COIL - R&D WORKSHOP, Prague'99

TECHNICAL PROGRAM

Monday 11 October

9:00 - 9:30
Welcome and Organization affairs

Session I
***Chair* : Gordon Hager**

9:30 - 10:10
Marsel V. Zagidullin
„The completely scaleable 1 kW class supersonic COIL"

10:10 – 10:50
Charles Helms
„Recent experimental results on the RADICL laser"

10:50 - 11:05 *Coffee break*

11:05 - 11:45
Otomar Špalek, Jarmila Kodymová, Vít Jirásek, Jan Kuželka
„Recent experimental results on COIL device in the Institute of Physics"

11:45 - 12:25
Frank Duschek *et* DLR colleagues
„Results of water vapor measurements in the COIL gas flow"

12:30 - 14:00 *Lunch break*

Session II
***Chair* : Martin Stickley**

14:00 - 14:40
Dov Furman and Zamik Rosenwaks
„Gain diagnostic in a supersonic COIL with transonic injection of iodine"

14:40 - 15:20
Karin Grünewald *et* DLR colleagues
„Results of COIL gain measurements"

REPORT DOCUMENTATION PAGE

Form Approved OMB No. 0704-0188

1. AGENCY USE ONLY (Leave blank)	2. REPORT DATE	3. REPORT TYPE AND DATES COVERED
	1999	Conference Proceedings

4. TITLE AND SUBTITLE

COIL R&D Worshop, Prague '99

5. FUNDING NUMBERS

F61775-99-WF077

6. AUTHOR(S)

Conference Committee

7. PERFORMING ORGANIZATION NAME(S) AND ADDRESS(ES)

Institute of Physics Academy of Sciences
Na Slovance 2
Prague 8 182 21
Czech Republic

8. PERFORMING ORGANIZATION REPORT NUMBER

N/A

9. SPONSORING/MONITORING AGENCY NAME(S) AND ADDRESS(ES)

EOARD
PSC 802 BOX 14
FPO 09499-0200

10. SPONSORING/MONITORING AGENCY REPORT NUMBER

CSP 99-5077

11. SUPPLEMENTARY NOTES

12a. DISTRIBUTION/AVAILABILITY STATEMENT

Approved for public release; distribution is unlimited.

12b. DISTRIBUTION CODE

A

13. ABSTRACT (Maximum 200 words)

The Final Proceedings for COIL R&D Worshop, Prague '99, 11 October 1999 - 12 October 1999

This is an interdisciplinary conference. Topics include latest achievements in R&D on COIL facilities supported by the USAF including gain measurements with various nozzle designs, efficiency measurements, gain distribution beyond the mixing zone, and new methods for preparing the active medium, especially iodine atoms.

14. SUBJECT TERMS

EOARD, Chemical oxygen iodine lasers

15. NUMBER OF PAGES

Too many to count

16. PRICE CODE

N/A

17. SECURITY CLASSIFICATION OF REPORT	18. SECURITY CLASSIFICATION OF THIS PAGE	19, SECURITY CLASSIFICATION OF ABSTRACT	20. LIMITATION OF ABSTRACT
UNCLASSIFIED	UNCLASSIFIED	UNCLASSIFIED	UL

NSN 7540-01-280-5500

Standard Form 298 (Rev. 2-89)
Prescribed by ANSI Std. 239-18
298-102

15:20 - 15:35 *Coffee break*

15:35 - 16:15
Boris Barmashenko and Ester Bruins
„Iodine dissociation and small signal gain in supersonic COILs"

16:15 - 16:55
Timothy J. Madden
„An investigation of supersonic mixing mechanisms for the chemical oxygen-iodine laser (COIL)"

16:55 – 17:35
Valery D. Nikolaev
„The gas dynamic parameters and efficiency of mixing in COIL with array of supersonic nozzles"

17:35 - 18:20
A separate meeting of the AFRL contingent with the Israeli Group for contract discussions

18:30 *Dinner*

Tuesday 12 October

Session III
Chair : **Charles Helms**

9:00 - 9:40
Gordon Hager
„The measurement of gain on the 1.315 μm transition of atomic iodine in a subsonic flow of chemically generated $NCl(a^1\Delta)$"

9:40 - 10:20
Vít Jirásek, Jarmila Kodymová, Otomar Špalek
„Thermodynamic and kinetic aspects of chemical generation of atomic iodine for a COIL and their consequences for experiments"

10:20 - 11:00
Nikolai N. Yuryshev
„A generation of atomic iodine for pulsed COIL by a dc discharge in alkyliodides"

11:00 - 11:15 *Coffee break*

11:15 - 12:00
A separate meeting of the AFRL contingent with the DLR Group for contract discussions

12:15 - 13:30 *Lunch break*

13:30 - 14:15
A separate meeting of the AFRL contingent with the Czech Group for contract discussions

14:15 - 14:45 **Round Table Discussion**
***Chair*: Willy Bohn**

15:00 *Departure from Lanna to the Institute of Physics*

15:30 - 16:30
Visit of COIL laboratory

16:30 *Departure to the Hotel Schwaiger*

19:00 *Closing working dinner*

N*otes:*

1/ A contribution will be given by the underlined colleagues
2/ A reserved time of 40 min for presentations includes the time for questions and discussion

ФИАН САМАРА Lebedev Physical Institute, Samara Branch

The completely scalable 1 kW class supersonic COIL

Zagidullin M.V.

Background

1. New compact Verty-JSOG operating stable up to 100 mmole/s of Cl_2
2. Minimization of $O_2(^1\Delta)$ losses when it is transported from JSOG to nozzle at high pressure and N2 dilution.
3. Optimization of geometry and gases flow rates.
4. COIL operation with slit nozzles because previously high efficiency was achieved with slit nozzle and 10 mmole/s of Cl2 and N2 dilution
5. Demonstration of high power with N_2 dilution and 5 cm gain length and new Verty-JSOG.
6. Operation at minimal volume pump rate as possible
7. Scalability of COIL

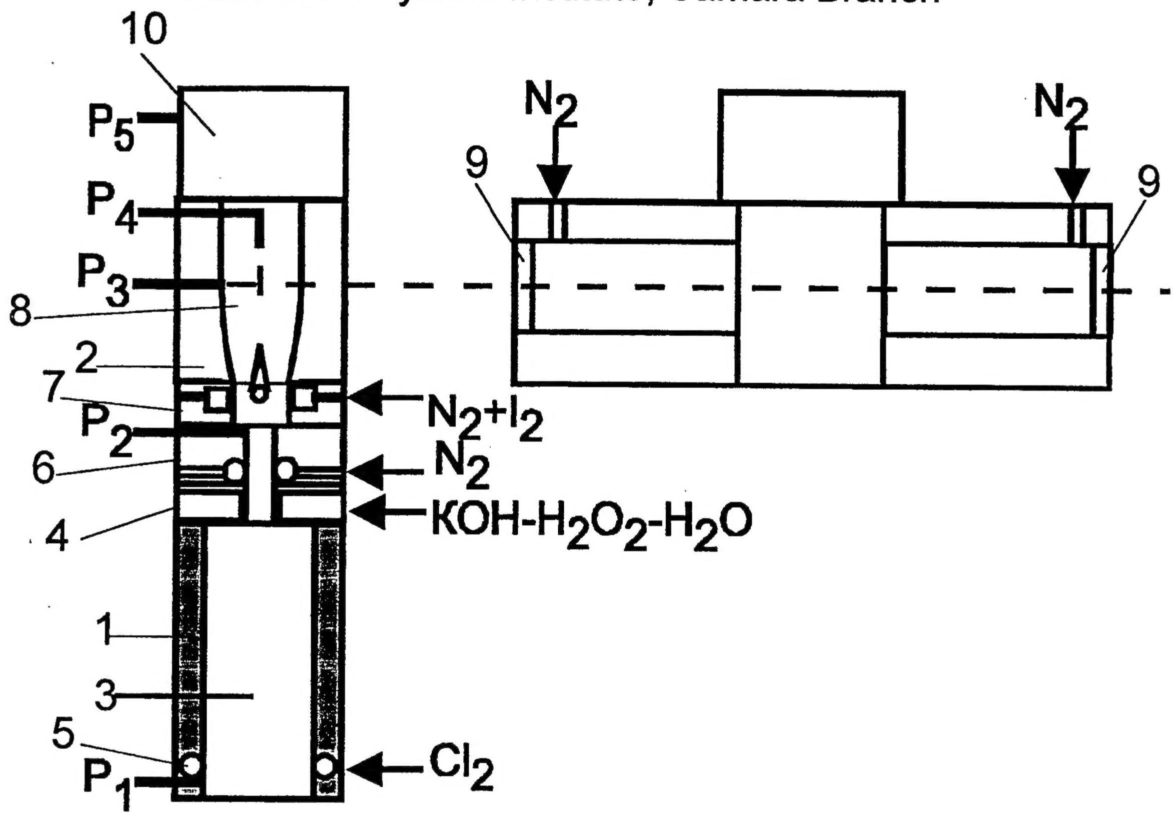

The set-up of COIL with Verty-JSOG and two slit nozzles

1- body of VJSOG ; 2- two slit nozzles ; 3 - counter-flow reactor ;4- the nozzle bank for BHP jets ; 5-the inlet for Cl_2, 6- mixing chamber 6 ; 7- iodine mixer ; 8- laser cavity ; 9-mirrors ; 10-vacuum duct

ФИАН САМАРА Lebedev Physical Institute, Samara Branch

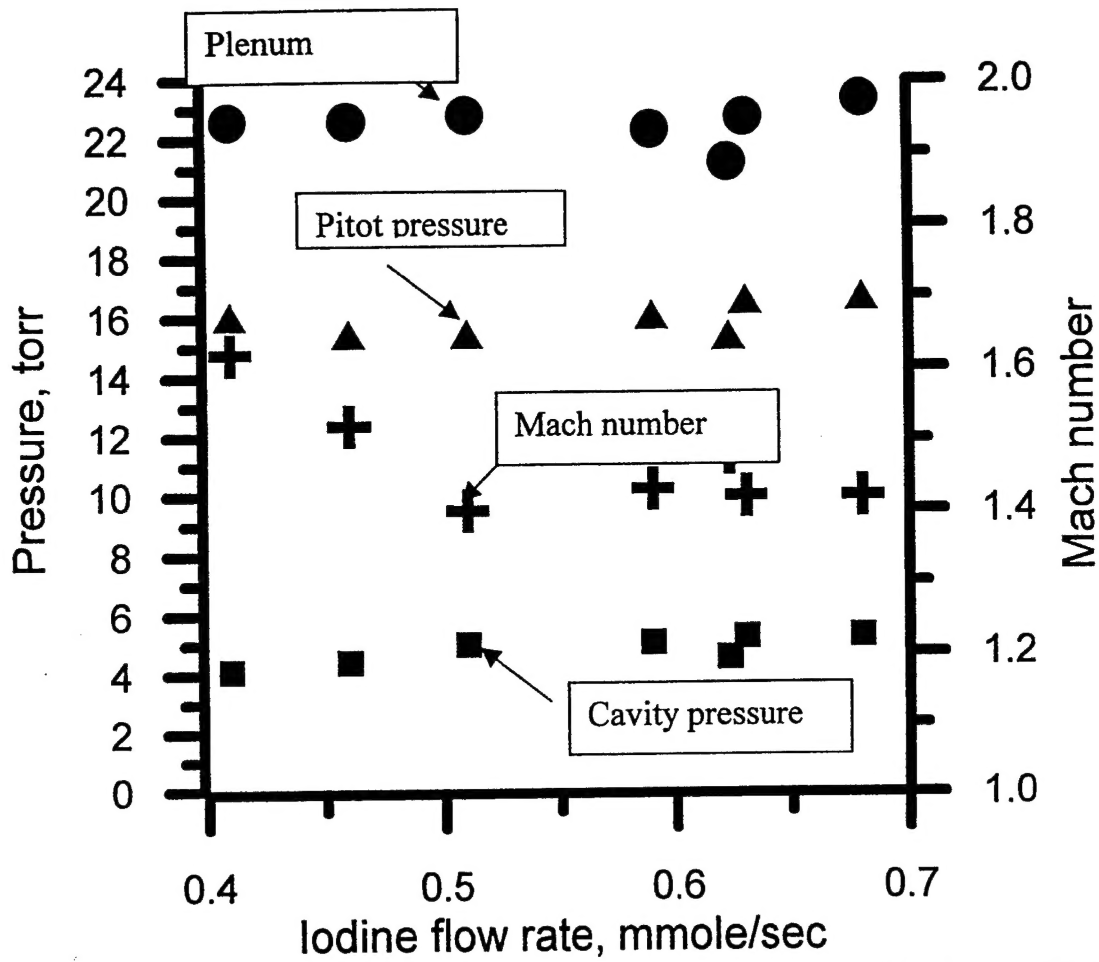

Pressures in gas-flowing part of the laser and the Mach number. $G_c:G_{N2P}:G_{N2S} = 1:2:1$. G_c=39.2 mmole/s., Pressure in JSOG 35 torr.

Lebedev Physical Institute, Samara Branch

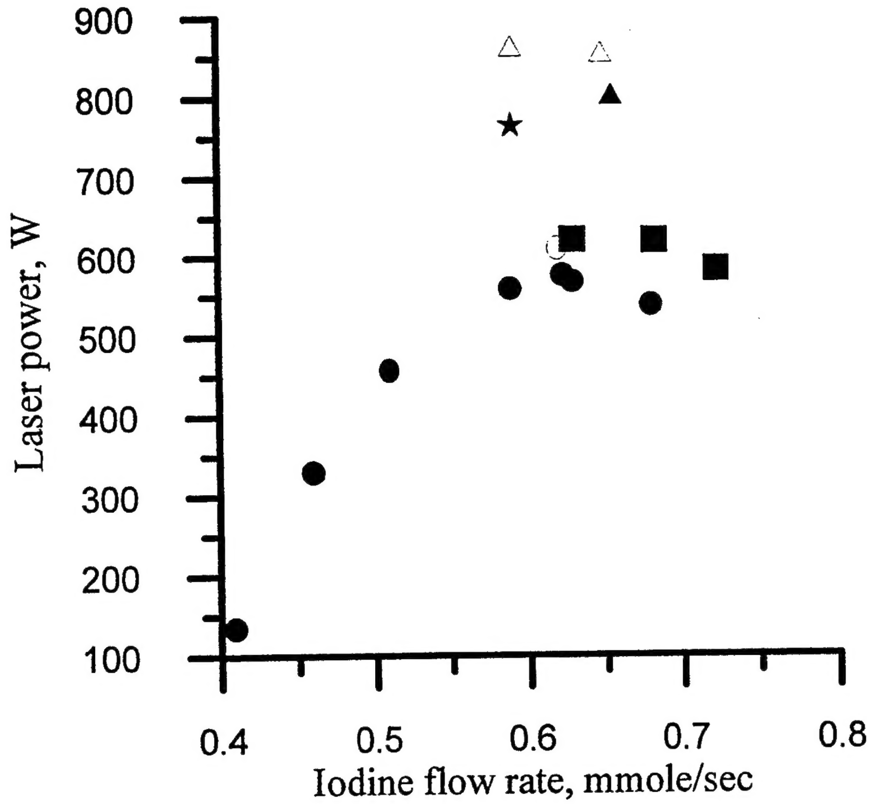

Dependence of output power on iodine flow rate and mirrors set at $Gc:G_{N2P}:G_{N2S} = 1:2:1$. G_c=39.2 mmole/s, Throat-optical axis distance L=55 mm

Symbol	T(N2P)	T_1,%	T_2,%
●	Room	0.9	0
❍	Cold	0.9	0
■	Room	1.3	0
▲	Room	1	0
Δ	Cold	1	0
★	Room	0.7	0.7

1. Change the primary gas flow rate.
Then ratio of gas flows was $G_C:G_{N2P}:G_{N2S} = 1:1:1$ to decrease pressure in JSOG and plenum pressure and decrease $O_2(^1\Delta)$ losses. P_{SOG}=28 torr, but lower Mach number and low power were obtained. At high I_2 flow rate the subsonic flow in cavity and zero power were obtained.
2. Change the throat-optical axis distance up to L= 80 mm. The power 467W was achieved for GI2=0.47 mmole/s (higher than 370W for L=55m). But for GI2 > 0.54 mmole/s the subsonic mode in cavity and zero power. Near GI2≈0.5 mmole/s the unstable subsonic or supersonic mode in cavity.

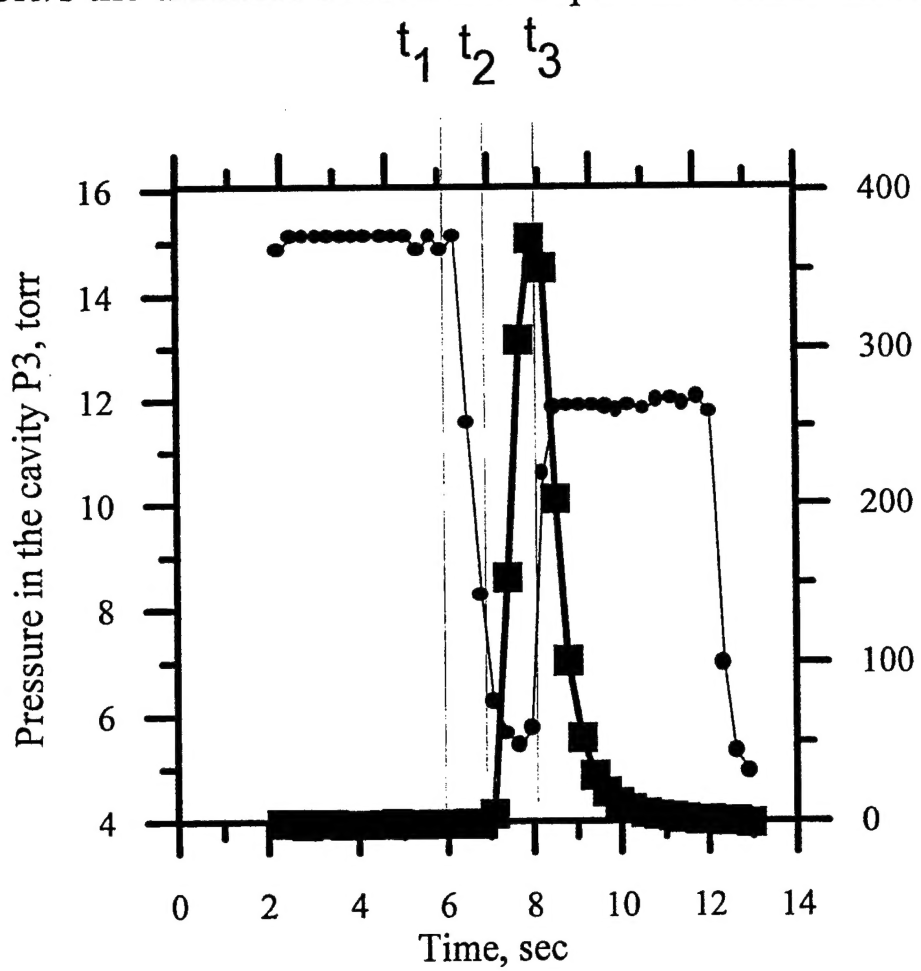

The transition from supersonic mode operation to subsonic mode. ● - pressure in the cavity, P_3 , ■ - laser power, L=80 mm.

OPERATION OF COIL WITH 68 MMOLE/S OF CHLORINE
$G_c:G_{N2P}:G_{N2S}$ = 1:2:1. L=55 mm. P_{SOG}=57 torr, Plenum pressure 36 torr.
If N2 flow rate for mirror purging from 4.5 mmole/s to 10 mmole/s power from 890W to 1035W, Mach number from 1.49 to 1.39, cavity pressure from 7.6 torr to 9.7 torr.

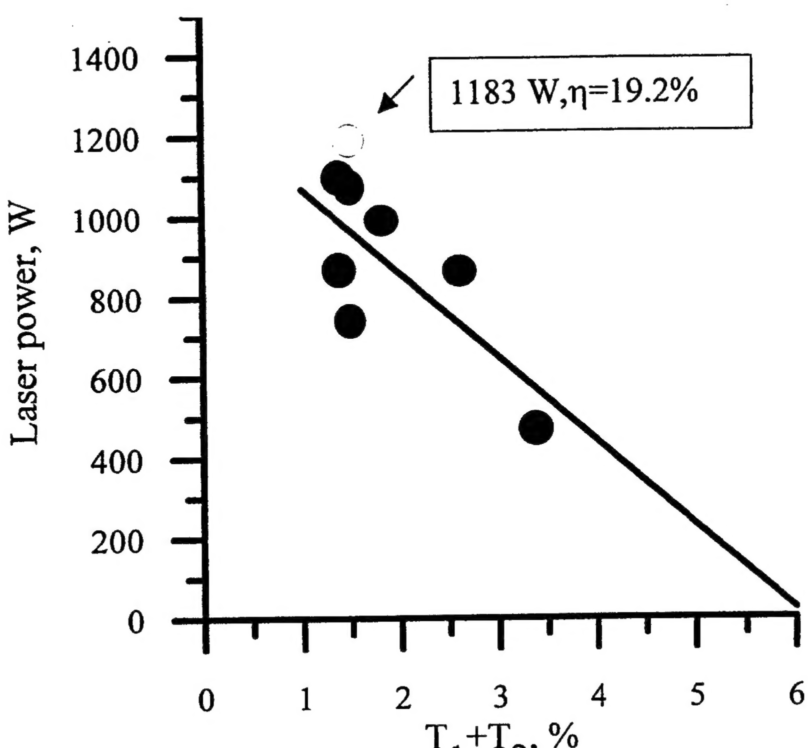

Dependence of output power on the total mirrors' transmissivity for G_c = 68 mmole/sec and G_{I2} =0.71 mmole/sec. ● - primary nitrogen at room temperature, ○ - cold primary nitrogen.
Estimated threshold transmission 6% , estimated losses 0.5%, estimated SSG $6.5x10^{-3}$ cm^{-1}.

OPERATION OF COIL WITH 75 MMOLE/S OF CHLORINE

G_c:G_{N2P}:G_{N2S} = 1:2:1. L=55 mm. P_{SOG}=67 torr, Plenum pressure 42 torr.

1. For N2 flow rate 2.7 mmole for mirror purging and GI2= 0.8 mmole/s Mach number 1.5 but power 0.
2. For N2 flow rate 6.8 mmole/s for mirror purging and GI2=0.89 mmole/s power 1030W was obtained (η=15%).(T1=0.94%, T2=0.9%)
3. The use of ratio G_c:G_{N2P}:G_{N2S} = 1:1:1 resulted in to subsonic mode and 0 power.
4. The use ratio G_c:G_{N2P}:G_{N2S} = 1:1:0.58 resulted in the same result.
5. The use ratio G_c:G_{N2P}:G_{N2S} = 1: 0.9 : 1.28 resulted in 1303 W (T1=0.8%, T2=0.7%).
6. The use ratio G_c:G_{N2P}:G_{N2S} = 1 : 1.28 : 1.28 resulted in 1408 W (T1=0.8%, T2=0.7%, GI2=0.7 mmole/s)

In last run mirrors were destroyed.

No cold primary N2 was used because we expected power more than 1500W and mirror destruction.

SUMMARY OF RESULTS

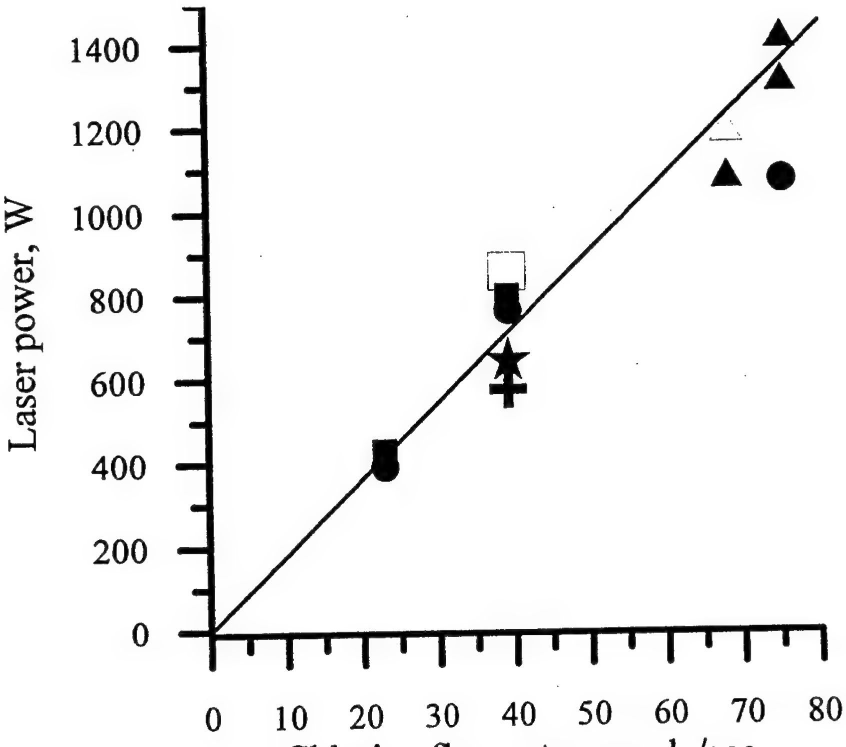

Dependence of laser power on chlorine flow rate. The direct line corresponds to chemical efficiency of 20%.

G_c	G_{N2S}	G_{N2P}	T_1,T_2, %	W	η, %	M
23	23,2	46.5	0.7;0.7	390(●)	18.7	1.24
23	23,2	46.5	1; 0	429(■)	20.6	1.24
39.2	39,2	78.4	0.9;0	574(✚)	16.2	1.48
39.2	43	78,4	1;0	798(■)	22.4	1.52
39.2	40	78,4	1.3;0	642(★)	18.1	1.51
39.2	39,2	78.4	0.7;0.7	764(●)	21.4	1.37
39.2	43	78.4*	1;0	858(□)	24.1	1.38
68	66	66	0.8;0.7	1074(▲)	17.4	1.51
68	66	66*	0.8;0.7	1183(Δ)	19.2	1.43
75	65.7	135.5	0.7;0.7	1074(●)	15.8	1.5
75	65.7	95.8	0.8;0.7	1303(▲)	19.2	1.4
75	82.	95.8	0.8;0.7	1408(▲)	20.7	1.5

*- cold primary nitrogen

ФИАН САМАРА Lebedev Physical Institute, Samara Branch

Conclusions

1. The output power growths close to linearly when for chlorine flow rates from 23 mmole/s to 75 mmole/s
2. The effect of gas heating on gas flow was observed (transition from supersonic to subsonic operation).
3. The power 1.4 kW (η=20.7%) for 75 mmole/s and η=24.1% (858W) for 39.2 mmole/s of Cl2 were achieved.
4. 5 kW per 1 liter of JSOG volume, δ-=100 W/cm^2, 2.7 W per 1 L/s of exhaust pump capacity.
5. The estimated SS gain 6×10^{-3} cm^{-1}.
6. Verty-JSOG is a good energy machine for COIL. The results obtained in this work can be as basis for comparison of other mixing-nozzles systems (reference point).
7. The gas flow section of high power COIL can be constructed as number of gas flow sections similar to considered.

Predicting the Performance of RADICL using the 3-D MINT Code

Oct 11, 1999

Charles Helms

Gas and Chemical Lasers Branch (DELC)

email: helmsc@plk.af.mil

phone: (505) 846-0519

Contributors

<u>Logicon RDA</u>

Dave Plummer
Peter Crowell
Alan Lampson

<u>SRA</u>

Richard Bugellin

<u>RADICL test team</u>

Brian Quillen
James Copland
Vince Valdez
John Oelfke
Greg Johnson
Teresa Neudecker

<u>DELC personnel</u>

Kip Kendrick
Gordon Hager
Tim Madden
Keith Truesdell

<u>Physical Sciences Inc.</u>

Measurements and Models can be combined to test our understanding of COIL

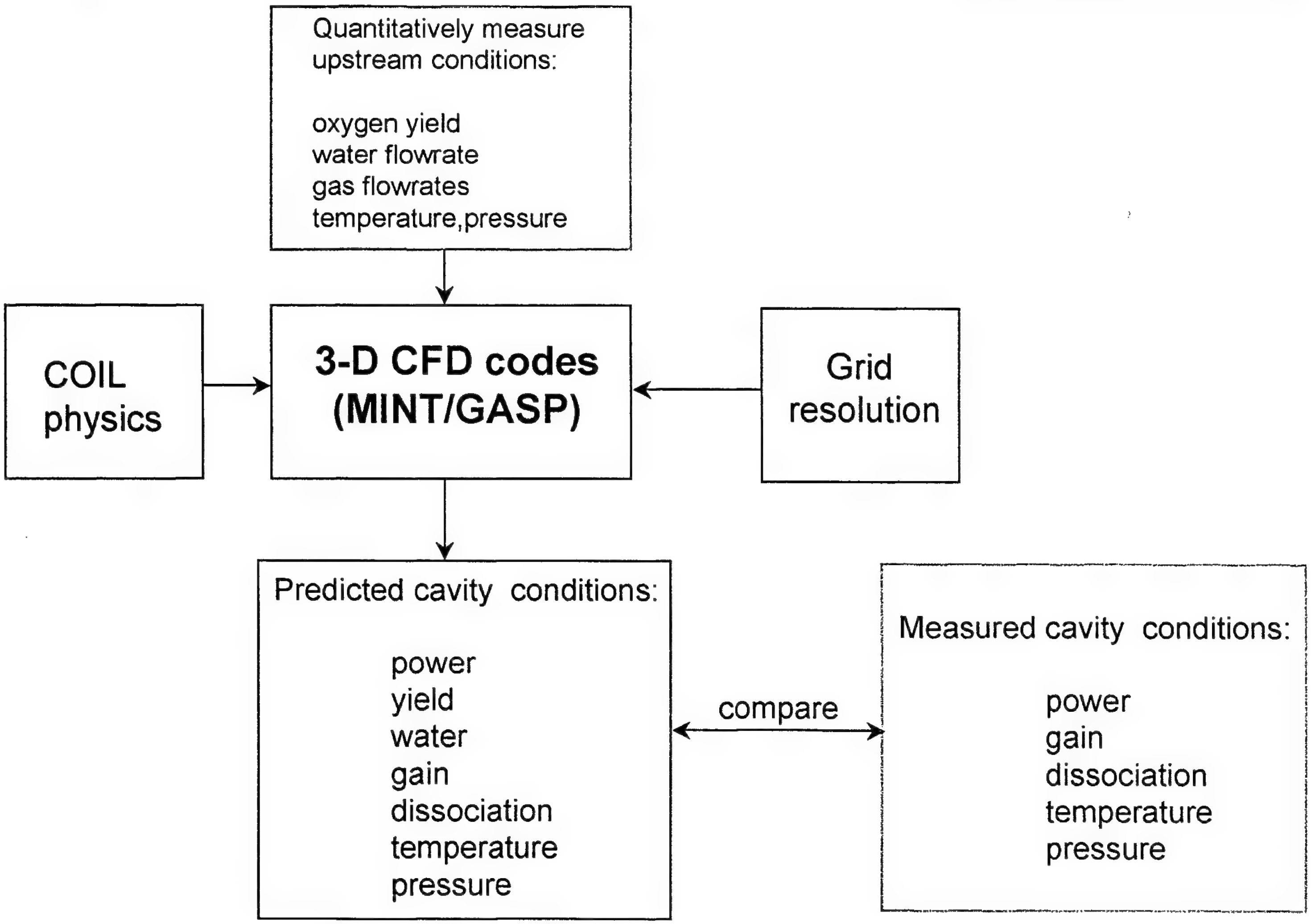

3-D MINT 7-Pack Validation Effort

- Goal: Determine the ability of the 3-D MINT code/kinetic rate package to predict the cavity conditions and power of the RADICL device at AFRL

- Approach:
  - Select a set of experimental conditions for which the results (power, gain, etc) are sensitive to the input flowrates
  - Carefully measure the input conditions and cavity conditions
  - Compare model predictions with experimental measurements

7 Selected RADICL Tests

1) baseline*............................optimized iodine and penetration
2) low iodine...........................poor dissociation and power
3) high iodine..........................reduced power due to losses in dissociation
4) low iodine penetration............reduced power due to poor mixing of oxygen and iodine
5) high iodine penetration ....poor dissociation and power
6) high diluent ratio..................poor dissociation and power
7) high water...........................reduced power due to water quenching and condensation

*.5 mol/sec Chlorine at 3/1 Helium/Chlorine

RADICL 2-D SLIT NOZZLE/ CAVITY

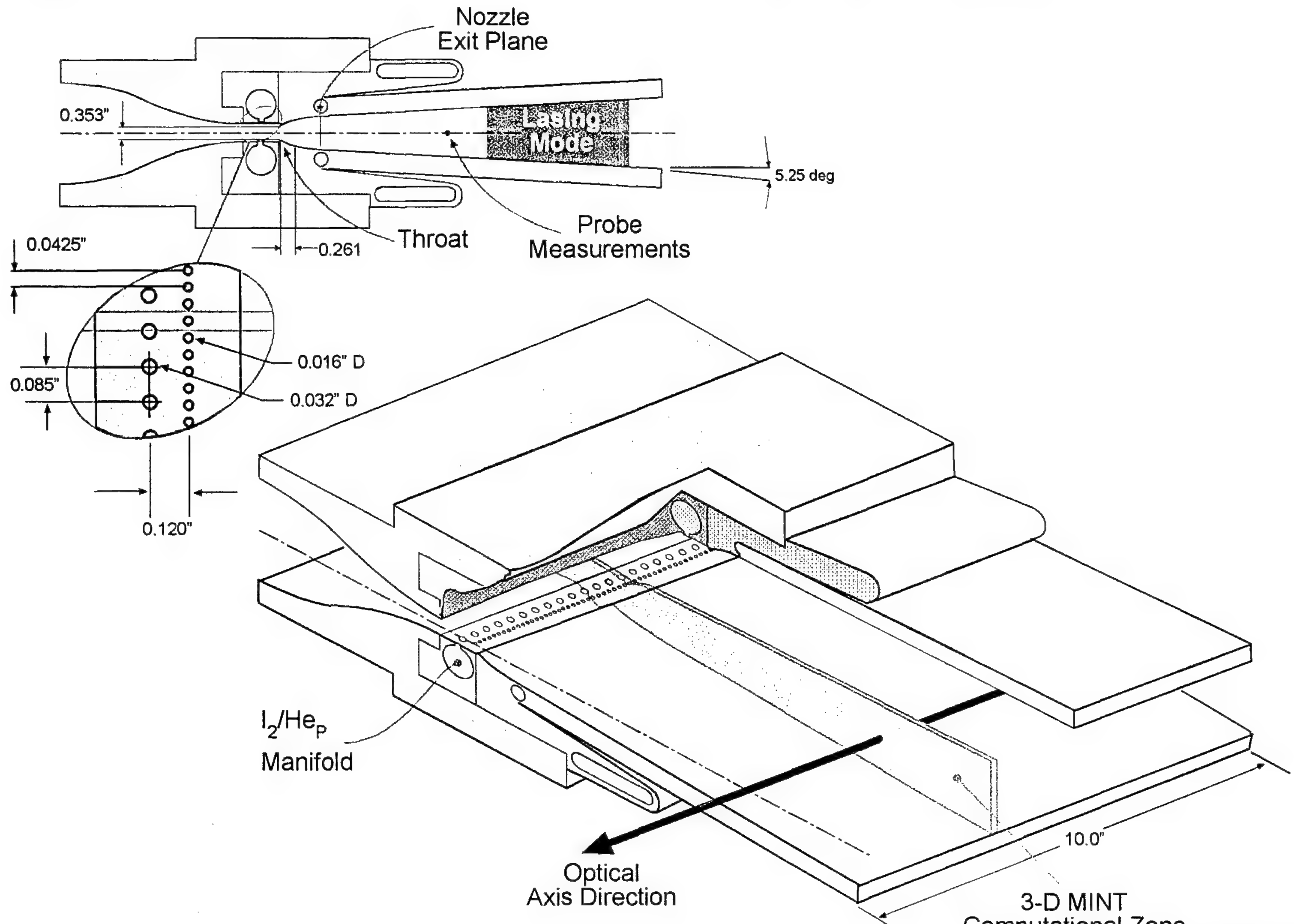

RADICL 2-D SLIT NOZZLE/ CAVITY

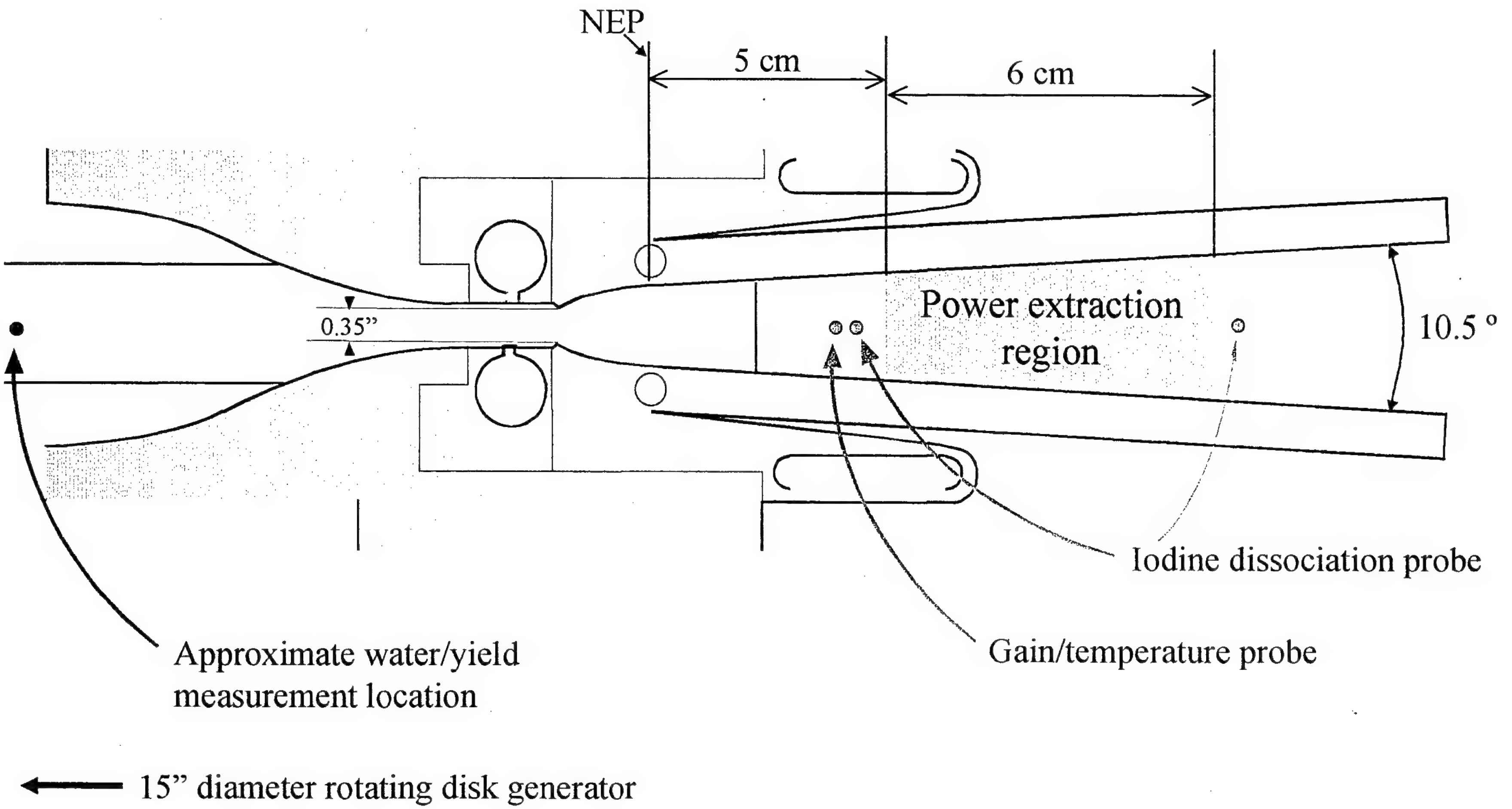

MINT Input Conditions for RADICL 7-Pack Comparisons

	Case						
Parameter	1	2	3	4	5	6	7
Primary Cl_2 (mole/s)	0.507	.508	0.51	0.505	0.509	0.513	0.501
He_p (mole/s)	1.513	1.492	1.52	1.513	1.52	2.937	1.479
H_2O (mmole/s)	42	47	39	47	39	58	81
U	0.88	0.90	0.90	0.91	0.81	0.83	0.93
Y	0.41	0.415	0.41	0.458	0.376	0.48	0.405 calculated
P (Torr)	74.9	73.5	74.3	64.9	87.7	103	75.7
T (K)	315	319	316	312	318	294	333
Secondary I_2 (mmole/s)	6.56	4.1	9.75	6.64	6.35	5.5	6.54
Hes (mole/s)	0.776	0.848	0.69	0.313	1.405	1.235	0.781
P_o (Torr)							
T_o (K)	421	415	419	421	412	417	421
I_2/O_2 (%)	1.49	0.897	2.15	1.49	1.39	1.29	1.40
Rate Parameter	4.2e-5	2.4e-5	7.0e-5	9.2e-5	2.6e-5	3.2e-5	3.9e-5
PEN (P_s/P_p)	4.8	4.7	4.7	2.7	6.5	4.9	4.7
PEN (AFRL)	0.14	0.14	0.14	0.09	0.19	0.14	0.14

"7-pack" Experimental Cavity Conditions

test description	ssg (%/cm)	cavity temp (K)	iodine dissoc upstream	iodine dissoc downstr.	power (kW)
baseline case	0.8	180	.94-.88	1	5.8
low iodine	.25-.45	145	.44-.37	1	2.7
high iodine	0.8	190	1	1	4.9
low penetration	0.4	185	0.99	0.98	4.3
high penetration	.35-.38	150-165	.31-.22	0.5	3
high diluent	0.22	150-160	.25-.15	0.29	1
high water	0.58	190-210	.86-.77	1	4.3

3-D MINT Code Features

- 3-D implicit, time-dependent, Navier-Stokes model
  - Central difference ADI solution scheme with artificial viscosity
- Effective binary diffusion model with pressure diffusion
- Laminar flow analysis (K-E turbulence model option)
- COIL kinetics (10 species & 21 reaction set)
  - Heterogeneous I* wall quenching included
- Finite rate condensation model including particle trajectory analysis
- Ray-trace stable resonator power model (or Fabry-Perot option)

COIL Kinetics Package

(AFWL Reduced Mod 1 - with Temperature Dependence)

	Reaction		**K_F (cm³/molecule-s)**
1)	$O_2(^1\Delta) + O_2(^1\Delta)$	-> $O_2(^1\Sigma) + O_2(^3\Sigma)$	$9.5 \times 10^{-28}\, T^{3.8}\, e^{700/T}$
2)	$O_2(^1\Sigma) + H_2O$	-> $O_2(^1\Delta) + H_2O$ **(M)**	6.7×10^{-12}
3)	$O_2(^1\Delta) + O_2(^3\Sigma)$	-> $O_2(^3\Sigma) + O_2(^3\Sigma)$	1.6×10^{-18}
4)	$O_2(^1\Delta) + H_2O$	-> $O_2(^3\Sigma) + H_2O$	4.0×10^{-18}
5)	$O_2(^1\Delta) + Cl_2$	-> $O_2(^3\Sigma) + Cl_2$	6.0×10^{-18}
6)	$O_2(^1\Delta) + He$	-> $O_2(^3\Sigma) + He$	8.0×10^{-21}
7)	$I_2(X) + O_2(^1\Sigma)$	-> $I + I + O_2(^3\Sigma)$	4.0×10^{-12}
8)	$I_2(X) + O_2(^1\Sigma)$	-> $I_2(X) + O_2(^3\Sigma)$	1.6×10^{-11}
9)	$I_2(X) + O_2(^1\Delta)$	-> $I_2^* + O_2(^3\Sigma)$	7.0×10^{-15}
10)	$I_2(X) + I^*$	-> $I_2^* + I$	3.8×10^{-11}
11)	$I_2^* + O_2(^1\Delta)$	-> $I + I + O_2(^3\Sigma)$	3.0×10^{-10}
12)	$I_2^* + O_2(^3\Sigma)$	-> $I_2(X) + O_2(^3\Sigma)$	5.0×10^{-11}
13)	$I_2^* + H_2O$	-> $I_2(X) + H_2O$	3.0×10^{-10}
14)	$I_2^* + He$	-> $I_2(X) + He$	4.0×10^{-12}
15)	$I + O_2(^1\Delta)$	-> $I^* + O_2(^3\Sigma)$	$4.54 \times 10^{-12}\, T^{0.5}$ **(M)**
16)	$I^* + O_2(^3\Sigma)$	-> $I + O_2(^1\Delta)$	$6.14 \times 10^{-12}\, T^{0.5}\, e^{-401.4/T}$ **(M)**
17)	$I + O_2(^1\Delta$	> $I + O_2(^3\Sigma)$	1.0×10^{-15}
18)	$I^* + O_2(^1\Delta)$	-> $I + O_2(^1\Sigma)$	$4.0 \times 10^{-24} T^{3.8}\, e^{700/T}$
19)	$I^* + O_2(^1\Delta)$	-> $I + O_2(^3\Sigma)$	5.0×10^{-14}
20)	$I^* + I$	-> $I + I$	1.6×10^{-14}
21)	$I^* + H_2O$	-> $I + H_2O$	2.0×10^{-12}

(M) = Modified from reduced AFWL Mod 1 rate package

3-d MINT RADICL Mesh
(Side View)

Full Grid (symmetric about centerline)

- 155,000 grid points

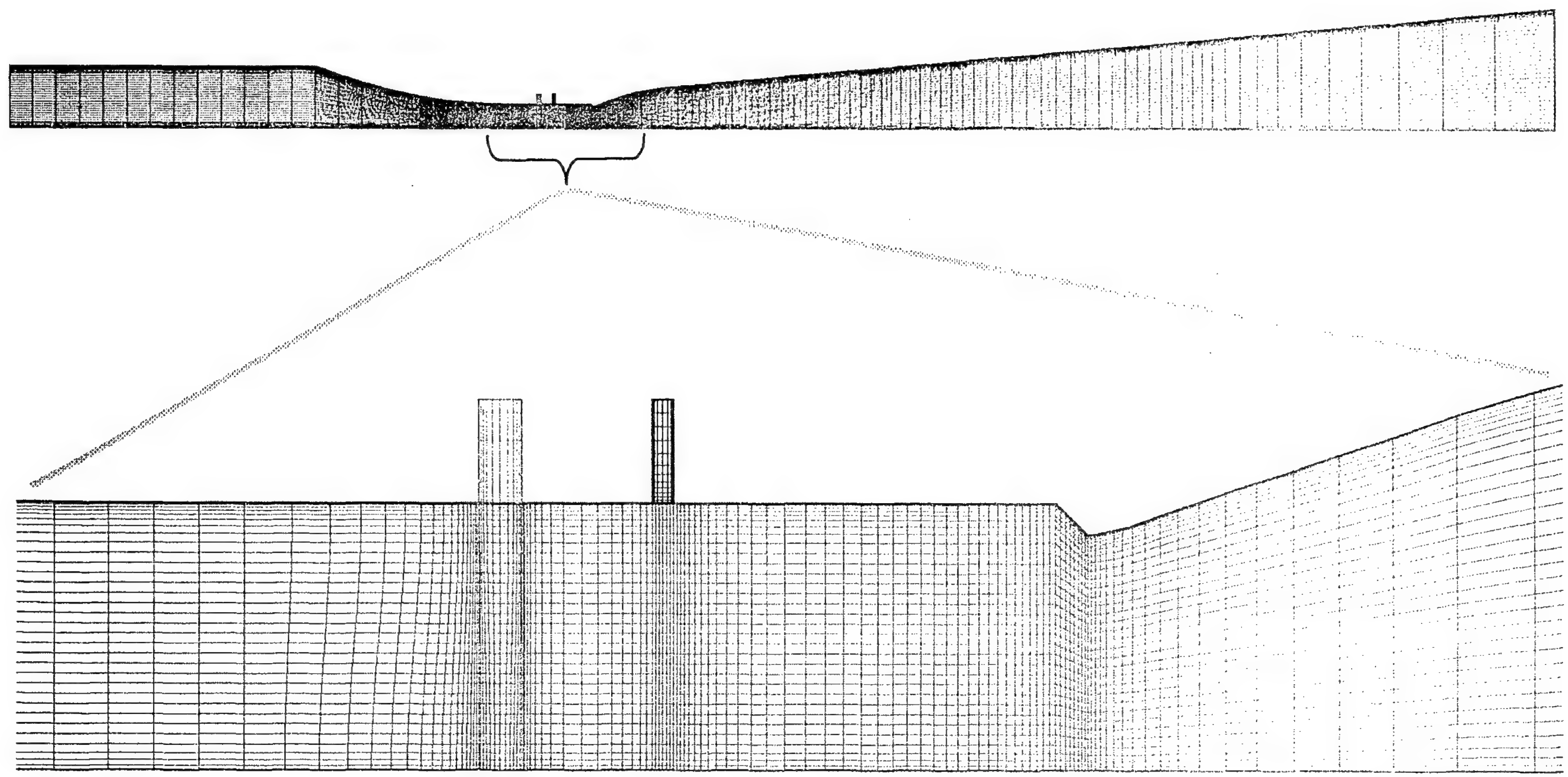

3-d MINT RADICL Mesh
(Top View)

Expanded View in Region
of Secondary Injection

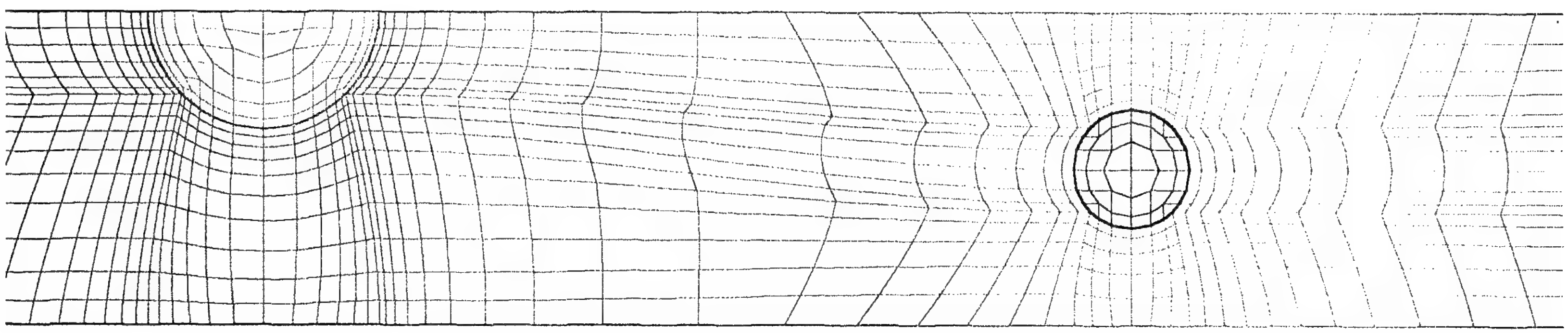

3-d MINT RADICL Mesh
(Top View)

Expanded View in Region
of Secondary Injection

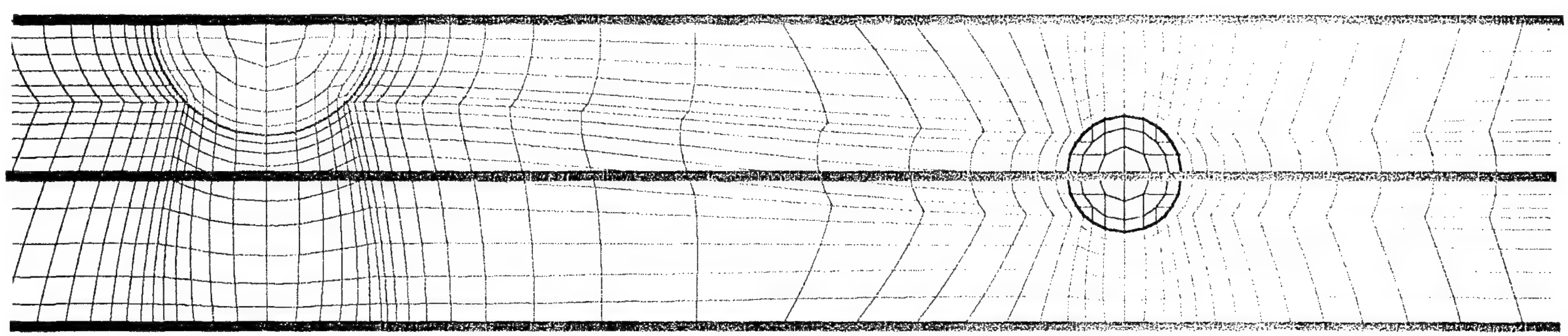

3-D MINT RADICL Intensity Profile
Case 1 - Baseline (Condensation)

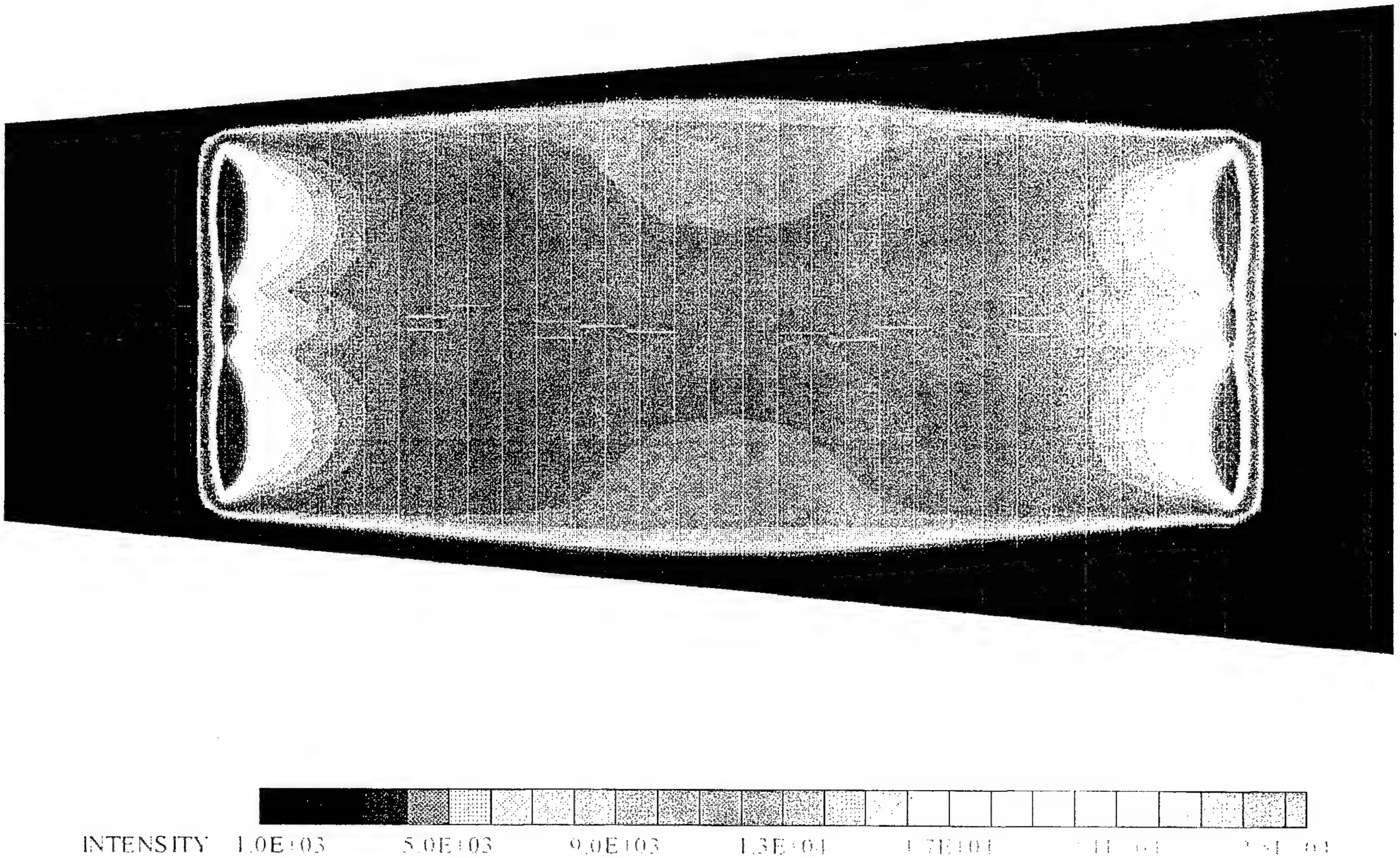

Comparison of 3-D MINT Plenum Pressure with RADICL 7-Pack Plenum Pressure Data

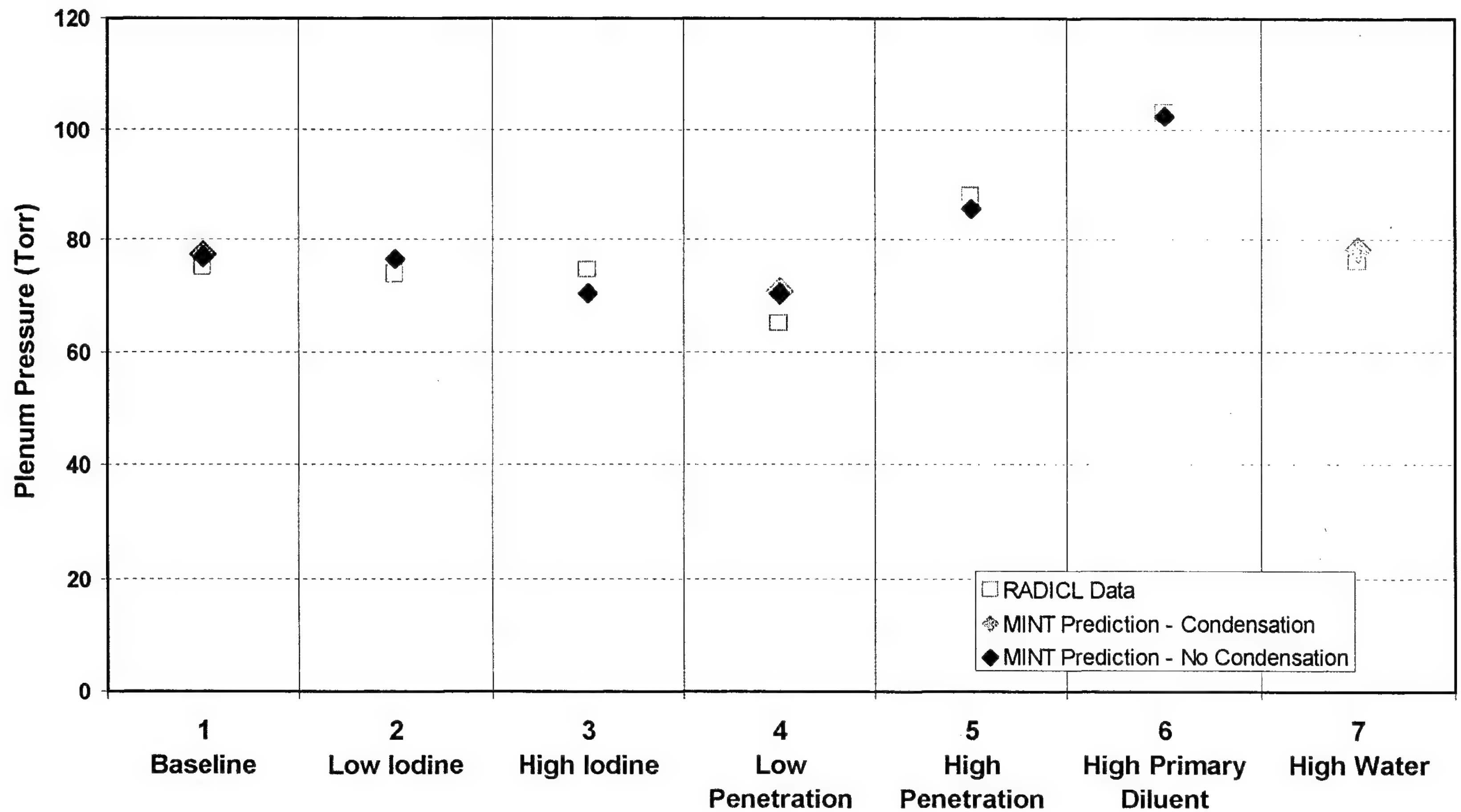

Comparison of 3-D MINT Avg Dissociation with RADICL 7-Pack Dissociation Data

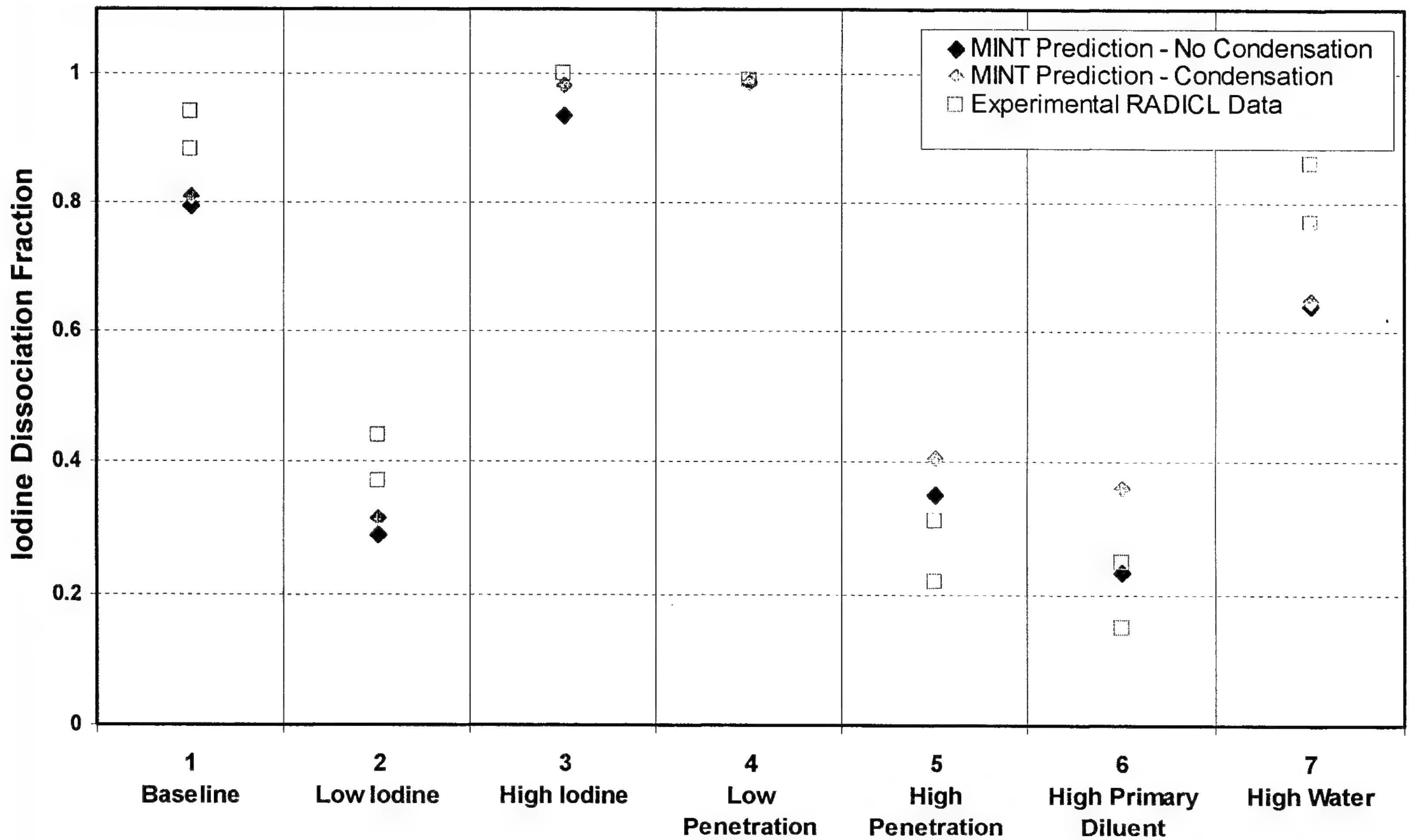

Comparison of 3-D MINT Probe Gain with RADICL 7-Pack Gain Probe Data

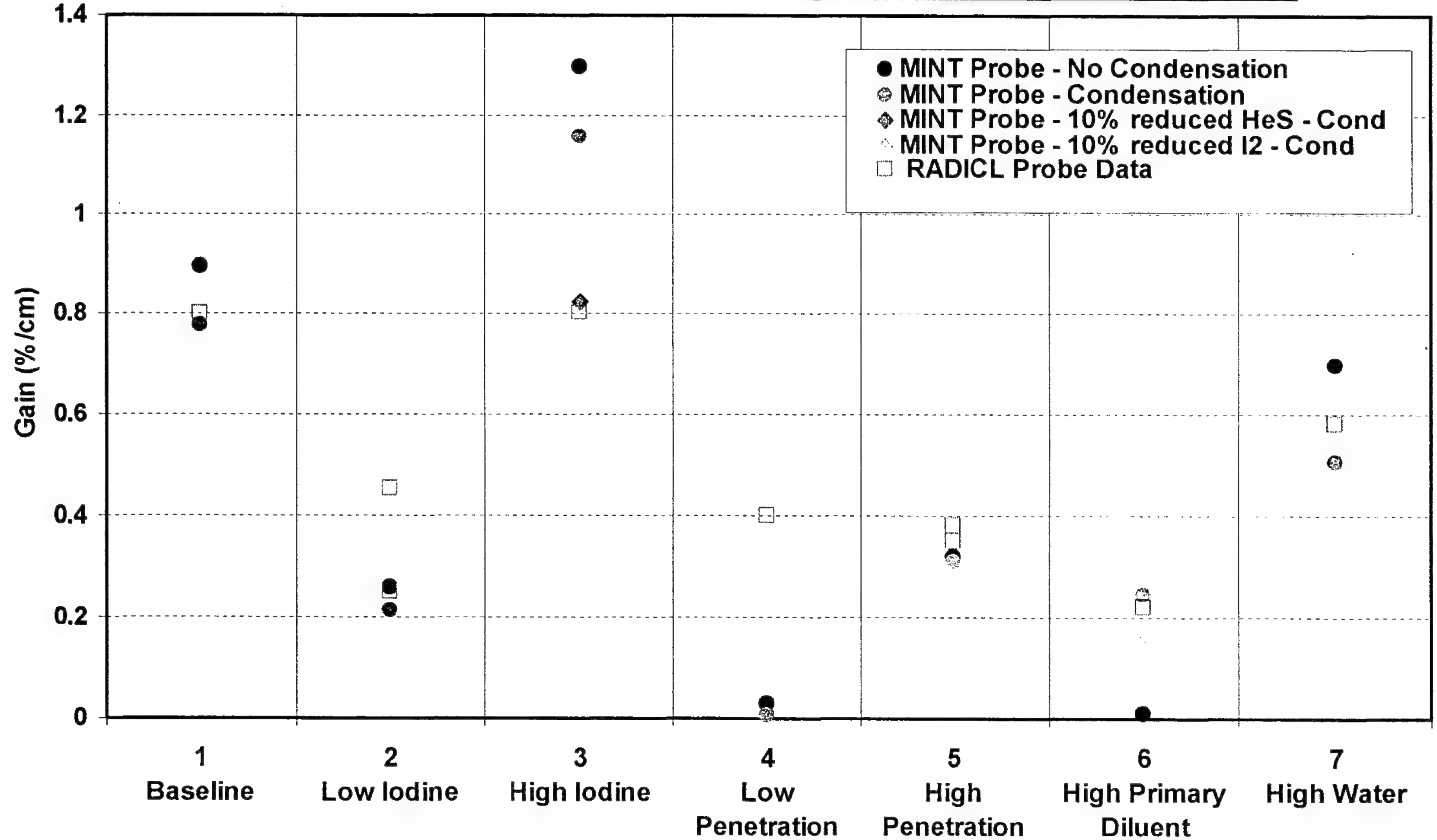

Vertical Gain Scan Comparison of 3-D MINT Probe Gain Vs RADICL 7-Pack Data

(Case 4 - Low Penetration)

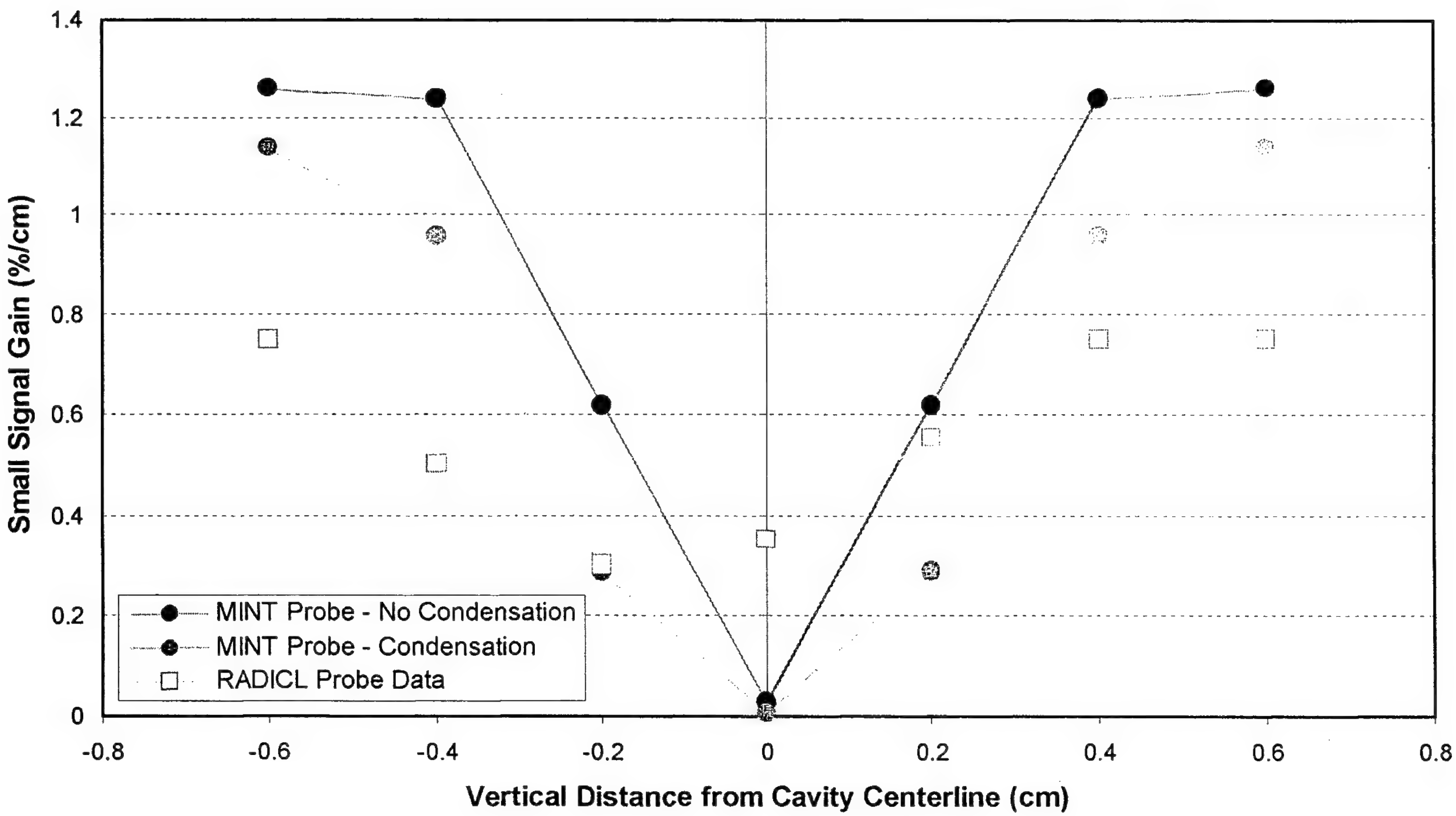

Comparison of 3-D MINT Cavity Temperature with RADICL 7-Pack Cavity Temperature Data

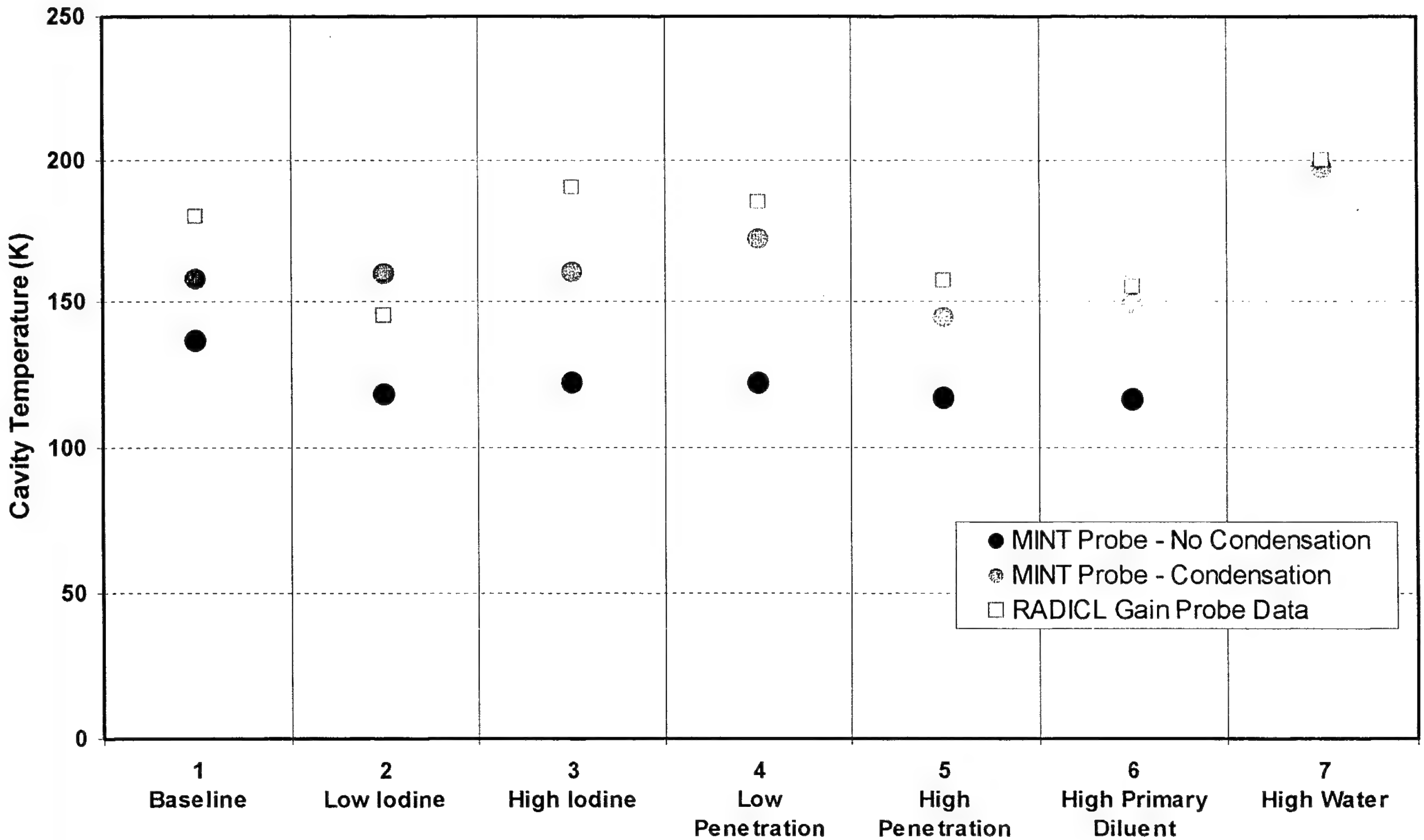

Comparison of 3-D MINT Power with RADICL 7-Pack Power Data

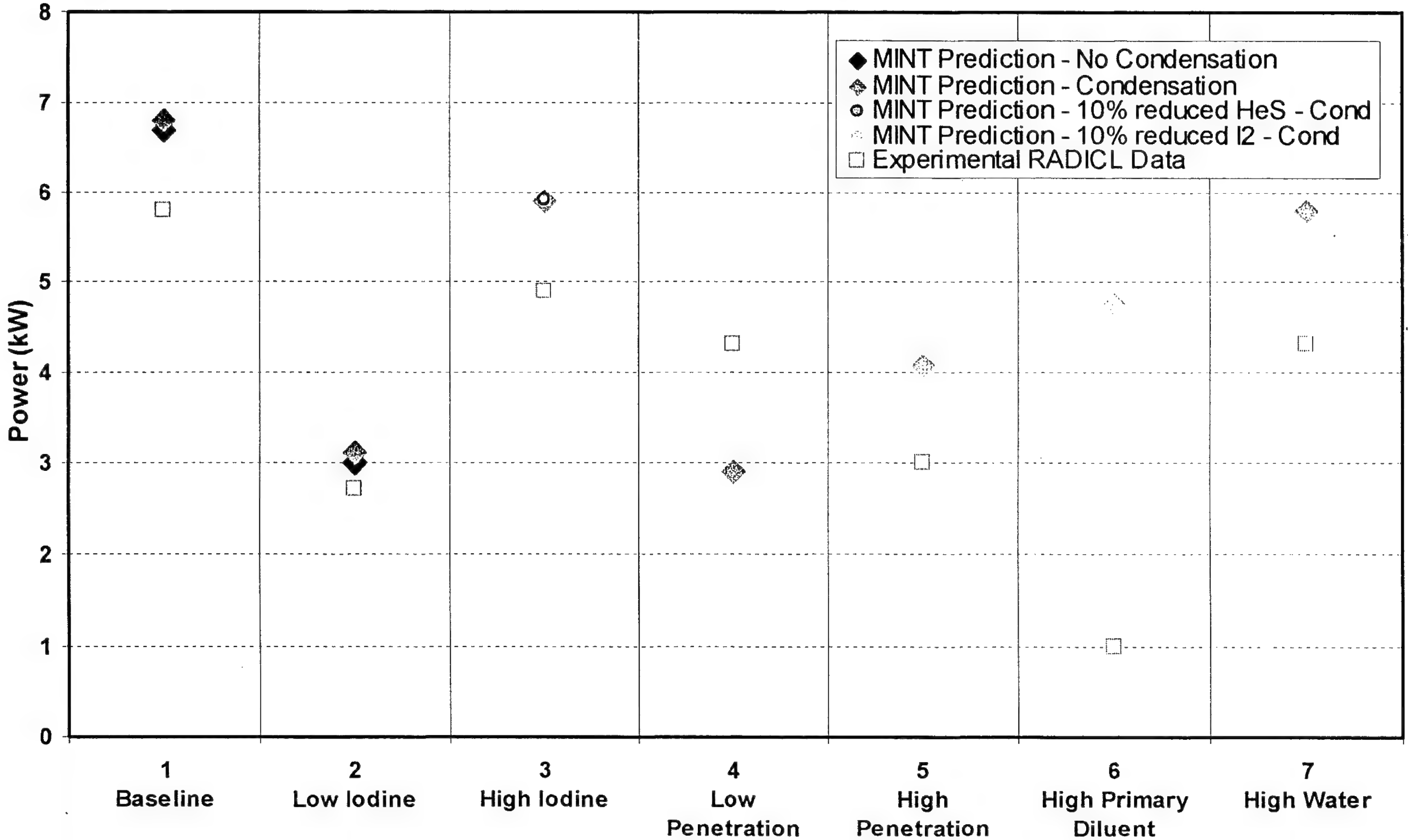

3-D MINT RADICL Dissociation Predictions Versus Dissociation Rate Parameter

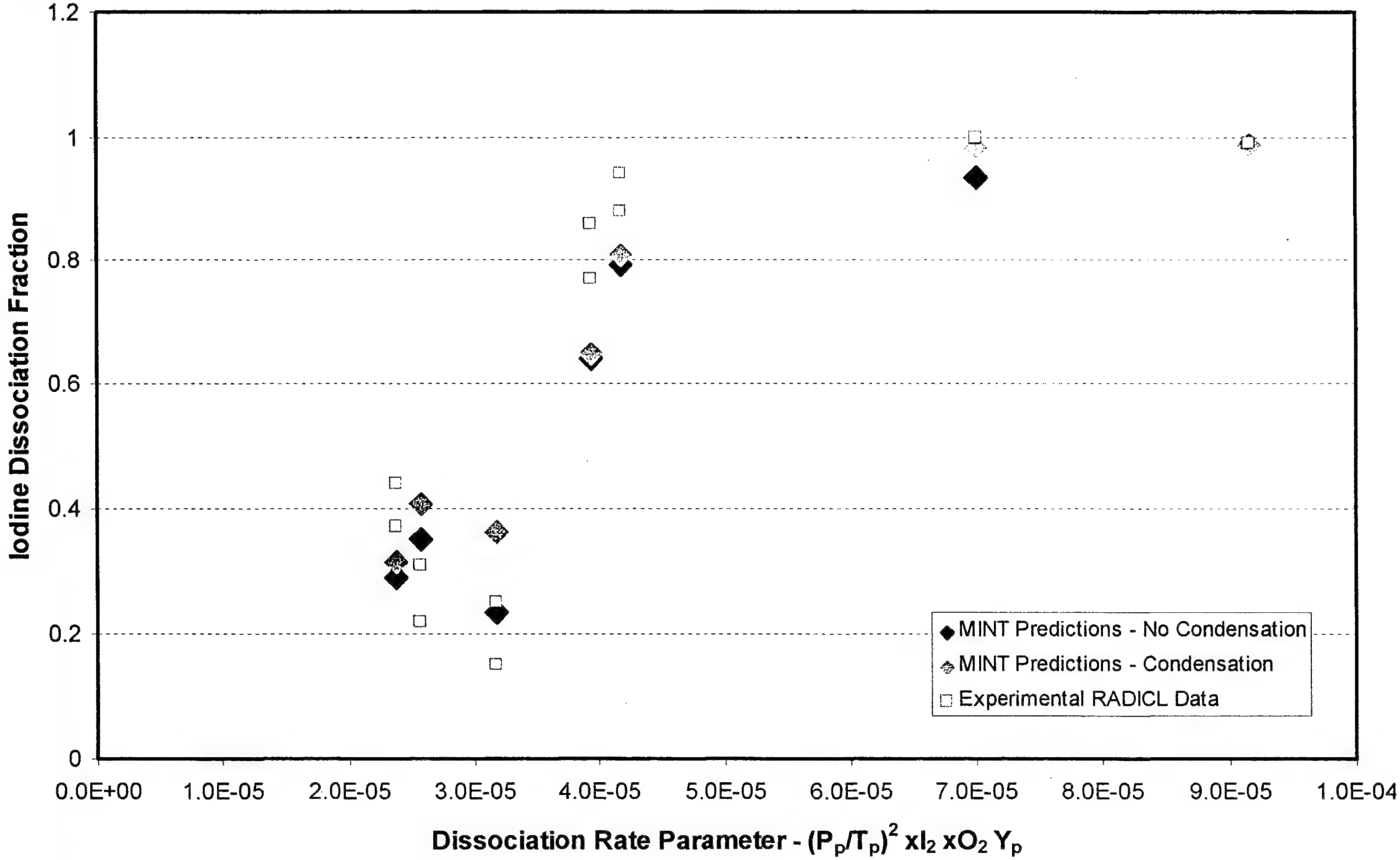

MINT Validation Preliminary Summary

- Very good prediction of experimental gain, dissociation, and cavity temperature TRENDS
- Fair to good prediction of experimental gain MAGNITUDES may mean adjustments in certain kinetic rates
- Water condensation seems to explain cavity temperature measurements
- Power comparisons show good agreement with trend but only fair agreement with magnitude
  – May be kinetics issue with respect to AFRL water quenching kinetics

Current/Future Work

- Conducting additional perturbation calculations
- Planning to assess grid resolution and solution accuracy
- Planning to demonstrate parallel MINT speedup on RADICL Case
- Planning to implement recommendations from MINT workshop

RECENT EXPERIMENTAL RESULTS ON COIL DEVICE IN PRAGUE

Otomar ŠPALEK, Jarmila KODYMOVÁ,
Vít JIRÁSEK, Jan KUŽELKA

Department of Gas Lasers
Institute of Physics, Academy of Sciences of the Czech Republic

EXPERIMENTAL

SSCOIL with JSOG - construction finished a year ago

Singlet oxygen generator

made of Plexiglas, cross section of 50 x 48 mm,
20 cm long BHP jets, 2 chlorine injectors in side walls (10 or 15 cm from top),
BHP jet injectors - 6 mm plate, 304 - 380 openings of 0.8 mm,
($S = 3.2 - 4.0\ cm^{-1}$),
liquid jets (velocity ~ 6 $m\ s^{-1}$) driven by ΔP created by a gear pump.

Close-loop BHP system

BHP tank with stainless steel heat exchanger, refrigerator (~2 kW),
BHP circulation - gear pump (110 $l\ min^{-1}$),
Liquiflo comp., model 312, frequency transducer,
continuous COIL operation at 40 mmol Cl_2/s up to ~ 4 minutes,
total time of JSOG operation with 15 litres of BHP ~ 40 min.

Generator gas outlet and subsonic channel (schema)

- throttle valve for choking the gas flow,
- electro-pneumatically controlled vacuum tight flat valve,
- diagnostic cell: $O_2(\Delta_g)$ emission at 1270 nm by Ge photodiode,
  $O_2(^1\Sigma_g)$ emission at 762 nm (Si photodiode) for c_{H2O},
  Cl_2 chlorine concentration measurement from light absorption (330 nm),
  gas pressure, temperature
- injector of primary He (2 rows of 25 x 0.7 mm i.d., ± 45 °).

Iodine injector (nozzle)

- stainless steel block with inner duct of 50 x 9.6 mm,
- 2 rows of openings (21 holes 0.8 mm and 42 holes 0.4 mm),
- heated by two transistors up to 60 - 90°C,
- a distance between I_2 injection and the sonic throat adjustable to 6 -10 mm..

Supersonic nozzle and optical cavity

- single horizontal slit(critical height 6.7 mm, width 50 mm),
- made of stainless steel (or Plexiglas), inserted into a laser body,
- shape designed according to the method of characteristics and still opened by 3°,
- distance between the throat and resonator optical axis from 35 to 55 mm,
- resonator 85 cm long, lasing gain region 5 cm,
- multimode output beam 3.7 cm x 1.6 cm.

Vacuum pumping system

- Roots blower and single-stage rotary pump (RUTA 3001/2, Leybold), 3000 $m^3 h^{-1}$,
- LN_2 trap with ribbed heat exchanger.

Iodine system

A new system of solid iodine evaporation by preheated He flowing through iodine bed,

Advantage - high area g/s interface for intensive heat transfer from preheated He to I_2 $\Rightarrow$ **high I_2 flow rates at small tank dimensions**,

Design: solid iodine in tank made of stainless steel cylinder with a glass liner,
- He heater upstream of the tank., He temperature up to 500 °C before entering the I_2 tank
- tank capacity ~30 min operation at 2 mmol I_2 /s,
- iodine concentration from light absorption (488 nm, $\varepsilon = 444.6$ l/mol cm, or $\sigma_{488} = 1.7 \times 10^{-18}$ cm^2),
- spectral photometer Spekol 11 with fibre optics,
- I_2 diagnostic cell: pressure and temperature sensing,
- I_2 flow rate from He flow rate, I_2 concentration, P and T in diagnostic cell,
- additional He through a line by-passing the iodine tank, enables to adjust required I_2 flow rate (automatic control is prepared).

Data acquisition system

Most of the measured parameters processed by A/D converter (32 channels) and by PC

TESTS OF COIL SUBSYSTEMS

Tests of jet SOG

Experiments with He_{prim} introduced downstream of the generator

Values $\mathbf{P_{gen}} \Rightarrow$ **$O_2(^1\Delta_g)$ yield easily controlled by choking exiting gas - Fig. 1a**.,

P in subsonic channel: 3.2 - 3.9 kPa (24 – 29 torr),

$O_2(^1\Delta_g)$ yield - **Fig. 1b**

water vapour pressure - **Fig.1c**

gas temperature in subsonic channel - **Fig.1c**

Experiments with He_{prim} admixed into Cl_2 upstream of the generator

$\mathbf{P_{gen}}$ on throttle valve position - **Fig. 2a**

$O_2(^1\Delta_g)$ yield - Fig. 2b

gas temperature in subsonic channel - **Fig. 2c, 3**

Effect of SOG run time on BHP temperature (40 mmol Cl_2 /s + 80 mmol He_{prim}/s, 15 l BHP): dT/dt = 5°C/min - **Fig. 3**,

BHP jets temperature by 2 – 4°C higher than bulk temperature,

Tests of gas dynamic conditions in COIL device

Tests at "cold flow run":

The average Mach number, M_1, in the subsonic channel[1]

$$n = (\kappa / R\,\mu)^{1/2} (A\,P_{stat} / T^{*1/2})\,M\,\{1 + M^2(\kappa - 1) / 2\}^{1/2}$$

n - total molar flow rate, κ - adiabatic constant, R - gas constant, μ - molecular weight, A - flow cross section, P_{stat} - static pressure, T^* - stagnation temperature.

Experimental conditions:

$n_{N2} = 22.3$ mmol/s, $n_{He} = 89.5$ mmol/s,

$P_{sub.\,ch.} = 2055$ Pa, A = 9,5 x 50 mm,

$T^* = 293$ K,

Resulting **average Mach number: $M_1 = 0.41$.**

Average Mach number in the resonator optical axis: $M_2 = 1.9 - 1.4$

Local Mach number in the centreline of ss cavity:

$$P_{stat} / P_{Pit} = \{2 / [(\kappa - 1)\,M_2^2]\}^{\kappa/(\kappa-1)}\,\{[2\,M_2^2\,\kappa / (\kappa + 1)] - [(\kappa - 1)/(\kappa + 1)]\}^{1/(\kappa-1)}$$

P_{Pit} - Pitot tube pressure, $A = 9.16\ 10^{-4}\ m^2$, h = 16 mm, w = 55 mm.

Local Mach number in the resonator optical axis: $M_2 = 2.4 - 2.2$

Tests of iodine vaporiser

- **study of I_2 flow rate**: controlled by He temperature, He flow rate, voltage and time of tank jacket heating.

Time dependence of I_2 flowrate - Fig. 4 (preheated tank, without He heating),

Fig. 5 (effect of He temperature),

$\Rightarrow$ **preheating of secondary gas can compensate** the **negative effect of iodine cooling** caused by evaporation heat,

- **iodine evaporation system with preheated gas can provide constant I_2 flow**

Mixing of primary (O_2 + He) and secondary (I_2 + He) flow

Iodine jet penetration given by **penetration parameter**[3]

$$\Pi = n_s / n_p \{(M_s T_s P_p / M_p T_p P_s)\}^{1/2}$$

Experiment : at P_{out} = 370 - 430 W:

primary flow: 37 mmol O_2/s + 1 mmol Cl_2/s + 80 mmol He/s

n_p = 118 mmol/s, $M_p = 13{,}35 \times 10^{-3}$ kg/mol,

T_p = 273 K, P_p = 3800 Pa,

secondary flow: 40 mmol He/s + 1.1 mmol I_2/s

n_s = 41.1 mmol/s, $M_s = 10.7 \times 10^{-3}$ kg/mol

T_s = 343 K, P_s = 13500 Pa

Resulting **penetration factor: Π = 0.093,**

A hardware design parameters $\Rightarrow$ **full penetration parameter**, Π_{full},[3]:

$$\Pi_{full} = d A_s / 5 D A_p$$

d - height of subsonic channel, D - diameter of iodine injector opening,

A_s - cross-section of secondary flow, A_p - cross-section of primary flow.

Our COIL: $\Pi_{full} = \mathbf{0.105}$,

$\Pi/\Pi_{full} = \mathbf{89\ \%}$

Experiments with laser generation

Main problem: entraining of BHP droplets and BHP foam into gas channel

- geometry of the generator near the gas outlet (extremely high gas velocity of gas crossing last rows of jets) - effect increases with increasing generator cross section,
- problems of liquid film creeping up the walls

Typical **experimental conditions:**

40 mmol Cl_2/s, 80 mmol He_{prim}/s, 40 mmol He_{sec}/s, 0 - 3.0 mmol I_2/s,

x = 6 mm or 10 mm (distance between the I_2 injector and nozzle throat),

δ_e = 0.85 - 2.6 % (resonator mirrors output coupling),

l = 35 or 55 mm (distance between the critical section and optical axis)

Experiments with prim. He downstream JSOG (behind throttle valve)

An output power 60 W - 150 W at I_2 flow rate of 0.5 - 1.25 mmol/s and δ_e = 0.85 - 2.6 %. Effects of the distance I_2 injector - nozzle throat, and nozzle throat - opt. axis - not revealed in this series for poor reproducibility for escaping liquid problems.

Primary He admixed into Cl_2 upstream of the generator

Earlier experimental series

P_L better (to 280 W) for shorter distance I_2 injector - nozzle throat (5 mm) - result of **smaller loss of I^* before nozzle throat.**

Study of effects of $\boldsymbol{P_{gen}}$, $\boldsymbol{n_{I2}}$, $\boldsymbol{n_{He,sec}}$, δ_e, and operation time:

- greater opening of the throttle valve resulting in lower generator pressure (below 6 kPa ~ 45 torr) **reduced laser power substantially (in contradiction to a higher $O_2(^1\Delta)$ yield) - Fig. 6**

- reason: light scattering in the laser active zone **on streaming liquid droplets,**

- water concentration was rather low (40 - 50 Pa vs. 580 Pa of $O_2(^1\Delta)$),

- effect caused by a lower P_{gen} and **higher gas velocity in the generator** (at more opened TV) and **increasing capture of liquid droplets** by gas.

Later experimental series

Suppression of escaping liquid increased the laser output power up to **430 W** (38 mmol Cl_2/s, η_{chem} = 12.5 %)

Laser power - mostly **affected by iodine flow rate - Fig. 7**

($\boldsymbol{P_L}$ between 375 W and 425 W, if $\boldsymbol{n_{I2}}$ between 1.0 and 1.75 mmol/s),

From this time dependence ⇒ **laser power** vs. **iodine flowrate - Fig. 8**

Effects of $\boldsymbol{n_{I2}}$ on laser power **at different output coupling - Fig. 9.**

From this dependence - the **small signal gain and saturation intensity.**

The Rigrod gain saturation model[4]

$$P_w = s\,\delta_e\,\{[\,2\,\alpha_{34}\,l_g / (\delta_e + \delta_o)]^2 - 1\}\,I_s$$

s is the output beam cross-section, δ_e - total external coupling, δ_o - internal cavity losses.

Our COIL: $s = 6.1\ cm^2$, $l_g = 5.5$ cm, and $\delta_o = 0.12$

n_{I2}, mmol s^{-1}	α_{34}, cm^{-1}	I_s, W cm^2
0.5	0.0137	3025
1.0	0.0163	3238
1.5	0.0155	4428

Very important effect of mirrors quality - a relatively stable P_L observed with some mirrors only (e.g. **Fig. 6**).

- often a **time decrease in *P_L*** caused by **worse quality mirrors (Fig. 10),**

Multimode **beam patterns** - see example

Comparison of our COIL (jet SOG-COIL) **with VertiCOIL** (disk SOG-COIL) from USAF Research Laboratory (data taken from Phipps *et al*[6] and Helms *al*[7])

	VertiCOIL in AFRL	**JetSOG-COIL in IP**
Total power	420 W	430 W
Chlorine flow rate	36 mmol/s	37.8 mmole/s
Primary He diluent	135 mmol/s	80 mmol/s
Generator pressure	38 torr	8 kPa (60 torr)
Diagnostic duct pressure	28 torr	3.8 kPa (28.5 torr)
Laser cavity pressure	4.5 torr	380 Pa (2.8 torr)
BHP inlet temperature	-30°C	-22°C
BHP outlet temperature	-19°C	-18°C
Diagnostic duct temp.	-10°C	+2°C
Penetration factor, Π	0.110	0.093
Full penetrat. factor, Π_{full}	-	0.105
Chemical efficiency	0.12	0.12
I_2/O_2	0.017	0.029
Starting BHP molarity	7.2 M HO_2^-/0.5 M H_2O_2	6.7 M HO_2^- /2.3M H_2O_2
$O_2(^1\Delta_g)$ yield	0.54 (assumed)	0.72
Mirror reflectivities	0.997/0.982	0.9995/0.981
Mirror scattering loss	0.0025/0025	not estimated
Mirror absorption loss	$10^{-5}/10^{-5}$	not estimated
Mode length	3.2 cm	3.7 cm
Gas velocity in cavity	1.0×10^5 cm/s	0.9×10^5 cm/s
Small signal gain	0.014 cm^{-1}	0.015 cm^{-1}
Saturation intensity	-	4 kW cm^{-2}

CONCLUSIONS

Experiments with **COIL subsystems**:

- our designed jet **SOG able to generate $O_2(^1\Delta_g)$** with **high excitation efficiency** and **low water content,**
- tests of **gas dynamic conditions** proved a **fast flow in the subsonic channel** and **supersonic flow in laser cavity,**
- originally **designed iodine vaporiser** using **pre-heated He may provide constant iodine flow rates** up to **3 mmol/s.**

COIL results:

- proved **very detrimental effect of liquid droplets in the laser cavity** and called for improvements, which resulted in **suppression of liquid droplet escaping from JSOG**,
- **found optimum experimental conditions suppressing this effect,**
- **achieved appropriate P_L and estimated small signal gain** and I_s.

Near plans:

- **to improve COIL parameters** (measurements at higher n_{Cl2}, using mirrors of better quality and greater aperture, to shorten subsonic channel)

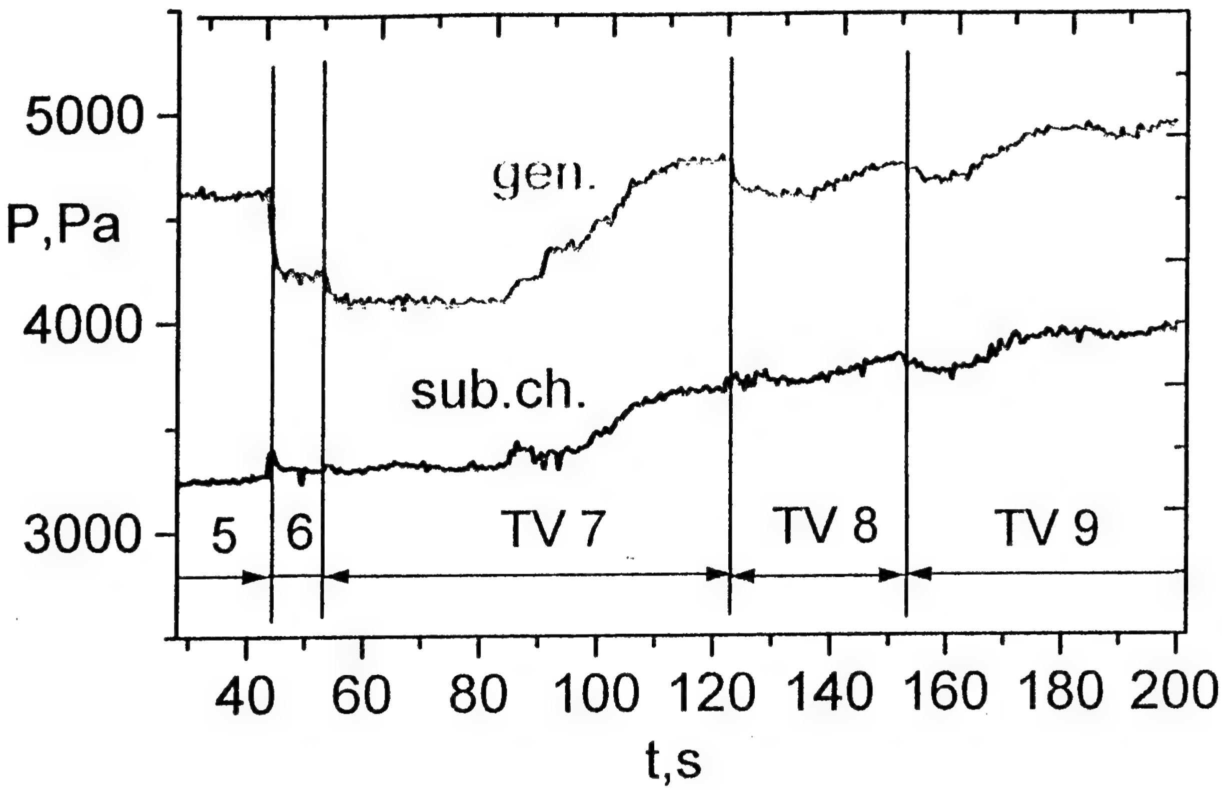

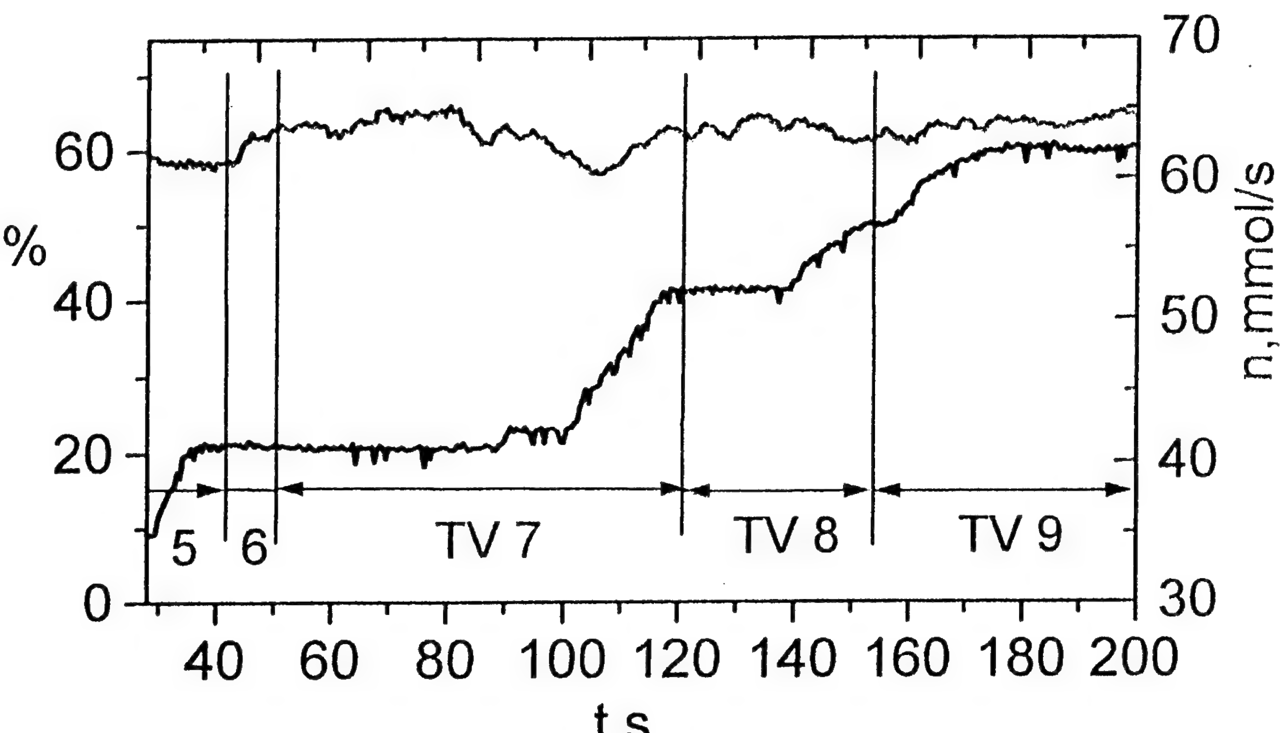

Fig.1a,b : Generator and subsonic pressure, $O_2(^1\Delta)$ yield and chlorine flowrate on time

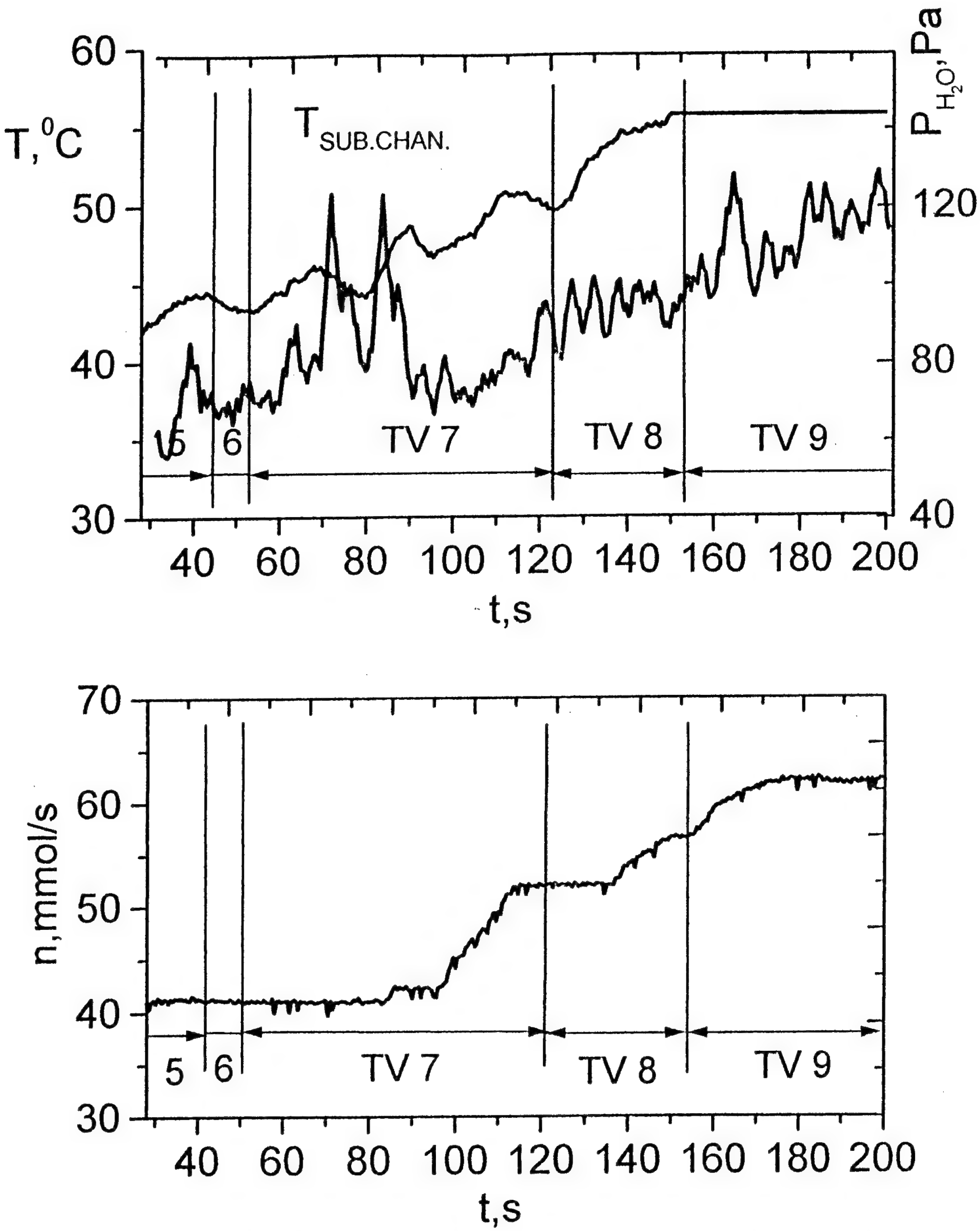

Fig.1c,d : Subsonic channel temperature,water vapor pressure and chlorine flowrate on time

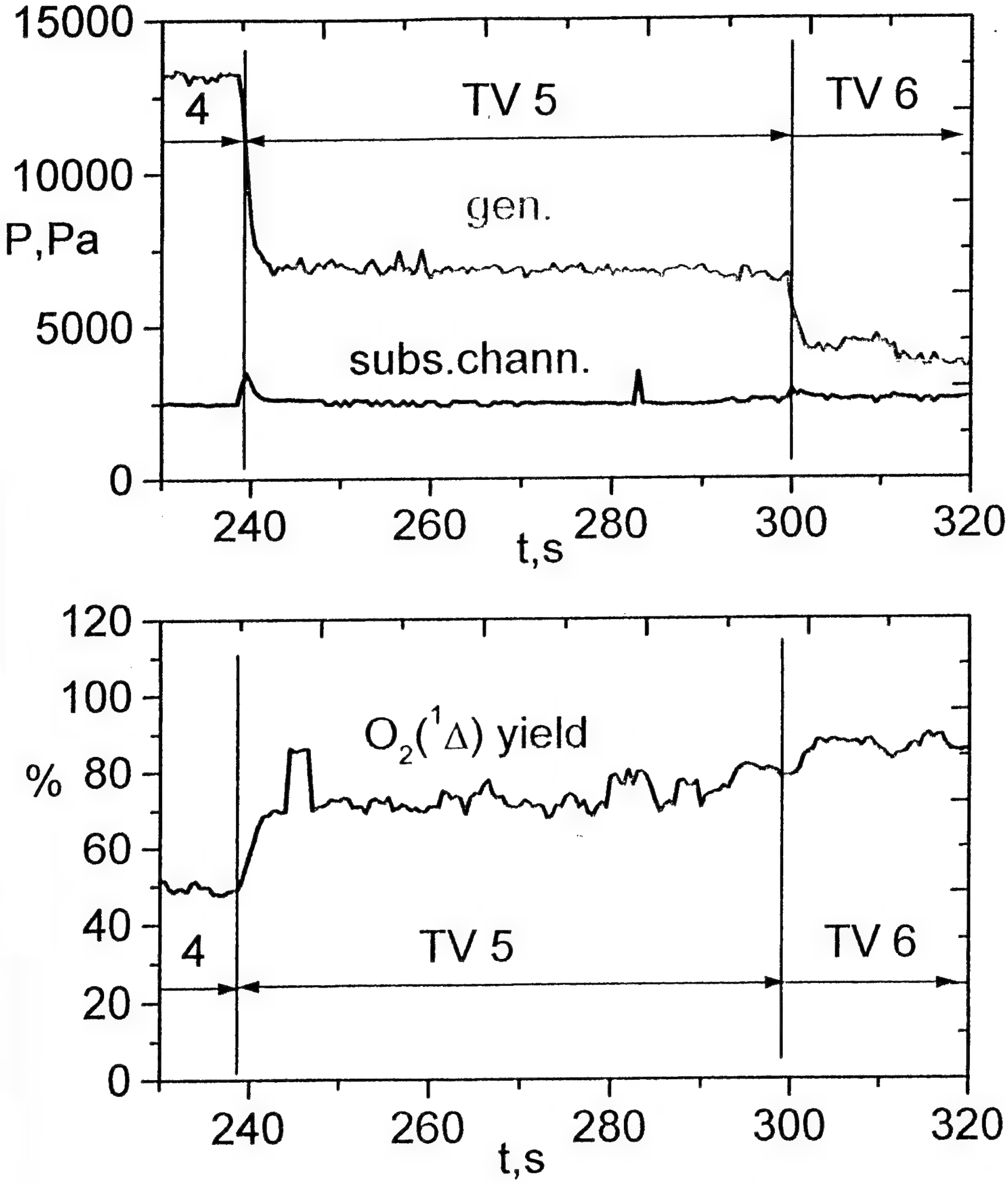

Fig.2a,b : Generator and subsonic channel pressure and $O_2(^1\Delta)$ yield on time (prim.He into chlorine)

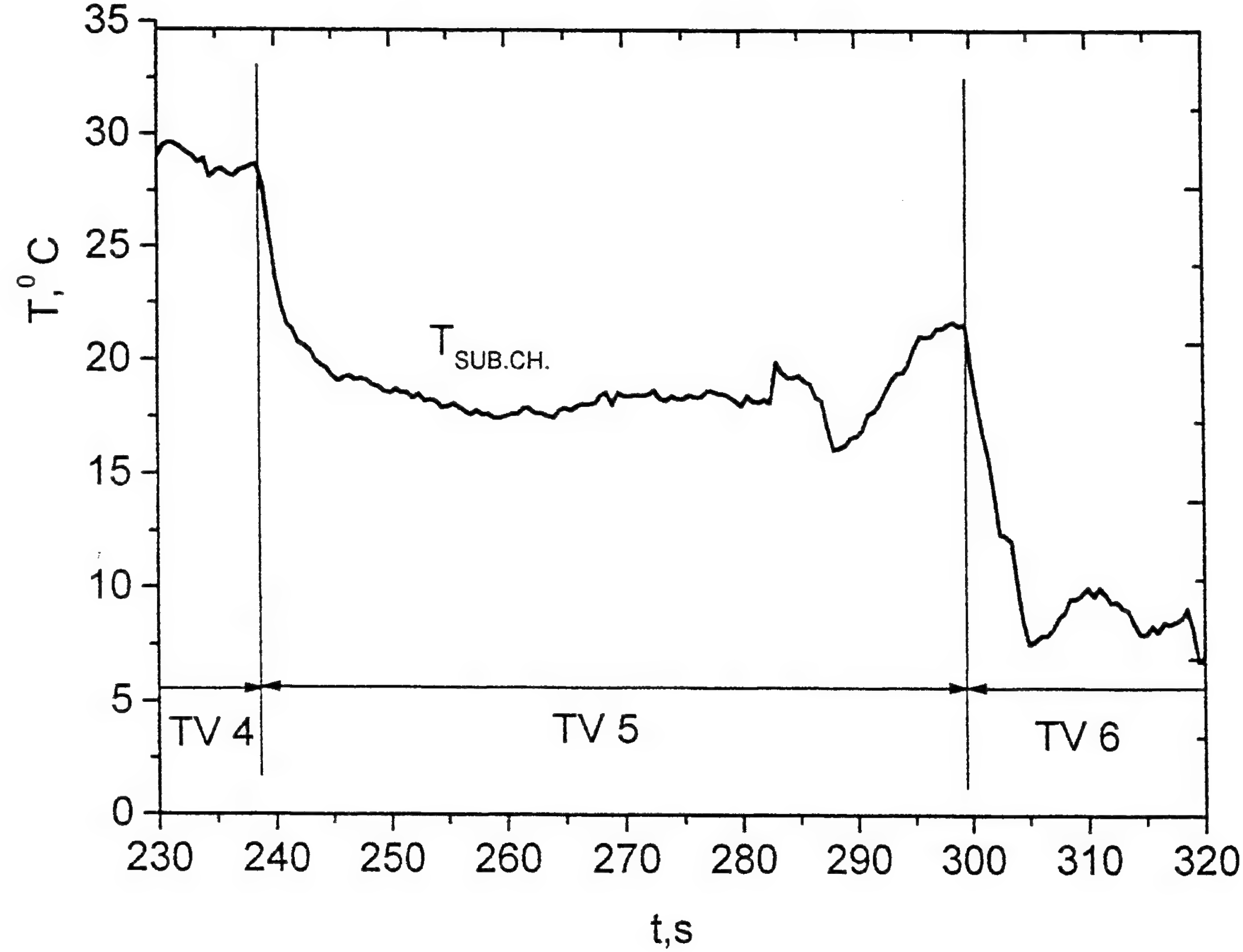

Fig.2c: Subsonic channel temperature on time
(40 mmol/s Cl_2, prim.He into chlorine)

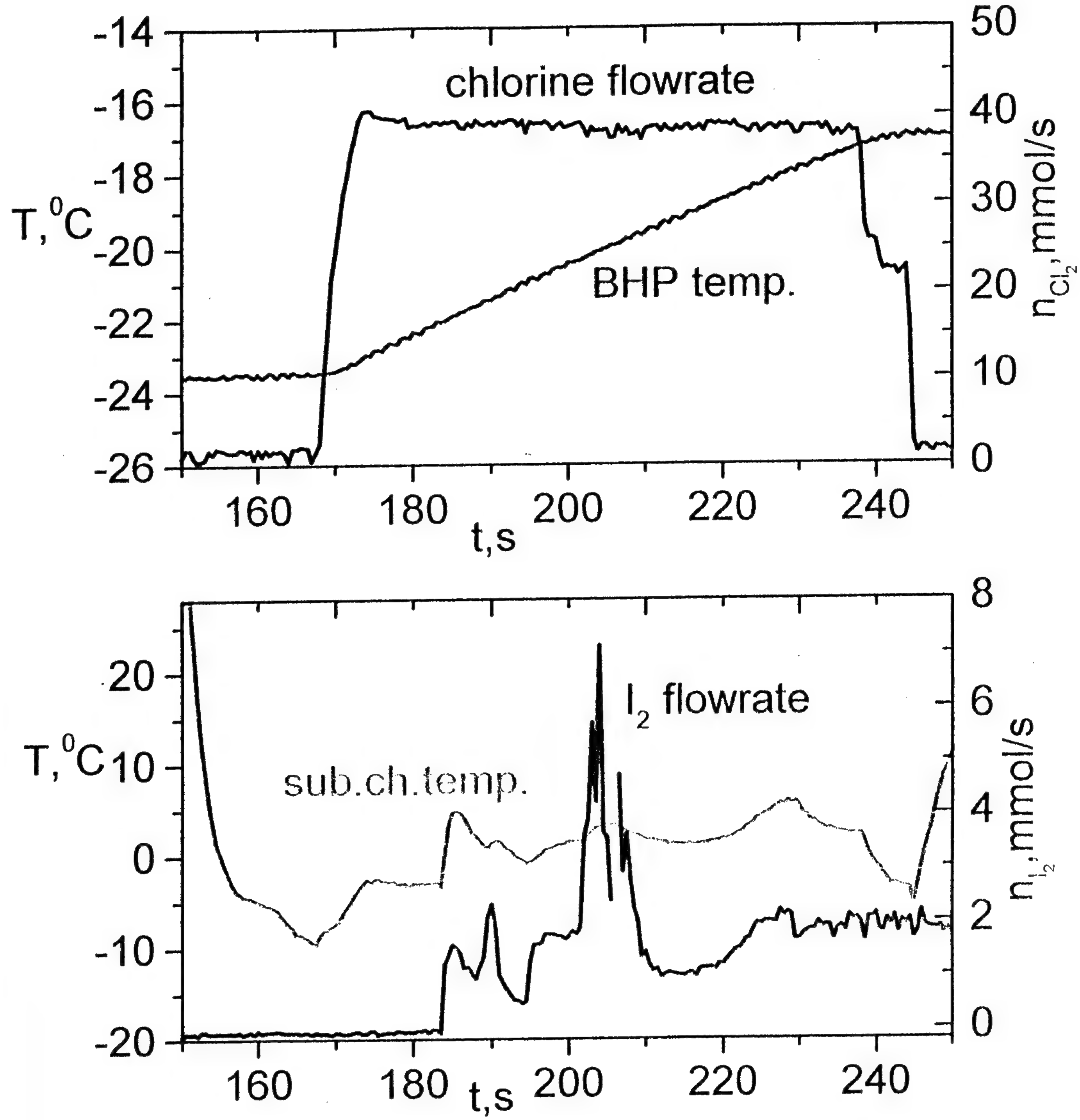

Fig.3. Time dependence of BHP and subsonic channel temperature

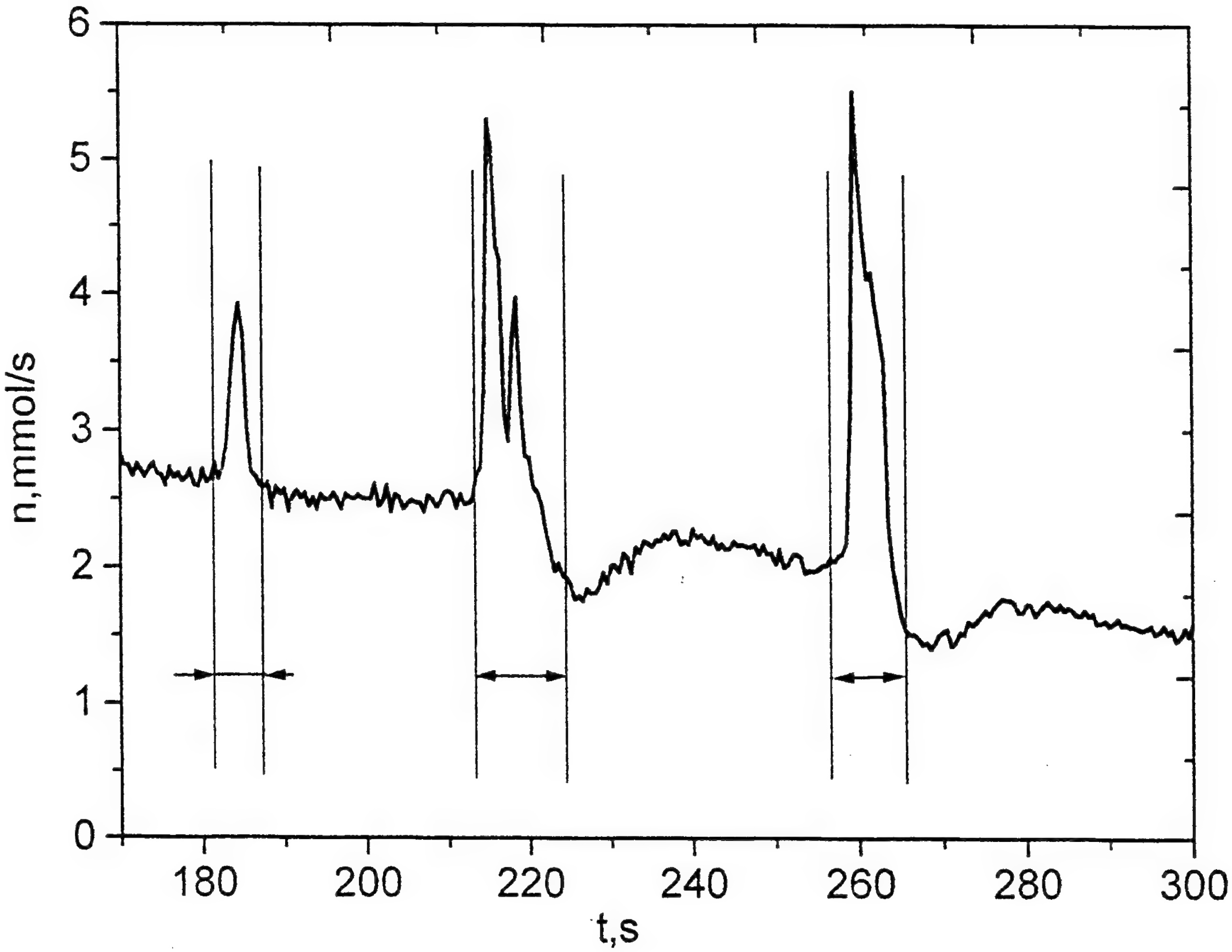

Fig.4: Plot of I_2 flowrate on time
(in regions between arrows higher flowrates tested)

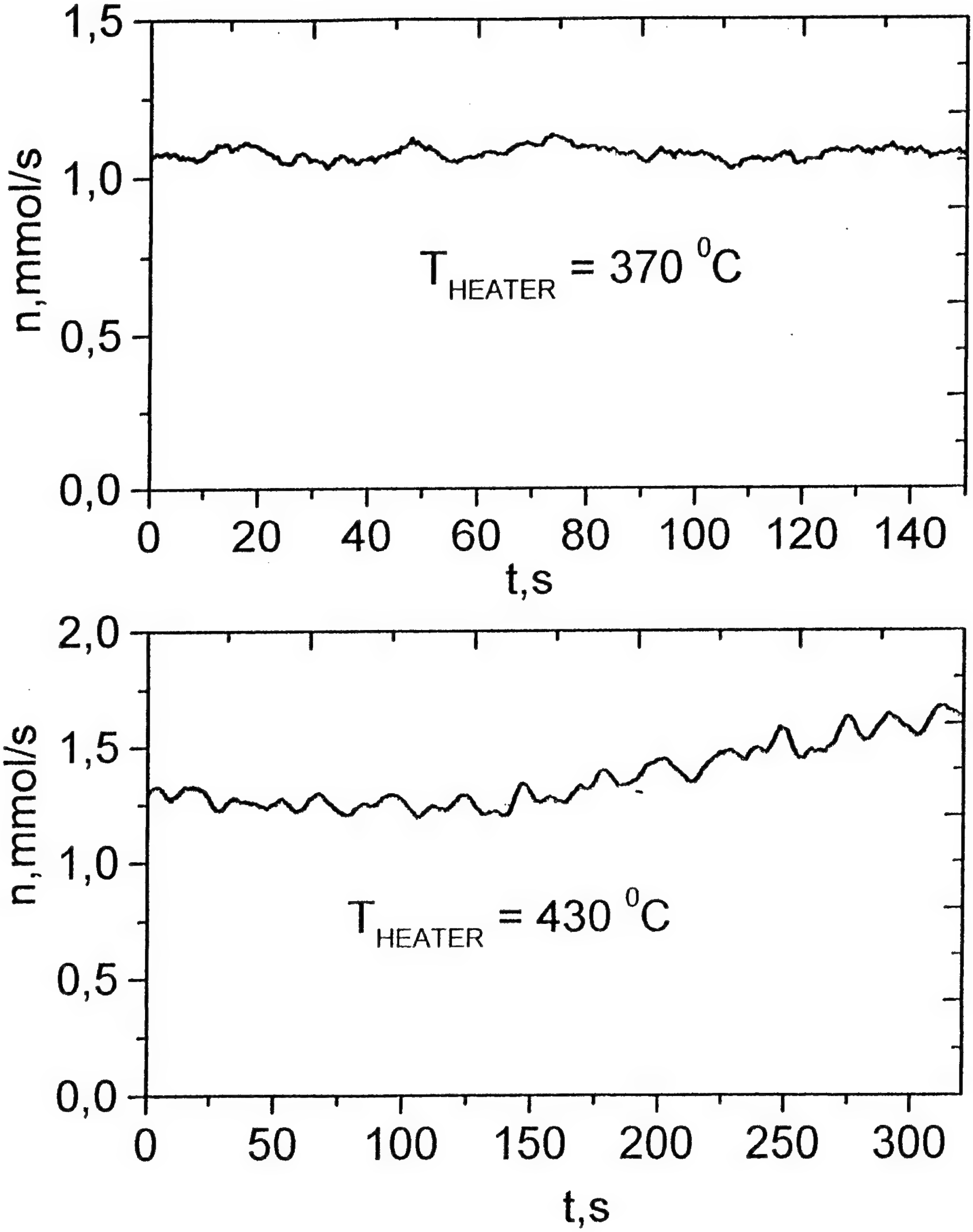

Fig.5 : Plot of I_2 flowrate on time

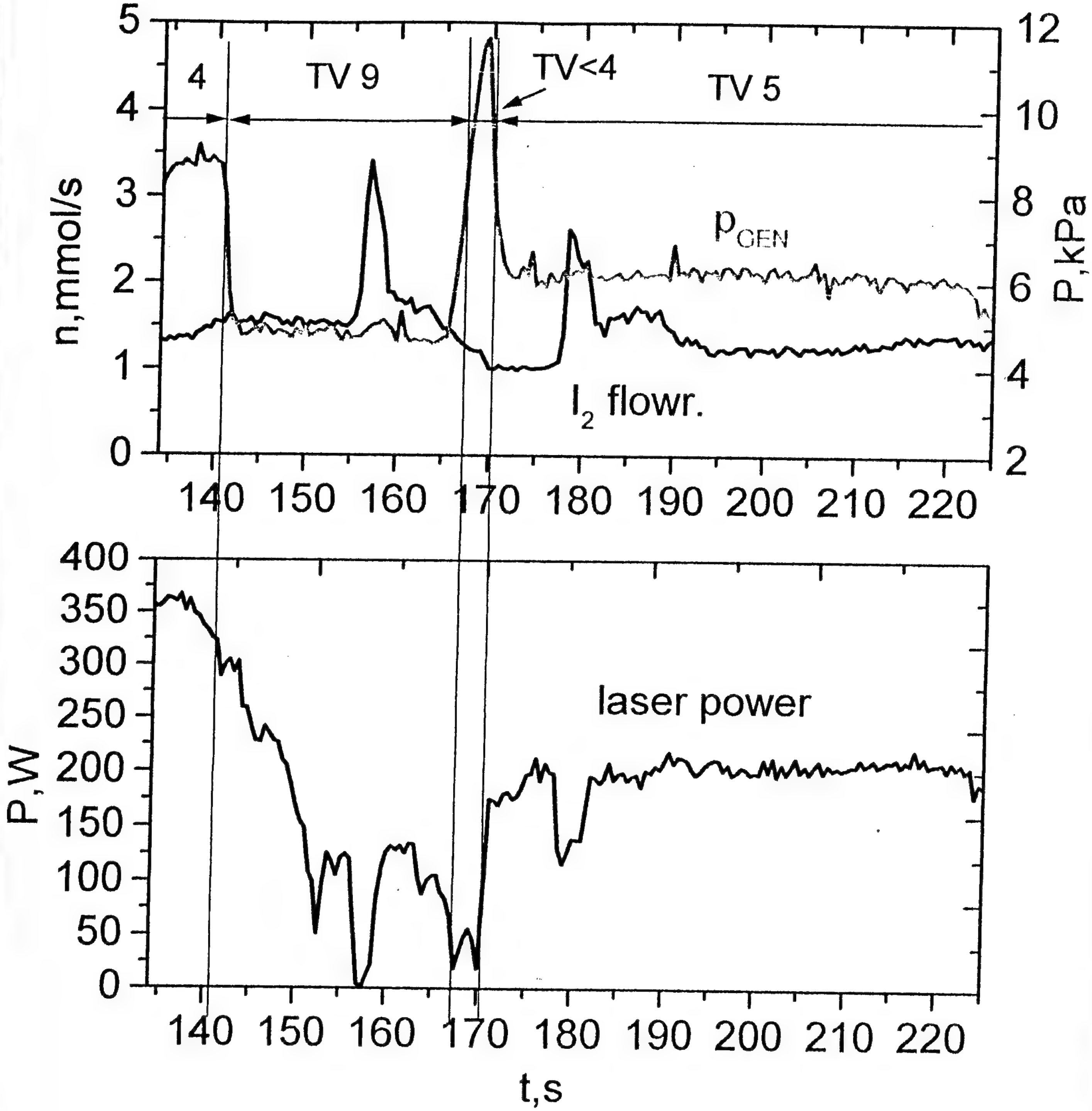

Fig.6.: Generator pressure, I_2 flowrate and laser power on time

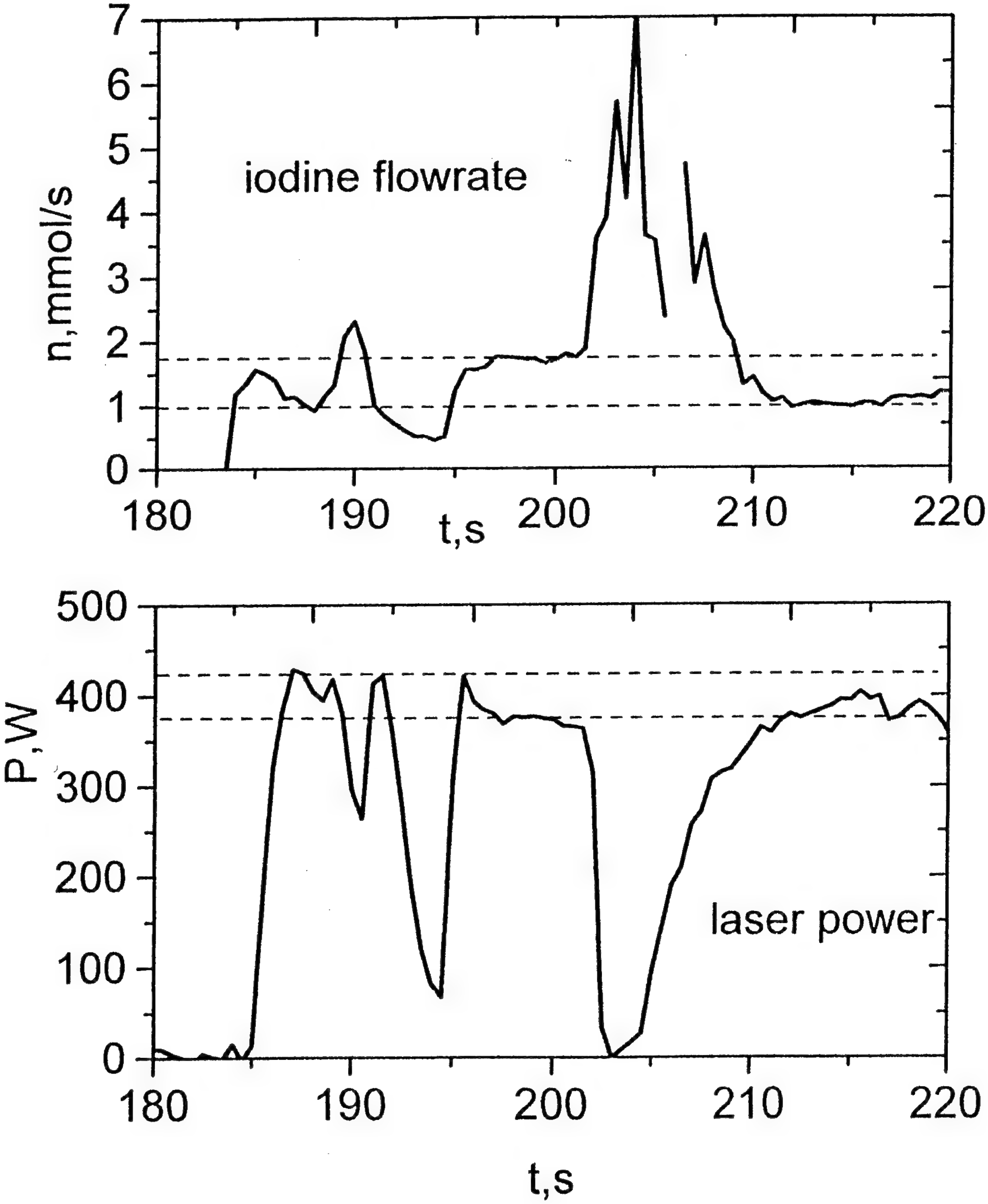

Fig.7: Iodine flowrate and laser power on time

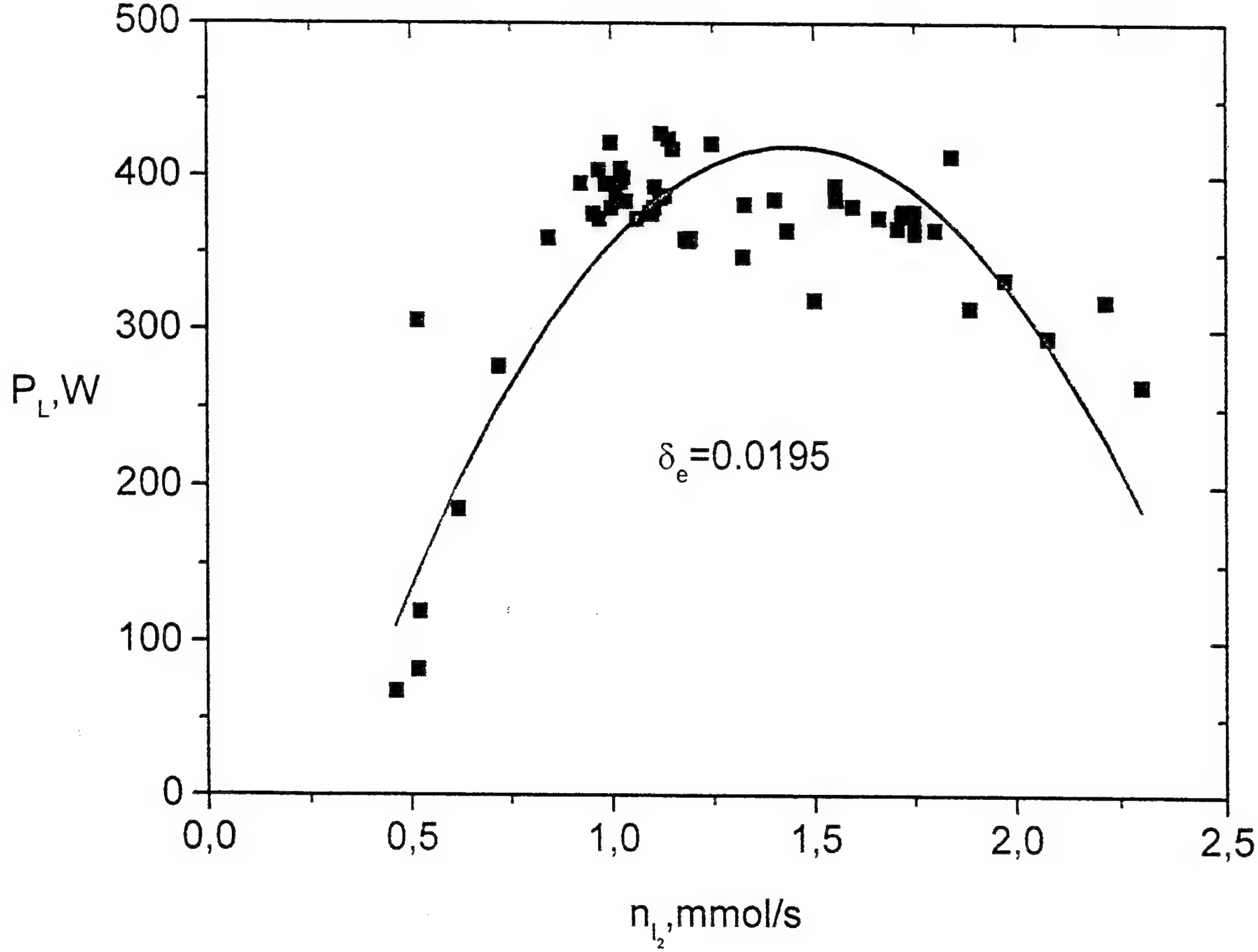

Fig.8 Laser power on iodine flowrate

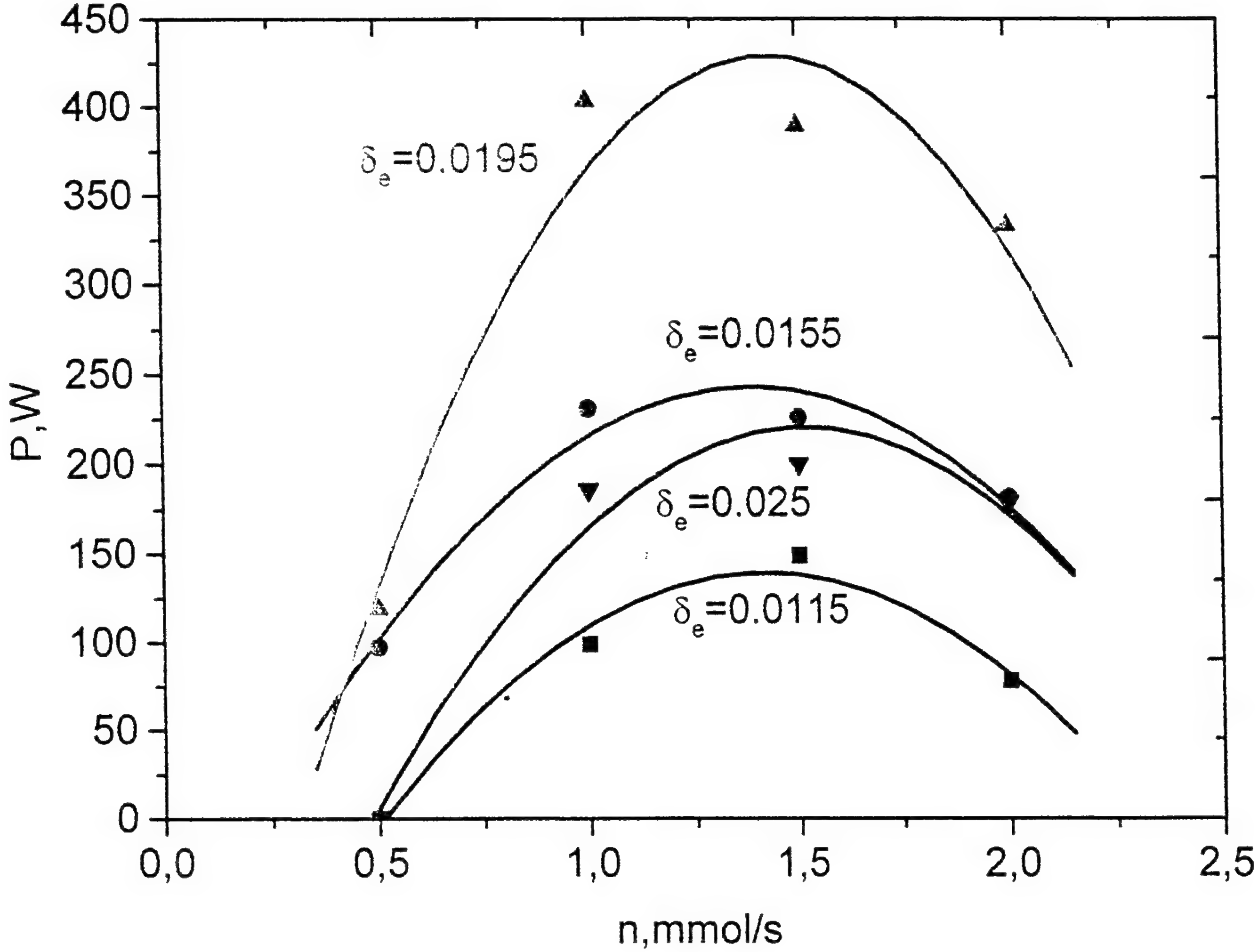

Fig.9 : Laser power on iodine flowrate for different outcoupling

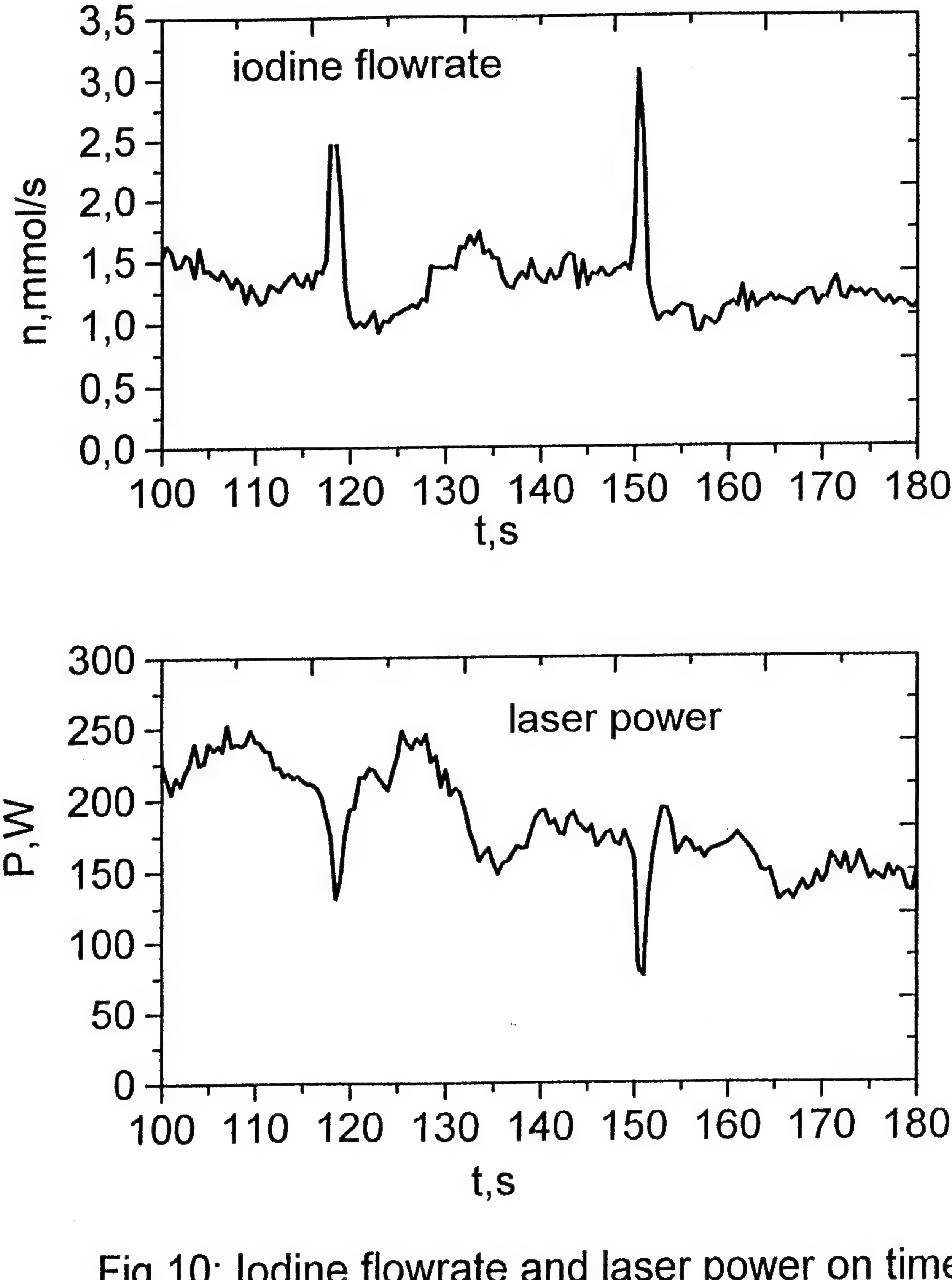

Fig.10: Iodine flowrate and laser power on time

Results of Water Measurements at the DLR COIL

Frank Duschek, Jürgen Handke, and Karin Grünewald

DLR Lampoldshausen

Outline

- Experimental setup
  - Built-in filter system
  - Reproducibility
- Measurements in the duct
- Measurements in the cavity
  - Condensation of water
- Substitution of optical diagnostics by a temperature dependent water vapor model

Deutsches Zentrum für Luft- und Raumfahrt e.V.

Optical Diagnostics in the COIL

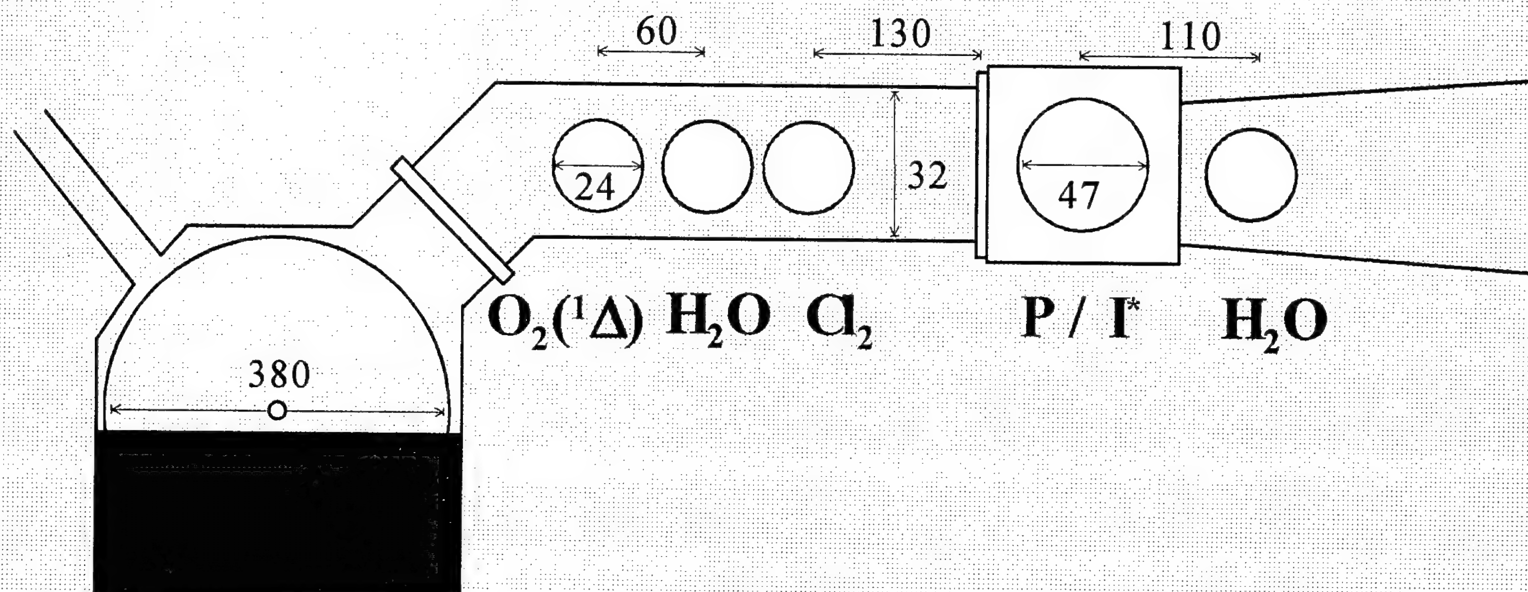

DLR

Deutsches Zentrum für Luft- und Raumfahrt e.V.

COIL System Emission Lines near 1.3

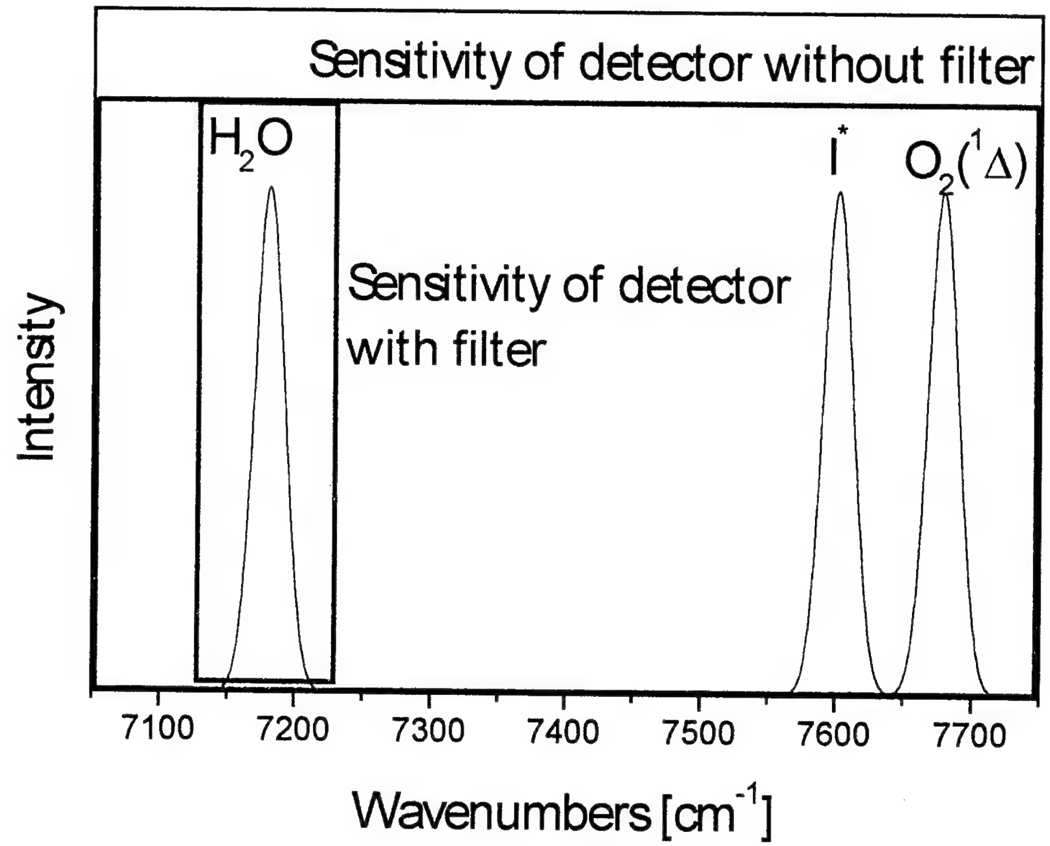

DLR

Deutsches Zentrum für Luft- und Raumfahrt e.V.

Measurement without Bandpass Filter

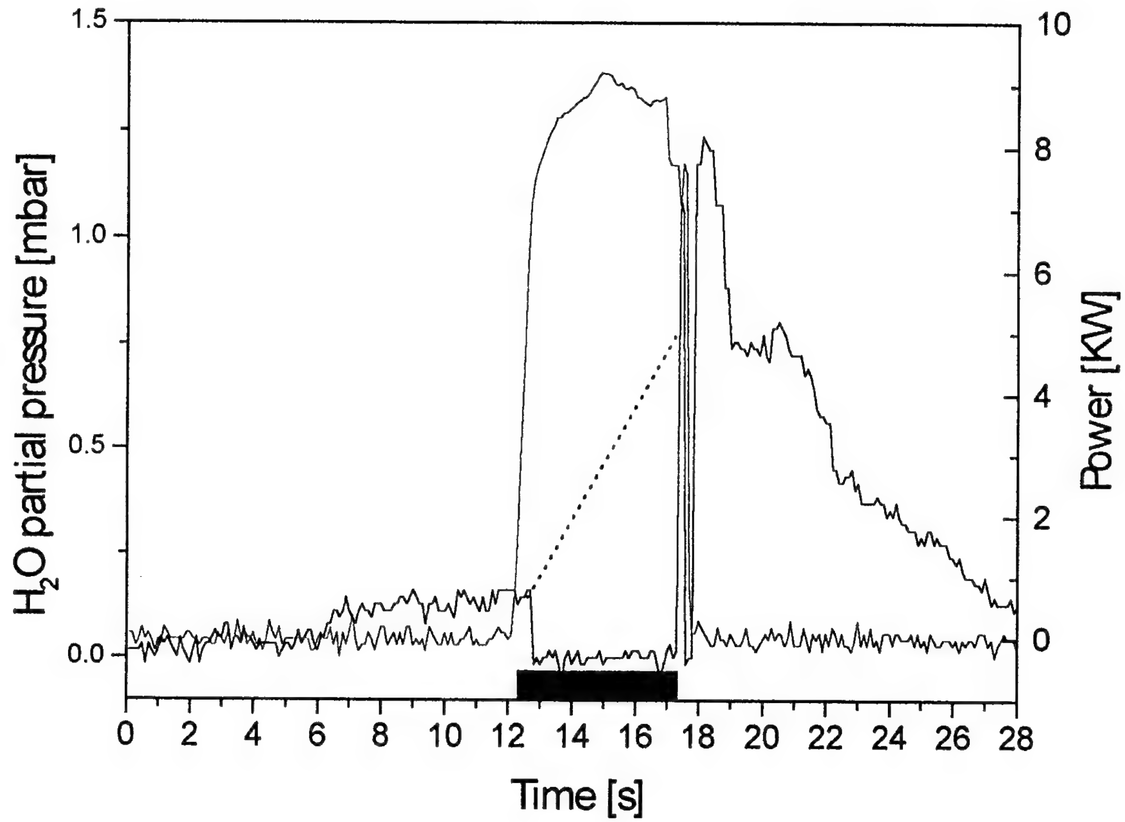

DLR

Deutsches Zentrum für Luft- und Raumfahrt e.V.

Measurement without Bandpass Filter

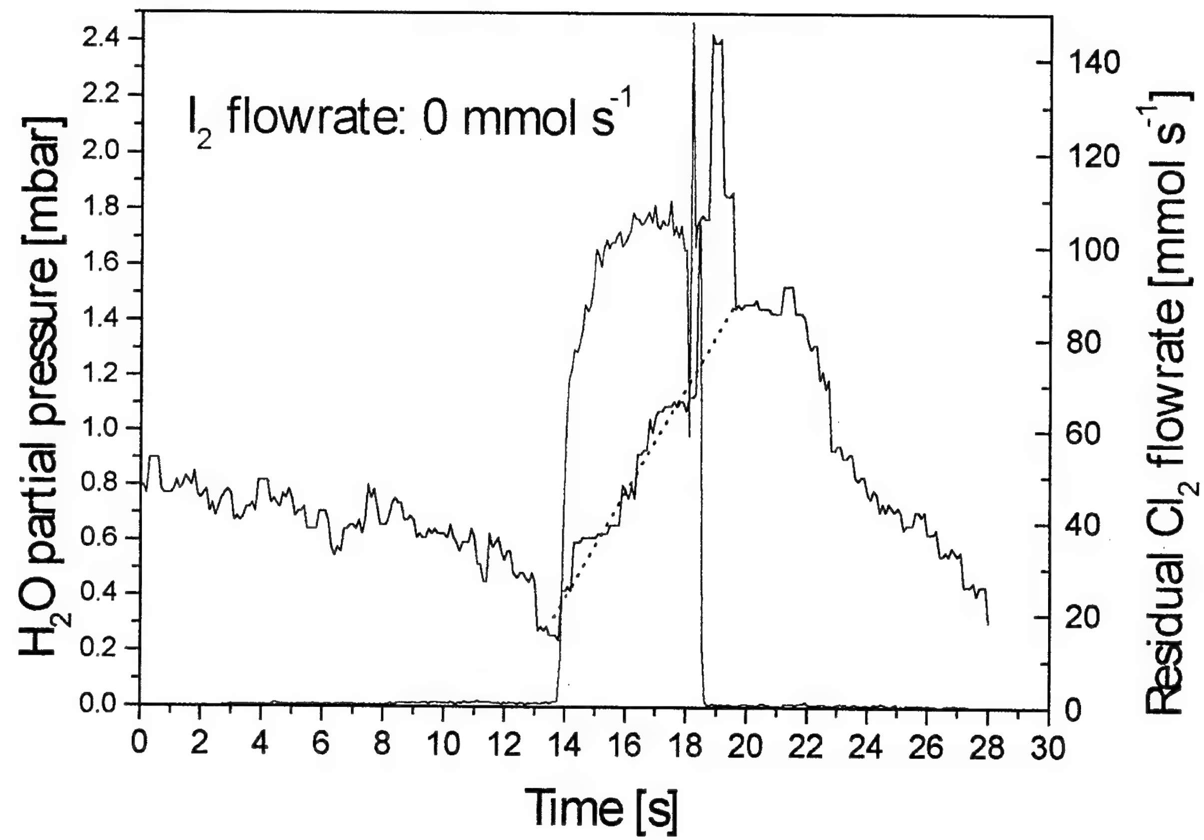

DLR

Measurement without Bandpass Filter

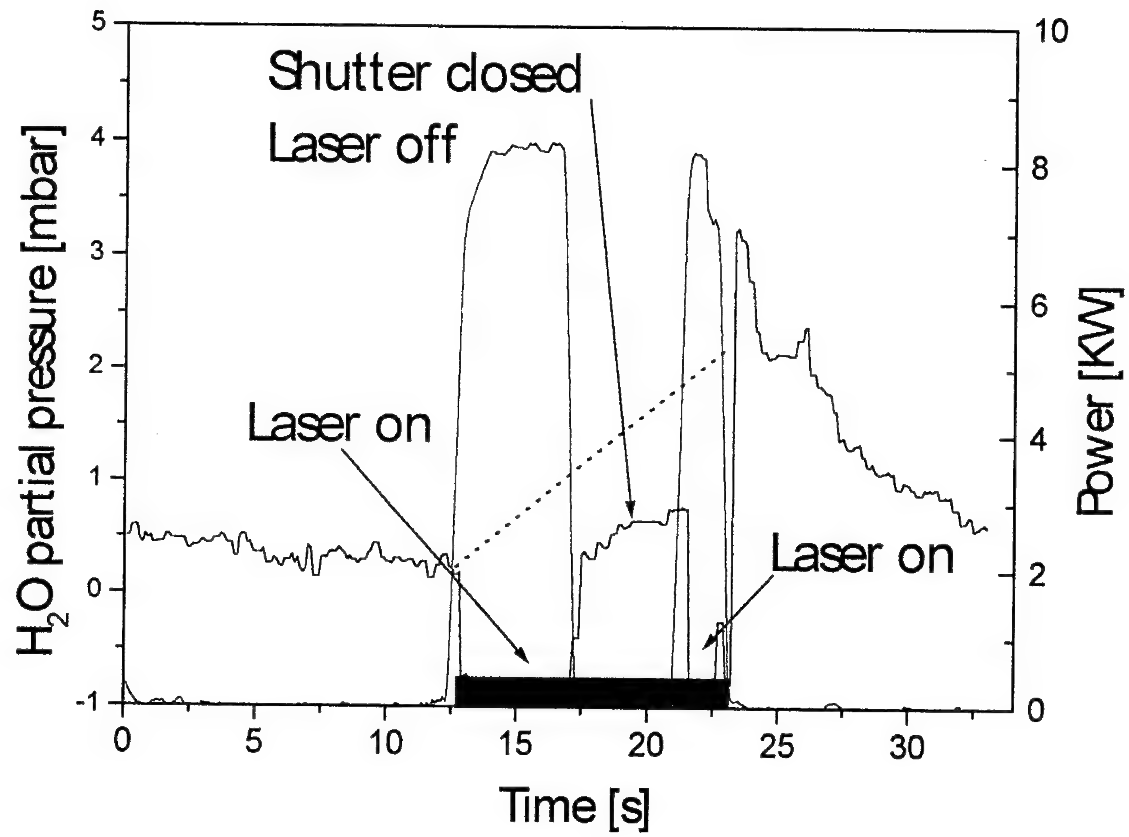

DLR

Measurement with Bandpass Filter

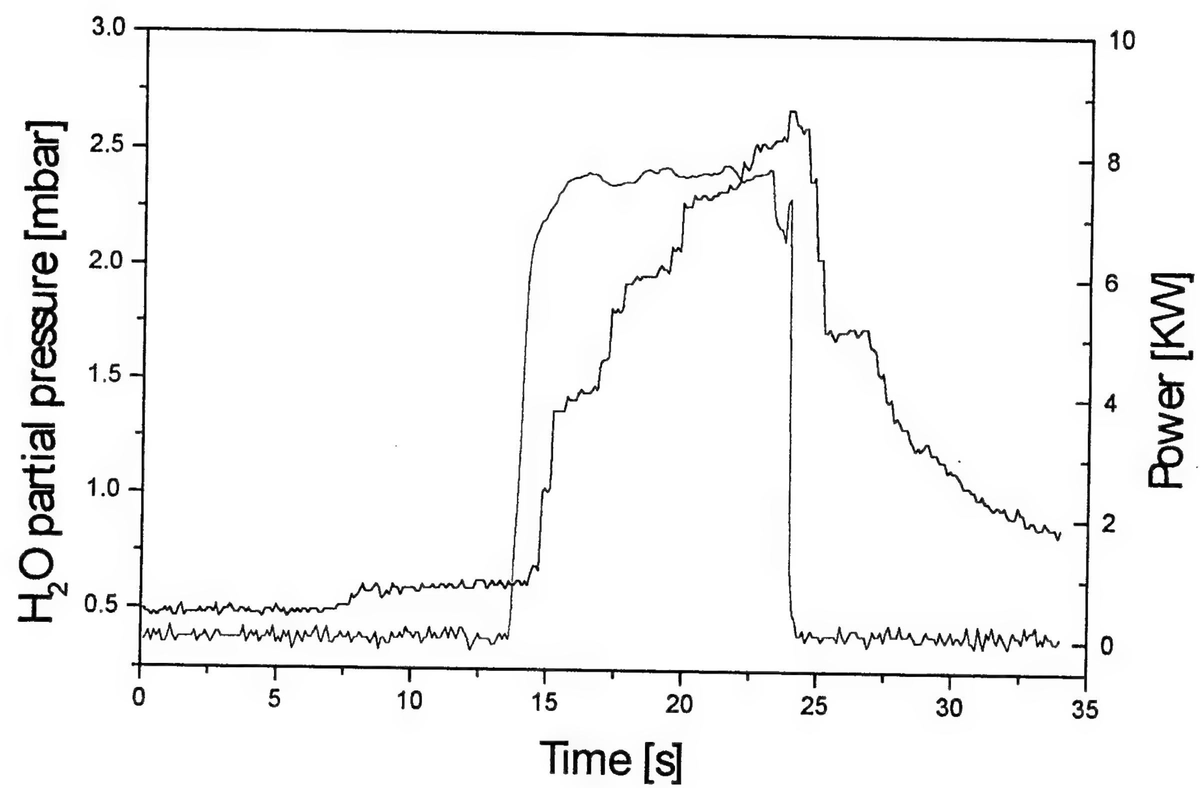

DLR

Deutsches Zentrum für Luft- und Raumfahrt e.V.

Reproducibility

H_2O molar flowrate in the duct

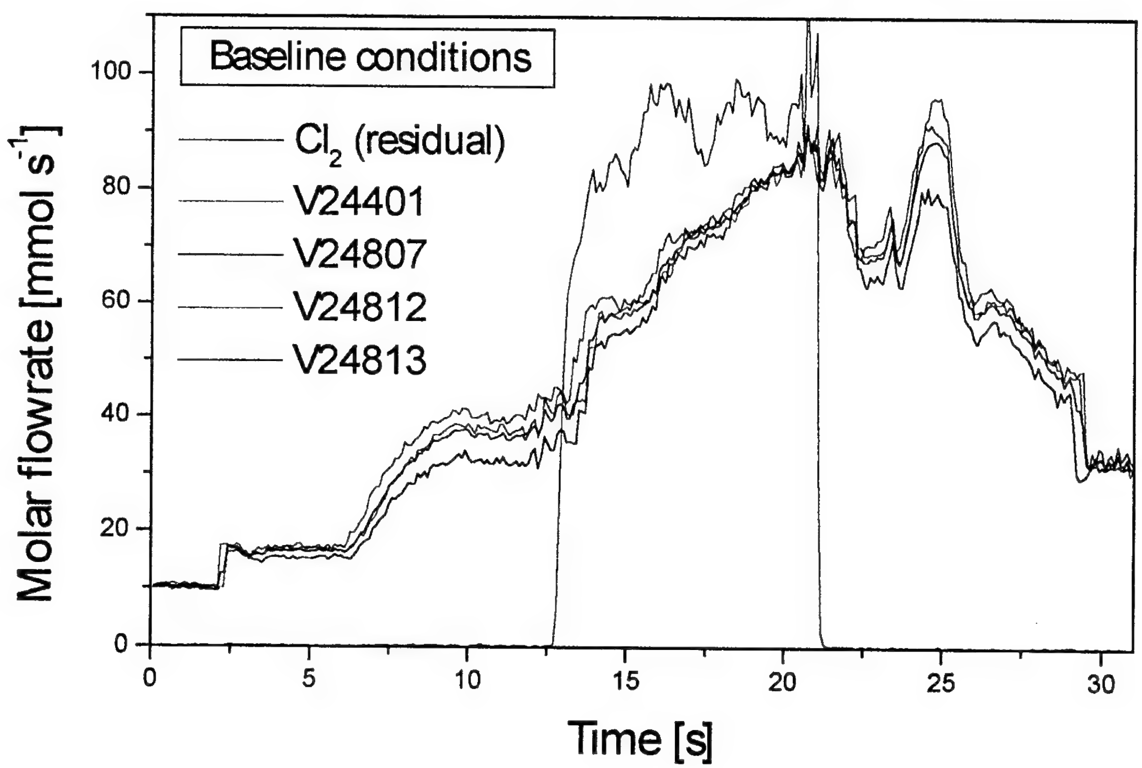

DLR

Simultaneous Measurement of H_2O in Duct and Cavity

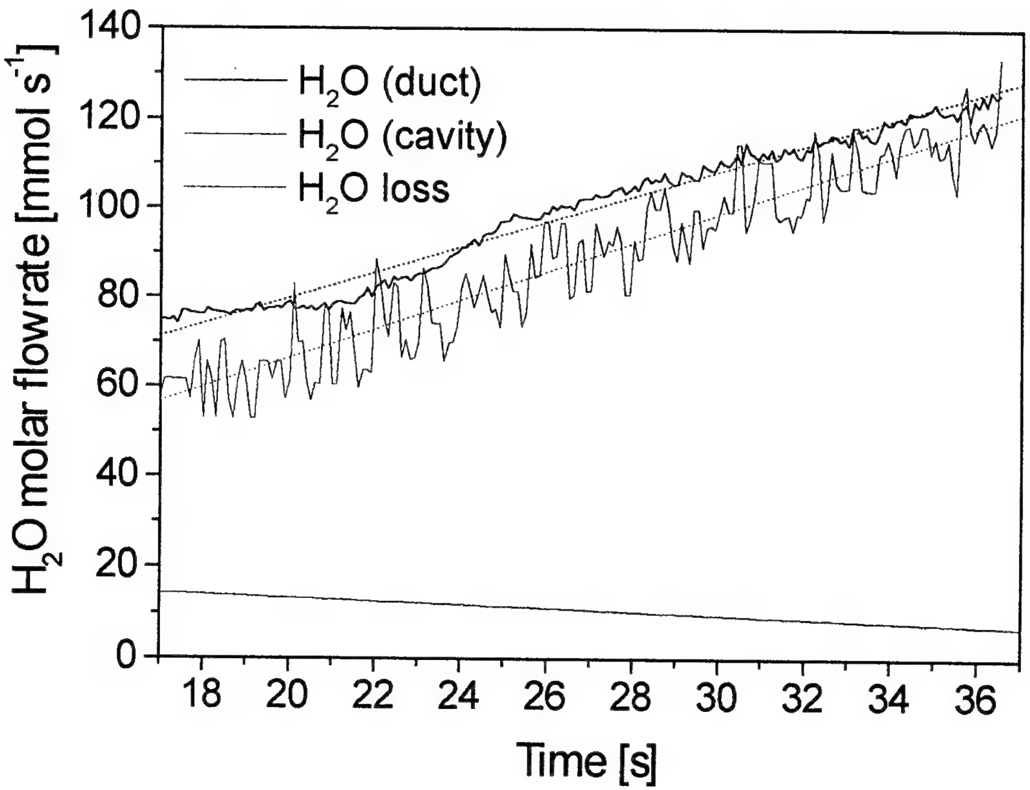

Correlation between H_2O in Duct and Cavity including different Disk Package Rotation Rates

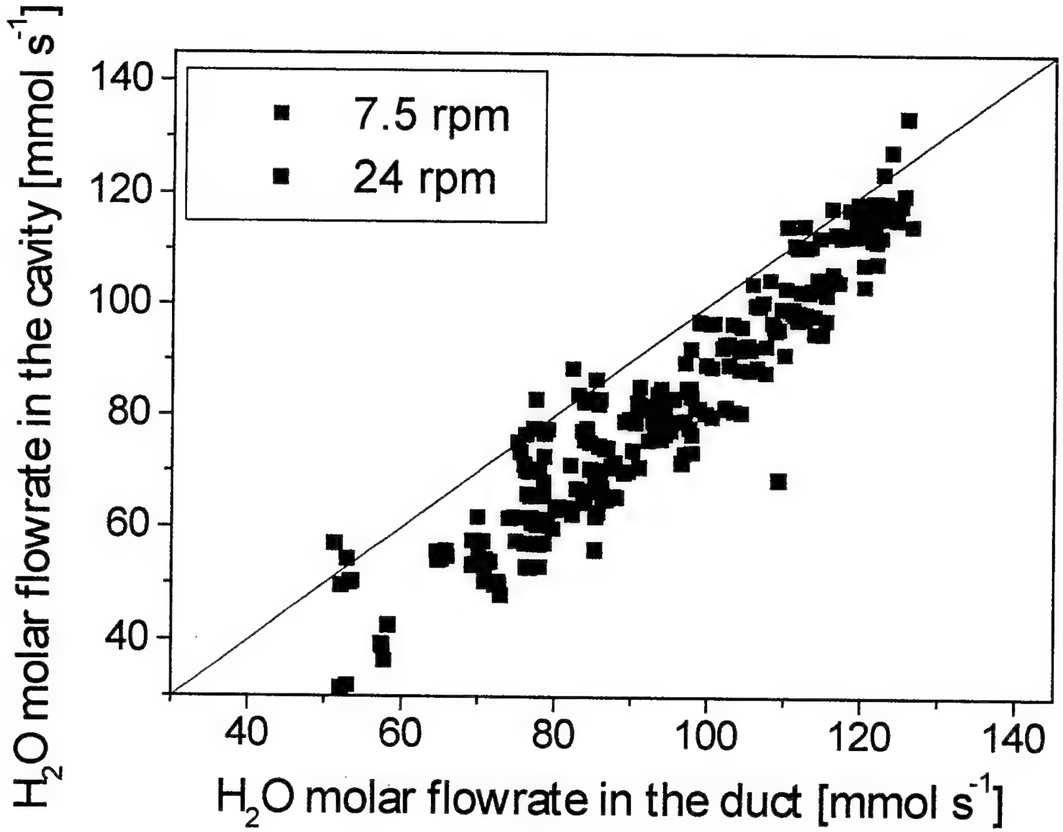

Temperature Change in the Cavity

- Thermodynamical calculation

$$\Delta H_{g\to l} + \Delta H_{l\to s} = C_p \Delta T$$
$$= \sum_i n_i c_{p,i} \Delta T$$

- i=He, O_2, Cl_2, I_2, H_2O,...

Deutsches Zentrum für Luft- und Raumfahrt e.V.

Temperature Change in the Cavity

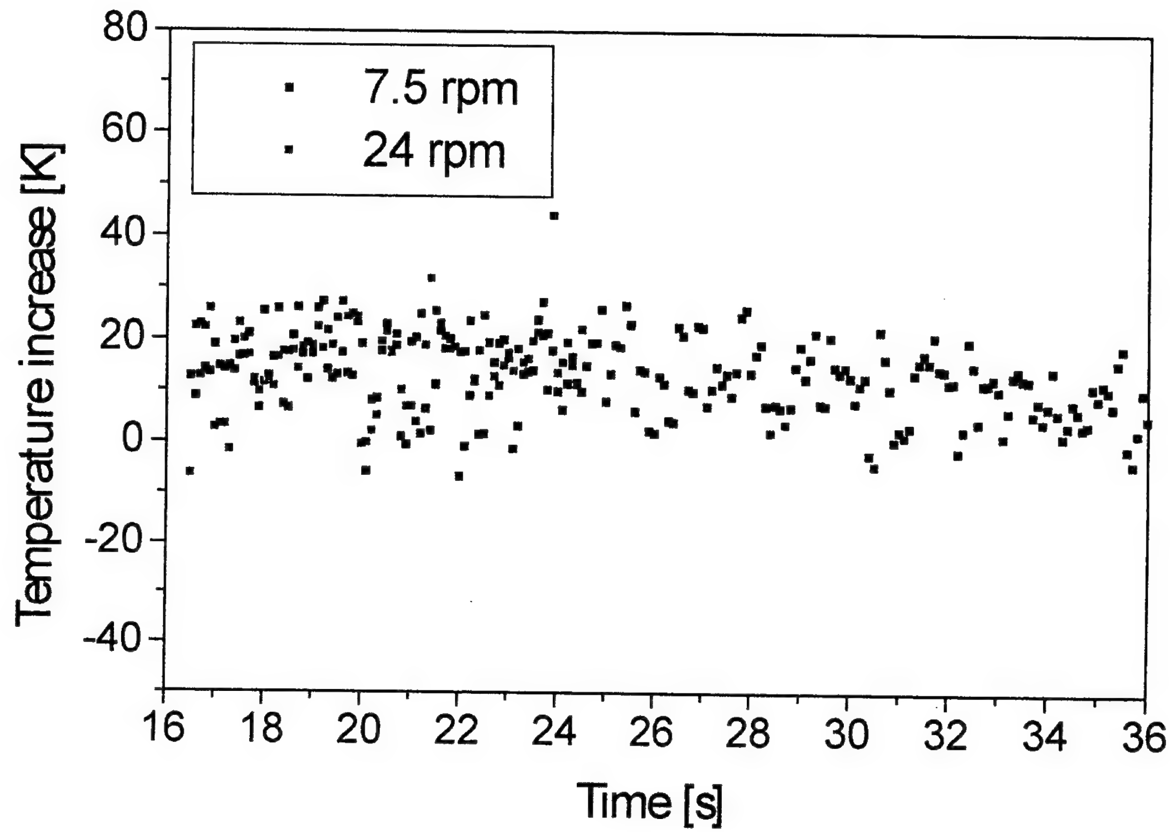

DLR

Influence of Disk Rotation Speed on the Water Content in the Duct

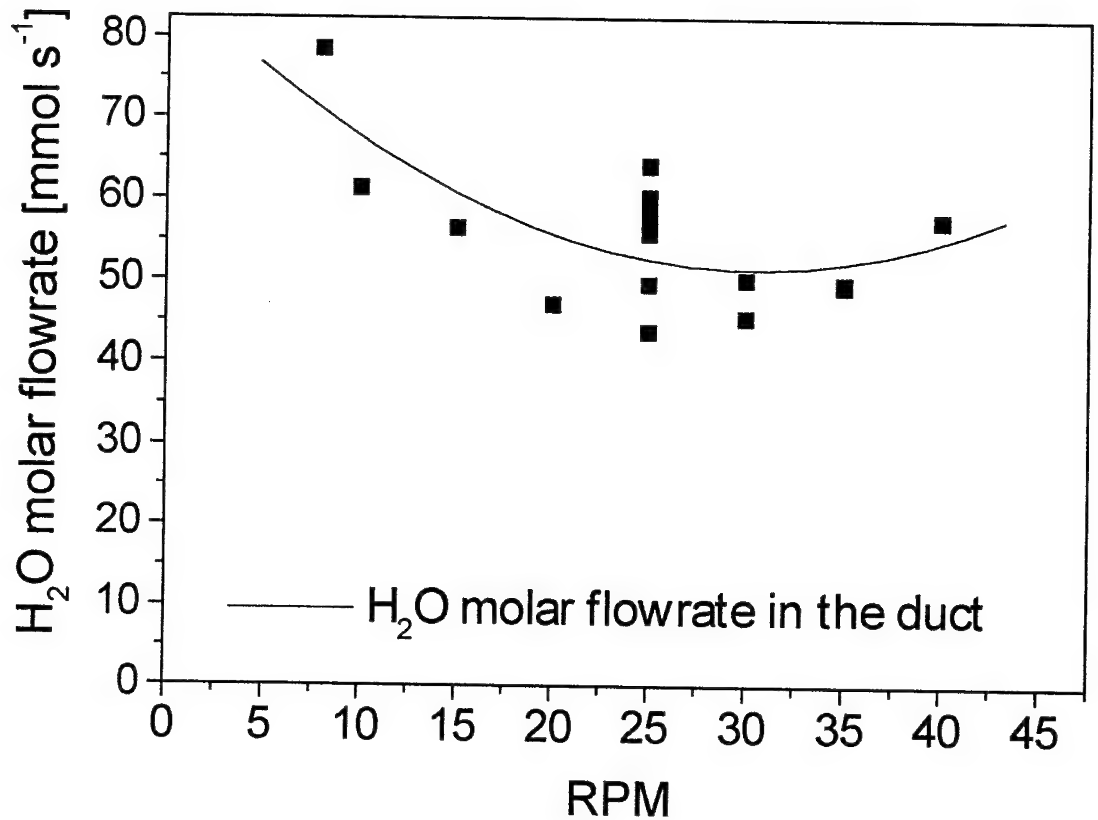

DLR

Deutsches Zentrum für Luft- und Raumfahrt e.V.

Influence of H_2O on the Output Power Short Time Operation

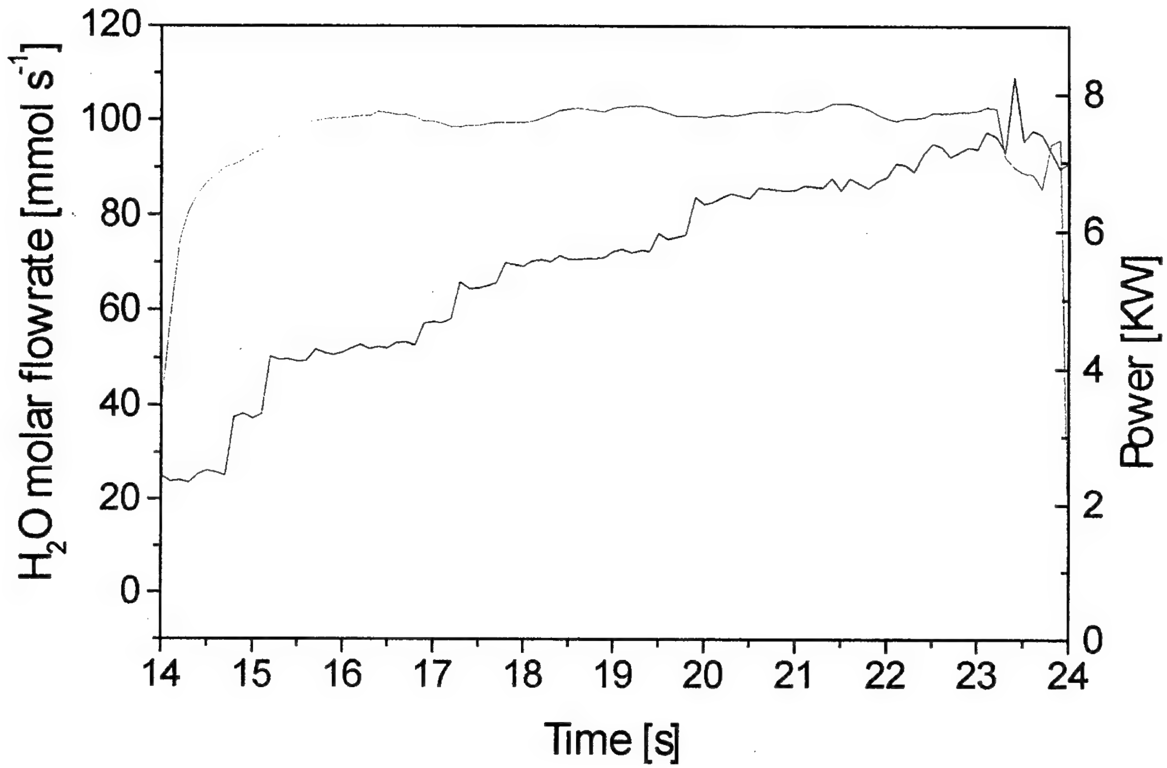

DLR

Empirical Function for Modeling H_2O Vapor Pressure*

$$p_{H_2O} = 10^{aT^{-1}+b+cT+dT^2}$$

$a = 9.758496\,\mathrm{K}$

$b = -2755.526$

$c = -8.410066 \times 10^{-3}\,\mathrm{K}^{-1}$

$d = 5.529658 \times 10^{-6}\,\mathrm{K}^{-2}$

* Ref.: Gase Handbuch, Messer-Griesheim GmbH, Frankfurt, 1989

Modeling H_2O Pressure

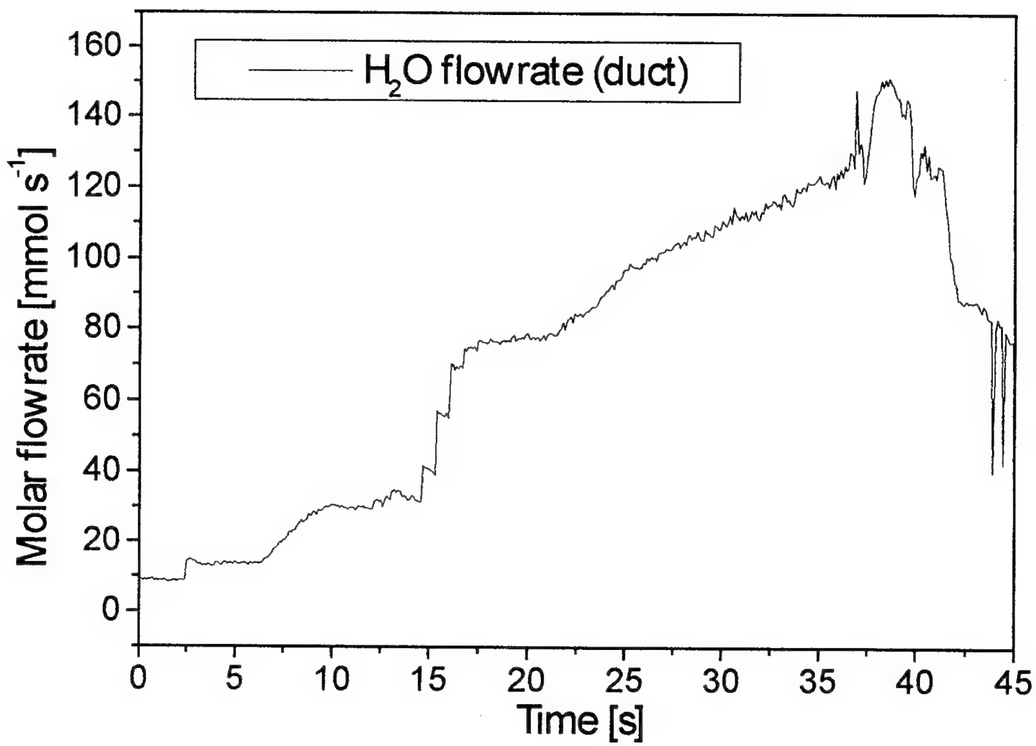

Deutsches Zentrum für Luft- und Raumfahrt e.V.

Temperatures for Modeling H_2O Pressure

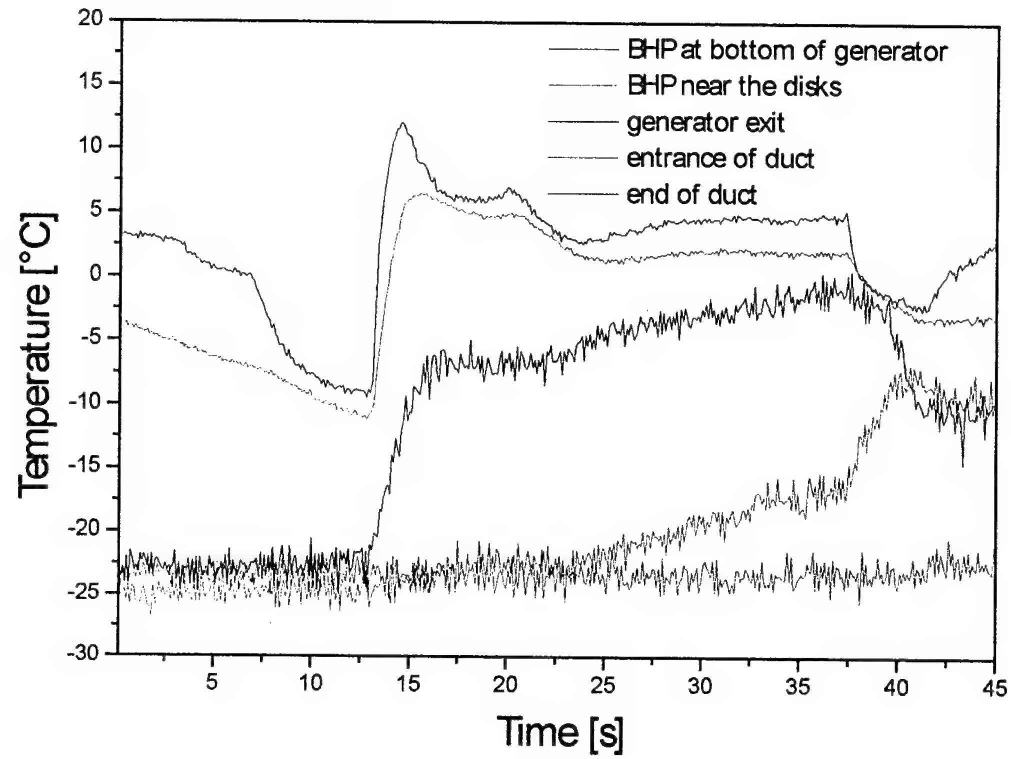

DLR

Modeling H_2O Pressure from Measured Temperatures

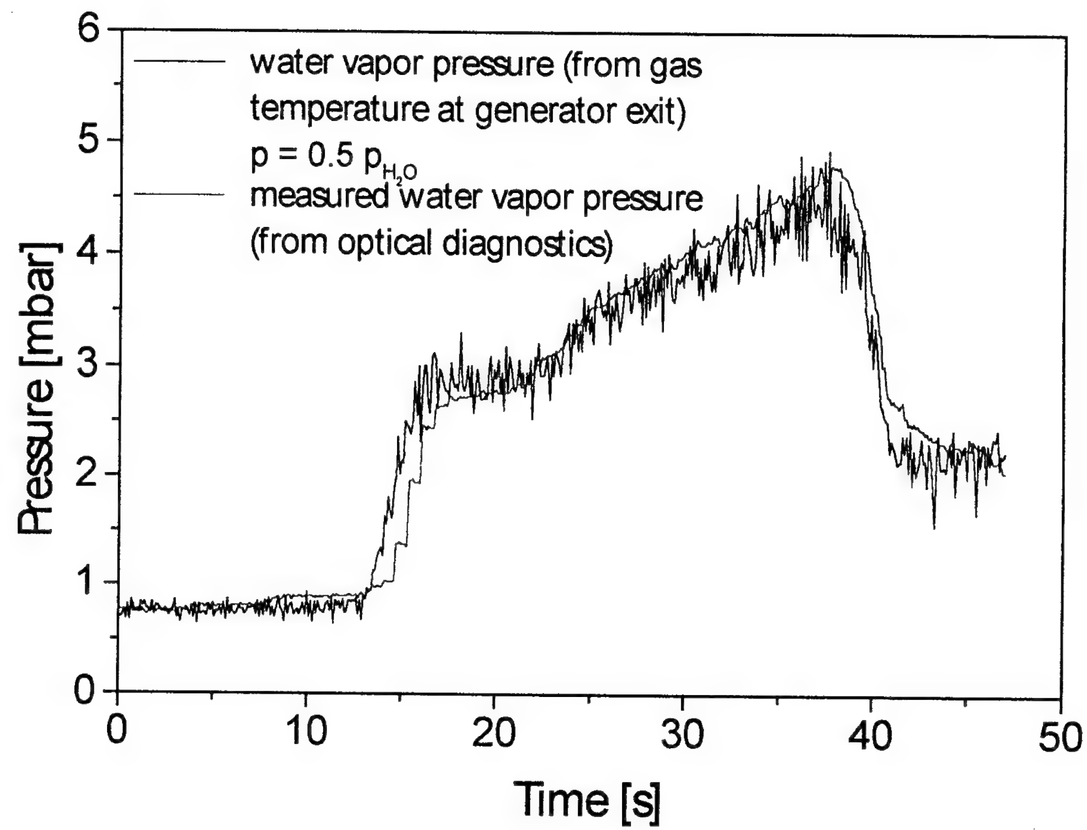

DLR

Modeling H_2O Pressure from Measured Temperatures

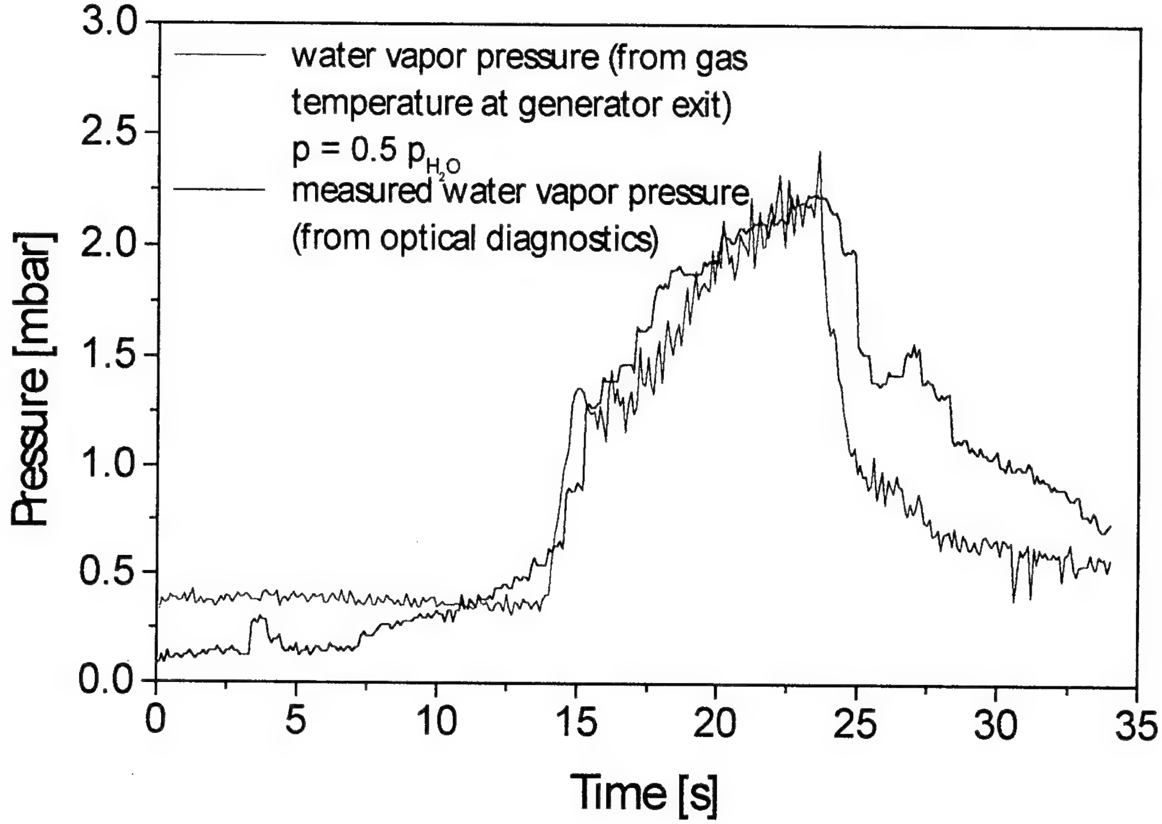

DLR

Results

- H_2O measurement without a filter system may lead to wrong water vapor pressures. This can be avoided with optical filter systems.
- Maximum 10-20 % of water condenses in the cavity.
- Increasing He and Cl_2 flow leads to higher water content.
- Disk rotation speed has minimum water in the laser gas at 24-30 rpm.
- Gas temperature at generator exit can be used to describe the water pressure.

DLR

GAIN DIAGNOSTIC IN A SUPERSONIC COIL WITH TRANSONIC INJECTION OF IODINE

D. Furman, E. Bruins, B. D. Barmashenko and S. Rosenwaks

Department of Physics,
Ben-Gurion University of the Negev,
Beer-Sheva, Israel

A 5-cm gain length supersonic COIL with maximum chlorine flow rat of 20 mmole/s.

Energized by a jet type singlet oxygen generator (JSOG).

Efficiently operates without a buffer gas (using transonic mixing of iodine)

Output power of 210 W with chemical efficiency of 20% was obtainec with chlorine flow rate of 11.8 mmole/s.

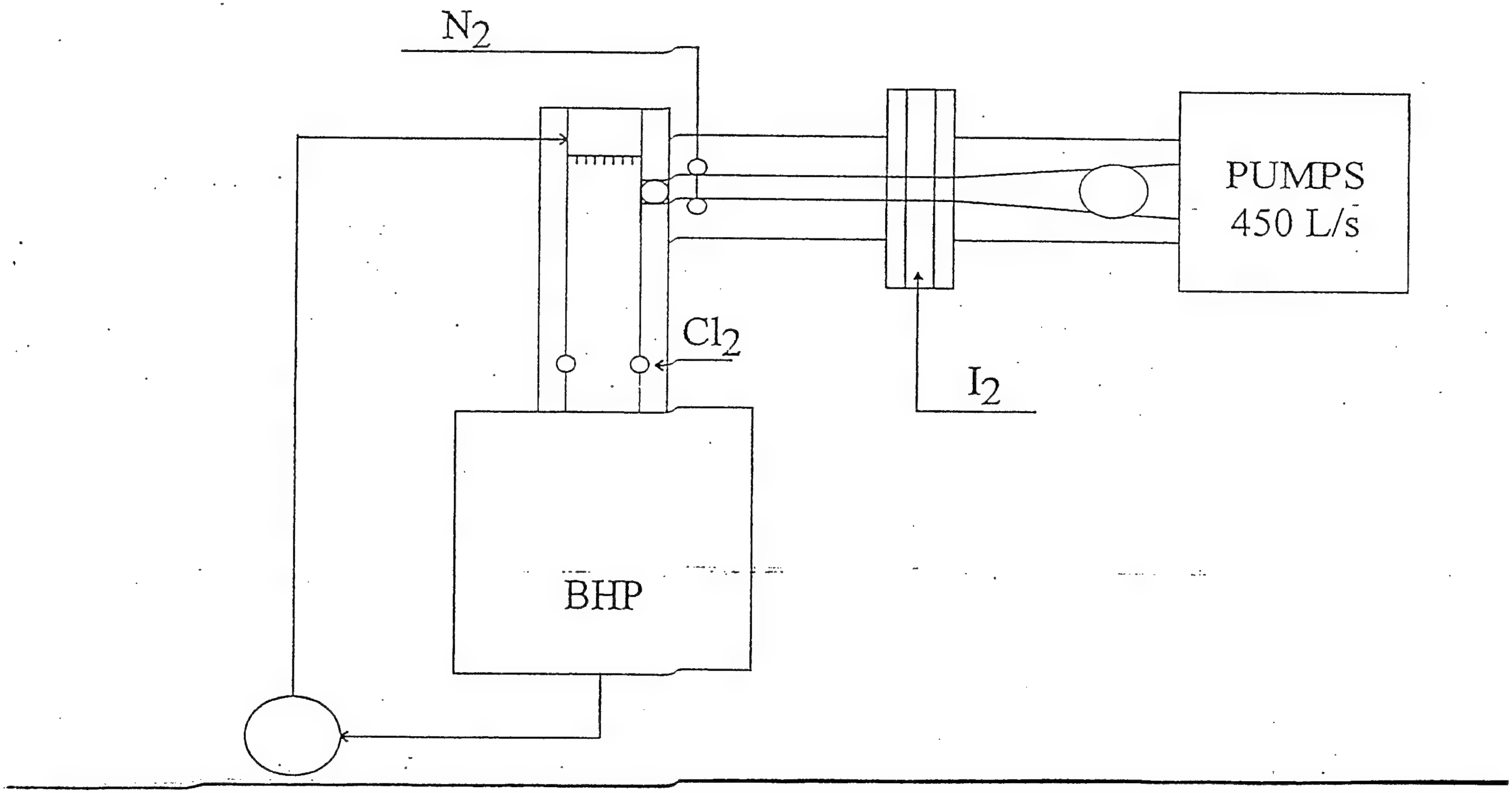

N_2
PUMPS
450 L/s
Cl_2
I_2
BHP

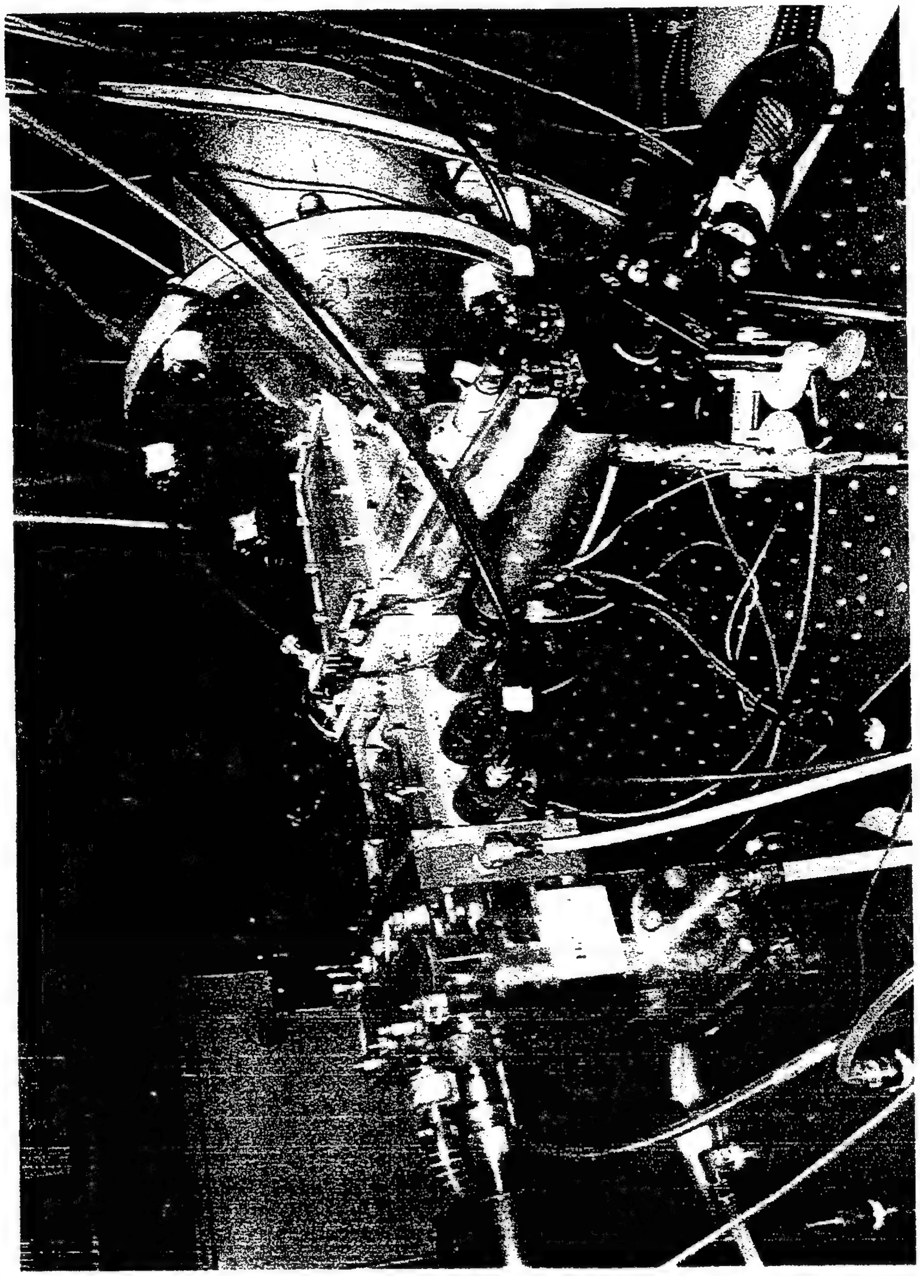

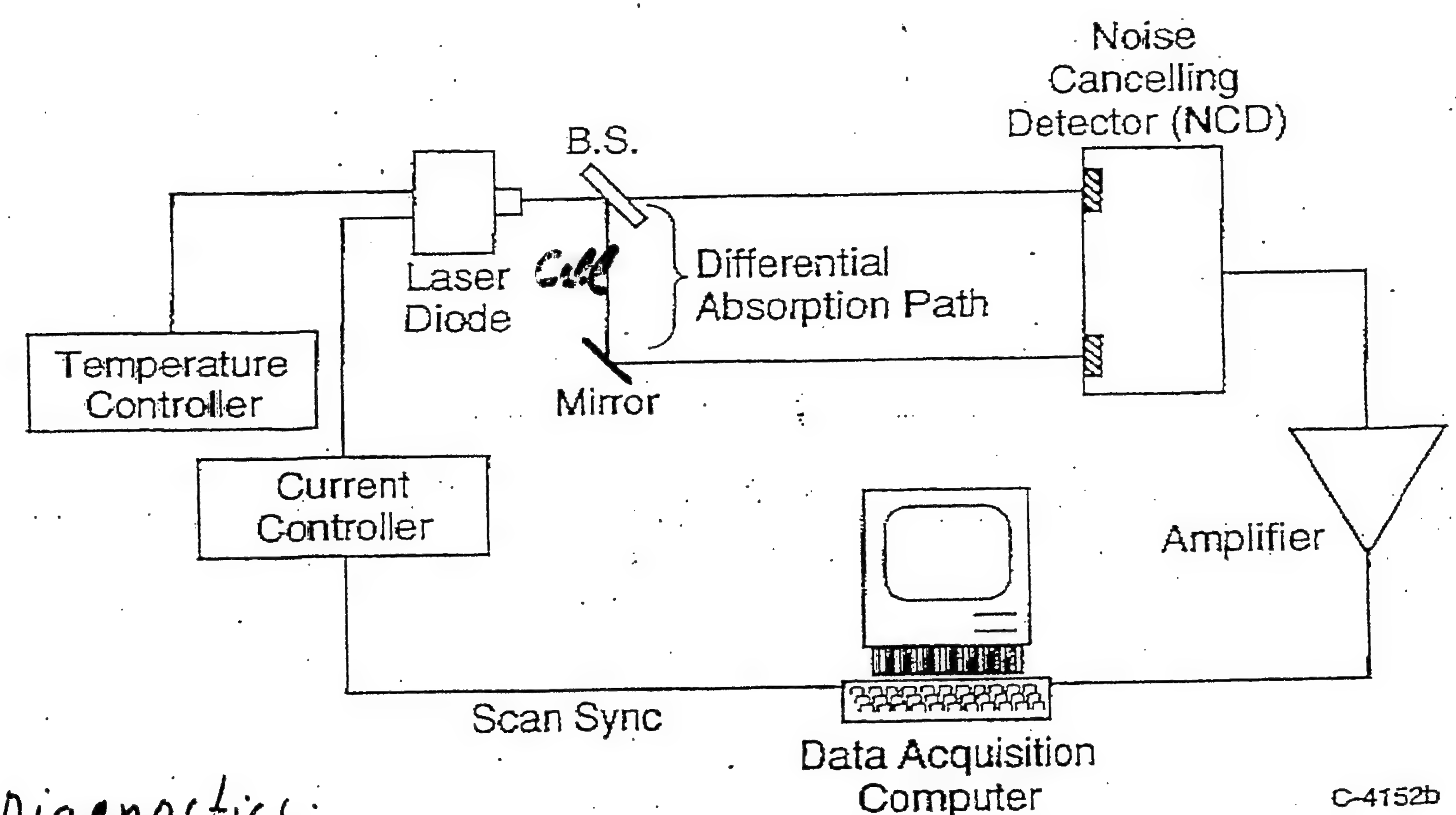

Diagnostics:

$O_2\,(^3\Sigma \rightarrow {}^1\Sigma)$, 760 nm

$I\,(^2P_{3/2} \rightarrow {}^2P_{1/2})$, 1315 nm

$H_2O\,(\nu_1+\nu_3)$, 1390 nm

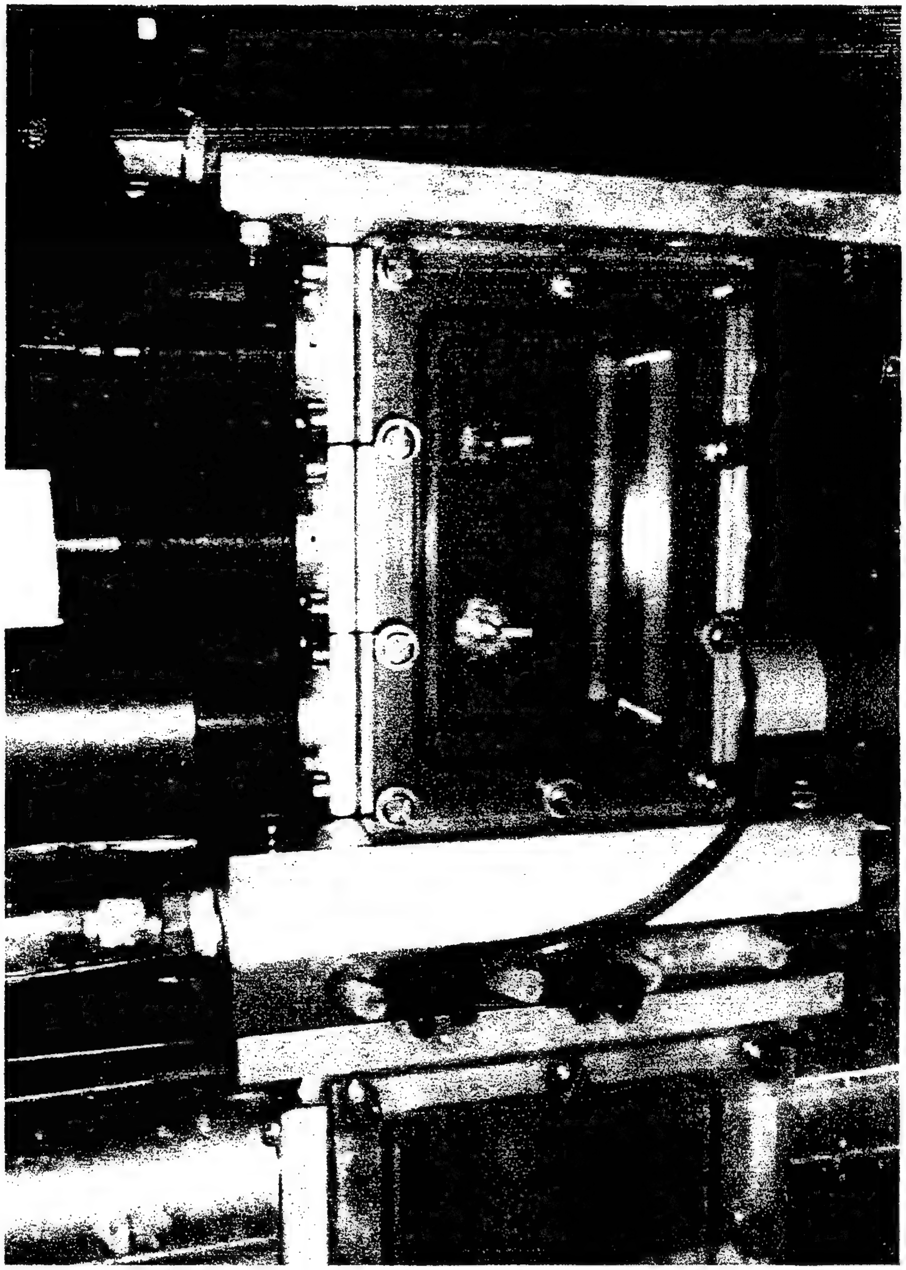

Injection Nozzles

i) Grid nozzle (transonic injection) consists of 10 rectangular brass tubes. There are 9 iodine injection holes, 0.5 mm i. d., on both sides o: each tube (5 on one side and 4 on the other).

Slit Nozzle No.1 (transonic injection): the first row has 24, 0.6 mm diameter holes, and the second row has 25, 0.4 mm diameter holes.

Slit Nozzle No.2 (transonic injection): the first row has 31, 0.6 mm diameter holes, and the second row 62, 0.4 mm diameter holes.

Slit Nozzle No.3 (supersonic injection): the first row has 49, 0.5 mm diameter holes, and the second row 50, 0.5 mm diameter holes.

Rectangular Brass Nozzles

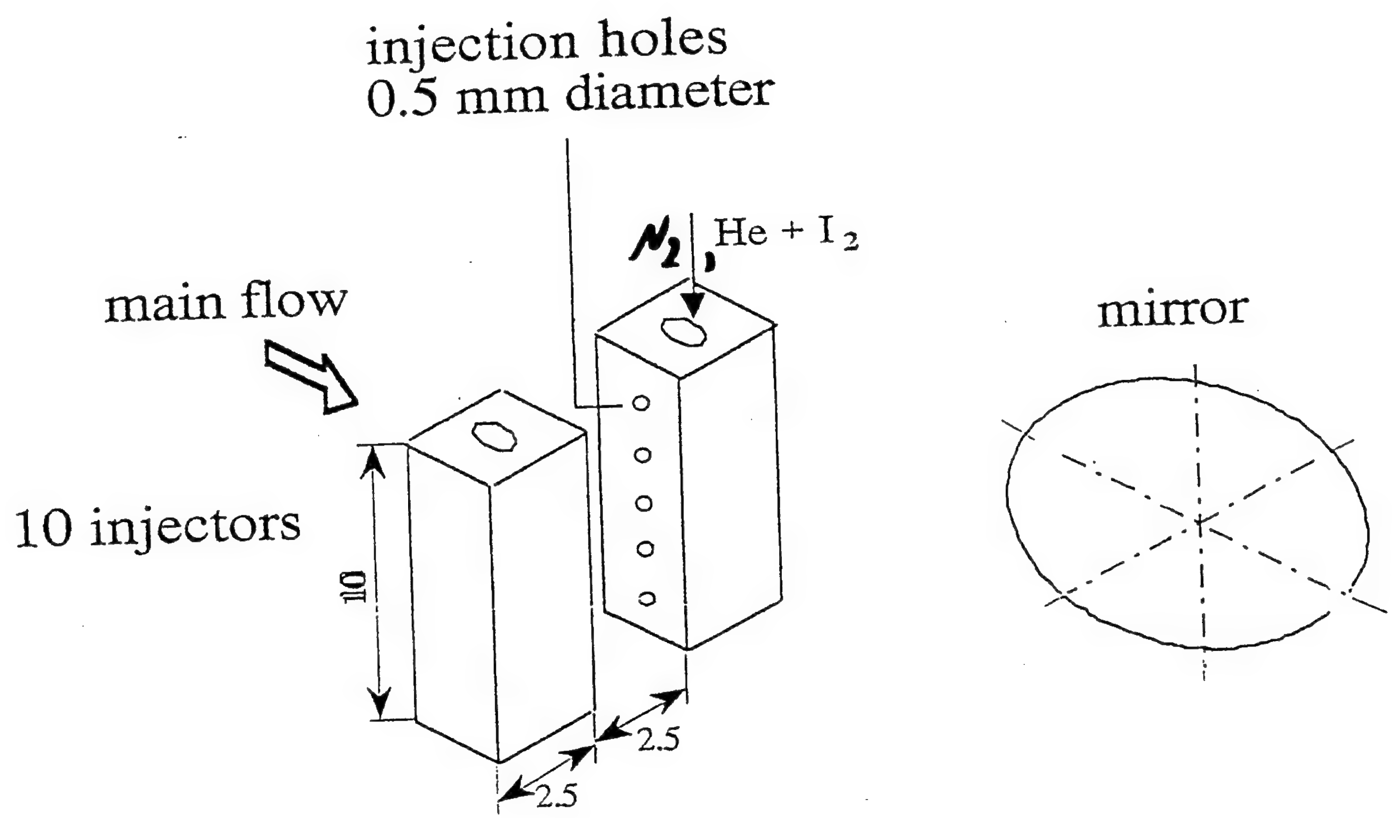

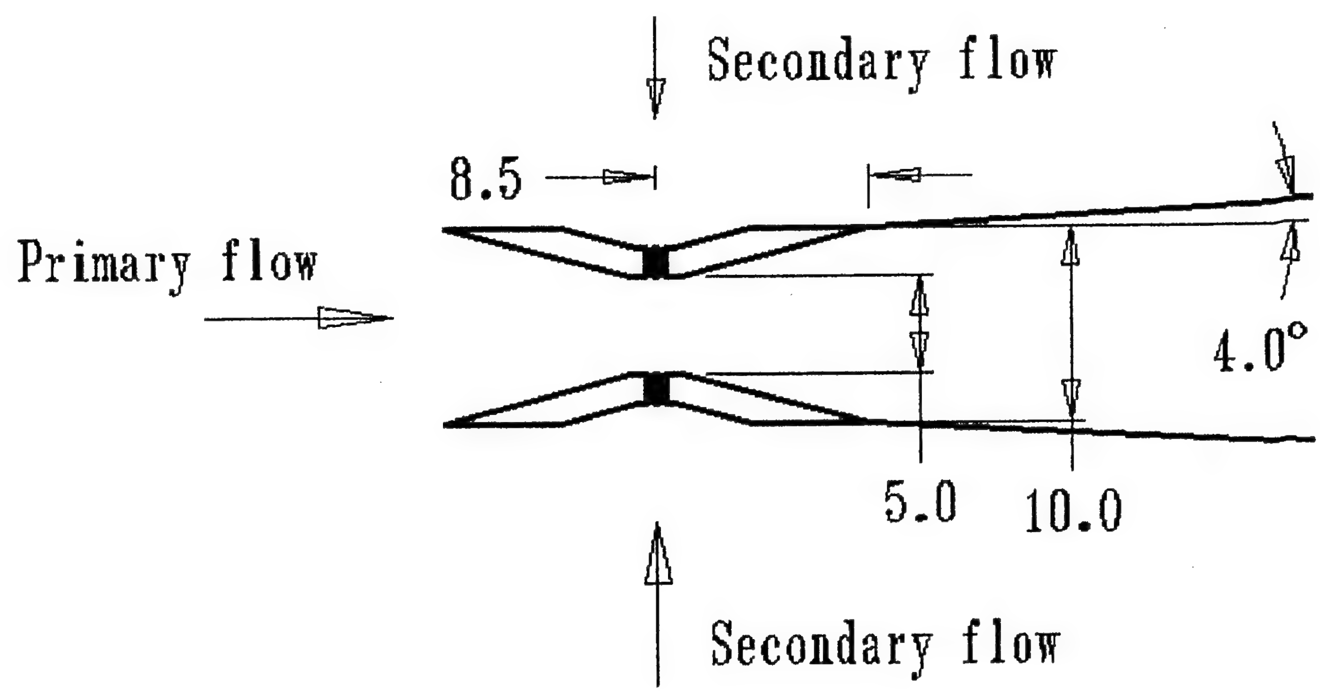

Secondary flow
8.5
Primary flow
4.0°
5.0
10.0
Secondary flow

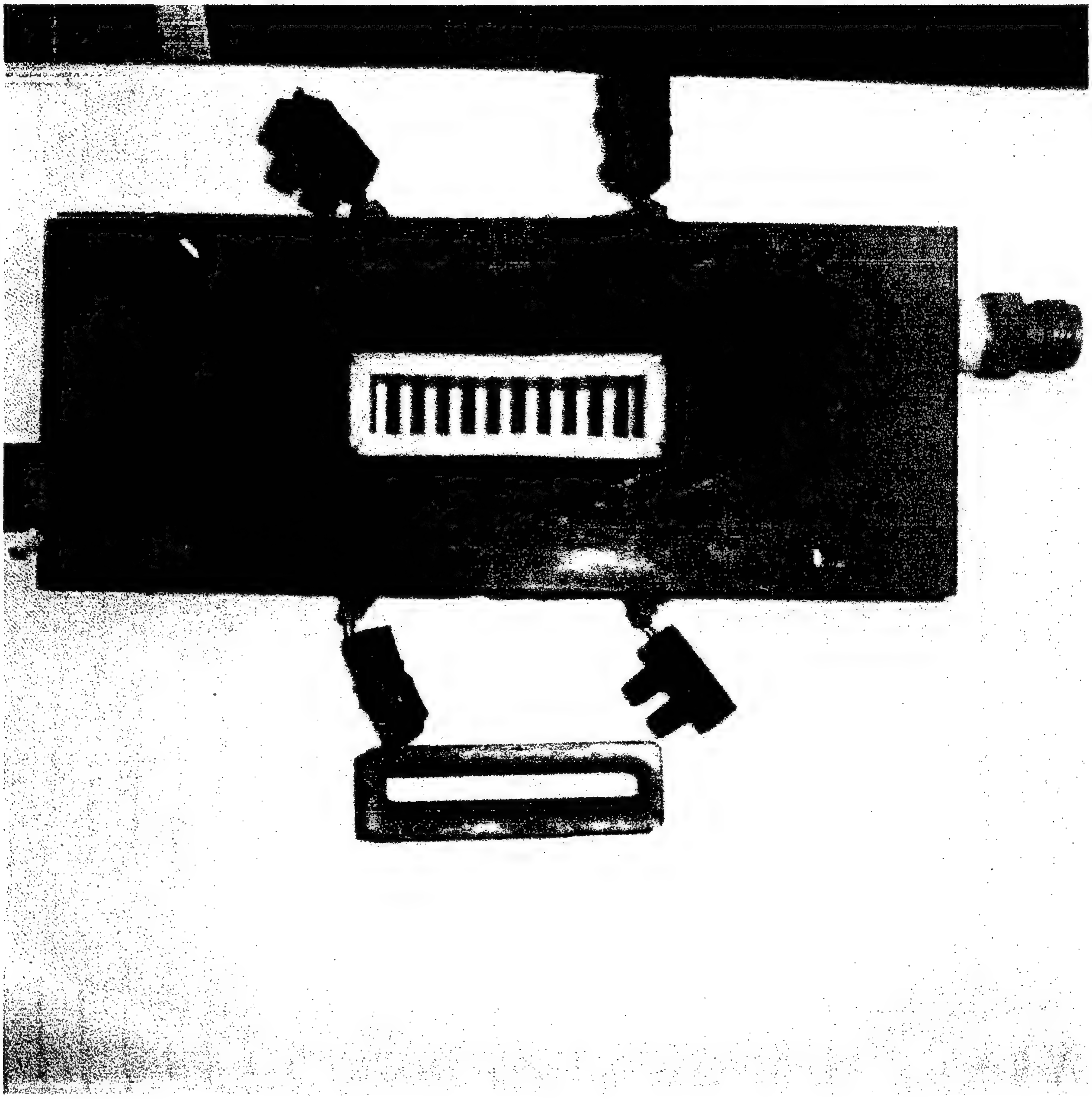

Grid nozzle

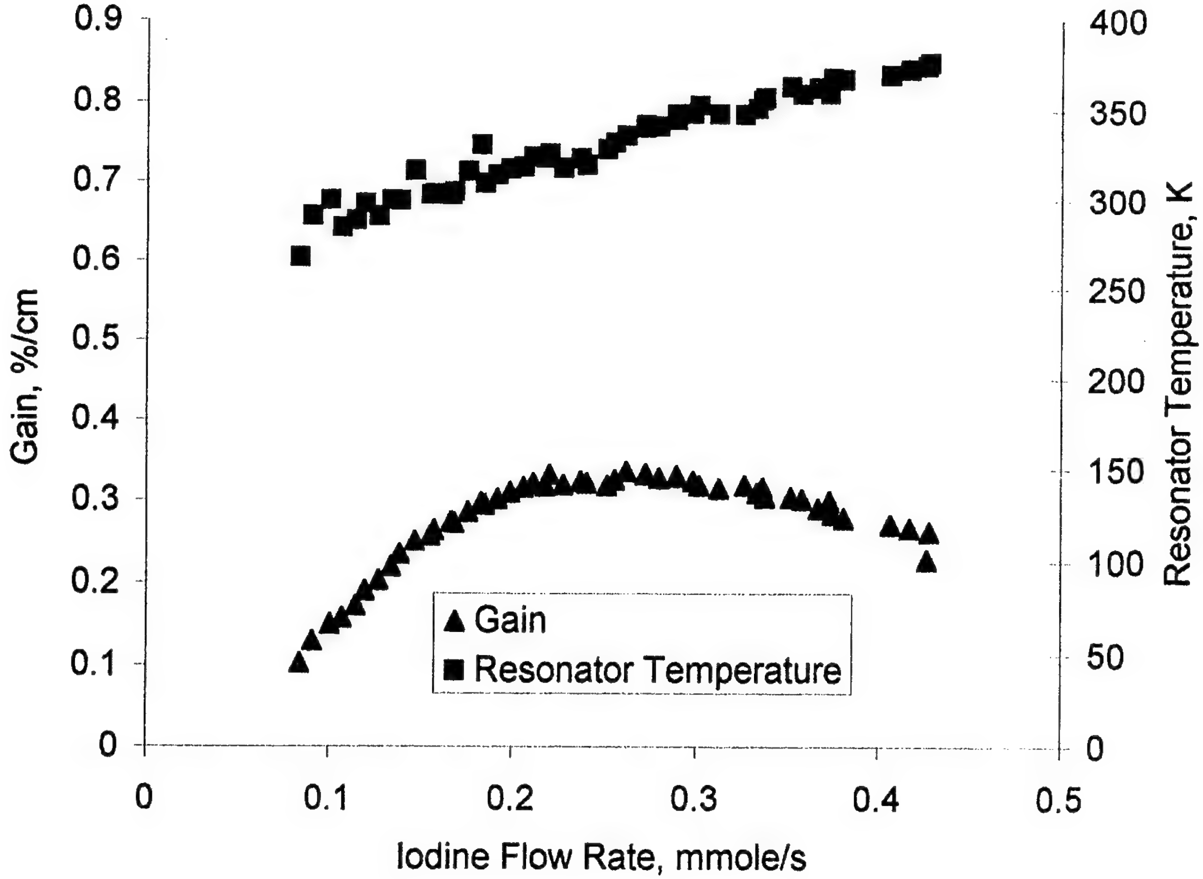

Cl2	11.7 mmol
Yield	0.65
Utilization	0.92
Water	0.12
Sec. N2	1.36 mmol
Stag. Temp.	340
Cold Res. Temp.	260
Res. Press.	1.4 Torr

Slit nozzle #1

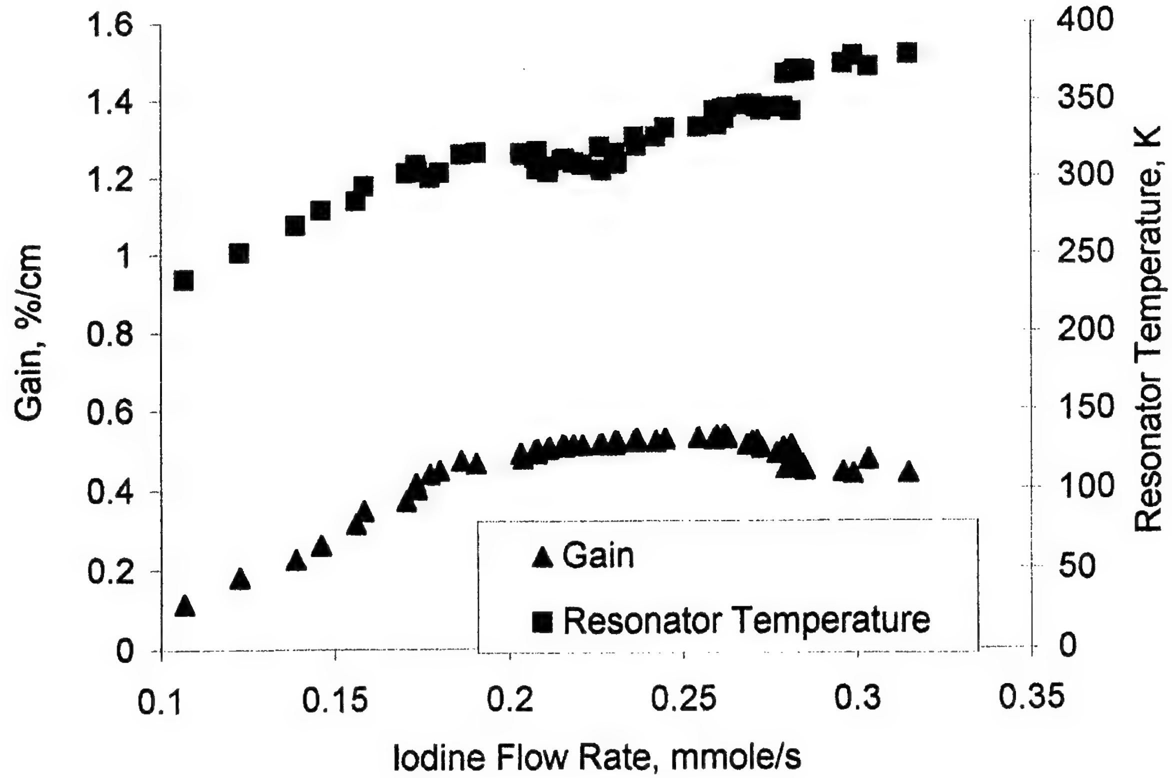

Cl2	11.7 mmole
Yield	0.6
Utilization	0.9
Water	0.12
Sec. N2	2.5 mmole/s
Stag. Temp.	320 K
Cold Res. Temp.	260 K
Res. Press.	1.4 Torr

Slit nozzle #1 (low resonator pressure)

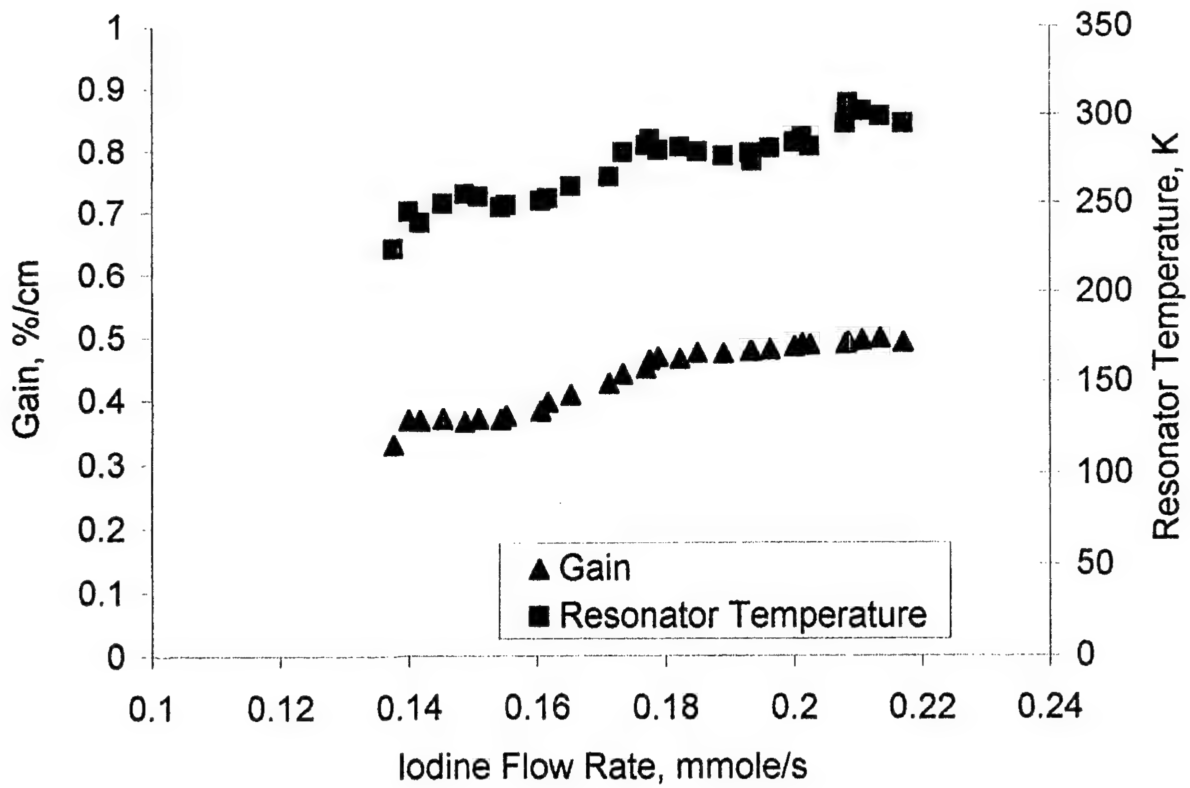

Cl2	11.7 mmol
Yield	0.55
Utilization	0.9
Water	0.12
Sec. N2	2.5 mmole/
Stag. Temp.	300
Cold Res. Temp.	190
Res. Press.	0.9 Torr

Slit nozzle #1 (high Cl2 flow rate)

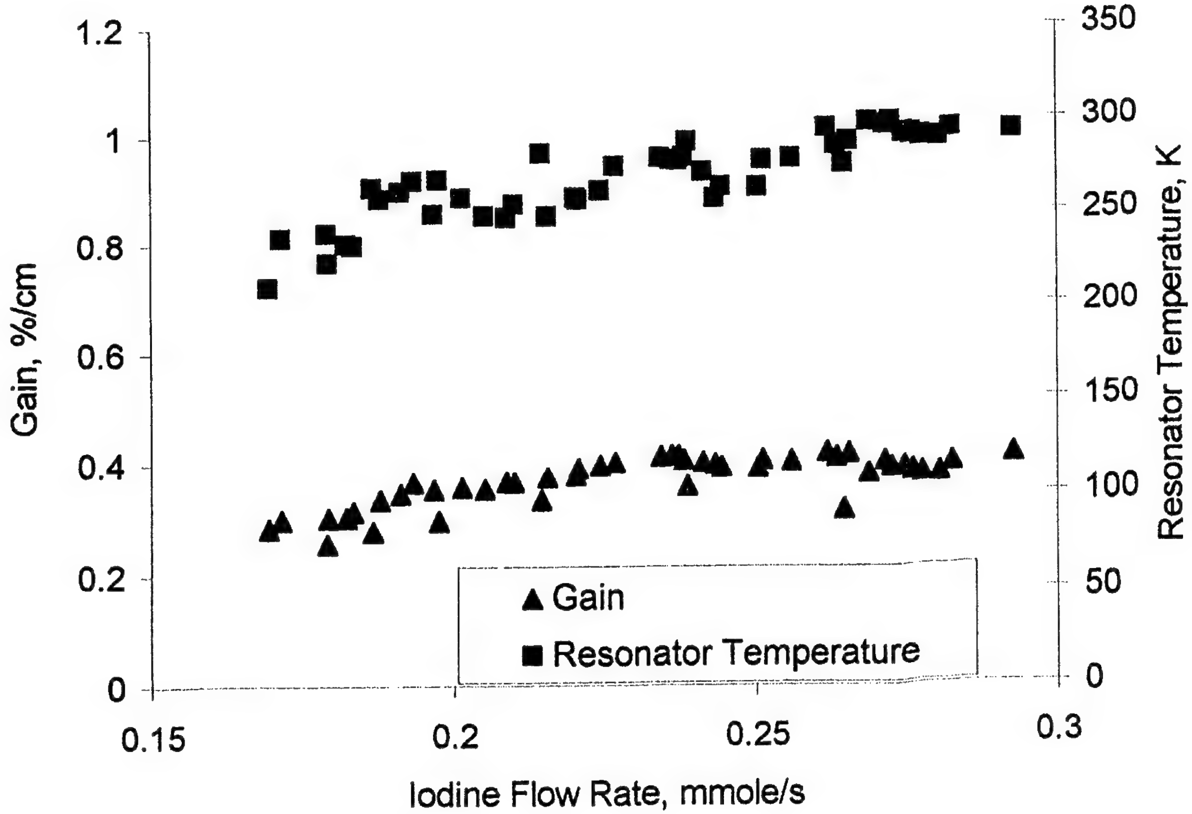

Cl2	19.5 mmol
Yield	0.55
Utilization	0.9
Water	0.12
Sec. N2	2.5 mmole/
Stag. Temp.	320
Cold Res. Temp.	230
Res. Press.	1.55 Torr

Slit nozzle #2

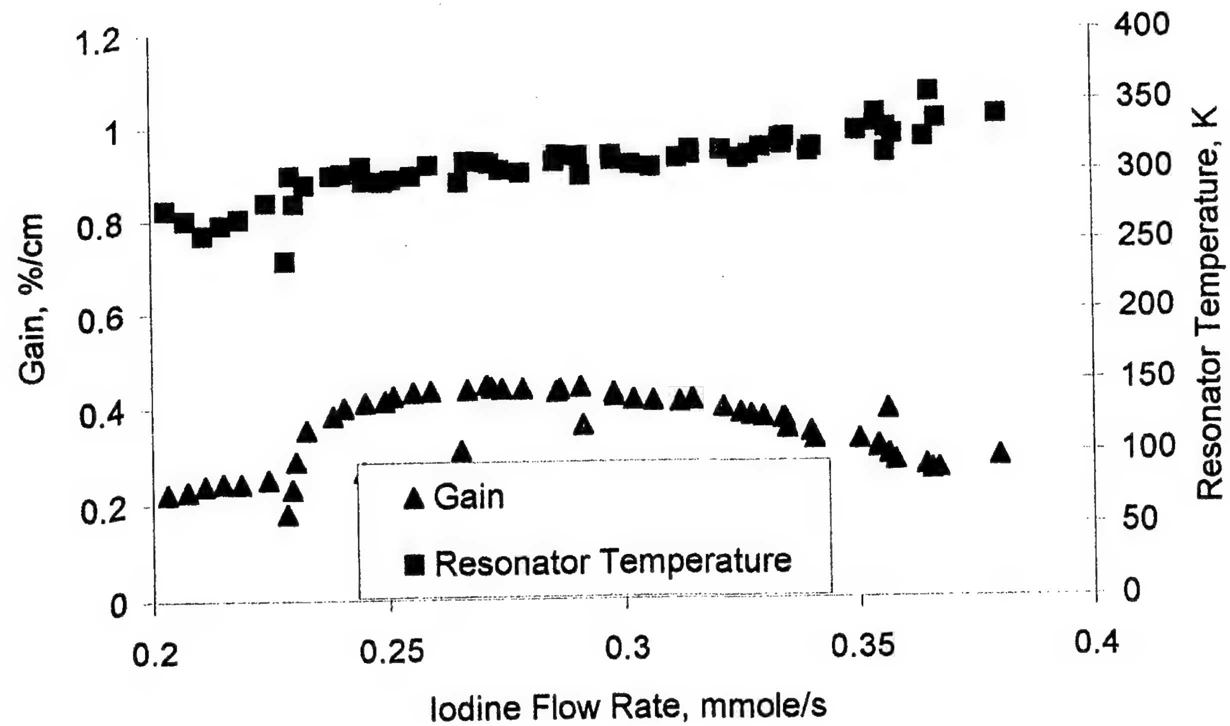

Cl2	11.8 mmole
Yield	0.55
Utilization	0.9
Water	0.12
Sec. N2	4 mmole/s
Stag. Temp.	350
Cold Res. Temp.	260
Res. Press.	1.45 Torr

Slit nozzle #3 (supersonic injection)

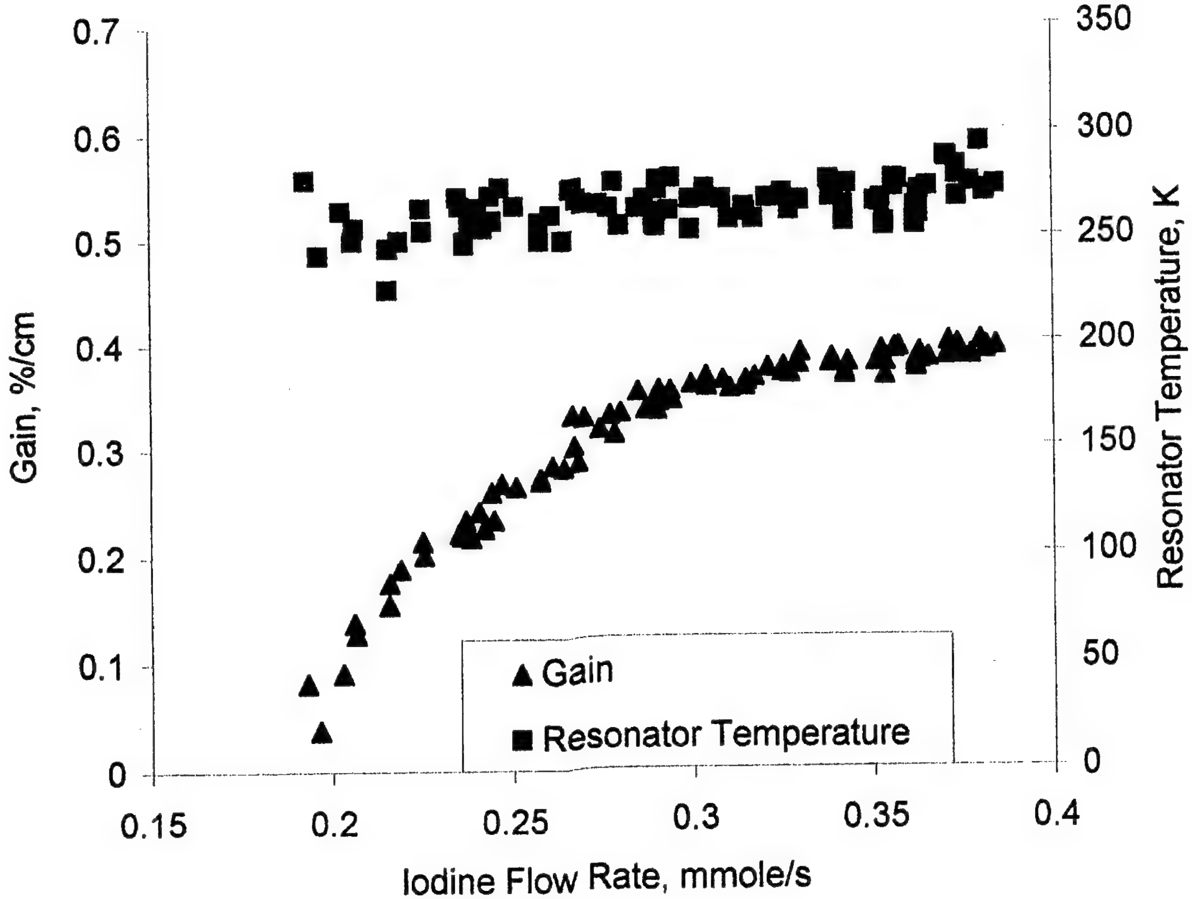

Cl2	11.7 mmole
Yield	0.55
Utilization	0.9
Water	0.12
Sec. N2	7 mmole/s
Stag. Temp.	320 I
Cold Res. Temp.	260 I
Res. Press.	1.55 Torr

Conclusions

1. We measured gain and temperature in resonator of a supersoni COIL without primary buffer gas for different I_2 injection scheme using diode laser based diagnostic.

2. Maximum gain of <u>0.54%/cm</u> was obtained for a slit nozzle with transonic injection. The temperatures in the resonator correspondir to the maximum gain was 320 K.

3. The gain is a non-monotonous function of I_2 flow rate, whereas th temperature increases with increasing I_2 flow rate.

4. The temperature in the resonator decreases with moving the injection point downstream.

Results of COIL Gain Measurements

K.Grünewald, F.Duschek, J.Handke

DLR

Outline

- Experimental Set-up
- Results of Stationary Measurements of SSG Coefficient and Temperature
- Local Scans of Gain and Temperature
- Effects of Gas Mixing Conditions on Small Signal Gain
- Localization of Dissociation Coefficient
- Summary

DLR

Deutsches Zentrum für Luft- und Raumfahrt e.V.

Comparison of Experimental Data with Results of "COIL simplified Saturation Model"

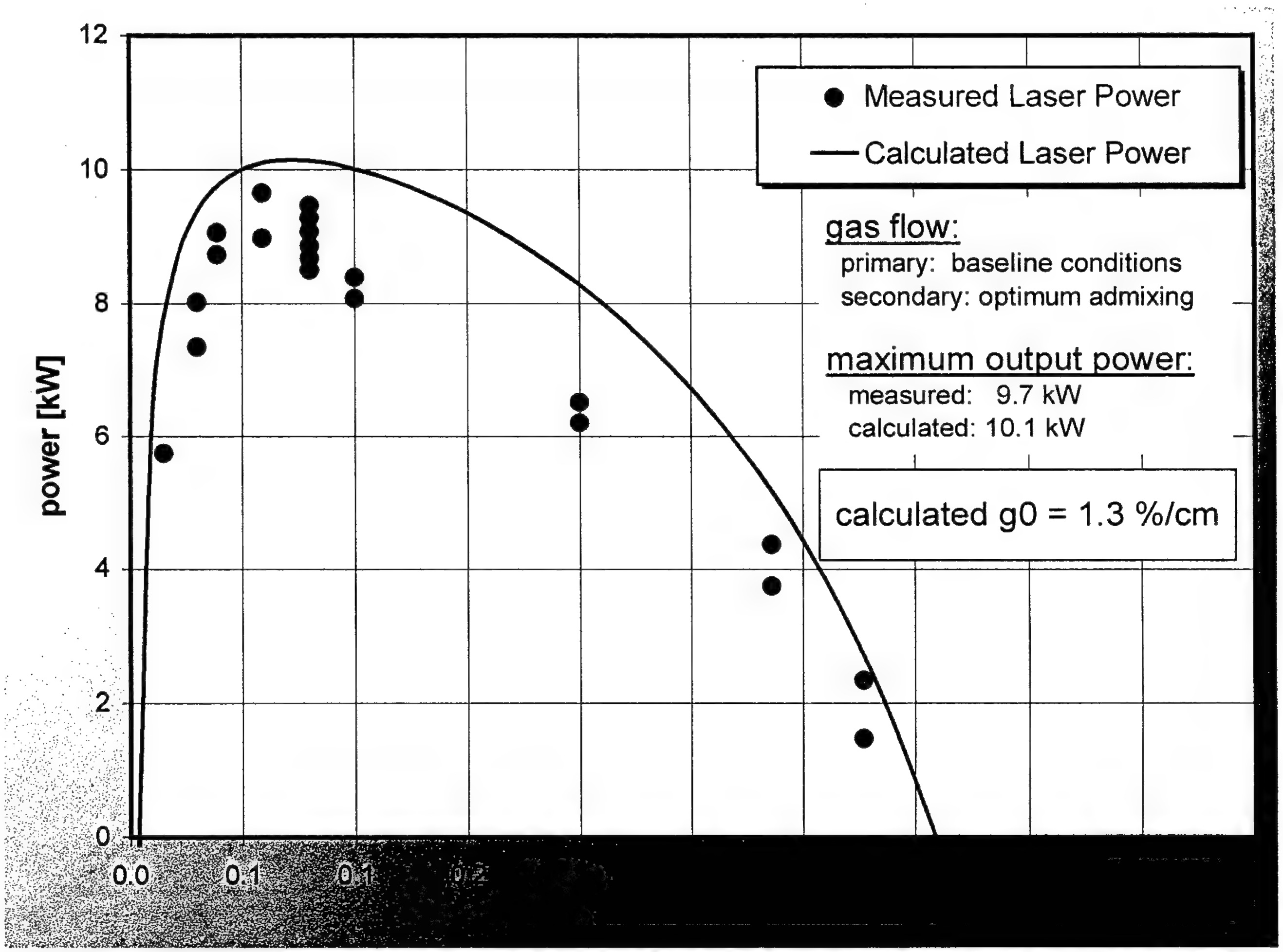

DLR

Measured Output Power for Different Outcoupling Configurations

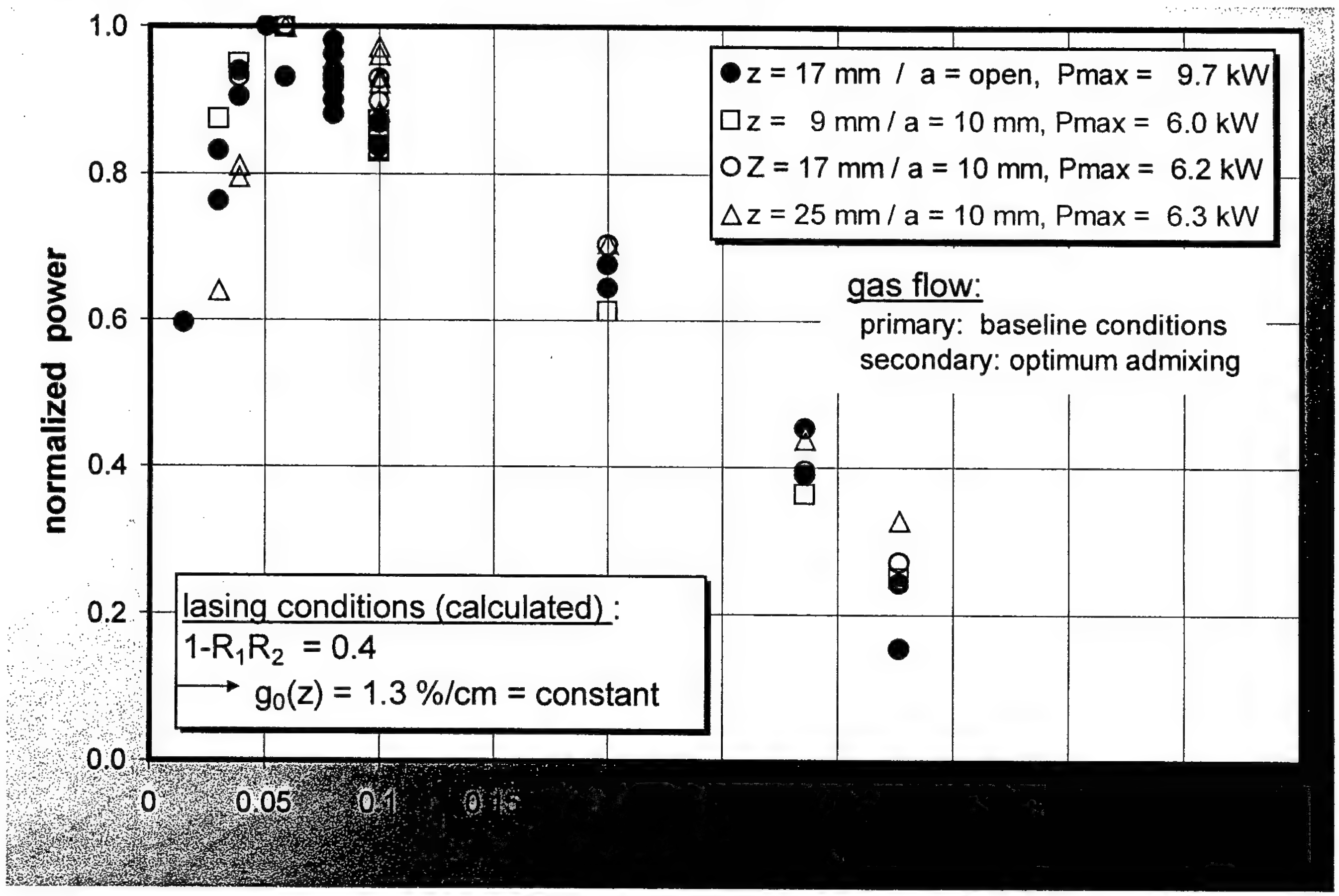

Deutsches Zentrum für Luft- und Raumfahrt e.V.

Scanning Equipment with Emitter / Detector Unit

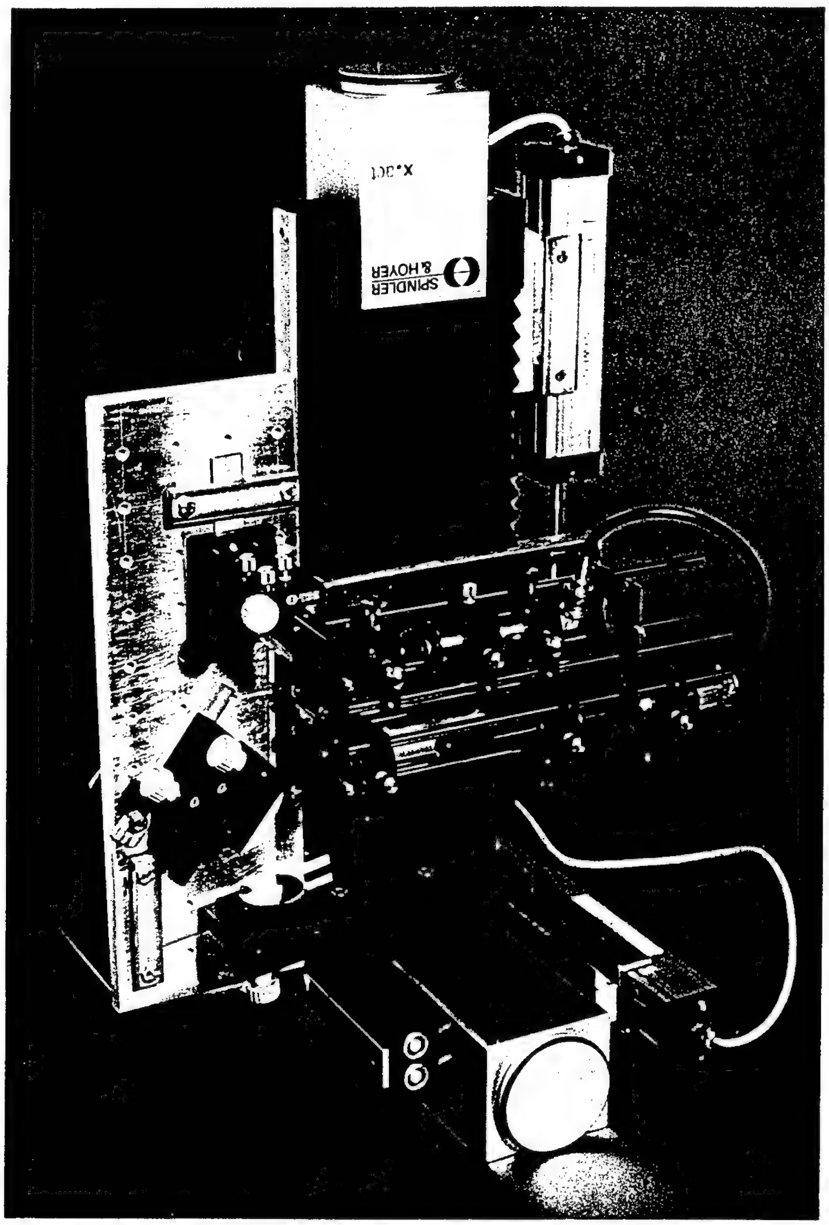

DLR

Deutsches Zentrum für Luft- und Raumfahrt e.V.

Experimental Set-up

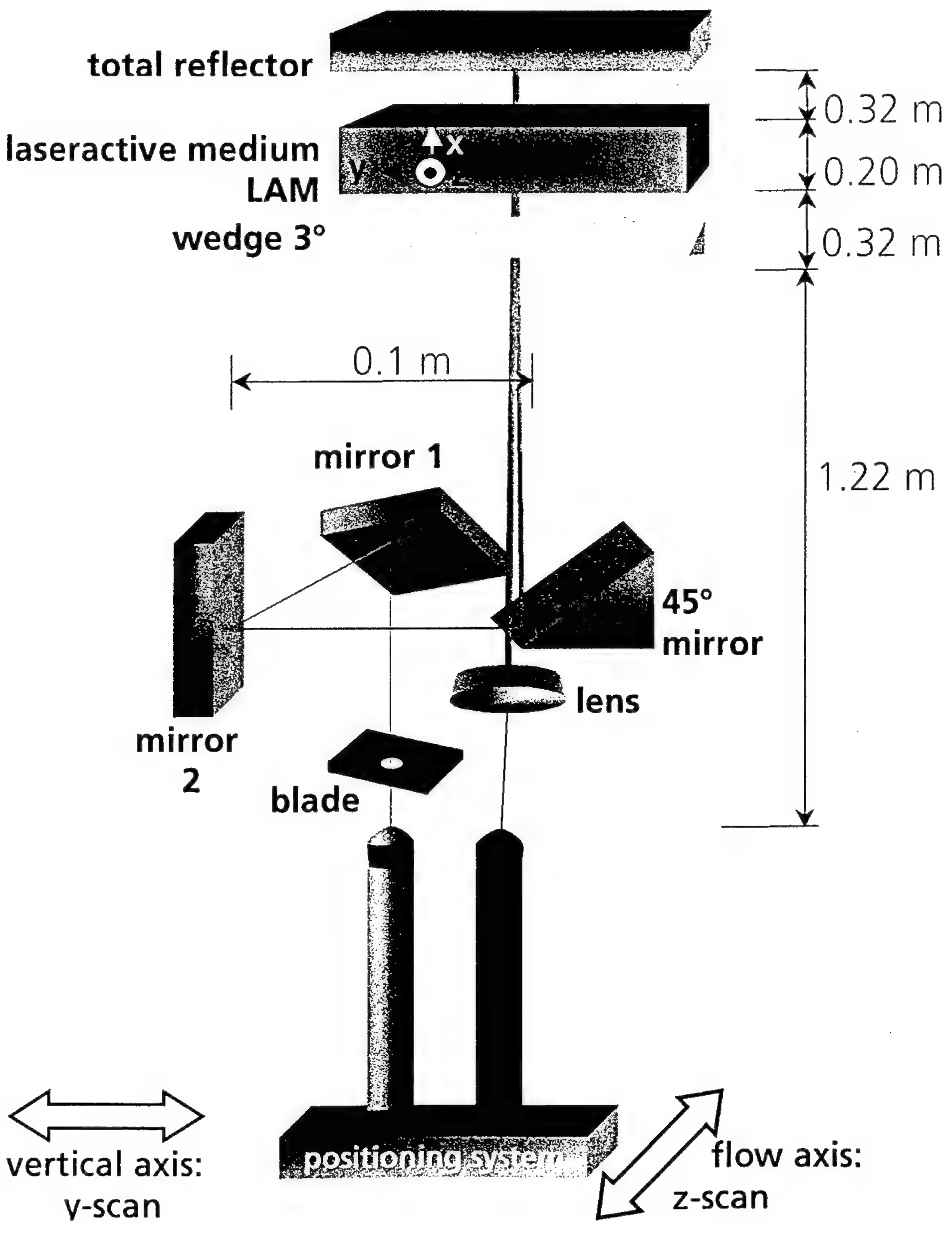

DLR

Deutsches Zentrum für Luft- und Raumfahrt e.V.

Spot Size and Position Definition

spot size:

direction → ↓ position	flow axis z	vert. axis z
reflector	5.4	5.4
LAM (⇒mirror)	6.2	7.1
LAM (⇒wedge)	6.6	8.1
wedge	7.4	9.7

measured beam divergence:
Θ = 2.3 mm·mrad

The dimensions of the beam at mirror 3 determine the minimum angle between the forwarded and the reflected beam

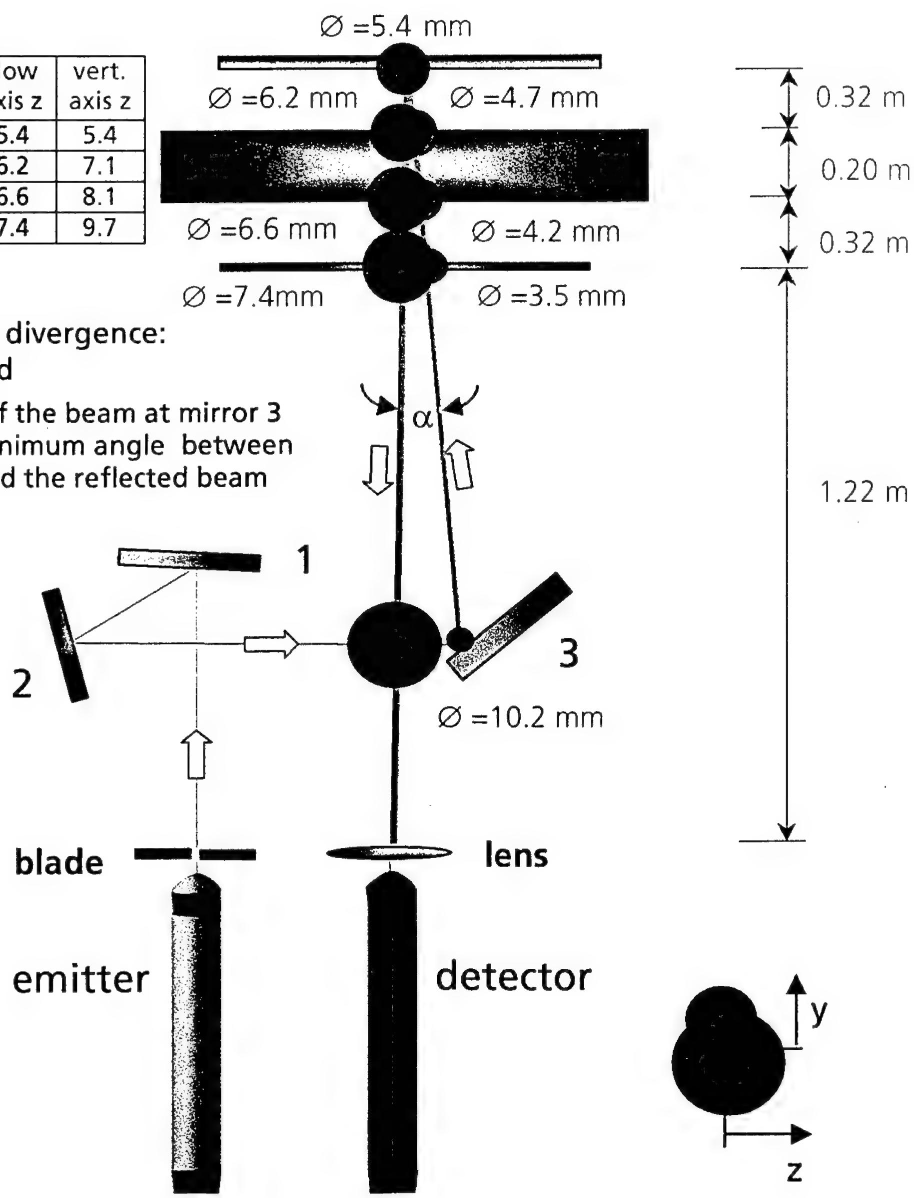

DLR

Measuring Positions

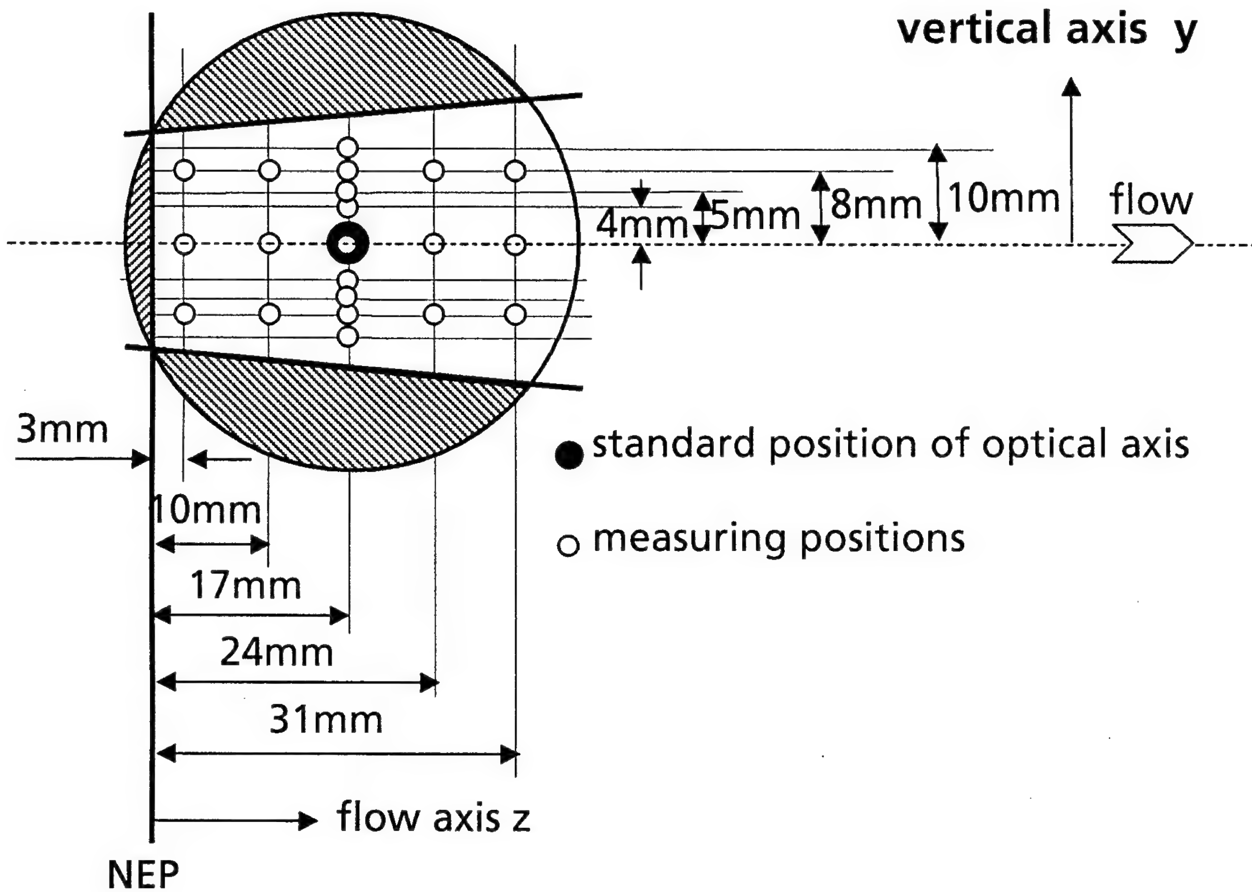

Readings of SSG Coefficient and Intra Cavity Temperature

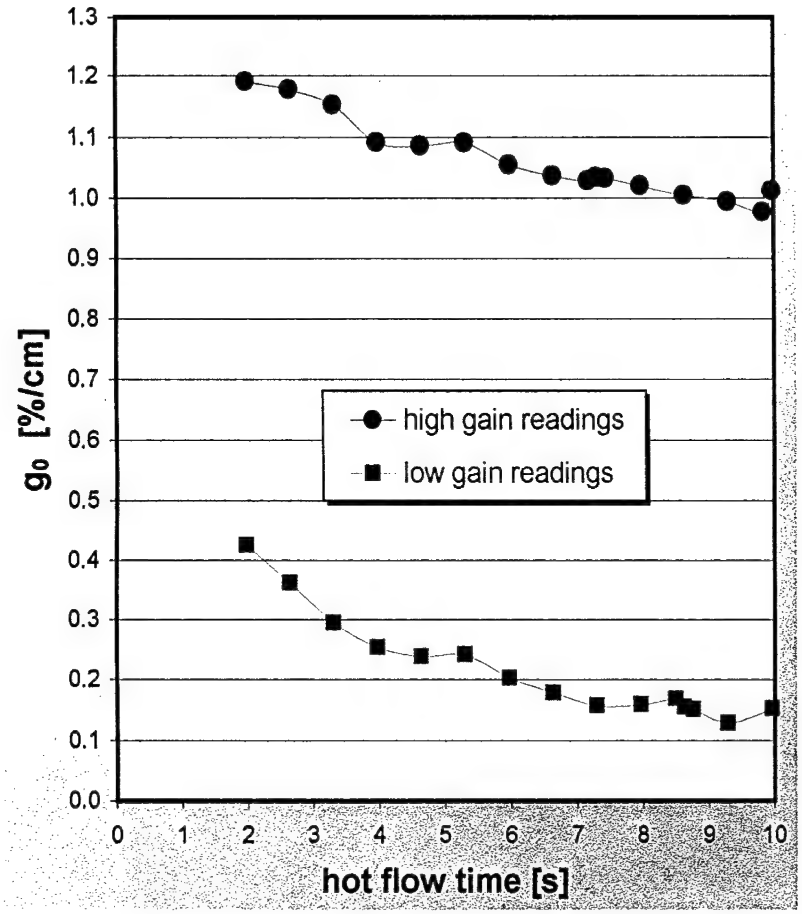

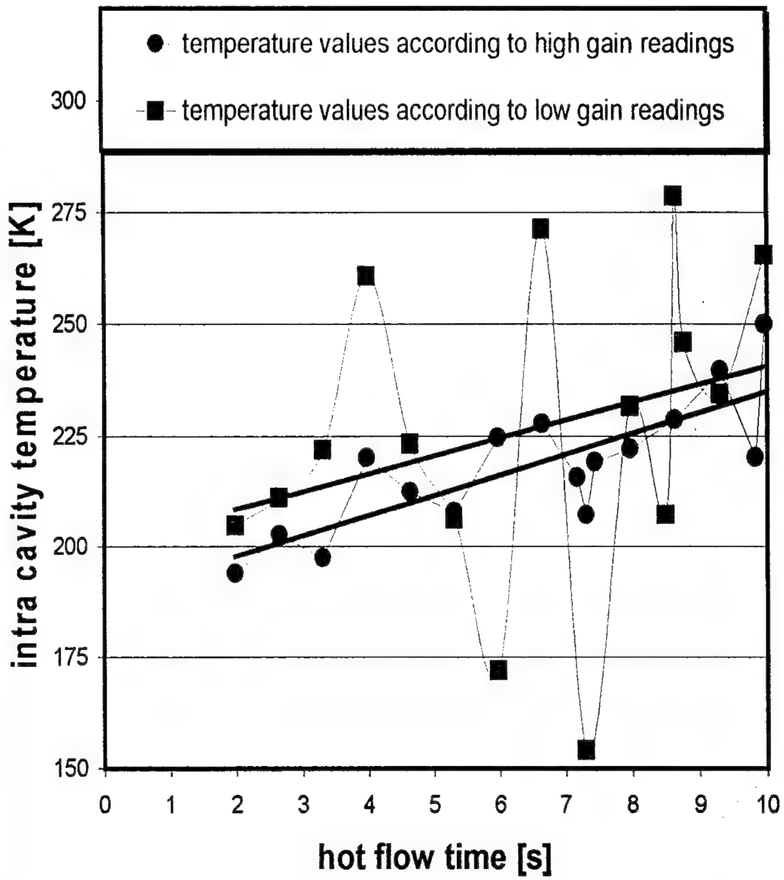

DLR

Deutsches Zentrum für Luft- und Raumfahrt e.V.

Time Dependent Small Signal Gain Coefficient in the Position of the Optical Axis

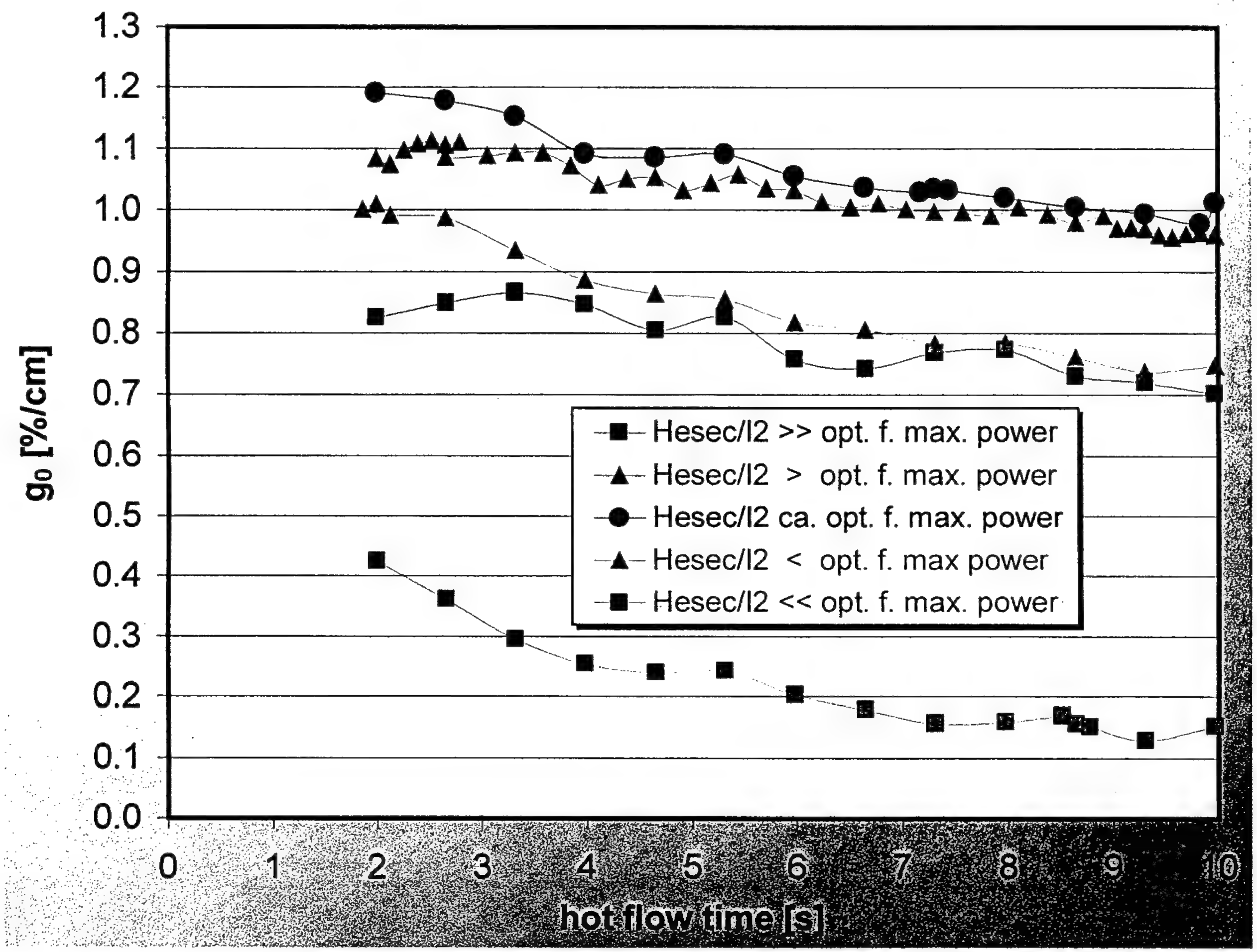

DLR

Time Dependence of Temperature at the Position of the Optical Axis

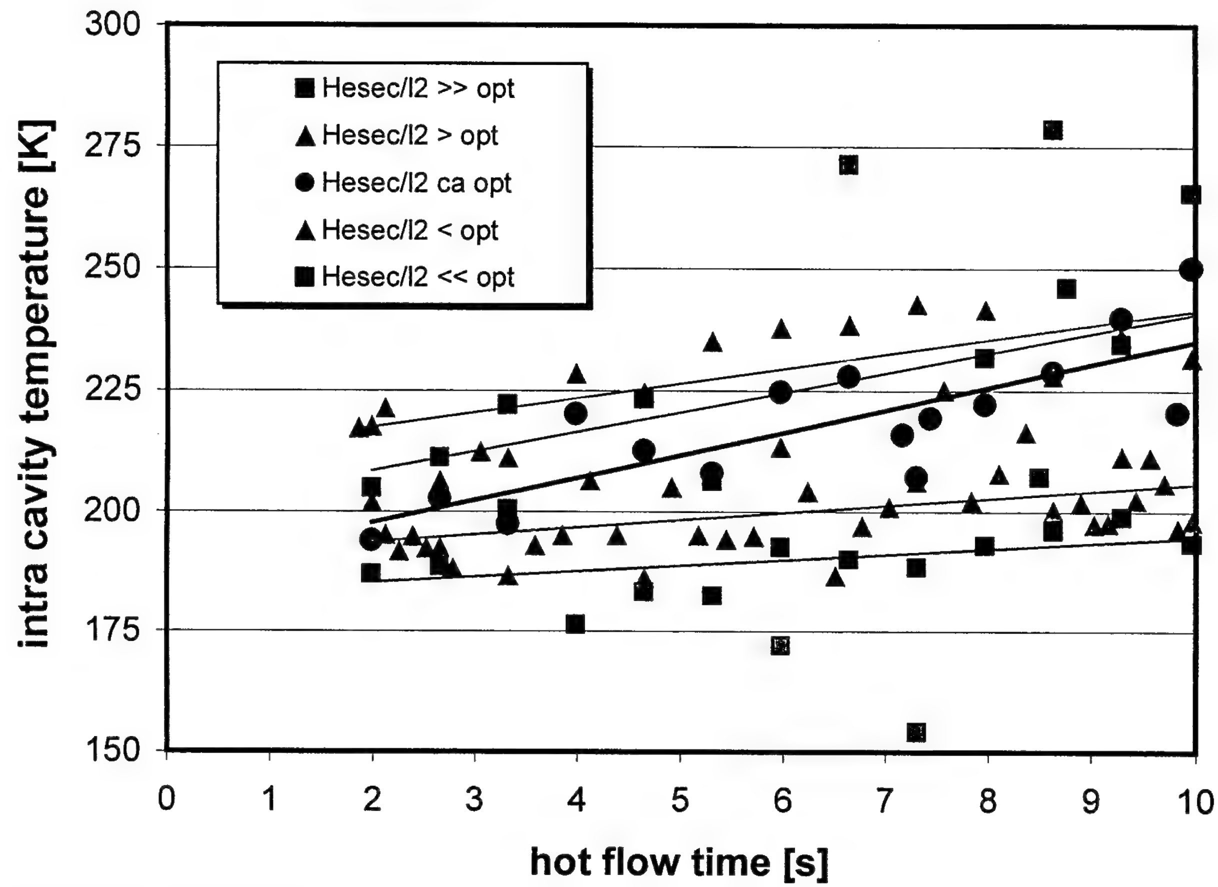

DLR

Time Dependence of Small Signal Gain Coefficient

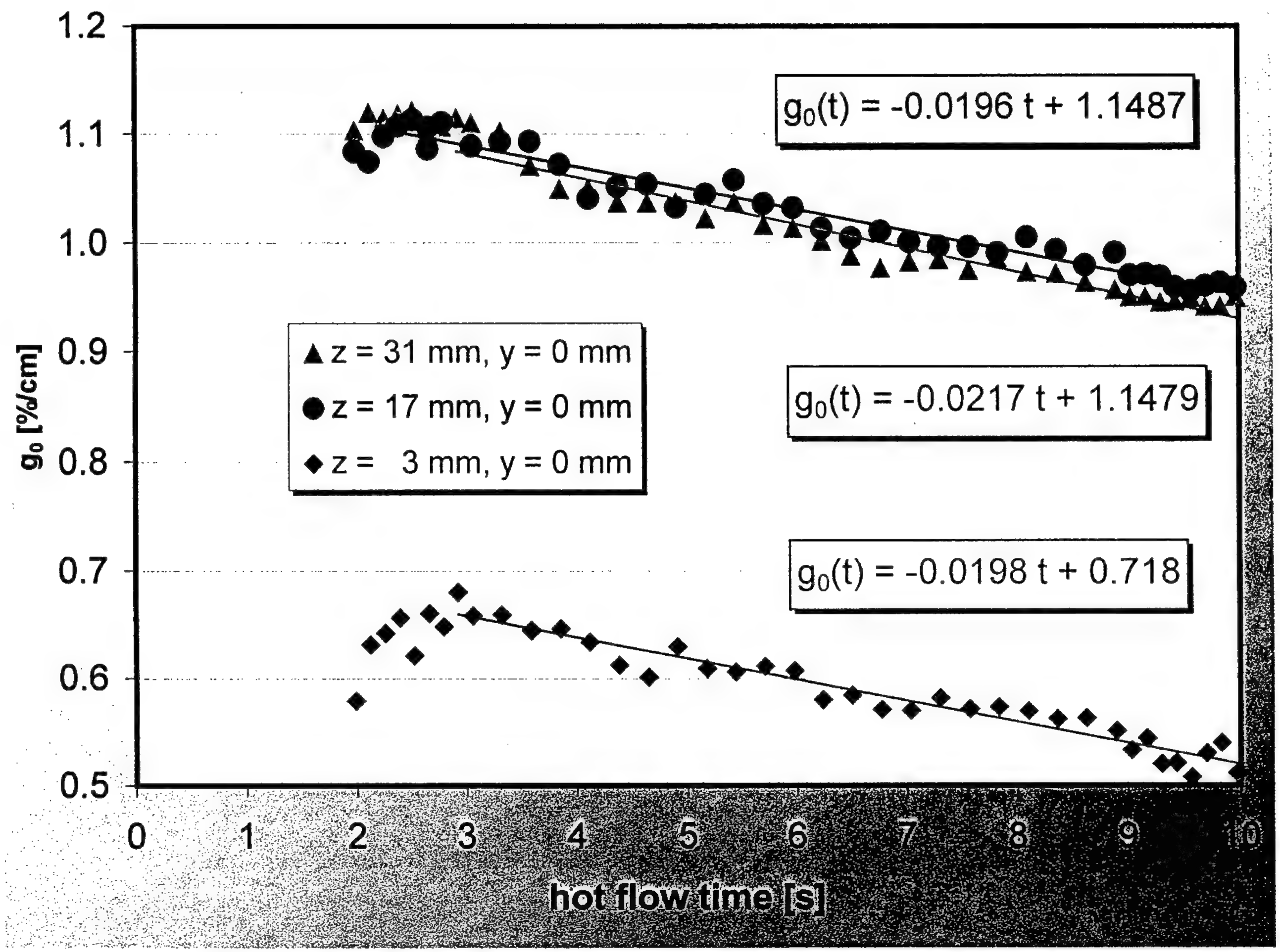

DLR

Deconvolution of Time Dependence for Local Scans of g_0

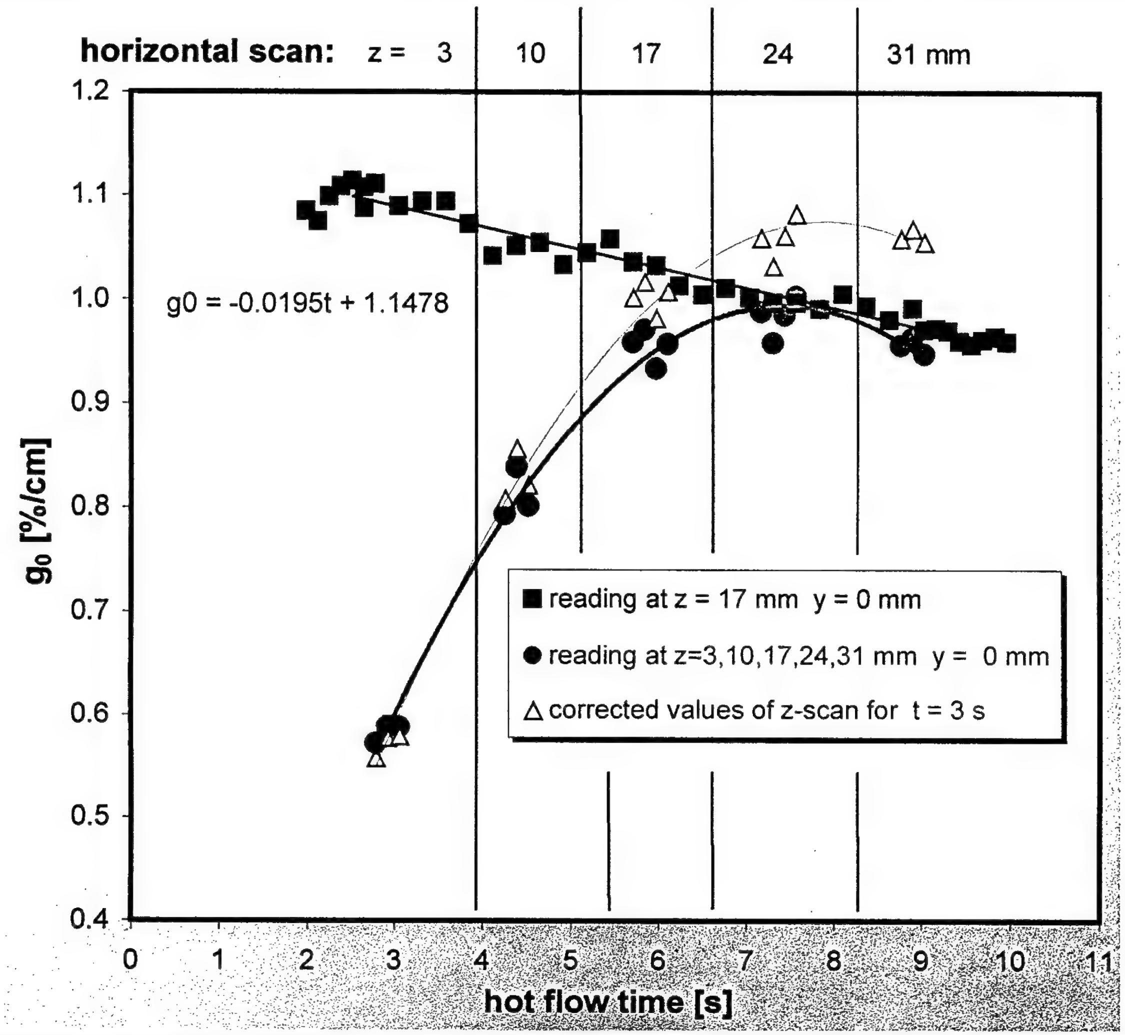

DLR

Deutsches Zentrum für Luft- und Raumfahrt e.V.

Local Dependence of the Small Signal Gain Coefficient

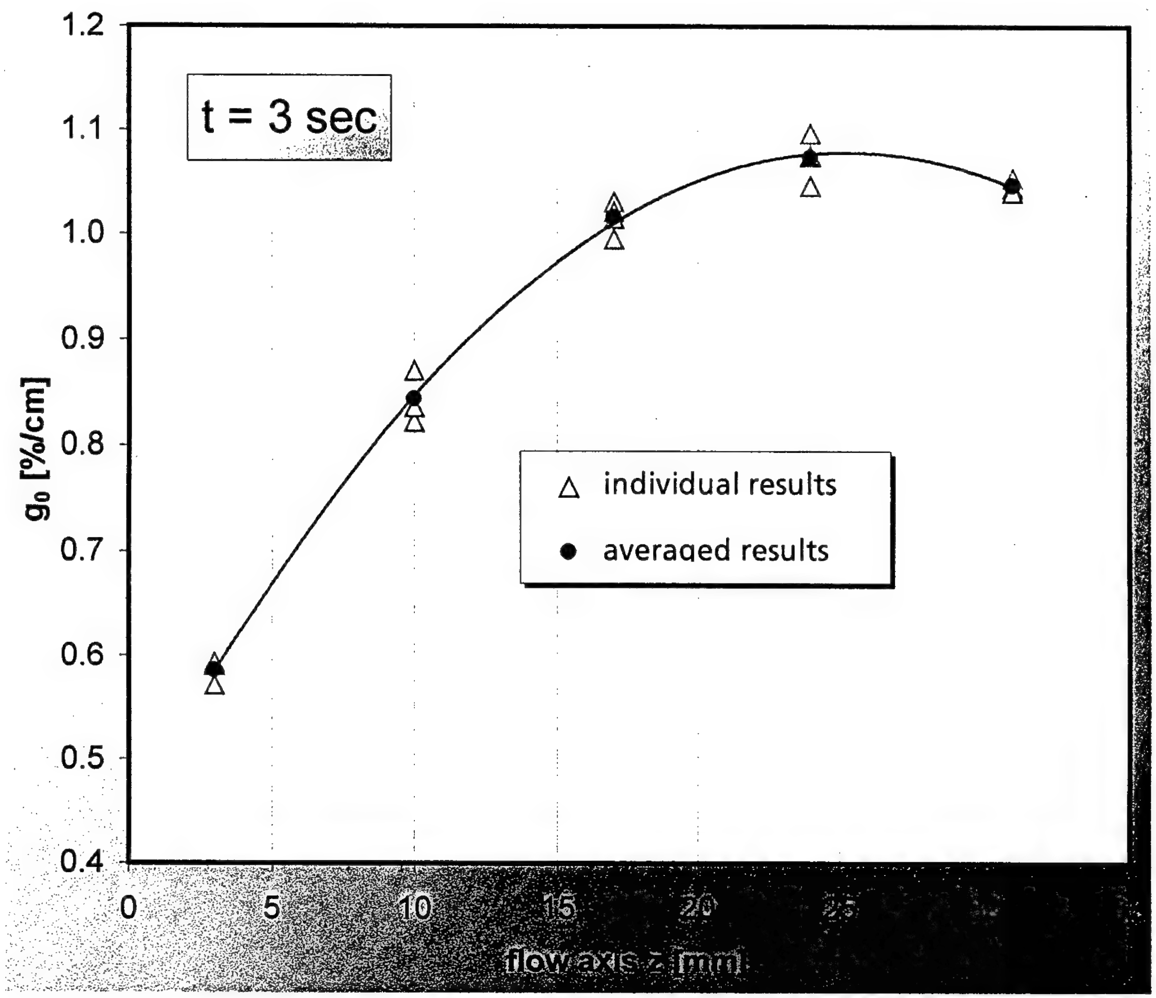

DLR

Performance of SSG Coefficient and Intra Cavity Temperature Along the Flow Axis at Different Vertical Positions*)

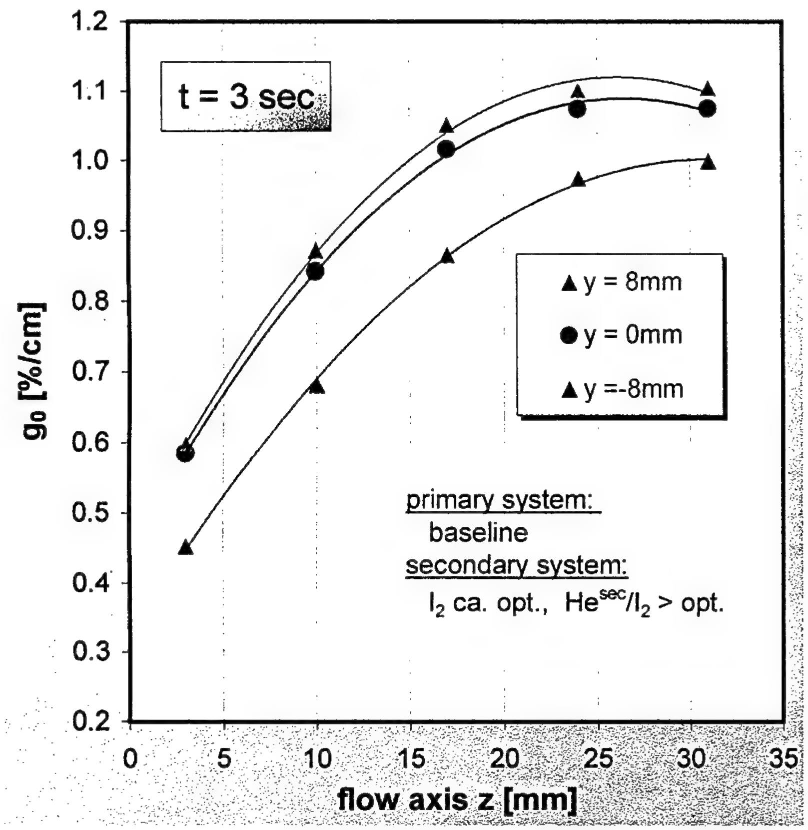

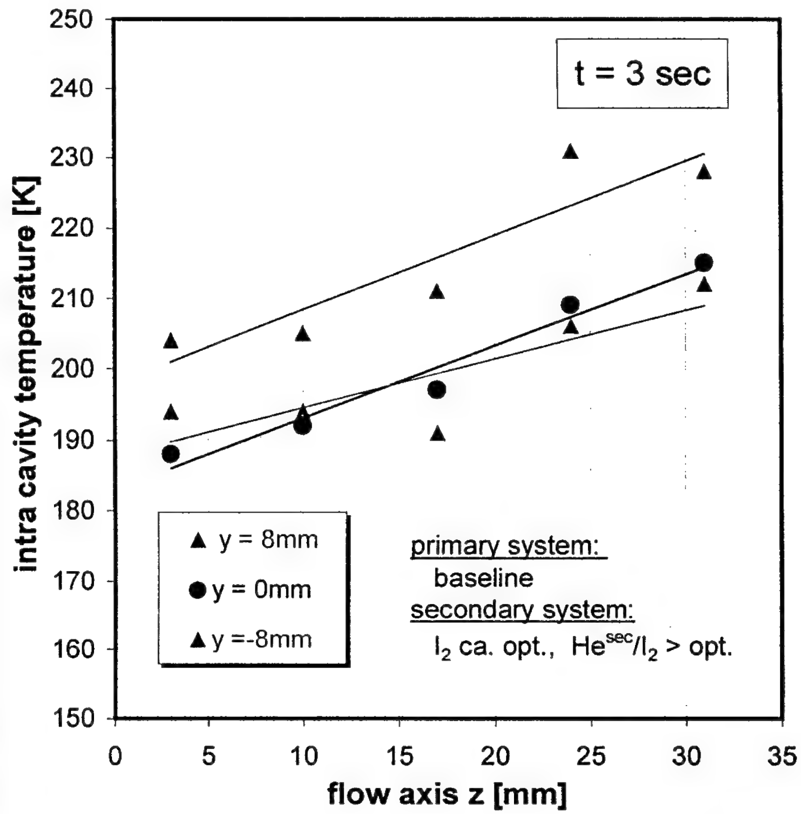

*) unchanged operating conditions: Γ > optimum for maximum power output

DLR

Deutsches Zentrum für Luft- und Raumfahrt e.V.

Reproducibility

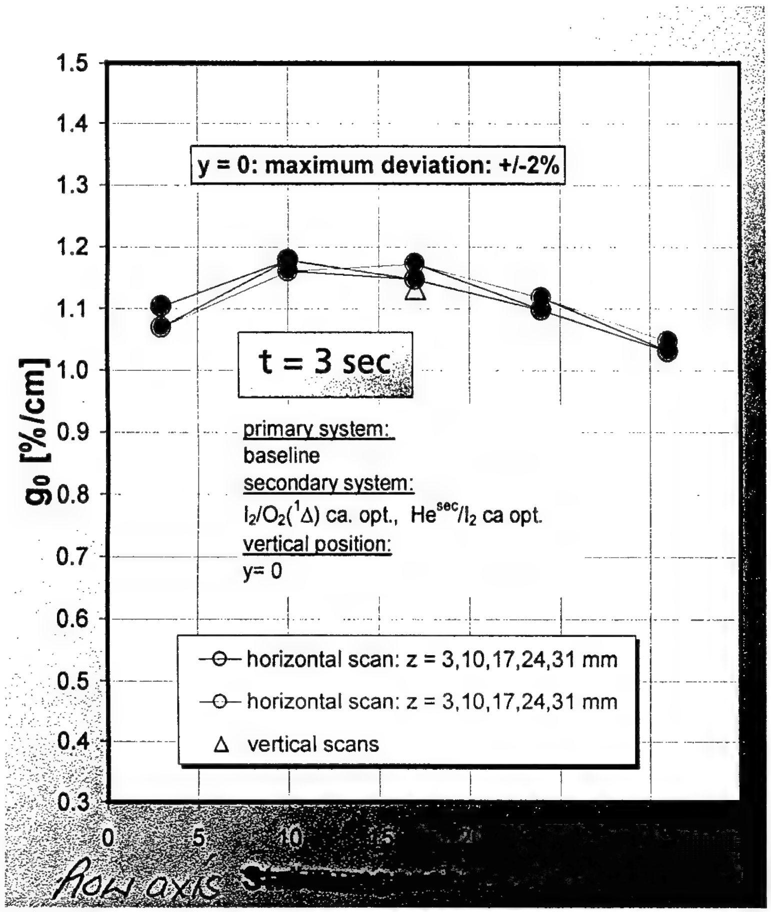

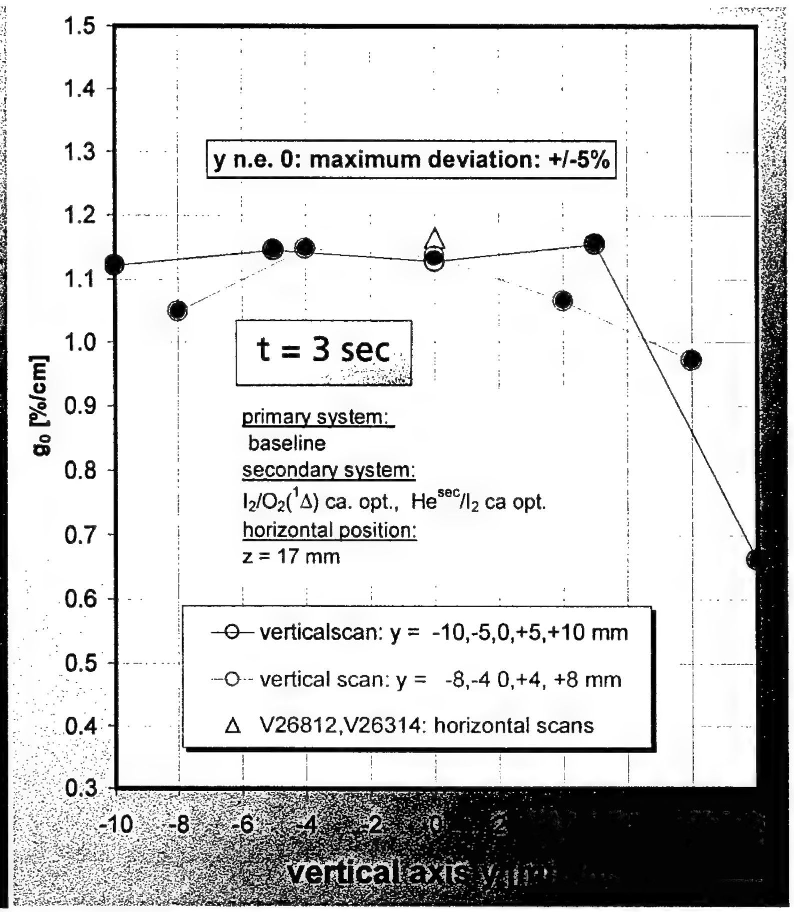

DLR

Time Dependence of Intra Cavity Temperature

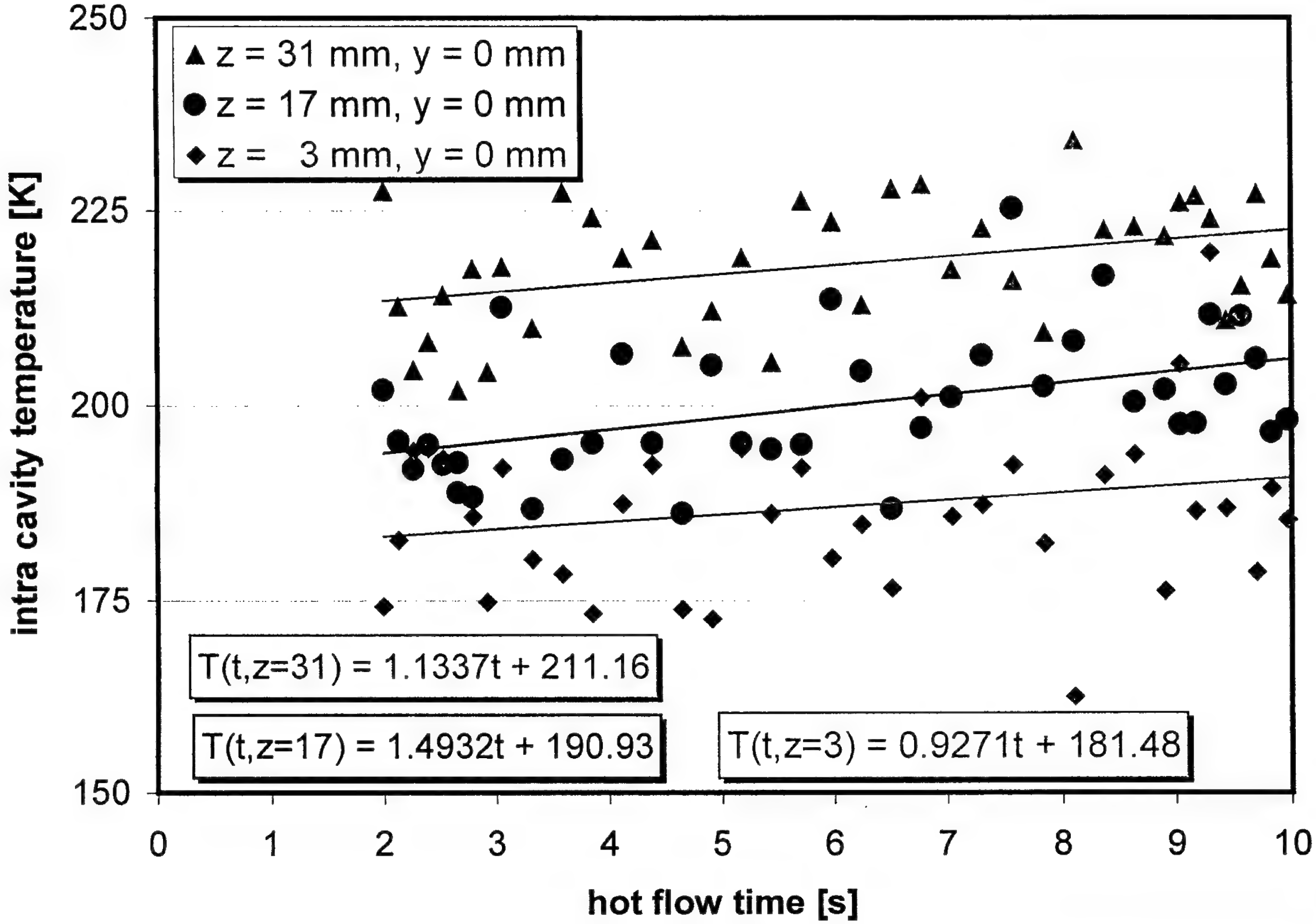

Deutsches Zentrum für Luft- und Raumfahrt e.V.

2D-field of SSG Coefficient

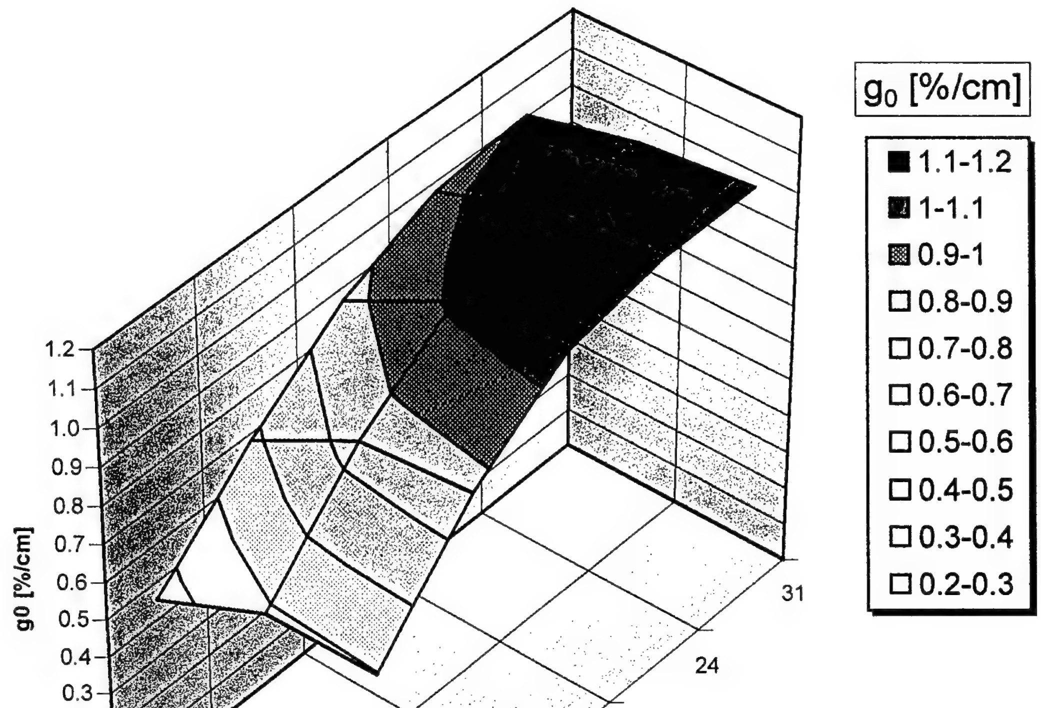

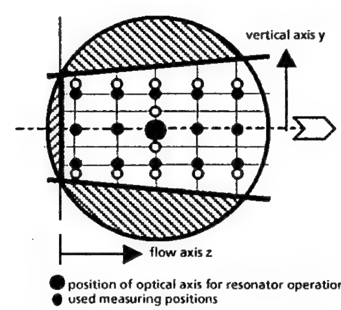

DLR

Variation of Secondary Helium Flow

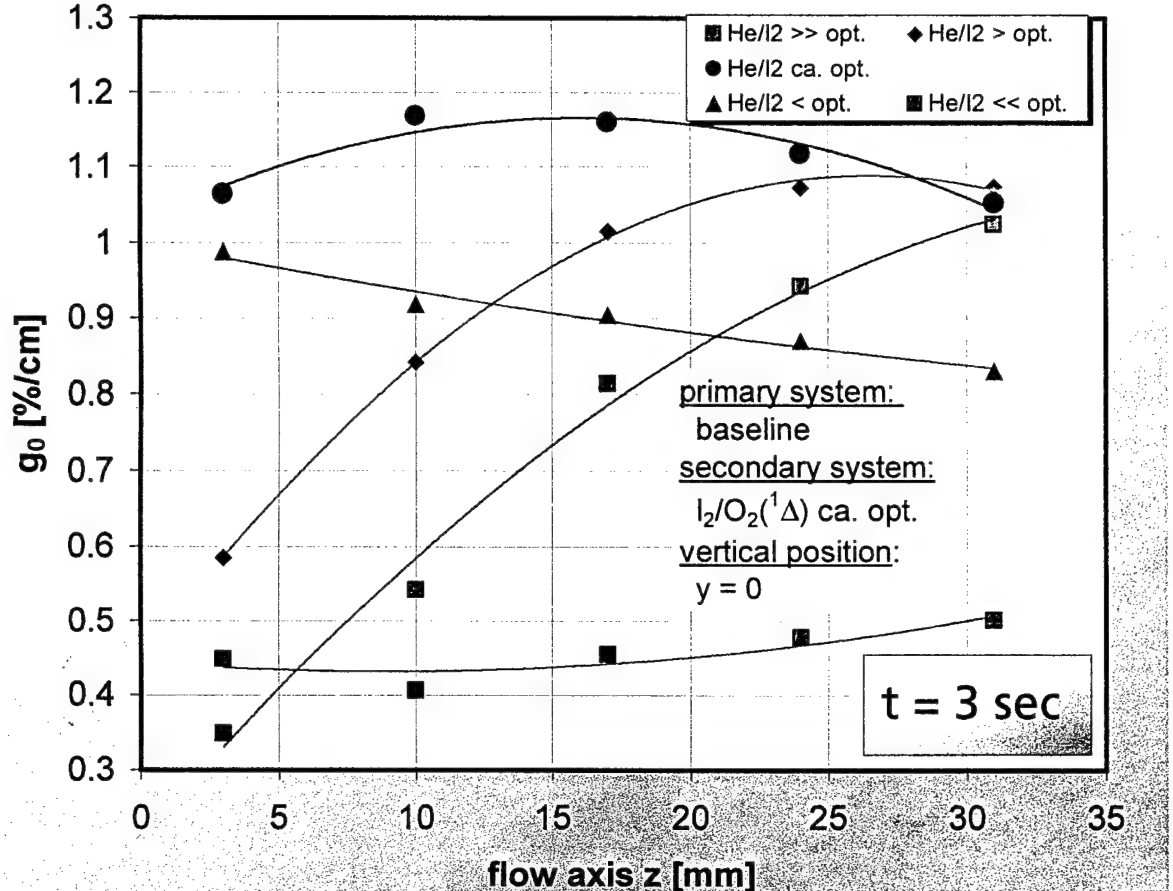

Comparison of Maximum Laser Power and Maximum Gain Variation of Secondary Helium Flow

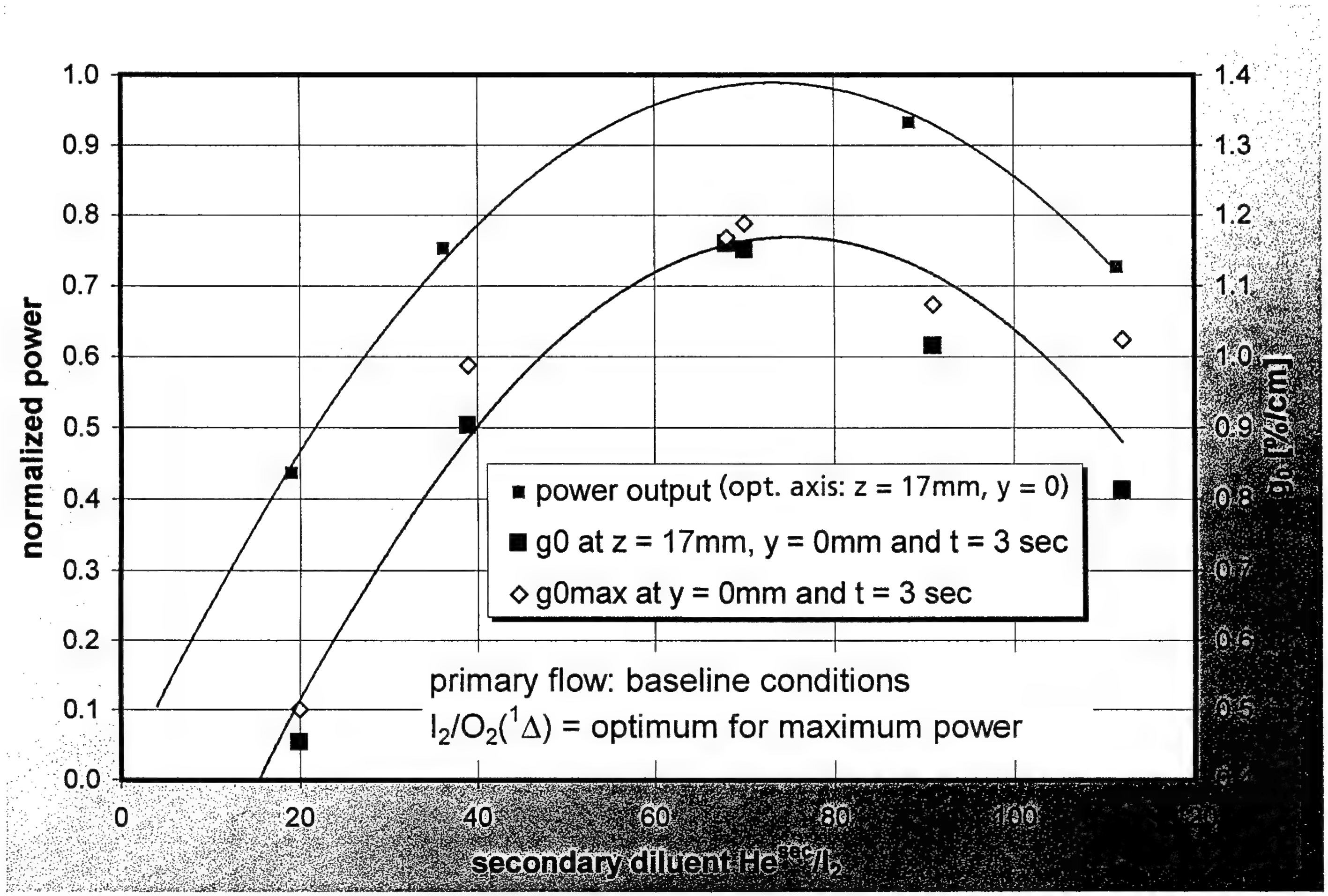

DLR

Comparison of Maximum Laser Power and Maximum Gain Variation of Iodine Flow

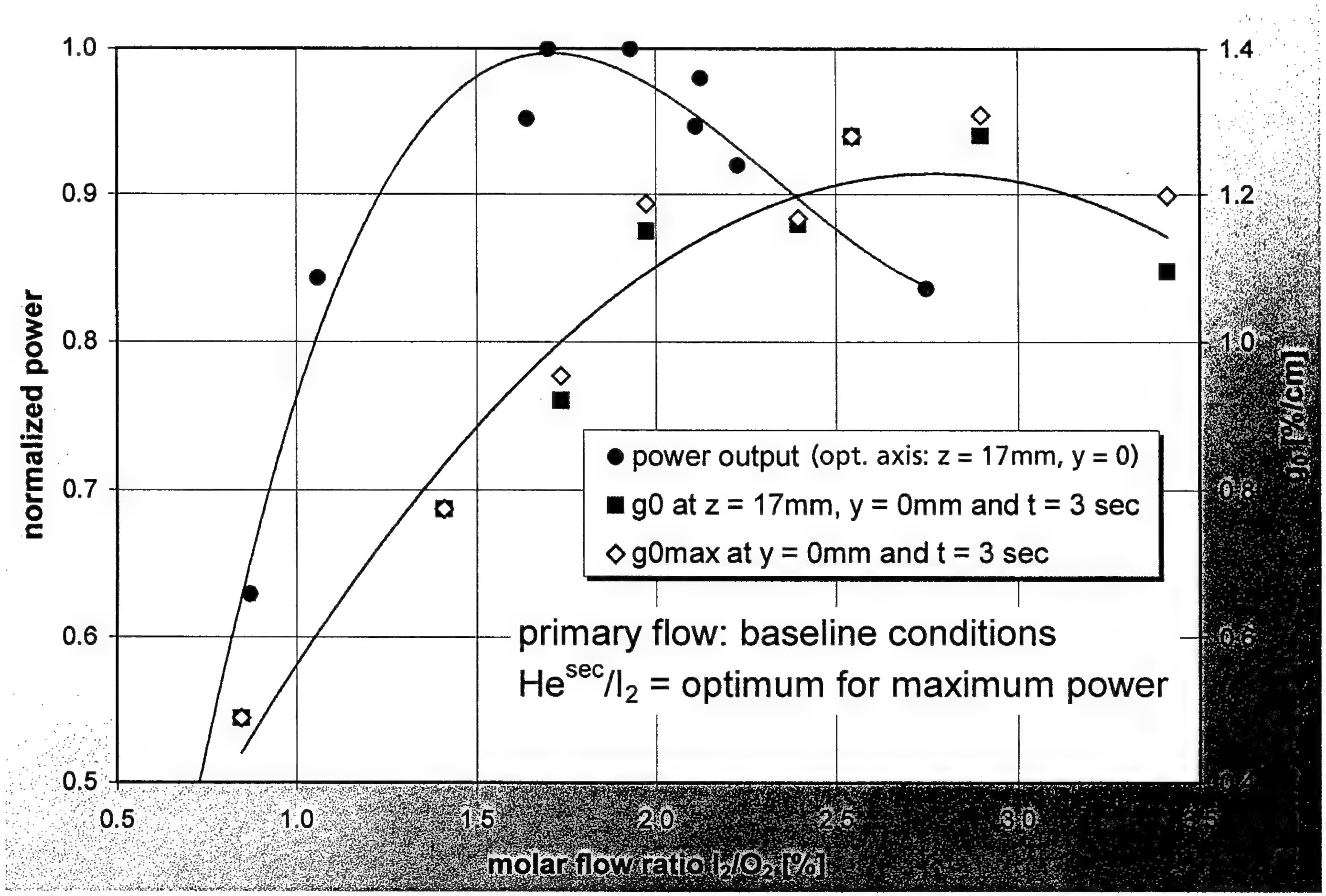

Variation of Iodine Flow

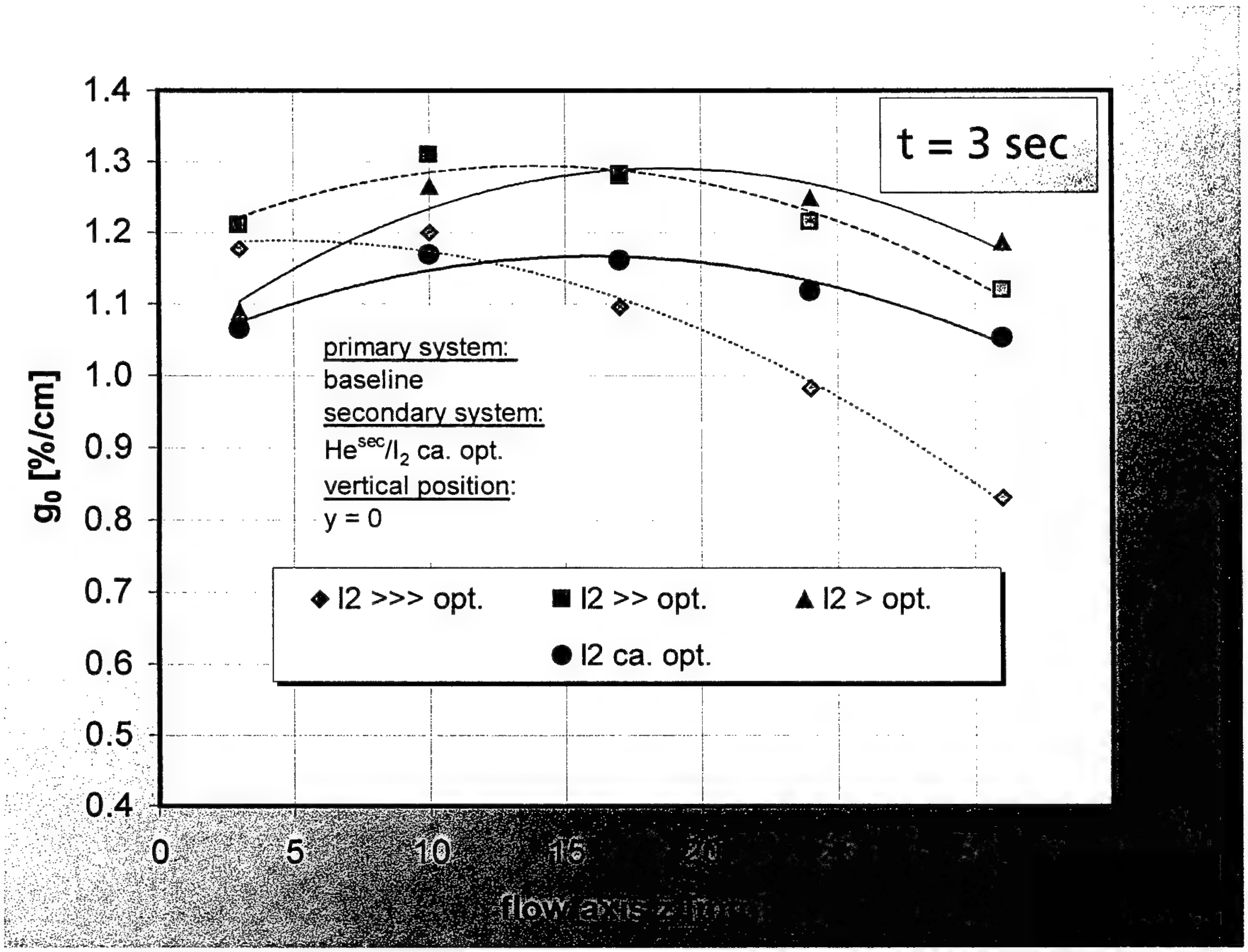

DLR

Variation of Iodine Flow

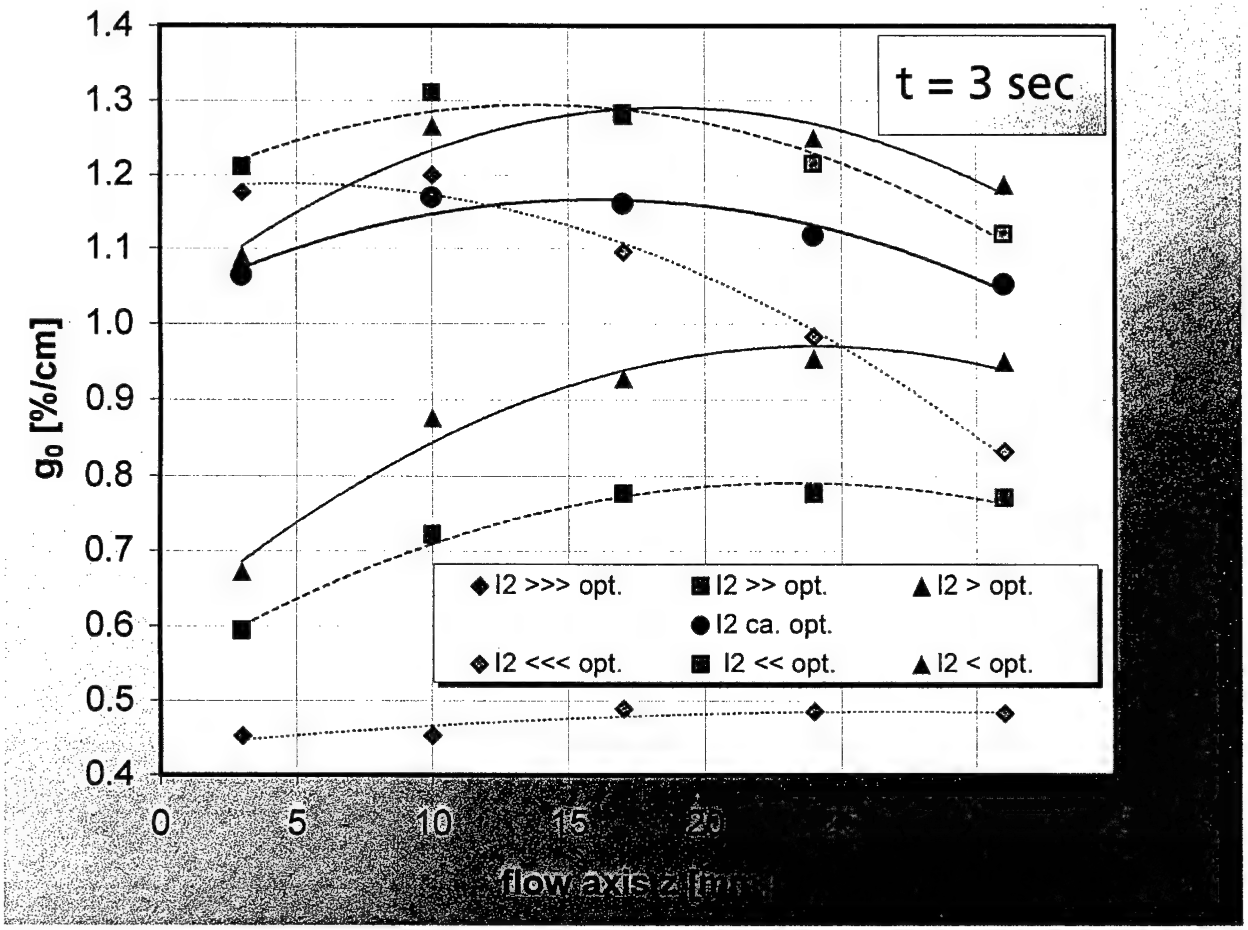

primary system:
baseline
secondary system:
Hesec/I2 ca. opt.
vertical position:
y = 0

DLR

Deutsches Zentrum für Luft- und Raumfahrt e.V.

Comparison of Measured Laser Power and Calculated Results

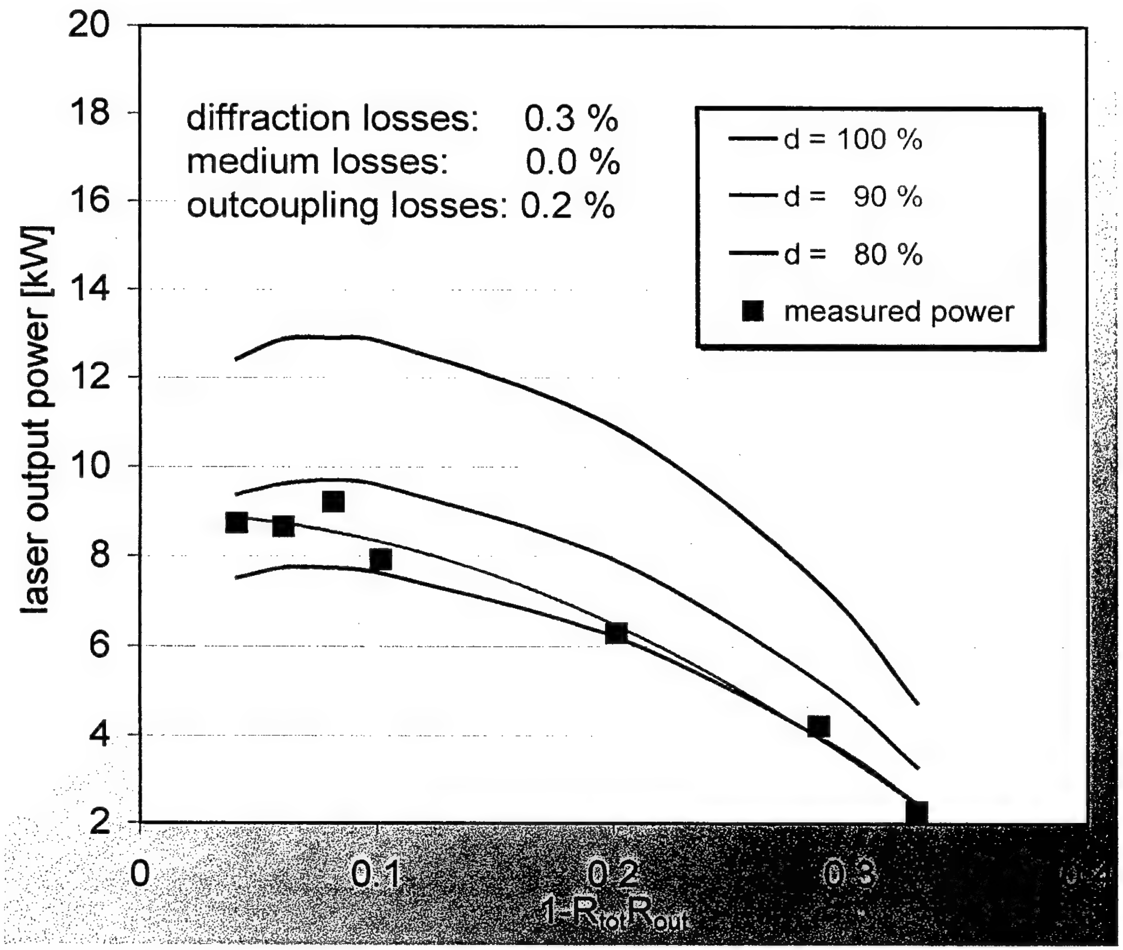

DLR

Calculated Laser Powers Dependent on the Dissociation Fraction

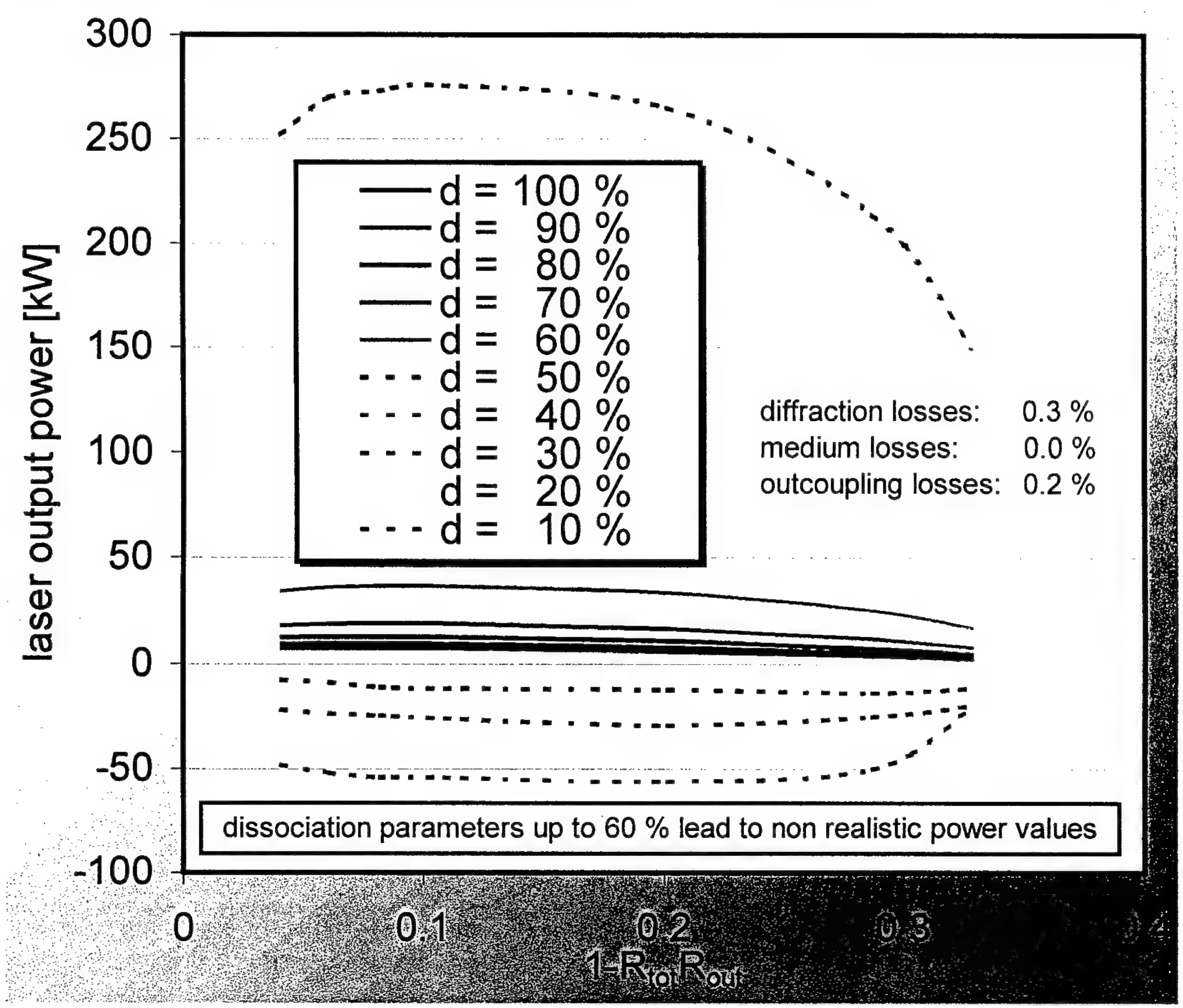

Summary

- Good accordance between predicted and measured values of ssg coefficient
- Linear time dependence of ssg coefficient (negative gradient) as well as of intra cavity temperatures (positive gradient)
- Intra cavity temperatures measured in a range of 200 K and above
- Local dependence of small signal gain coefficient is determined by gas mixing

  For optimum mixing conditions :
  - Ssg Coefficient of about 1.2 %/cm, nearly constant along the flow axis.
  - Dissociation coefficient in a range of 70 % - 90 %

  Non optimum mixing conditions:
  - Non constant local dependence of small signal gain coefficient
  - SSg Coefficient (averaged over the cavity length) smaller than 1.2 %/cm only exception: increased iodine molar flow rate

IODINE DISSOCIATION AND SMALL SIGNAL GAIN IN SUPERSONIC COILS

B. D. Barmashenko, D. Furman, E. Bruins and S. Rosenwaks

Department of Physics, Ben-Gurion University of the Negev,
Beer-Sheva 84105, Israel

COIL

$$I^*(^2P_{1/2}) \rightarrow I(^2P_{3/2}) + h\nu\ (1.315\mu m)$$

$$O_2(^1\Delta) + I(^2P_{3/2}) \rightarrow O_2(^3\Sigma) + I(^2P_{1/2})$$

Measurements: dependencies of the gain g and temperature T in t resonator on the iodine flow rate nI_2 for different kinds of nozzles. addition Y, U, water vapor fraction and T_{0i} were measured.

An analytical method for calculation of the iodine dissociation fracti F and the number N of $O_2(^1\Delta)$molecules lost in the region of iodi dissociation per I_2 molecule.

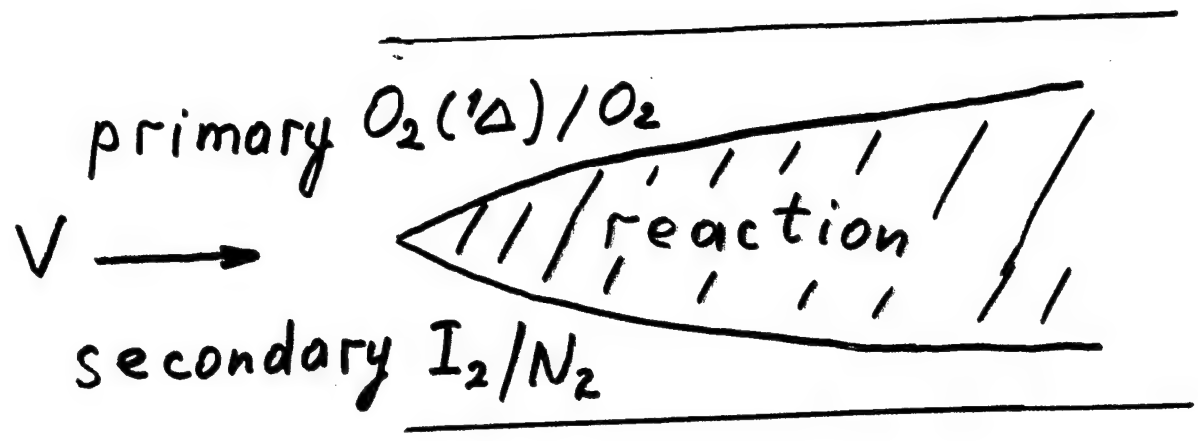

η_p, η_s — fractions of the primary or secondary flows present in the reaction zone

Relation between g, F and the $O_2(^1\Delta)$ yield Y at the optical axis:

$$g = \sigma_0 \left(\frac{300}{T} \right)^{1/2} \frac{p}{kT} \frac{n\mathrm{I}_2}{n} F \frac{(2K_e + 1)Y - 1}{(K_e - 1)Y + 1}, \qquad (1)$$

where $\sigma_0 = 7.5 \times 10^{-18}\ \mathrm{cm}^2$ and $Ke = 0.75 \exp(402/T)$ is the equilibriu constant of reaction (1).

Slit nozzle: right hand side of Eq. (1) is multiplied by

$$n/(n_p\eta_p + n_s\eta_s),$$

where $n_p = (n\mathrm{Cl}_2)_0 + n\mathrm{H2O}$ and $n_s = n\mathrm{N}_2 + n\mathrm{I}_2$, η_p and η_s are the mixi
efficiencies of the primary and secondary flow.

$$Y = Y_i - \frac{n\mathrm{I}_2 F}{n\mathrm{O}_2\eta_p} N, \tag{2}$$

N can be found from the energy conservation equation:

$$c_p[(n_p\eta_p + n_s\eta_s)T_0 - n_p\eta_p(T_{0i})_p - n_s\eta_s(T_{0i})_s] = q_\Delta n\mathrm{I}_2FN - q_{\mathrm{I}_2}n\mathrm{I}_2F -$$

$$q_{\mathrm{I}^*}n\mathrm{I}_2F\frac{2K_eY}{(K_e-1)Y+1}, \qquad (3$$

where c_p = 7/2 k , T_0 is the stagnation temperature of the flow in tl reaction zone, $(T_{0i})_p$ and $(T_{0i})_s$ are the stagnation temperatures of tl primary and secondary flows, q_Δ = 11,340 K, q_{I_2}= 18,400 K and $q_{\mathrm{I}*}$ 10,954 K

Find T_0

p is constant hence flow velocity V is constant ($\rho V\, dV/dx$ = - dp/dx =

$V^2/2 + c_p T = c_p T_0$, hence $\Delta(T_0/\mu) = \Delta(T/\mu)$:

$$T_0 = T_{0c}\frac{\mu}{\mu_c} + T - T_c\frac{\mu}{\mu_c},$$

where T_c and T_{0c} are static and stagnation temperatures in the "col runs without iodine.

T_c is found from $T(n\mathrm{I}_2)$ by extrapolation to to $n\mathrm{I}_2$, corresponding to ze gain.

g and *F* are nonmonotonous functions of nI_2.

This was predicted in B. D. Barmashenko, A. Elior, E. Lebiush and S. Rosenwaks, J. Appl. Phys., **75**, 7653 (1994).

For low $nI_2 < (nI_2)_c$, *F* increases with nI_2. This is due to an increase of [I*] that serve as the chain carriers for the dissociation reactions

$$O_2(^1\Delta) + I \rightarrow O_2(^3\Sigma) + I^*, \qquad I^* + I_2 \rightarrow I + I_2^*,$$

$$O_2(^1\Delta) + I_2^* \rightarrow O_2(^3\Sigma) + 2I$$

For high $nI_2 > (nI_2)_c$, *F* decreases with increasing nI_2. $O_2(^1\Delta)$, I^* and I_2 are quenched by I_2 which results in a retardation of the dissociation.

Grid nozzle

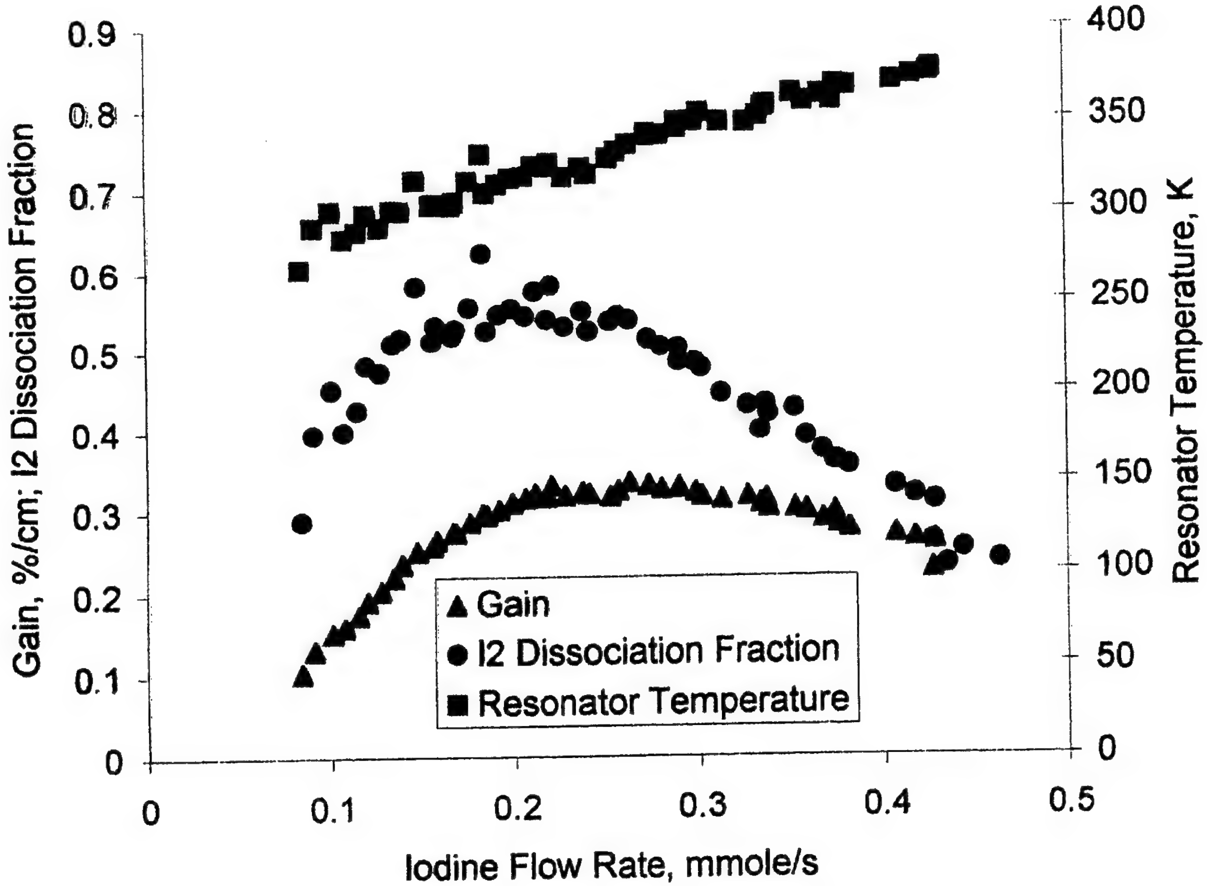

Cl2	11.7 mmol
Yield	0.65
Utilization	0.92
Water	0.12
Sec. N2	1.36 mmol
Stag. Temp.	340
Cold Res. Temp.	260
Res. Press.	1.4 Torr

To find η_p and η_s we compared $N(n\mathrm{I}_2)$ with the theoretical value of N

$$N_{th} = 1 + 1/\eta_{dis} - \frac{\left(k_w n\mathrm{H_2O} + k_o Y n\mathrm{O_2}\right)}{\eta_{dis} k_7 n\mathrm{I}_2} \frac{\eta_p}{\eta_s} \frac{\ln(1-F)}{F} + \frac{2K_e Y}{(K_e - 1)Y + 1},$$

$\eta_{dis} = k_1[\mathrm{O_2}(^1\Delta)]/(k_1[\mathrm{O_2}(^1\Delta)] + \sum_M k_{qM}[M])$ is the dissociation efficiency, k_1 is the rate of reaction $\mathrm{O_2}(^1\Delta) + \mathrm{I}_2^* \rightarrow \mathrm{O_2}(^3\Sigma) + 2\mathrm{I}$

B. D. Barmashenko and S. Rosenwaks, AIAA Journal, **34**, 2569 (1996)

V. Quan, Proc. SPIE, **2989**, 114 (1997).

Grid nozzle

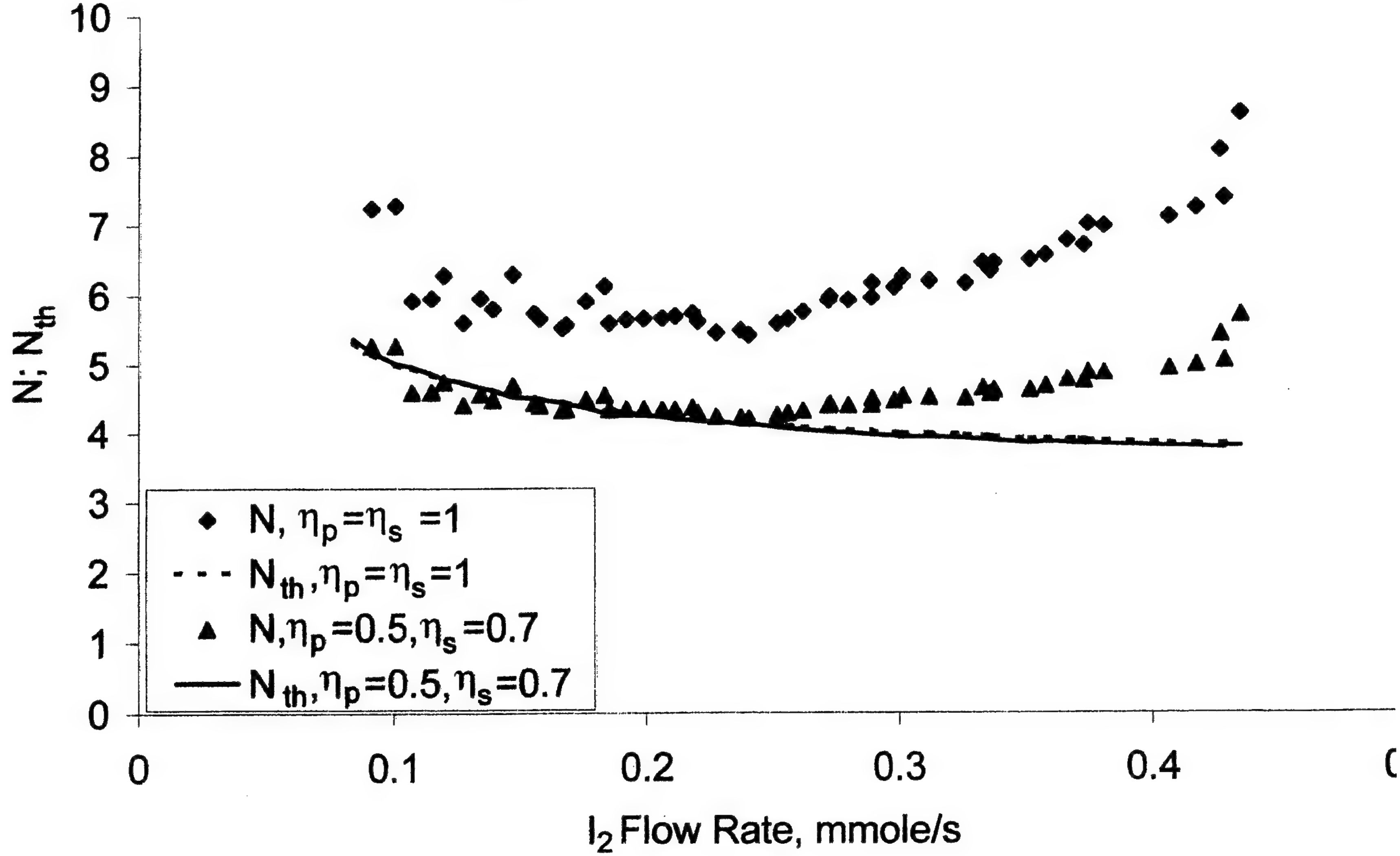
10
9
8
7
6
5
4
3
2
1
0
N; N_th
0
0.1
0.2
0.3
0.4
I_2 Flow Rate, mmole/s
N, η_p=η_s =1
N_th,η_p=η_s=1
N,η_p=0.5,η_s=0.7
N_th,η_p=0.5,η_s=0.7

Slit nozzle #1

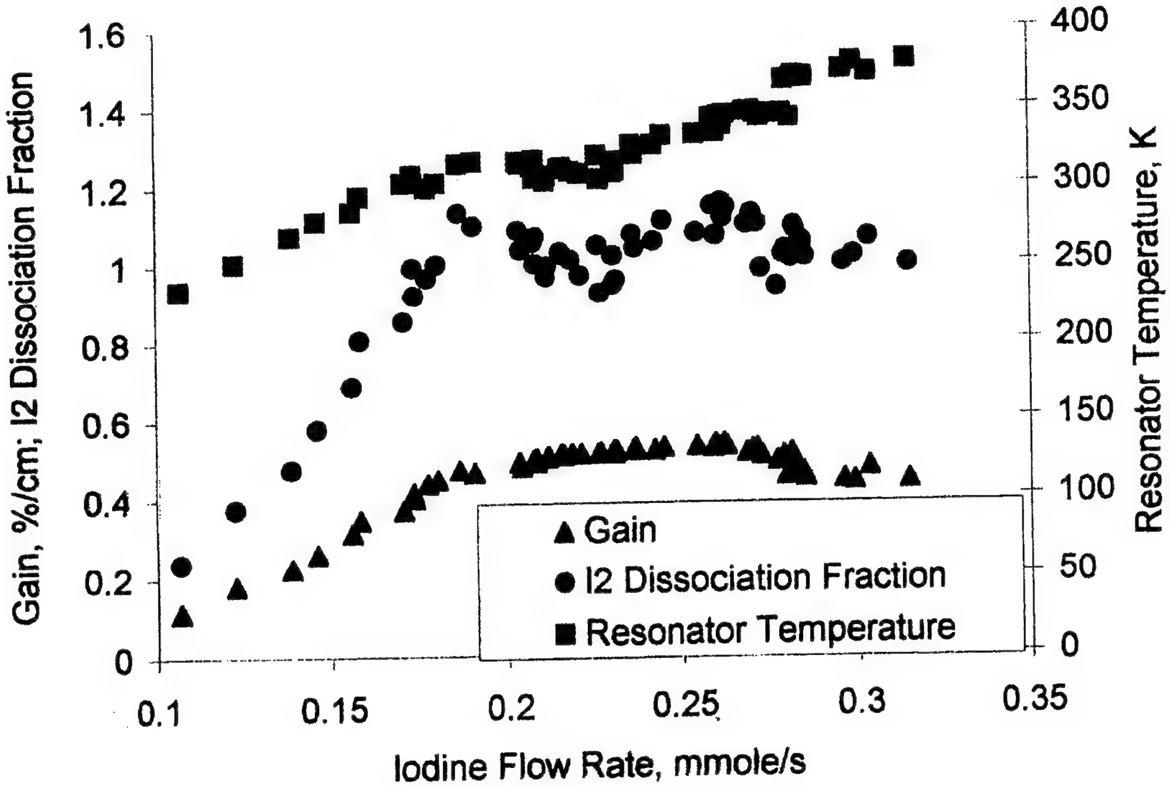

Cl2	11.7 mmol
Yield	0.6
Utilization	0.9
Water	0.12
Sec. N2	2.5 mmole/
Stag. Temp.	320
Cold Res. Temp.	260
Res. Press.	1.4 Torr

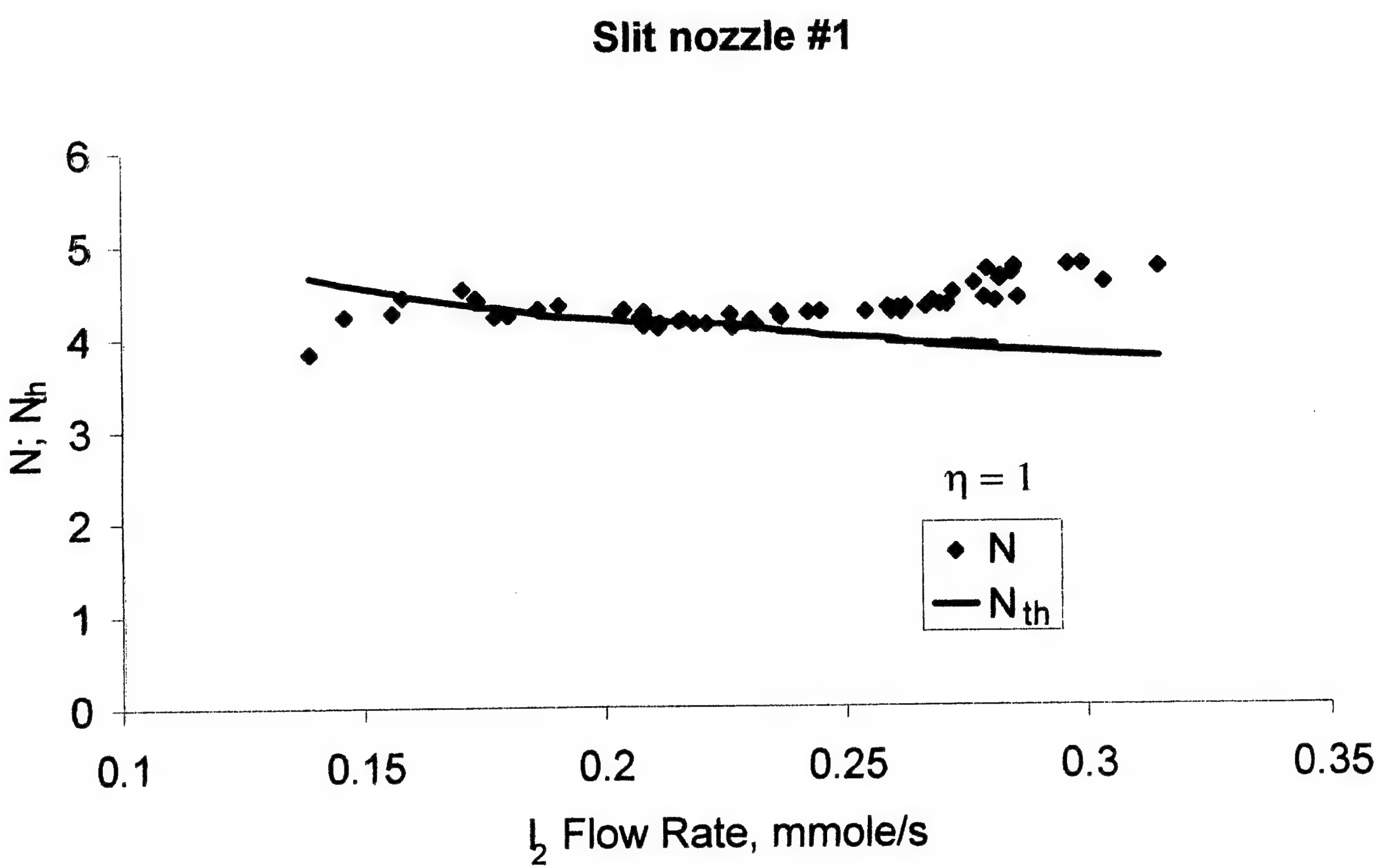

Slit nozzle #1
N; Nth
0
1
2
3
4
5
6
0.1
0.15
0.2
0.25
0.3
0.35
I2 Flow Rate, mmole/s
η = 1
N
Nth

Slit nozzle #1 (high Cl2 flow rate)

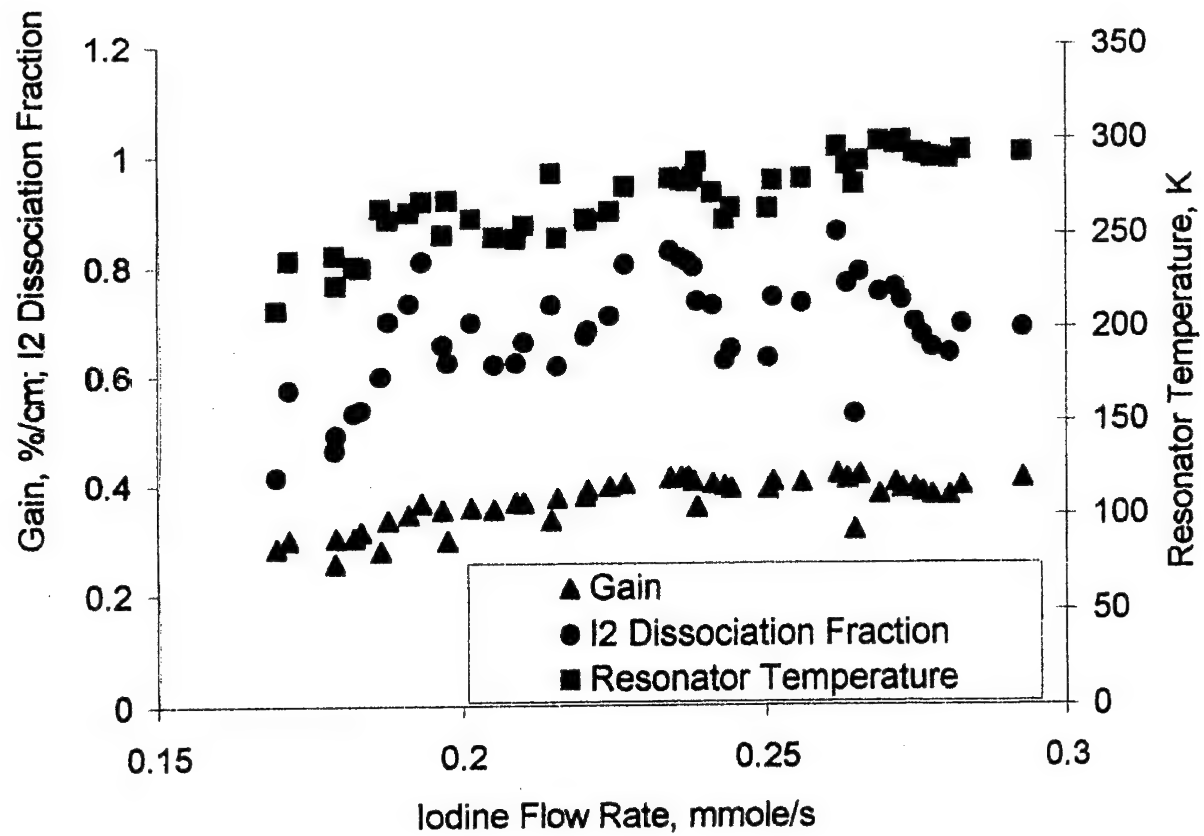

Cl2	19.5 mmole
Yield	0.55
Utilization	0.9
Water	0.12
Sec. N2	2.5 mmole/
Stag. Temp.	320
Cold Res. Temp.	230
Res. Press.	1.55 Torr

Slit nozzle No. 1 (high Cl_2 flow ra

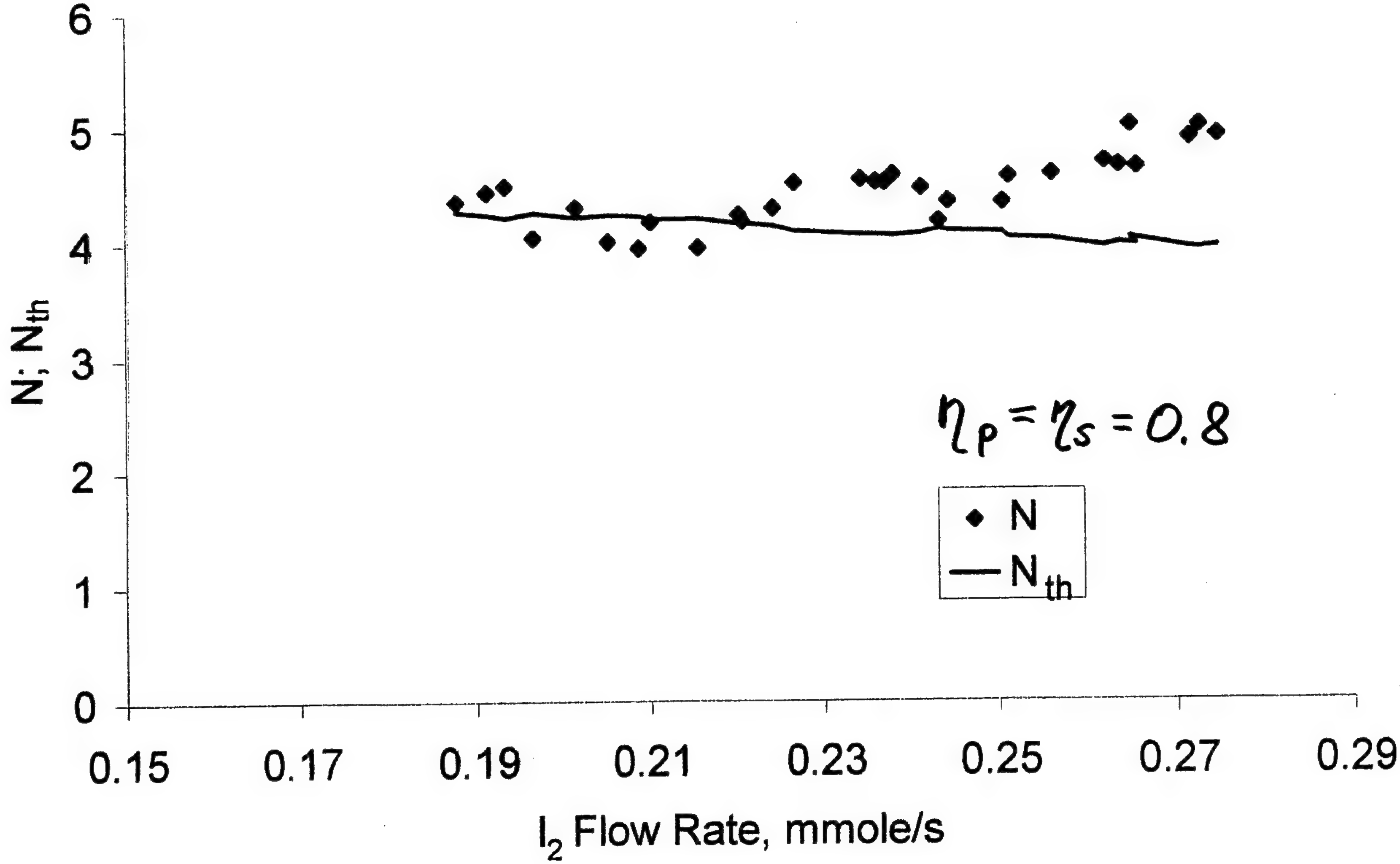

Slit nozzle #2

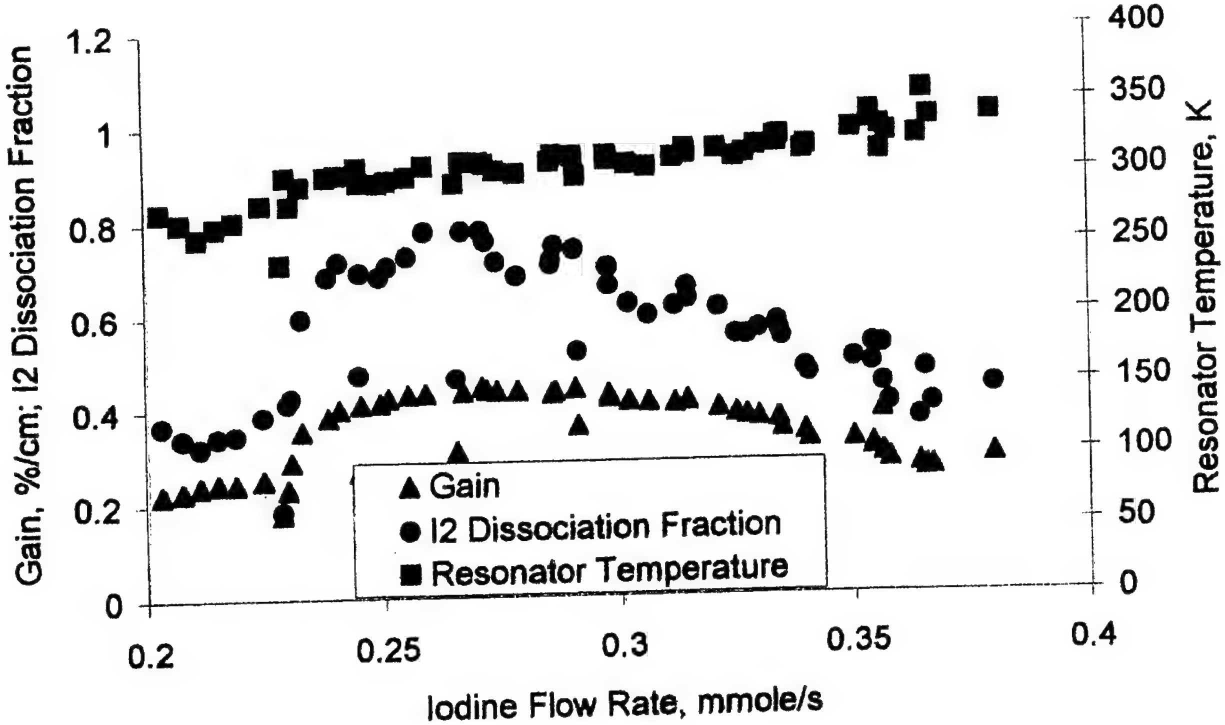

Cl2	11.8 mmole
Yield	0.55
Utilization	0.9
Water	0.12
Sec. N2	4 mmole/s
Stag. Temp.	350
Cold Res. Temp.	260
Res. Press.	1.45 Torr

Slit nozzle No. 2

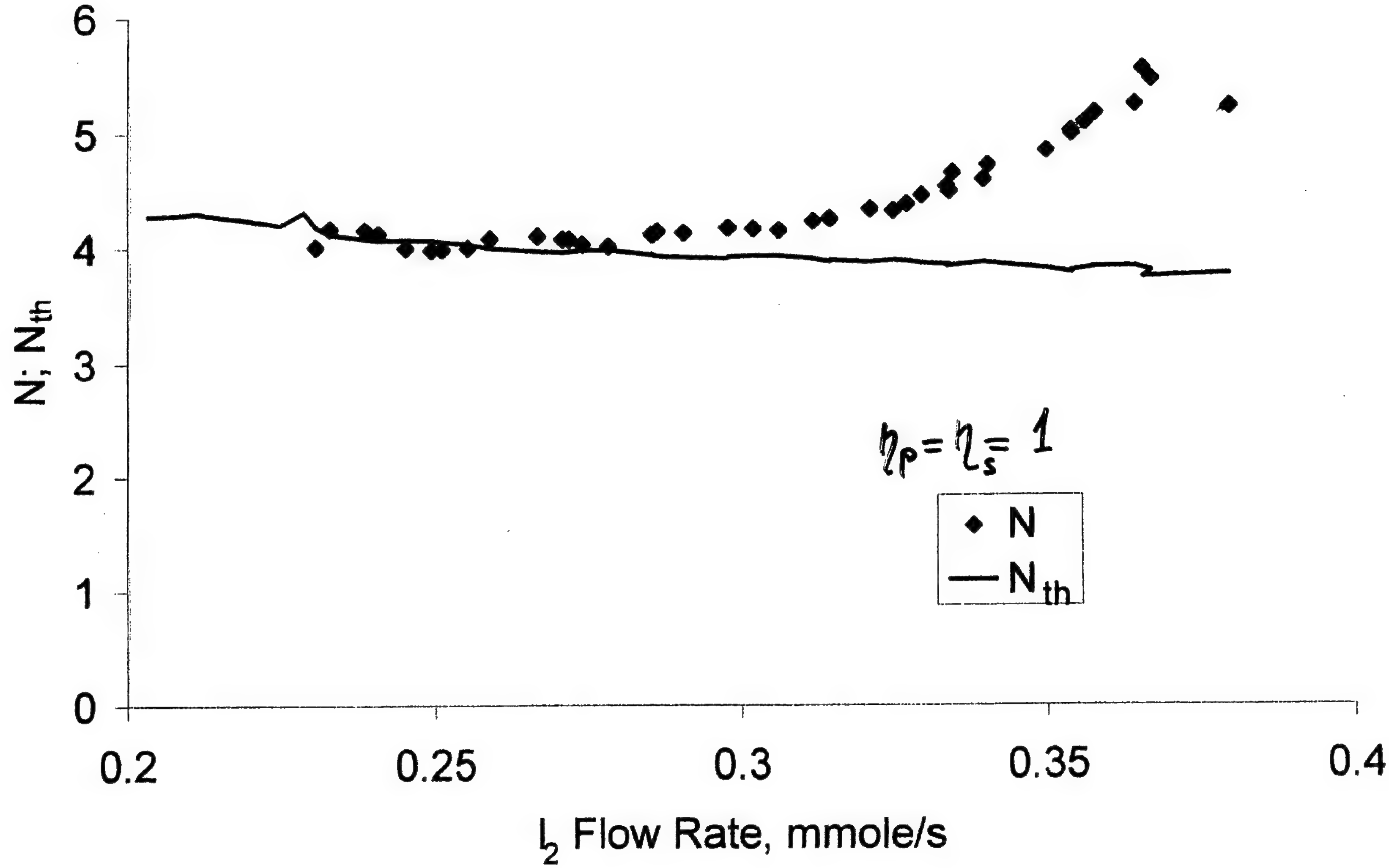

Slit nozzle #3 (supersonic injection)

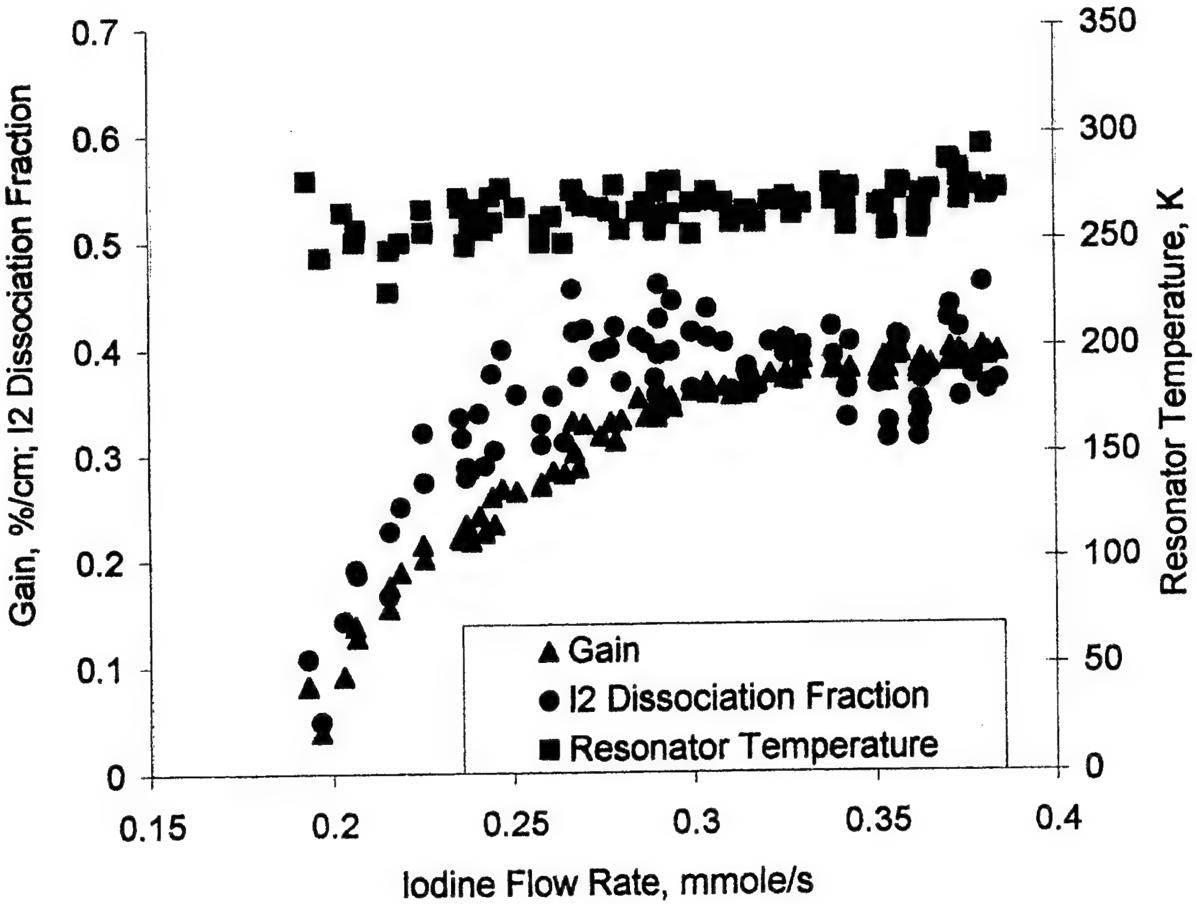

Cl2	11.7 mmol
Yield	0.55
Utilization	0.9
Water	0.12
Sec. N2	7 mmole/s
Stag. Temp.	320
Cold Res. Temp.	260
Res. Press.	1.55 Torr

Grid nozzle: $F = 0.55$ can be explained by slow mixing rate.
Both η_s and η_p are small.

Slit nozzle No. 1: for low Cl2 (11.7 mmole/s) $F = 1$, is much higher than for the grid nozzle due to higher mixing efficiency caused by larg optimal penetration. For higher Cl2 (19.5 mmole/s) F is about 0.8; smaller F is due to smaller mixing efficiency and higher flow velocity.

Slit nozzle No. 2: F is ~ 0.8, i. e. smaller than for the nozzle No.1.

Slit nozzle No. 3 (supersonic injection): F is ~ 0.45, i. e. much smaller than for the nozzle No.1.

Conclusions

1. An analytical method is developed, which enables the use (dependencies of g and T in the resonator of the supersonic CO $n\mathrm{I}_2$, for calculation of F and N.
2. F is a nonmonotonous function of $n\mathrm{I}_2$.
3. Maximum values of F are found for different types of the nozzle The highest $F\sim$ 1 is achieved for slit nozzle No. 1 with transon injection of iodine and small Cl2 flow rate of 11.7 mmole/s.
4. For the grid nozzle the mixing efficiencies are small (~ 0.5 – 0.7 For the slit nozzle No.1 the mixing efficiency is much higher th for the grid nozzle (~1).For higher Cl2 flow rate mixing efficiency smaller (~ 0.8).

An Investigation of Supersonic Mixing Mechanisms for the Chemical Oxygen-Iodine Laser (COIL)

Dr. Timothy Madden and Dr. Gordon Hager

Air Force Research Laboratory

Alan Lampson and Dr. Peter Crowell

Northrup Logicon Division

Outline

- Introduction
- Methodology
- Results
- Summary and Conclusion

Introduction

- Traditional COIL's have injected the I_2/diluent mixture in the subsonic region of the mixing nozzle.
  - This placement was driven by the interplay between mixing, I_2 dissociation, and transport through the nozzle flow.
- Can the I_2/diluent mixture be injected in the supersonic region of the nozzle without degrading performance?

Introduction (cont.)

- Supersonic injection offers potential performance improvements.
  - De-couples the generator from the injection process.
  - Improved mirror loadings.
  - Lower deactivation losses.
    - Introduces the possibility of injecting I atoms with minimal I* deactivation.
    - Supersonic injection is logical for I atoms because it minimizes I* deactivation losses during transport.

Methodology

- The different injection concepts are modeled using the MINT CFD code from Scientific Research Associates.
  - Solves the 3D Navier-Stokes equations coupled to finite-rate chemistry, detailed molecular diffusion, and Fabry-Perot power extraction models.
  - Extensively validated as an accurate tool for modeling COIL flowfields.

Methodology (cont.)

AFRL Standard COIL Chemistry Mechanism

	Reaction	Rate (cc/molecule-sec)
1	$O_2(^1\Delta) + O_2(^1\Delta) \rightarrow O_2(^1\Sigma) + O_2(^3\Sigma)$	$2.7\cdot10^{-17}$
2	$O_2(^1\Sigma) + H_2O \rightarrow O_2(^3\Sigma) + H_2O$	$6.7\cdot10^{-12}$
3	$O_2(^1\Delta) + O_2(^3\Sigma) \rightarrow O_2(^3\Sigma) + O_2(^3\Sigma)$	$1.6\cdot10^{-18}$
4	$O_2(^1\Delta) + H_2O \rightarrow O_2(^3\Sigma) + H_2O$	$4.0\cdot10^{-18}$
5	$O_2(^1\Delta) + Cl_2 \rightarrow O_2(^3\Sigma) + Cl_2$	$6.0\cdot10^{-18}$
6	$O_2(^1\Delta) + He \rightarrow O_2(^3\Sigma) + He$	$8.0\cdot10^{-21}$
7	$I_2 + O_2(^1\Sigma) \rightarrow 2I(^2P_{3/2}) + O_2(^3\Sigma)$	$4.0\cdot10^{-12}$
8	$I_2 + O_2(^1\Sigma) \rightarrow I_2 + O_2(^1\Delta)$	$1.6\cdot10^{-11}$
9	$I_2 + O_2(^1\Delta) \rightarrow I_2^* + O_2(^3\Sigma)$	$7.0\cdot10^{-15}$
10	$I_2 + I(^2P_{1/2}) \rightarrow I(^2P_{3/2}) + I_2^*$	$3.8\cdot10^{-11}$
11	$I_2^* + O_2(^1\Delta) \rightarrow 2I(^2P_{3/2}) + O_2(^3\Sigma)$	$3.0\cdot10^{-10}$
12	$I_2^* + O_2(^3\Sigma) \rightarrow I_2 + O_2(^3\Sigma)$	$5.0\cdot10^{-11}$
13	$I_2^* + H_2O \rightarrow I_2 + H_2O$	$3.0\cdot10^{-10}$
14	$I_2^* + He \rightarrow I_2 + He$	$3.2\cdot10^{-11}$
15	$I(^2P_{3/2}) + O_2(^1\Delta) \rightarrow I(^2P_{1/2}) + O_2(^3\Sigma)$	$2.33\cdot10^{-8}/T$
16	$I(^2P_{1/2}) + O_2(^3\Sigma) \rightarrow I(^2P_{3/2}) + O_2(^1\Delta)$	$3.1\cdot10^{-8}/T$ $\cdot\exp(-401.4/T)$
17	$I(^2P_{3/2}) + O_2(^1\Delta) \rightarrow I(^2P_{3/2}) + O_2(^3\Sigma)$	$1.0\cdot10^{-15}$
18	$I(^2P_{1/2}) + O_2(^1\Delta) \rightarrow I(^2P_{3/2}) + O_2(^1\Sigma)$	$1.1\cdot10^{-13}$
19	$I(^2P_{1/2}) + O_2(^1\Delta) \rightarrow I(^2P_{3/2}) + O_2(^3\Sigma)$	$5.0\cdot10^{-14}$
20	$I(^2P_{1/2}) + I(^2P_{3/2}) \rightarrow I(^2P_{3/2}) + I(^2P_{3/2})$	$1.6\cdot10^{-14}$
21	$I(^2P_{1/2}) + H_2O \rightarrow I(^2P_{3/2}) + H_2O$	$2.0\cdot10^{-12}$

Methodology (cont.)

- One subsonic and two supersonic injection concepts are modeled:
  - Subsonic and supersonic I_2/He injection.
  - I/DF/He injection
    - I atoms are assumed to be the product of the reaction $F+DI \rightarrow DF+I$.

Methodology (cont.)

- Flow conditions
  - $He/Cl_2 = 4/1$
  - $I_2/O_2 = 0.018$, $I/O_2 = 0.036$
  - Yield nominally > 50%
  - Low H_2O - condensation assumed negligible.

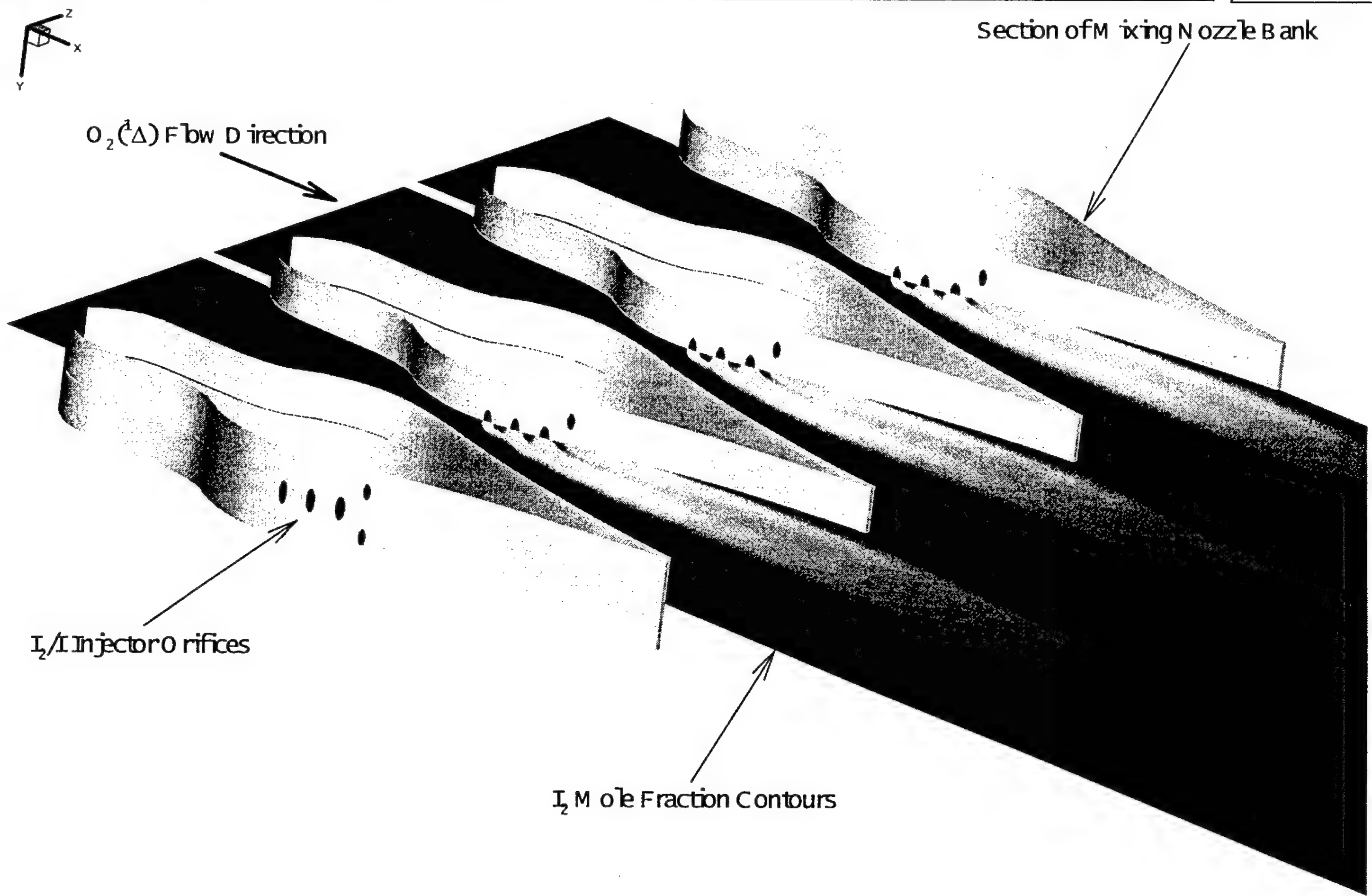

3D MINT CFD Simulation of Supersonic Injection of I_2 into $O_2(^1\Delta)$ Flow

Results

- Subsonic I_2/He injection.

Total Iodine Mass Fraction from MINT Simulation of COIL Mixing Nozzle with Subsonic Injection, I_2 Injected

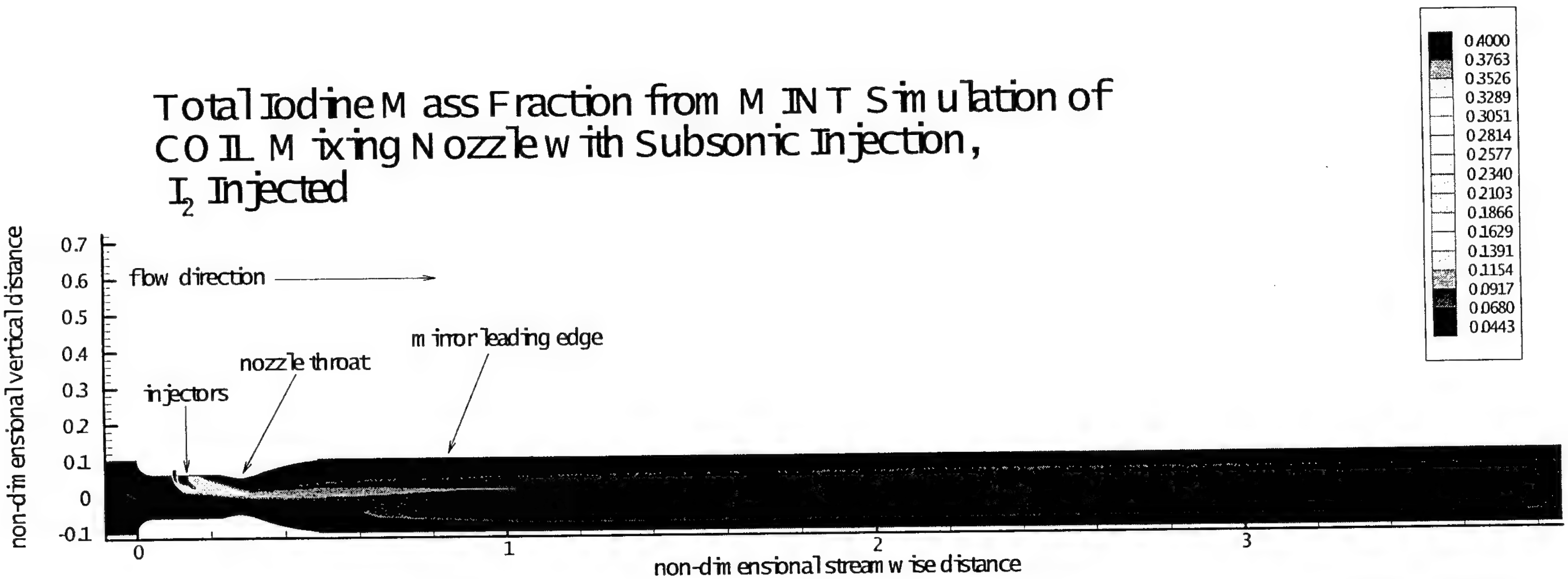

I_2 Mass Fractions from MINT Simulation of COIL Mixing Nozzle with Subsonic Injection, I_2 Injected

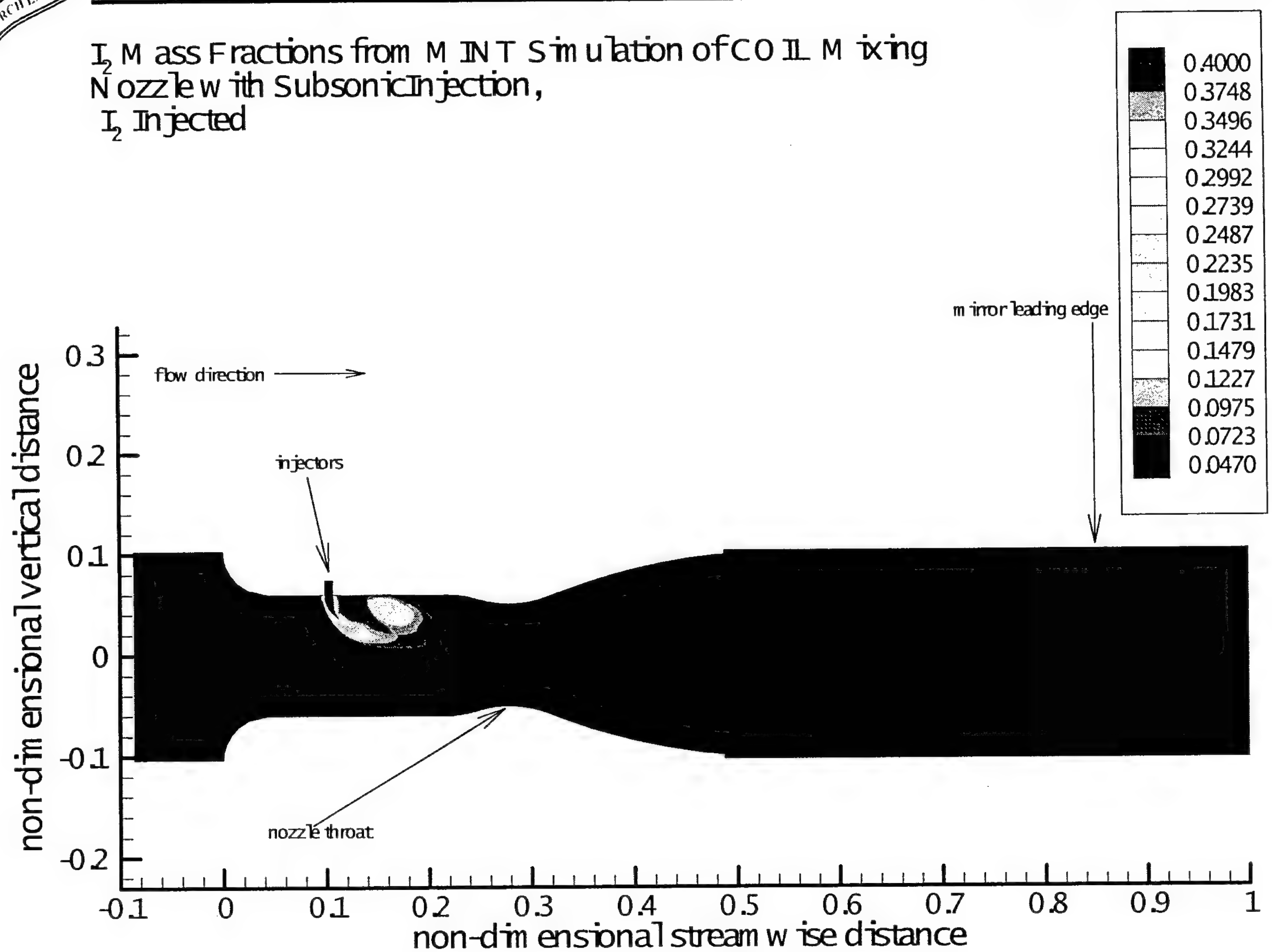

Gain (cm^{-1}) from MINT Simulation of COIL Mixing Nozzle with Subsonic Injection, I_2 Injected

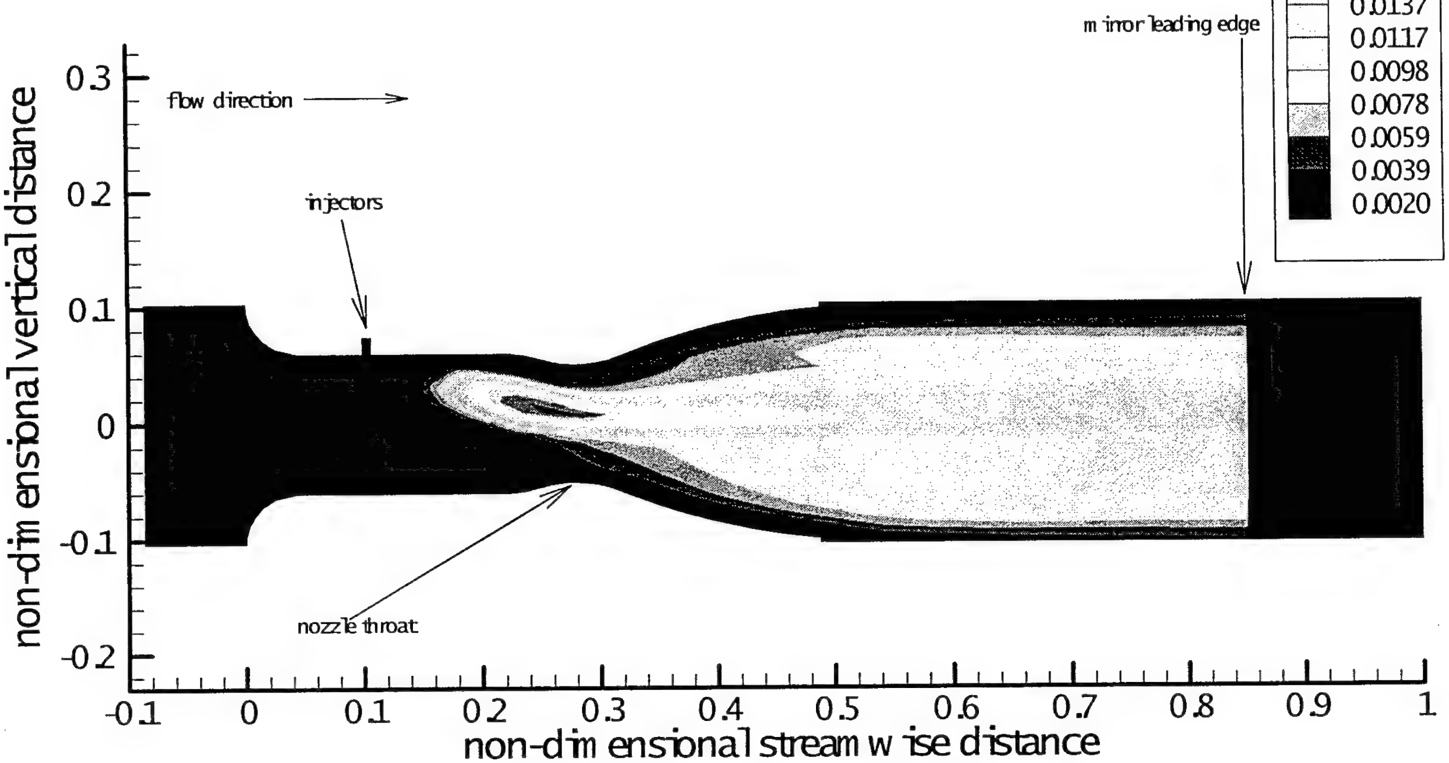

Results

- Supersonic I_2/He injection.

Total Iodine Mass Fraction from MINT Simulation of COIL Mixing Nozzle with Supersonic Injection, I_2 Injected

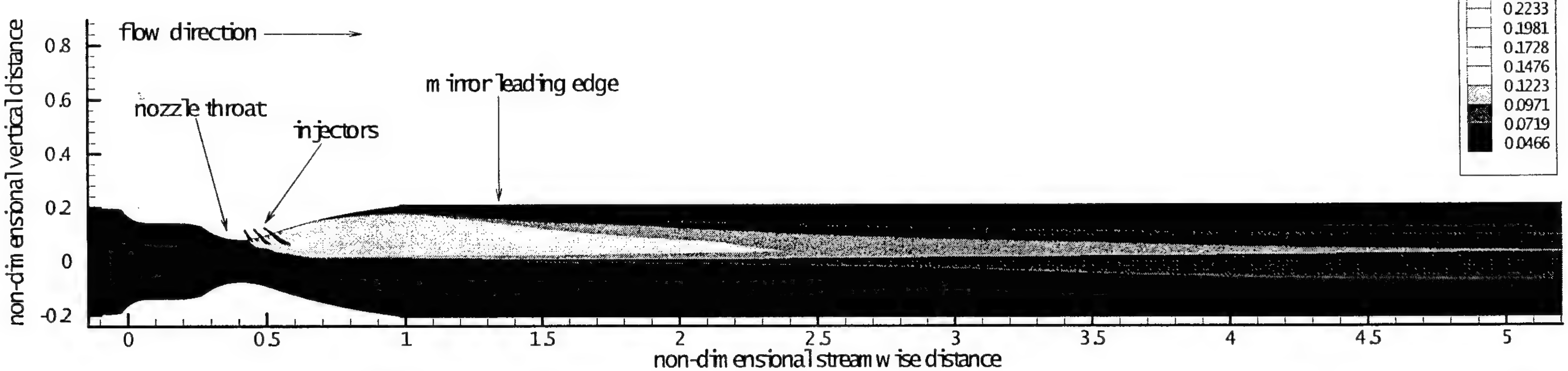

I_2 Mass Fractions from MINT Simulation of COIL Mixing Nozzle with Supersonic Injection, I_2 Injected

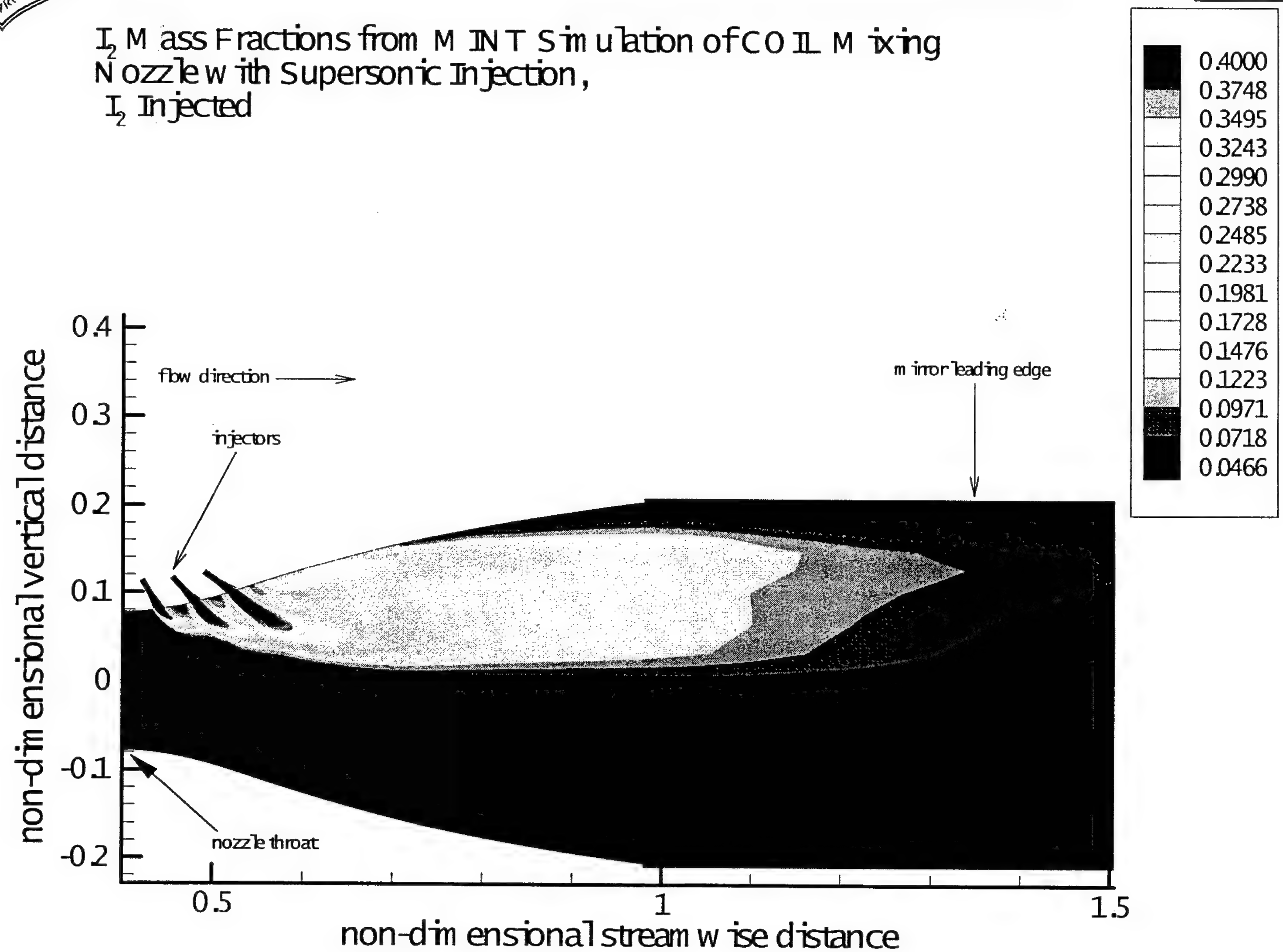

Gain (cm^{-1}) from MINT Simulation of COIL Mixing Nozzle with Supersonic Injection, I_2 Injected

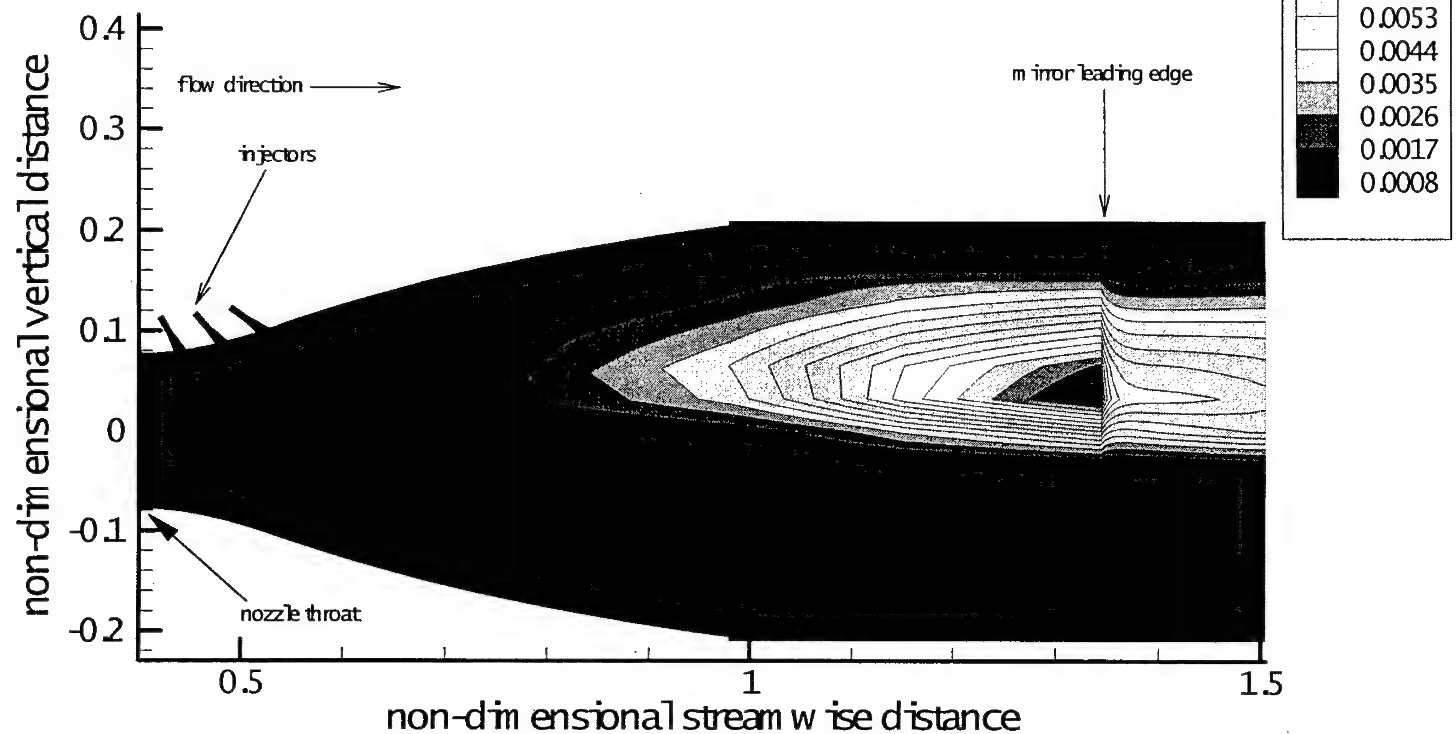

Results

- I/DF/He injection

I Mass Fraction from MINT Simulation of COIL Mixing Nozzle with Supersonic Injection, I atoms Injected

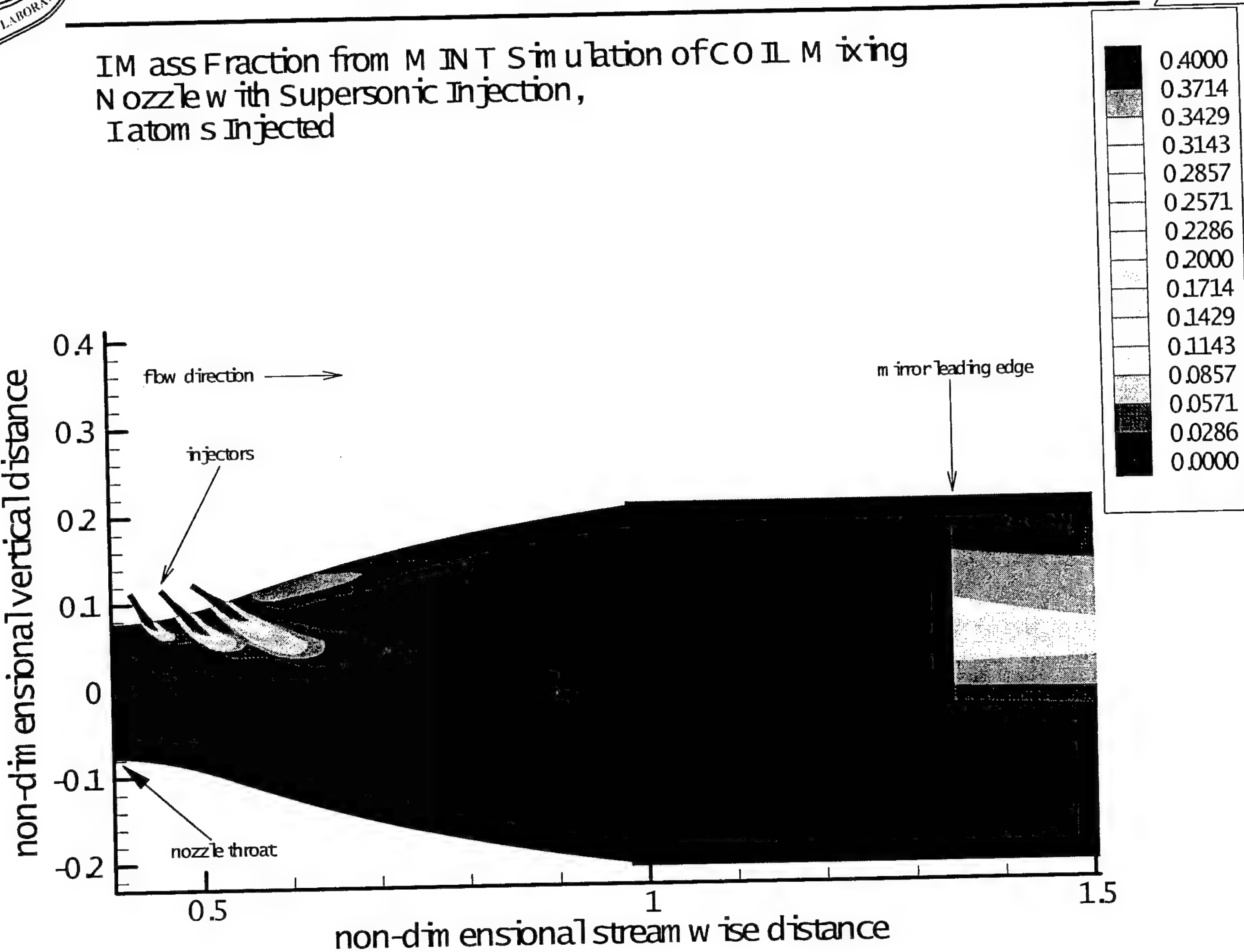

Gain (cm^{-1}) from MINT Simulation of COIL Mixing Nozzle with Supersonic Injection, I atoms Injected

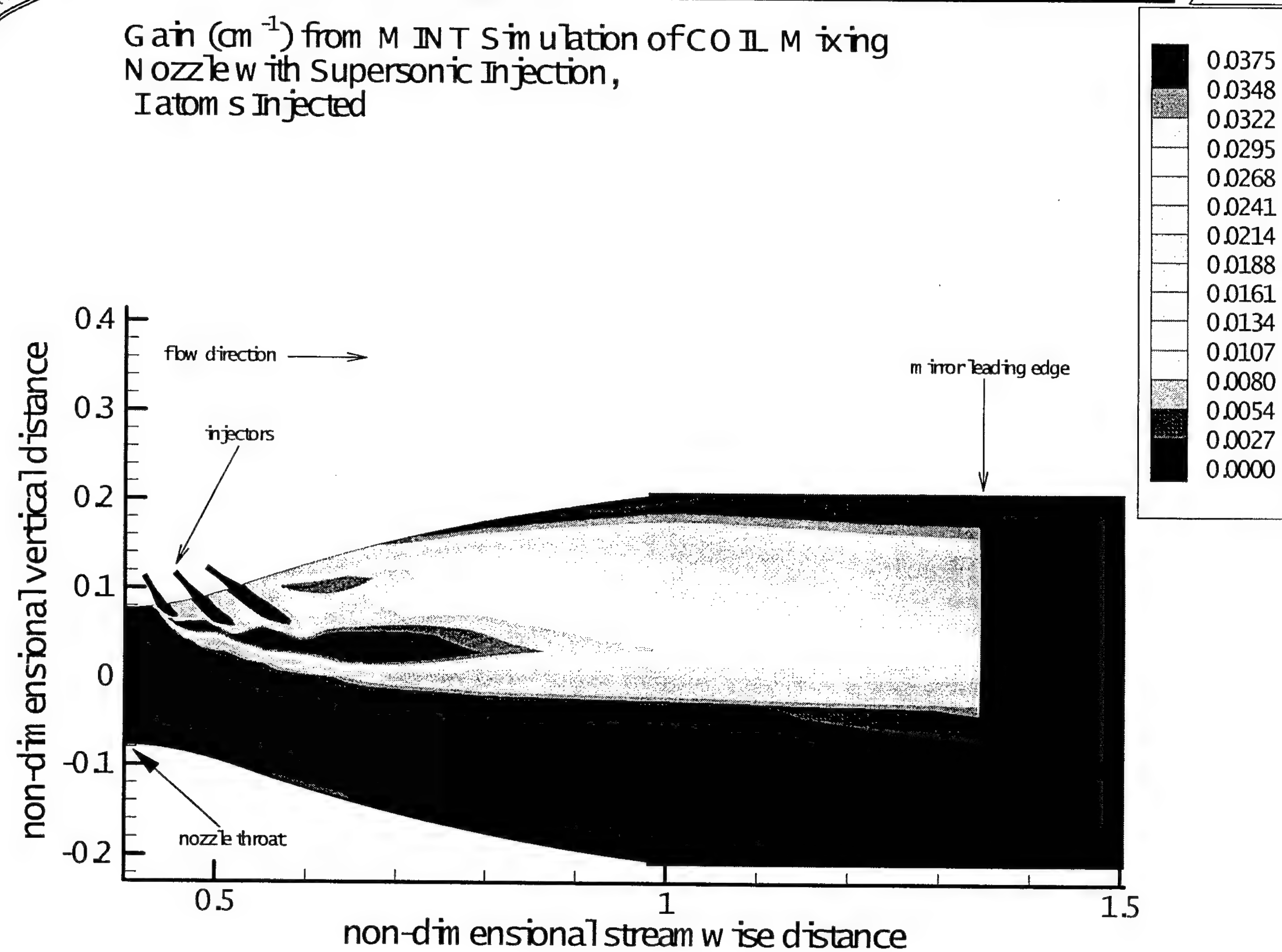

Comparison of MINT Model Predictions of Average Gain using Subsonic and Supersonic Injection

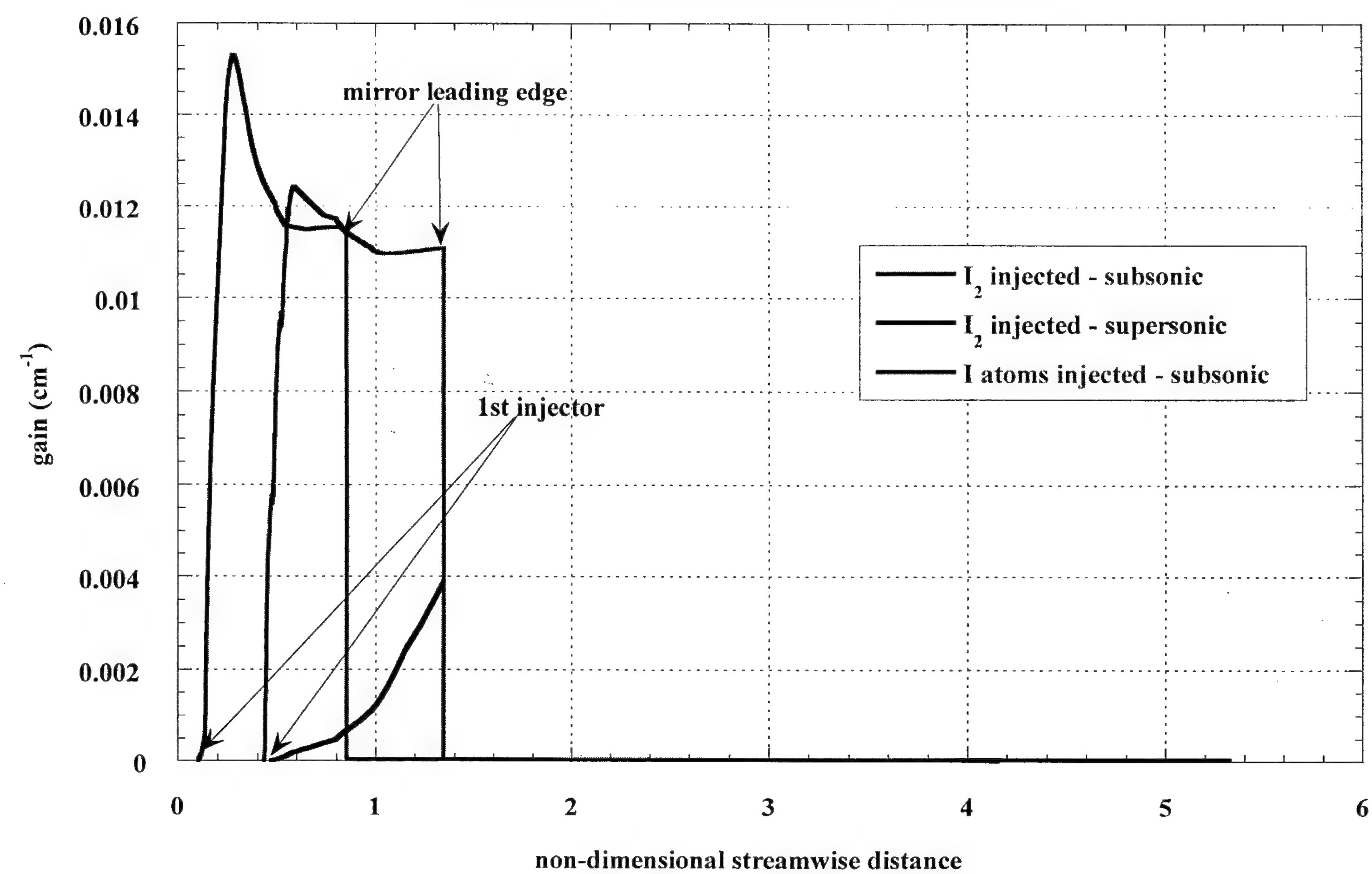

Comparison of MINT Model Predictions of I_2 Dissociation using Subsonic and Supersonic Injection

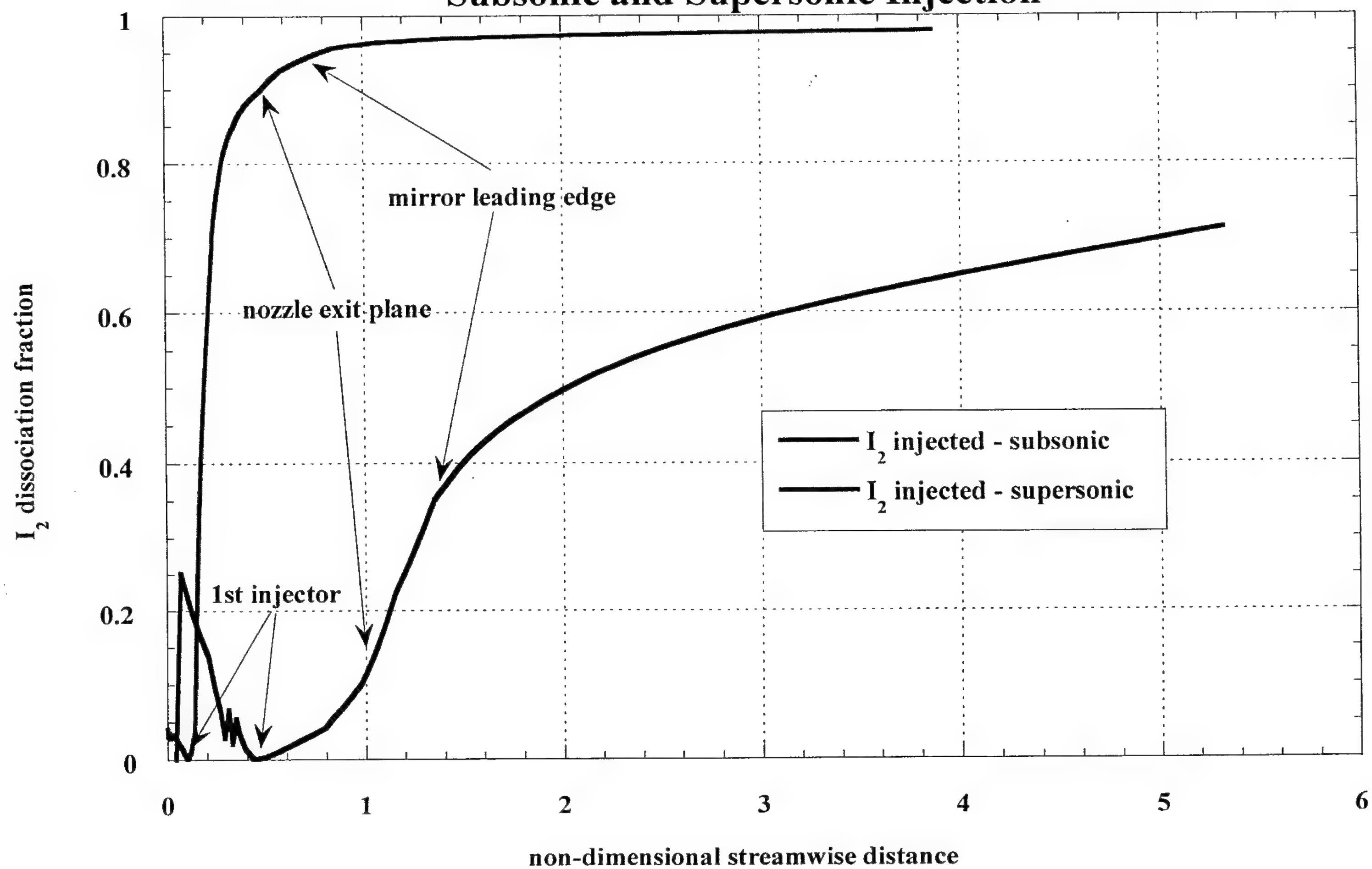

Comparison of MINT Model Predictions of Power Extraction using Subsonic and Supersonic Injection

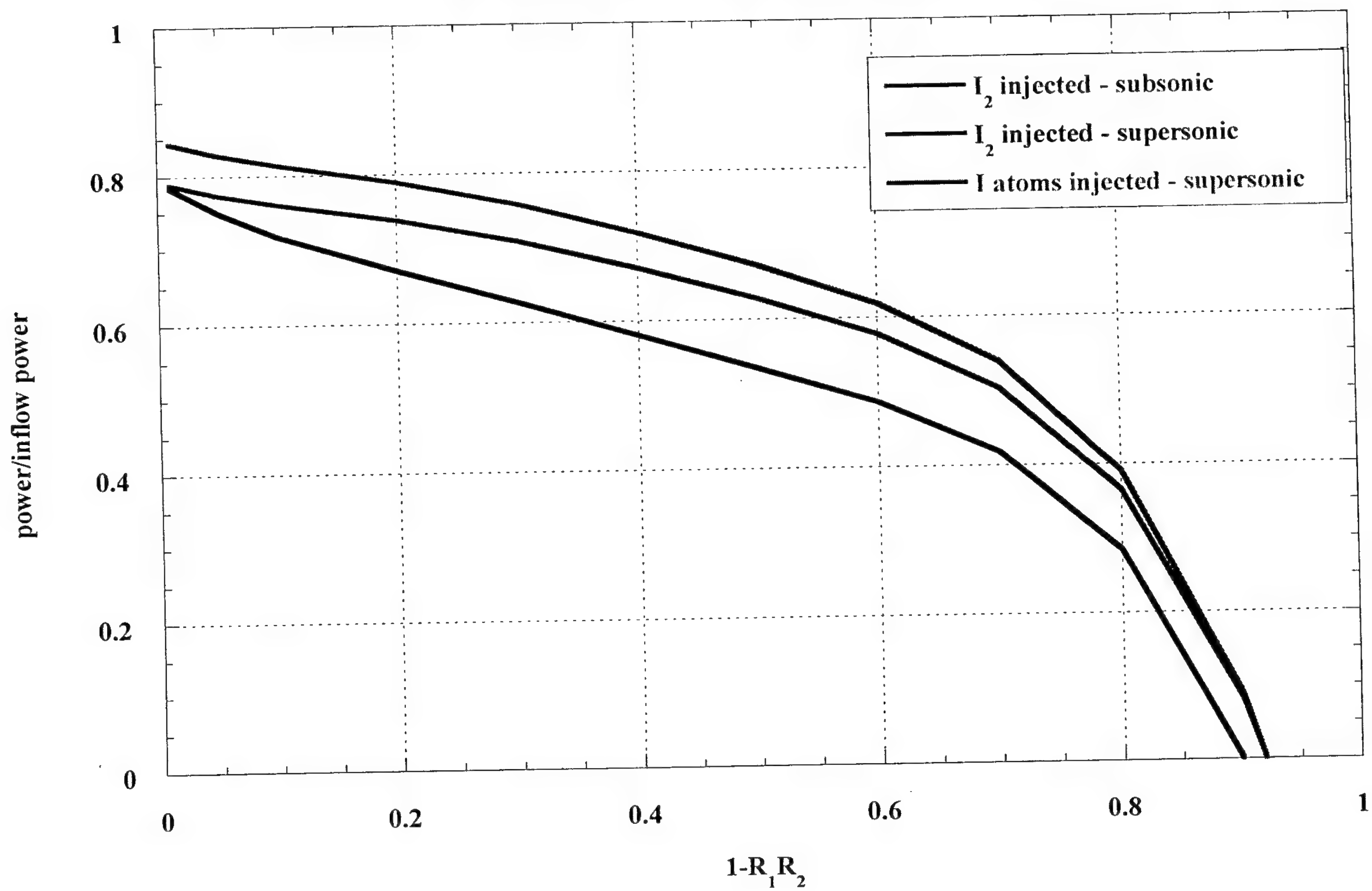

Comparison of MINT Model Predictions of $O_2(^1\Delta)$ Energy Removal using Subsonic and Supersonic Injection

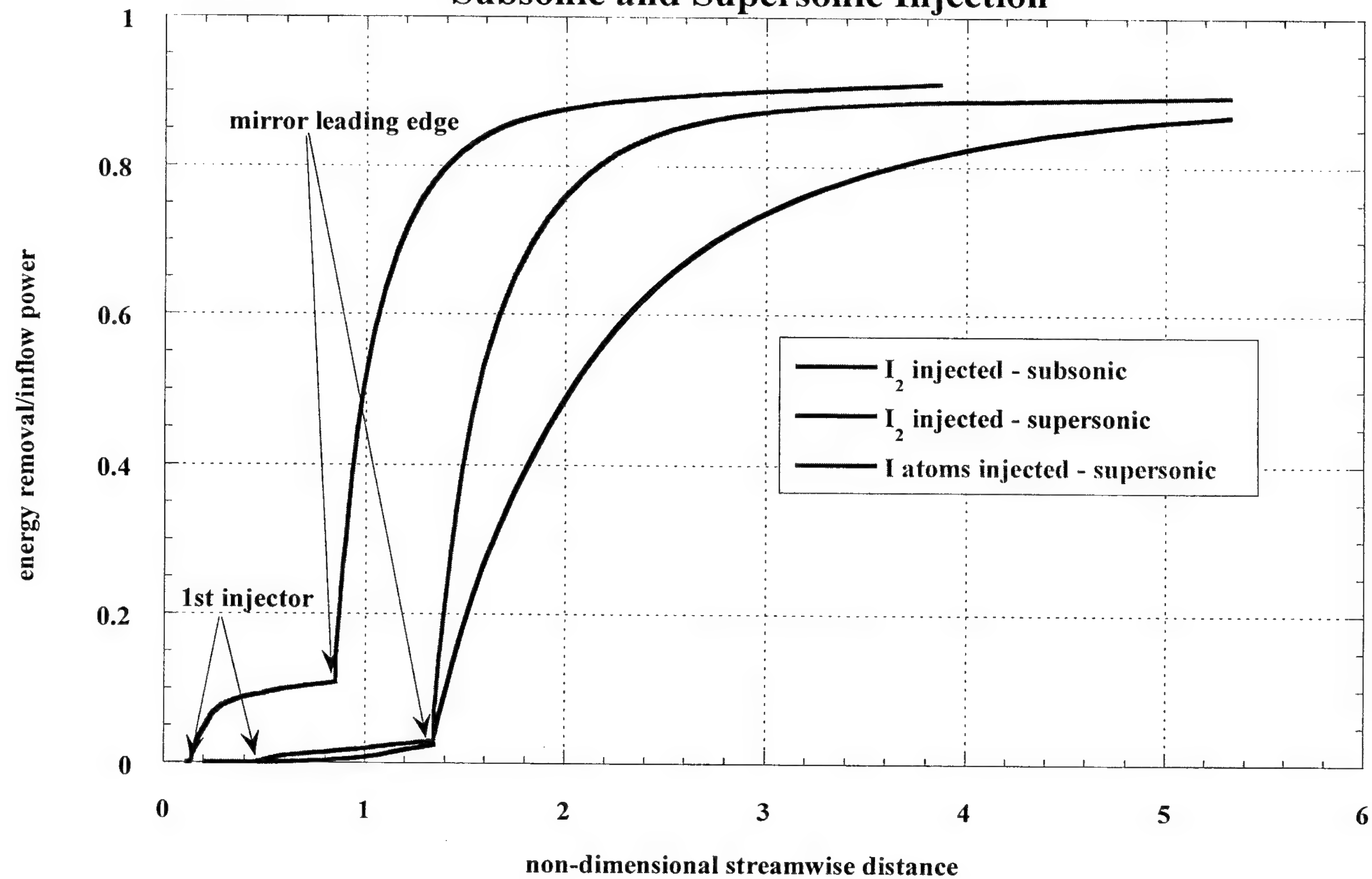

	Subsonic I_2 Injection	Supersonic I_2 Injection	Supersonic I Atom Injection
Quantity/Inflow Power			
Power Extracted	78.8%	78.3%	84.3%
Power in Flow at Cavity Exit	8.9%	13.2%	10.6%
available	2.6%	4.9%	2.2%
unavailable	6.3%	8.3%	8.4%
Lost Upstream of Resonator	10.9%	2.6%	3.1%
Losses in the Resonator	1.4%	6.0%	2.0%
Losses before Cavity Exit	12.3%	8.5%	5.1%
Total Losses	21.2%	21.7%	15.7%
Cavity Temperature (K)	151	169	170
Cavity Mach Number	2.25	1.91	1.99

Summary and Conclusions

- I_2 supersonic injection shows potential as an alternative to subsonic injection.
  - 0% outcoupling power equals subsonic power despite incomplete dissociation.
- I atom supersonic injection allows more power to be extracted than the I_2 injection schemes over all of the outcoupling range.
  - No I_2 dissociation cost.

COIL-R&D WORKSHOP, *Prague' 99*

Lebedev Physical Institute, Samara Branch

Nikolaev V.D., Zagidullin M.V.

The gas dynamic parameters, efficiency of mixing and lasing in COIL with ejector array of supersonic nozzles

ФИАН САМАРА Lebedev Physical Institute Samara Branch

Dependence of Mach number on iodine molar flow rate
Conditions: optical axis-nozzles 89 mm, chlorine flow rate 39.2 mmole/s, primary nitrogen molar flow rate 400 mmole/s, secondary nitrogen 40 mmole/s, mirror purging 10 mmole/s.

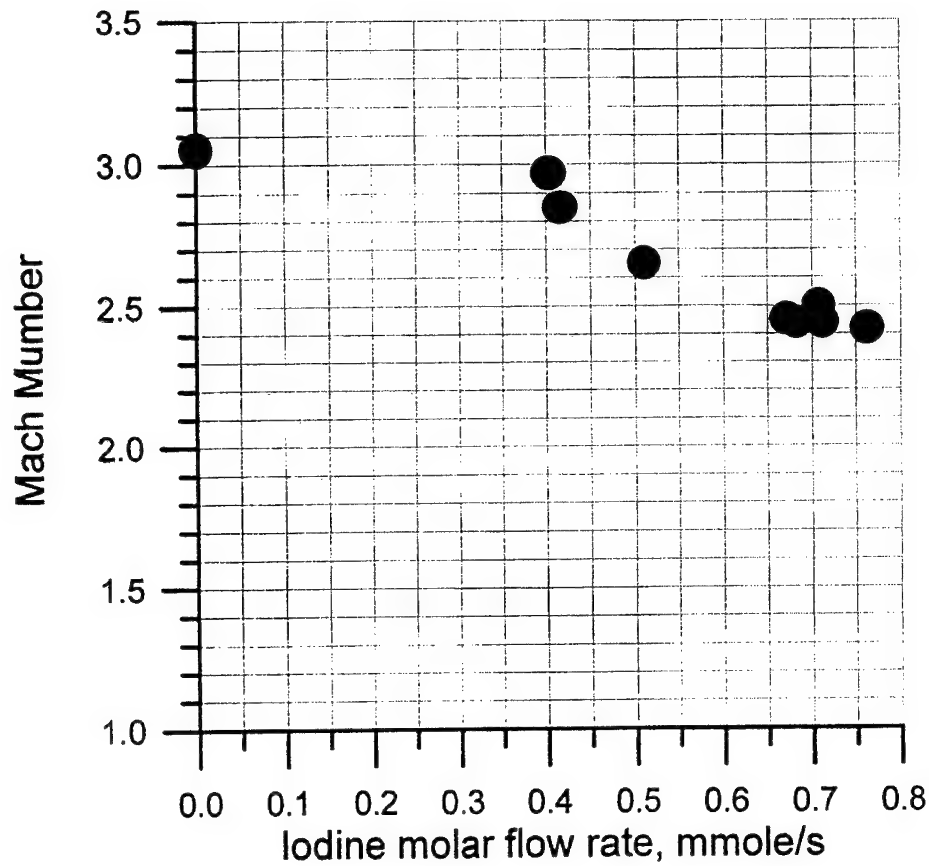

ФИАН САМАРА Lebedev Physical Institute Samara Branch

Dependence of output power on iodine molar flow rate

Conditions: optical axis-nozzles 89 mm, chlorine flow rate 39.2 mmole/s, primary nitrogen molar flow rate 400 mmole/s, secondary nitrogen 40 mmole/s, mirror purging 10 mmole/s, mirrors T1=0.8%, T2=0.014% (nonresonant loses were unknown)

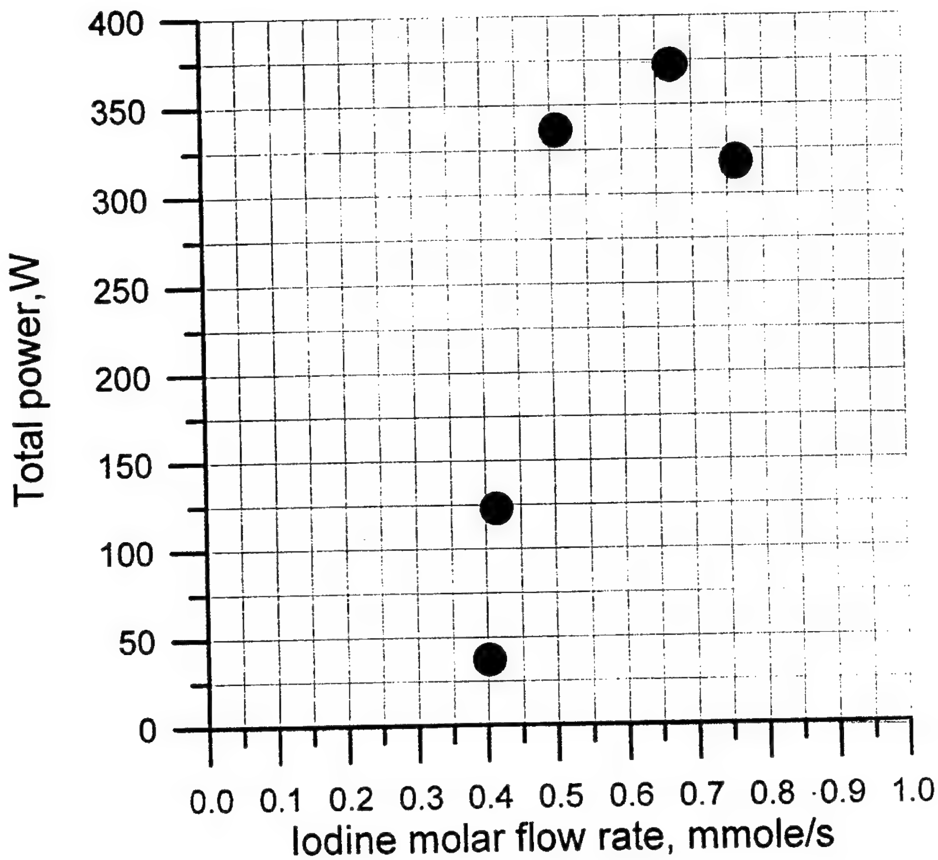

ФИАН САМАРА Lebedev Physical Institute Samara Branch

Dependence of output power on total mirror transmission

Conditions: optical axis-nozzles 89 mm, chlorine flow rate 39.2 mmole/s, primary nitrogen molar flow rate 400 mmole/s, secondary nitrogen 40 mmole/s, mirror purging 10 mmole/s,

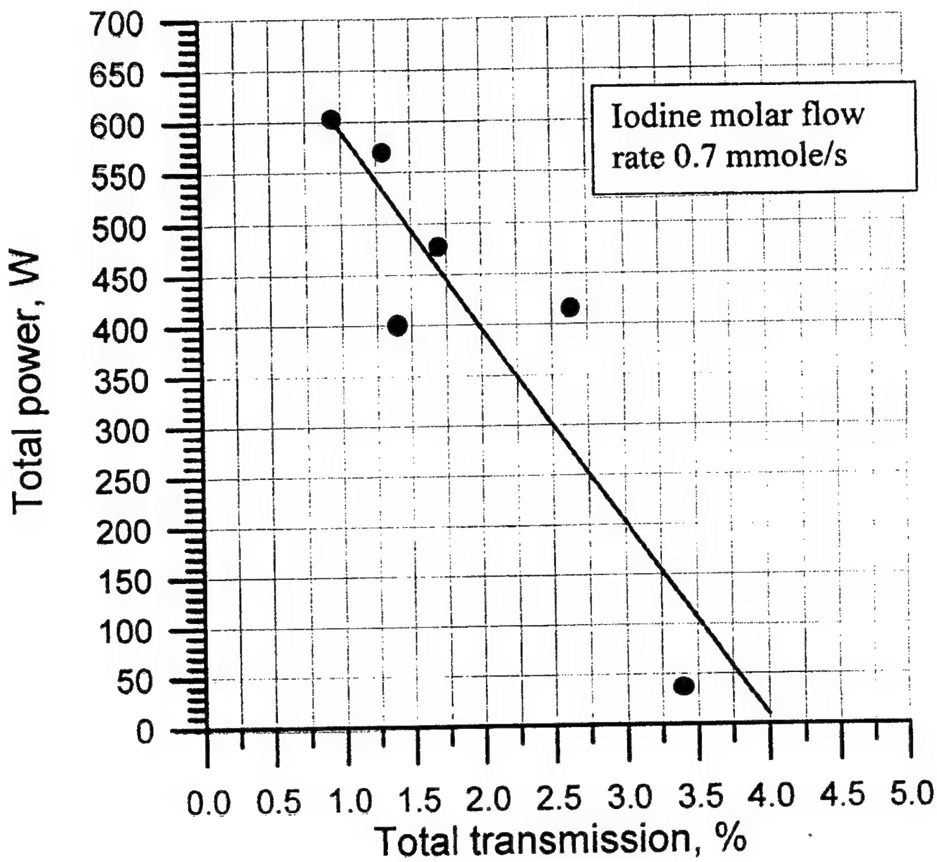

The video of mixing-dissociation zone showed that the length iodine dissociation was shorter 50 mm

Pressures at maximum output power conditions:

SOG: 41 torr , Plenum : 35.2 torr

Laser cavity: 11.9 torr, Pitot: 81 torr, Mach: 2.2

Total pressure of gas flow in cavity 128 torr

Dependence of output power on iodine molar flow rate
Conditions: optical axis-nozzles 64 mm, chlorine flow rate 39.2 mmole/s, primary nitrogen molar flow rate 400 mmole/s, secondary nitrogen 40 mmole/s, mirror purging 10 mmole/s,

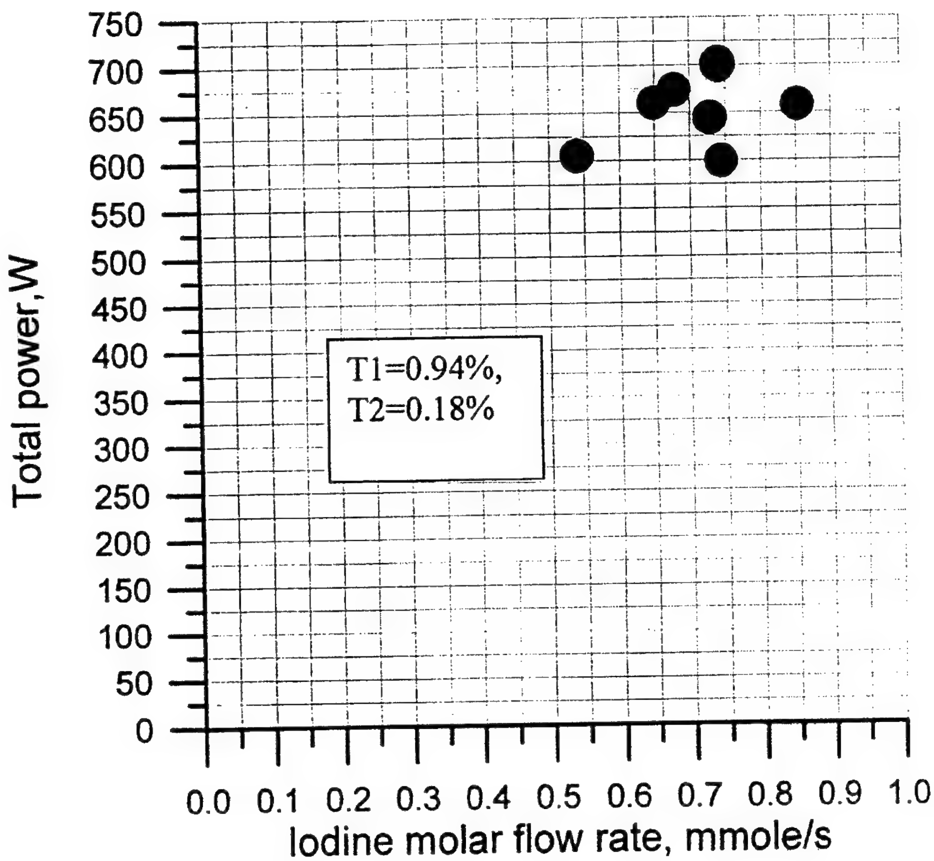

ФИАН САМАРА Lebedev Physical Institute Samara Branch

Dependence of output power on total mirror transmission

Conditions: optical axis-nozzles 64 mm, chlorine flow rate 39.2 mmole/s, primary nitrogen molar flow rate 400 mmole/s, secondary nitrogen 40 mmole/s, mirror purging 10 mmole/s.

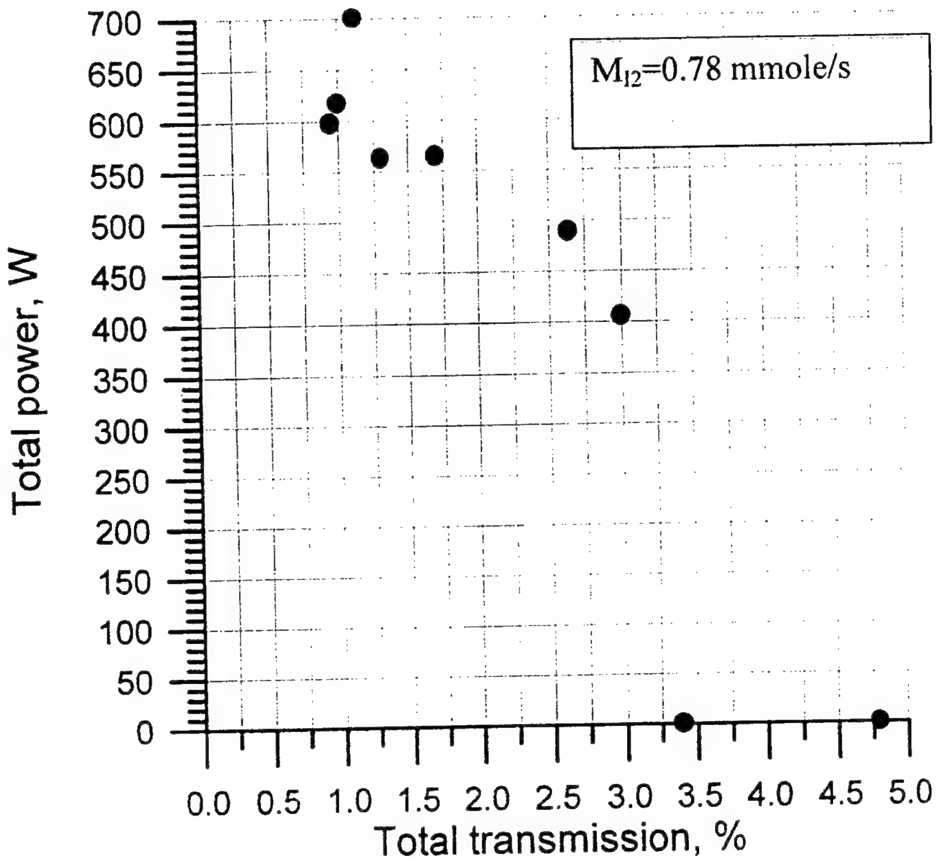

Pressures at maximum output power (M_{I2}= 0.78 mmole/s):
SOG- 39.4 torr, Plenum- 33 torr, Laser cavity –11.2 torr, Pitot- 101 torr, Mach-2,6.
Total pressure of gas flow in laser cavity =218 torr.
For M_{I2}= 0, Laser cavity –9.5 torr, Pitot- 98.3 torr, Mach-2,9.
Total pressure of gas flow in laser cavity =300 torr.

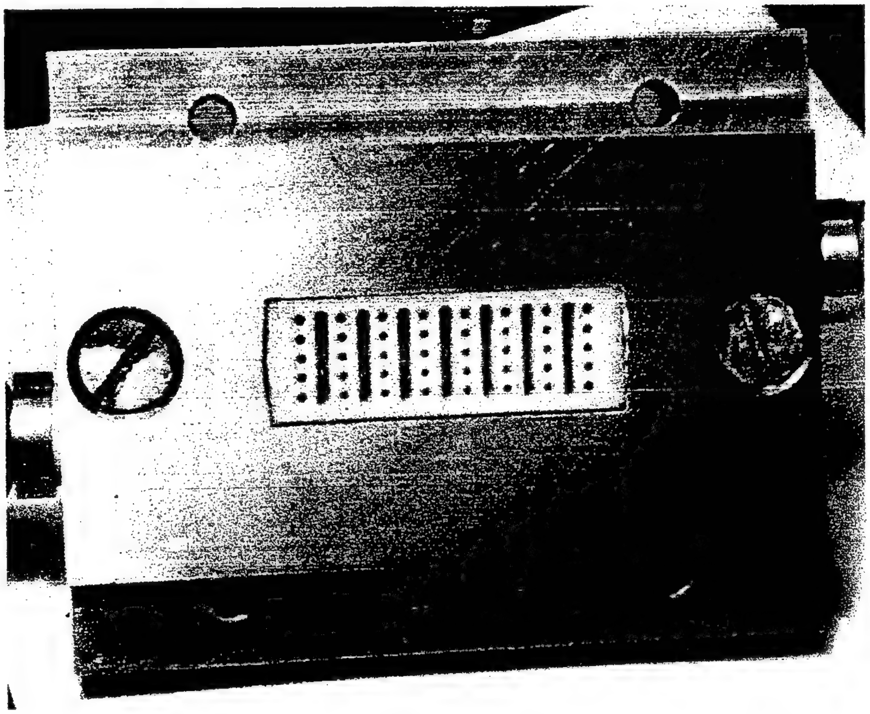

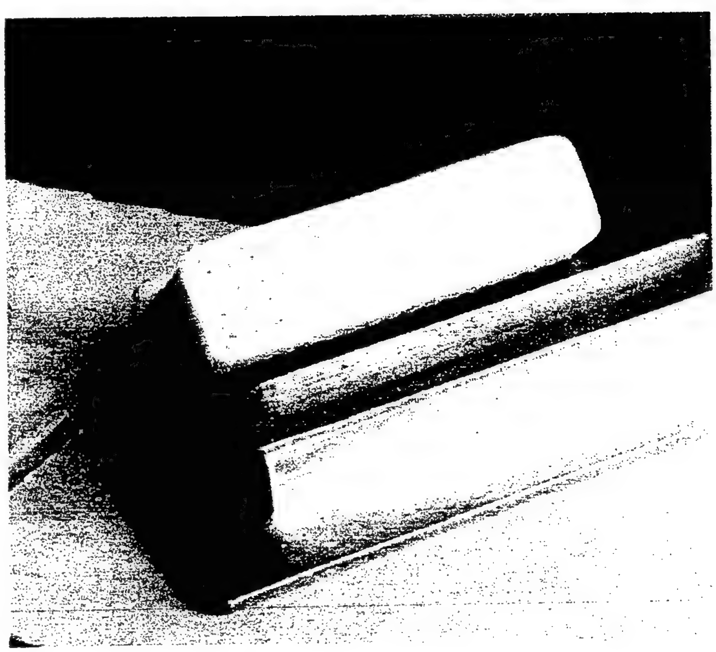

New ejector grid nozzle Scale 4:1

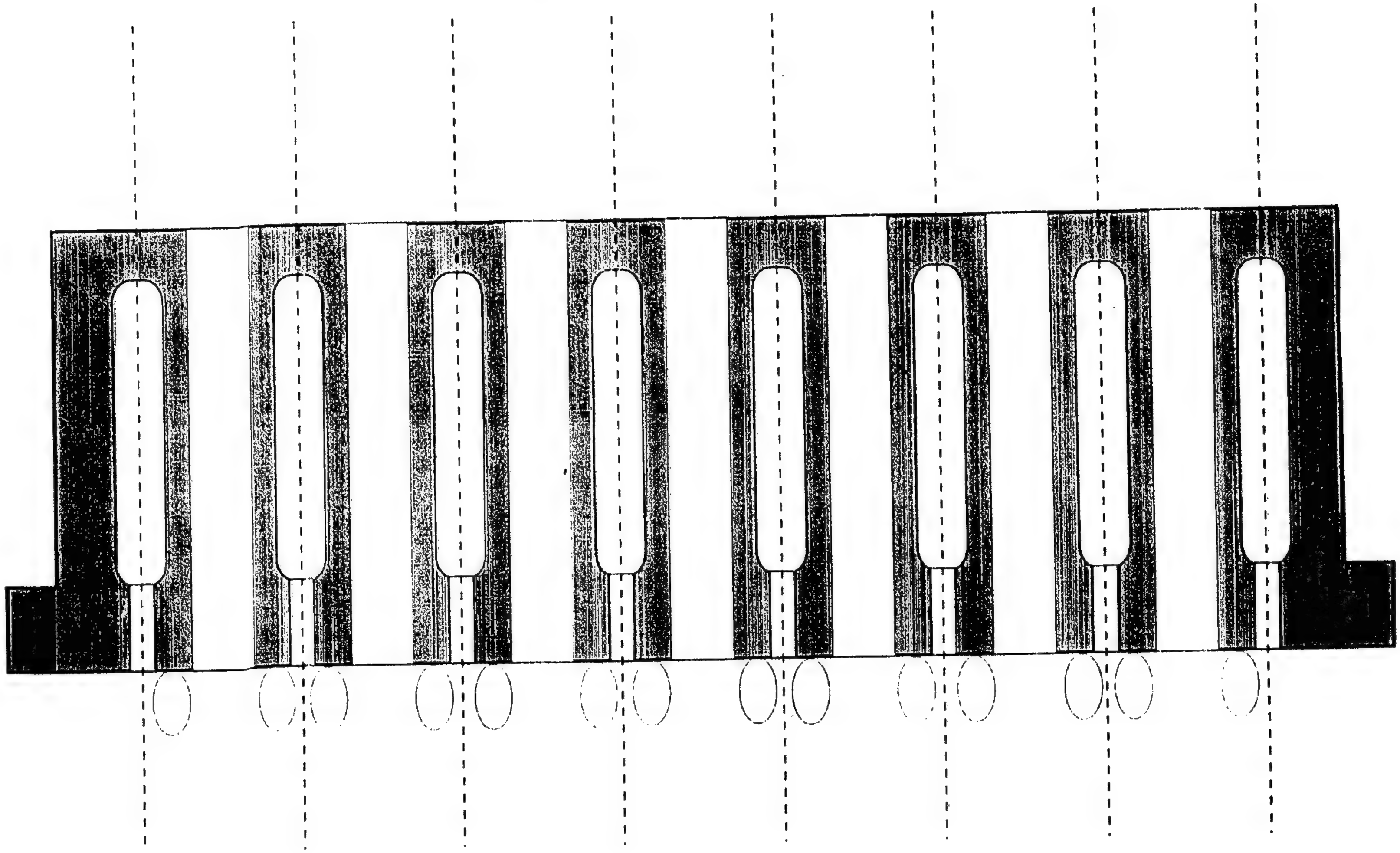

The tubes for iodine injection have i.d. of 2mm and wall thickness of 0.1mm. These tubes have been deformated to elliptical shape with small axis of 1,5mm. 15 orifices of 0.5mm i.d. (one row) were drilled in each tube.

Scale 4:1

The assembly of JSOG with nozzle bank
(high pressure nitrogen flow mixing with oxygen and injection of iodine into boundary layer)

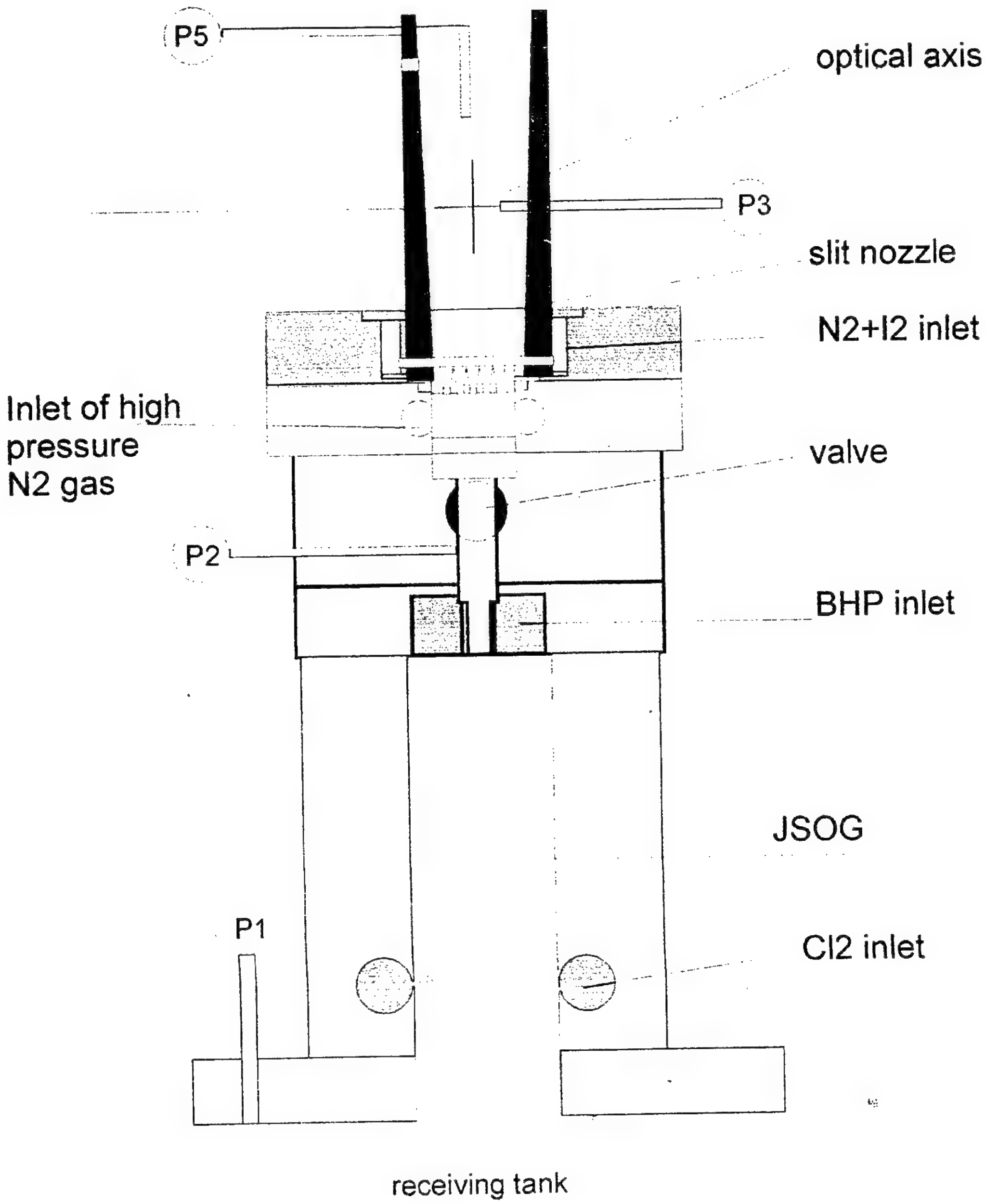

A Second Iodine Laser Breakthrough

Recent Progress in the Development of an All Gas Phase Iodine Laser (AGIL)

by

Dr. Thomas L. Henshaw, Dr. Timothy J. Madden, Dr. Gerald C. Manke II, Dr. John M. Herbelin, Mr. Brian T. Anderson, Mr. Ralph F. Tate, and Dr. Gordon D. Hager

Air Force Research Laboratory/DELC, Kirtland AFB
3550 Aberdeen Ave. SE
Kirtland AFB, NM 87117-5776

All Gas-Phase Iodine Laser Experiment (AGILE) Overview

1. ***Perform direct and quantitative measurement of gain resulting from the NCl(a) - I transfer reaction***

2. ***Determine if NCl(a)-I system gain will scale with reagent densities***

All Gas-Phase Iodine Laser (AGIL) Overview

- **The AGIL system is based on an efficient energy transfer reaction between electronically excited NCl ($a^1\Delta$) metastable molecules and ground state iodine atoms,**

$$\mathrm{NCl}\,(a^1\Delta) + \mathrm{I}\,(^2P_{3/2}) \rightarrow \mathrm{NCl}\,(X^3\Sigma) + \mathrm{I}^*(^2P_{1/2})$$

- **Subsequent lasing is generated on the I $^*(^2P_{1/2}) \rightarrow$ I $(^2P_{3/2})$ transition at 1.315 μm:**

$$\mathrm{I}^*(^2P_{1/2}) + h\nu \rightarrow \mathrm{I}\,(^2P_{3/2}) + nh\nu \quad (\lambda = 1.315\ \mu m)$$

$NCl(a^1\Delta)$ Energetics

- **Interest in $NCl(a^1\Delta)$ energetics:**

  - **Potential energy carrier in all gas phase I* laser system**

  - **$NCl(a^1\Delta)$ metastable isovalent to $O_2(a^1\Delta)$**

  - **$O_2(a^1\Delta)$ 0.98 eV, $NCl(a^1\Delta)$ 1.1 eV**

- **Similar $I^*(^2P_{1/2})$ Transfer Mechanism:**

$$O_2(a^1\Delta) + I(^2P_{3/2}) \rightleftharpoons I^*(^2P_{1/2}) + O_2(X^3\Sigma),\ \Delta E = -279\ cm^{-1}$$

$$NCl(a^1\Delta, v=0) + I(^2P_{3/2}) \longrightarrow I^*(^2P_{1/2}) + NCl(X^3\Sigma, v=2),\ \Delta E = -50\ cm^{-1}$$

- ***Can NCl(a) be a viable chemical energy substitute for H_2O_2 based COIL?***

Motivation

Limitations of COIL in ABL/SBL :

- **Aqueous chemistry heavy**
- **H_20 a strong quencher of I***
- **Heat remains in BHP**
- **Zero - g**

AGIL a potential chemical substitute for H_2O_2-based COIL:

- ✓ **purely gas phase reaction, heat rejection in exhaust**
- ✓ **exhibits higher specific energy content (KJ/Kg)**
- ✓ **operational in zero-g environments**
- ✓ **maintains short wavelength, single line lasing**

Chemical Generation of $NCl(a^1\Delta)$ and $I^*(^2P_{1/2})$

Subsonic Flow Reactor

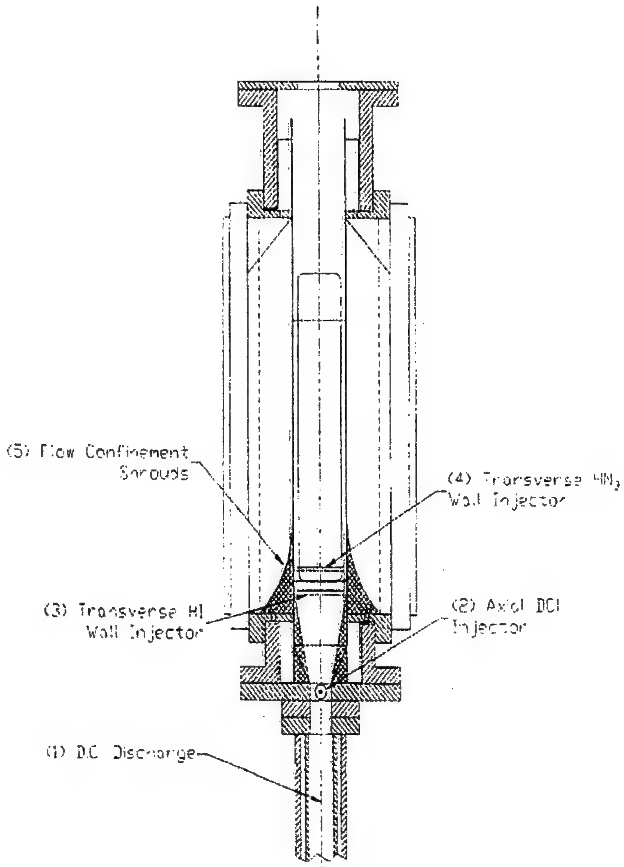

Chemical Mechanism

Step 1: F,Cl, I Atom Production:

1. $F_2 / He \xrightarrow{\text{dc discharge}} F, F_2$
2. $F + DCl \longrightarrow DF + Cl$, $k = 1 \times 10^{-11}\ cm^3/s$
3. $Cl + HI \longrightarrow HCl + I$, $k = 8 \times 10^{-11}\ cm^3/s$

Step 2: NCl(a) Production:

4. $Cl + HN_3 \longrightarrow HCl + N_3$, $k = 1 \times 10^{-12}\ cm^3/s$
5. $Cl + N_3 \longrightarrow NCl(a) + N_2$, $k = 2 \times 10^{-11} cm^3/s$

Step 3: I* Production:

6. $NCl(a) + I \longrightarrow I^* + NCl(X)$, $k = 2 \times 10^{-11}\ cm^3/s$

AGIL SUBSONIC FLOW APPARATUS

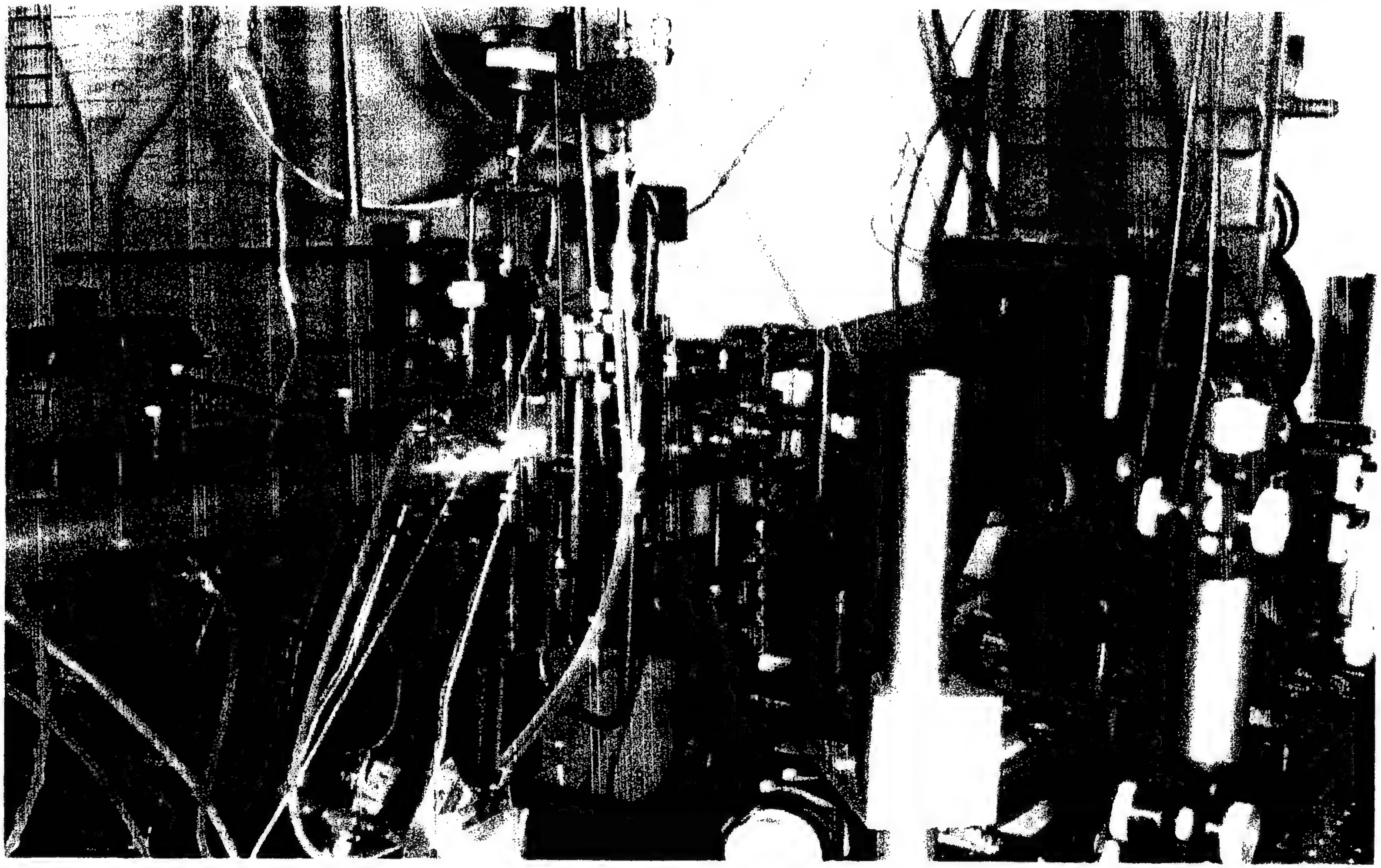

System Diagnostics

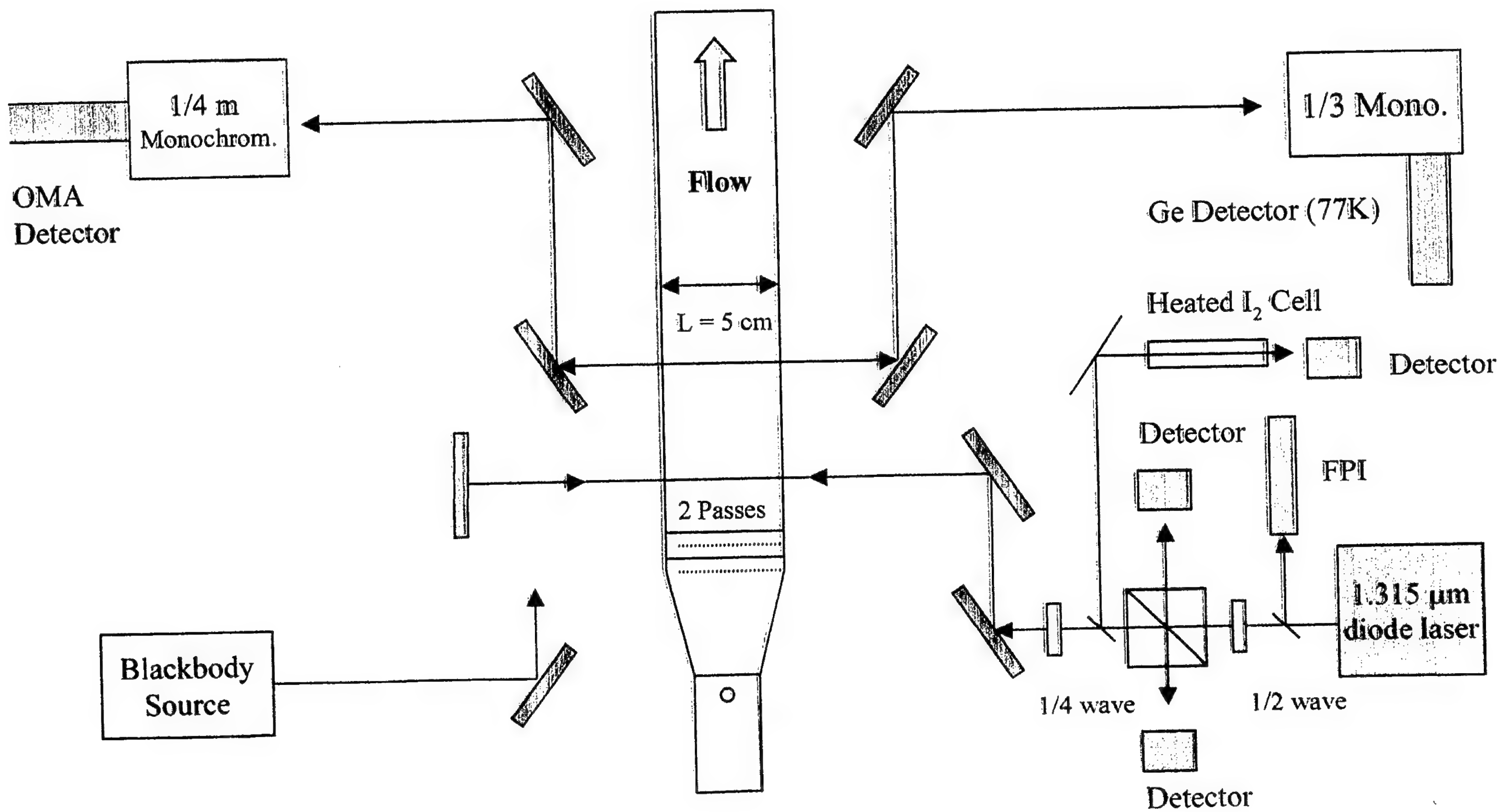

ATOMIC IODINE HYPERFINE SPECTRUM

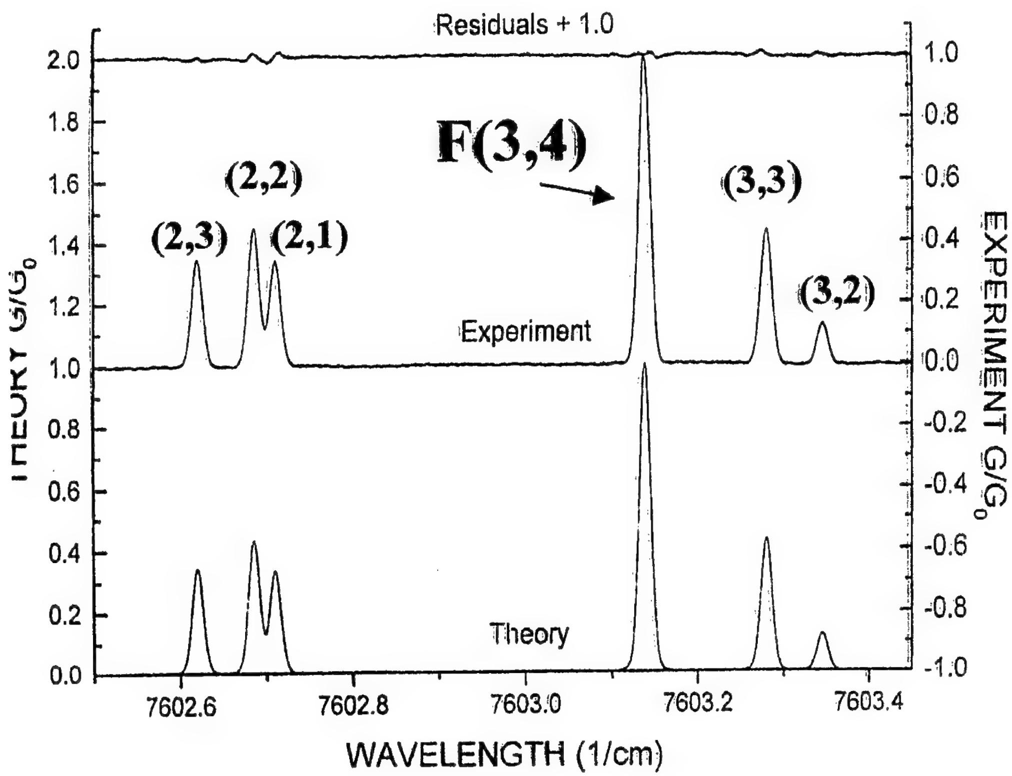

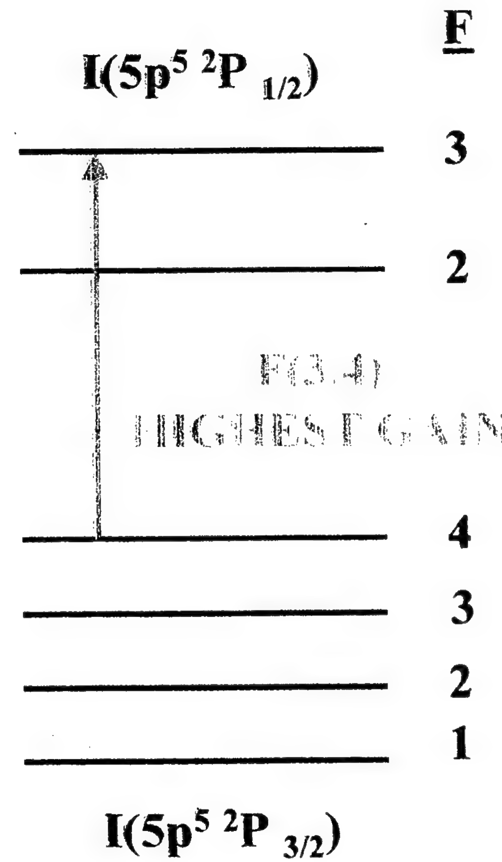

Absorption Line Shape Analysis

$$I = I_0 \exp(\gamma L), \quad \gamma = \sigma \Delta N, L = 10\,cm$$

$$I(\nu) = I_0(\nu) \exp(\sigma(\nu) \Delta N L)$$

$$\sigma(\nu) = \frac{A_{3,4}\lambda^2}{8\pi} f(\nu), \quad f(\nu) = Voigt\ Line\ Function$$

$$\Delta N = \left(N_u - \frac{g_u}{g_l} N_l\right) = \left[\frac{7}{12}\left(I^* - \frac{1}{2}I\right)\right]$$

$$\int_{-\infty}^{\infty} \gamma(\nu) d\nu = Area = \frac{A_{3,4}\lambda^2}{8\pi} \int_{-\infty}^{\infty} f(\nu)\, d\nu \left[\frac{7}{12}\left(I^* - \frac{1}{2}I\right)\right] L$$

$$where \int_{-\infty}^{\infty} f(\nu)\, d\nu \equiv 1$$

Absorption Spectrum of $I(^2P_{3/2})$, F(3,4)

$$F + HI \longrightarrow I + HF$$

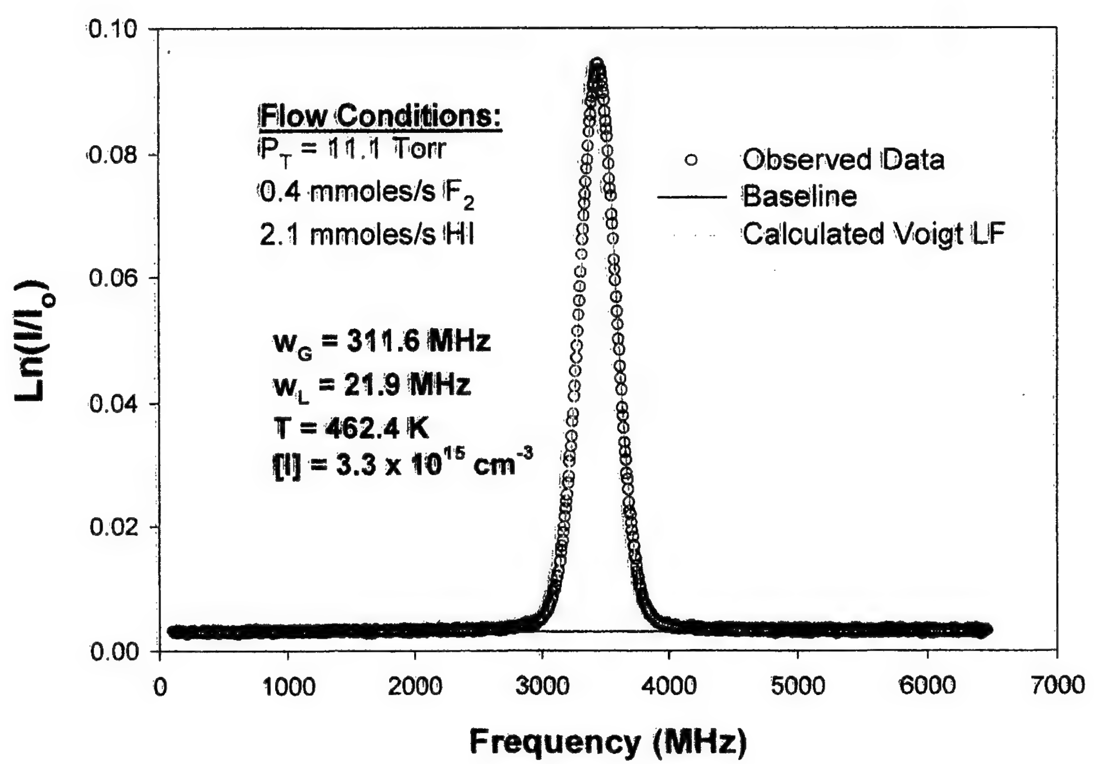

Nominal Flow Parameters for I* Gain Measurement

Reagent Species	Molar Flow Rate, mmole/s	Reactor Pressure, Torr	Reagent Density, cm^{-3}	Cross Sectional Area, cm^2	Flow Velocity, cm/s	Flow Temperature, K
He	151.28	15.50	3.0×10^{17}	10	2.9×10^{4}	470
F_2	0.66		1.3×10^{15}			
DCl	2.00		4.0×10^{15}			
HN_3	3.32		6.6×10^{15}			
HI	0.032		6.3×10^{13}			
Total	157.29		3.1×10^{17}			

Direct Measurement of $I^*(^2P_{1/2})$ Gain

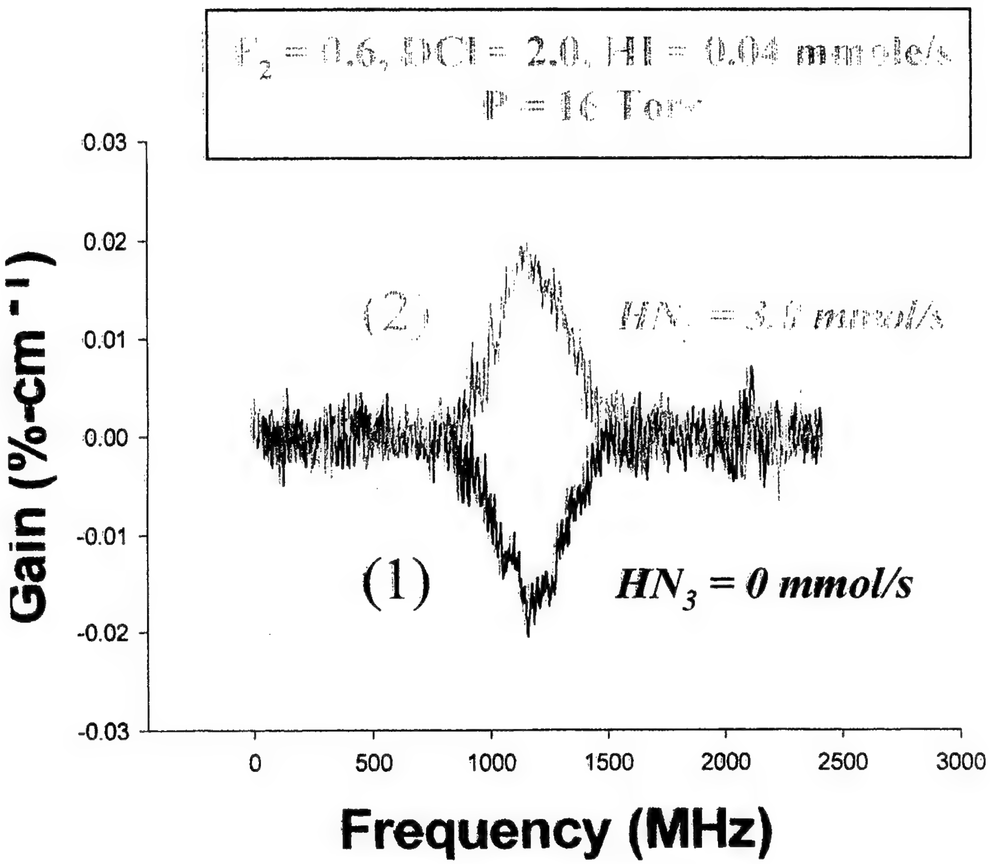

Curve 1: Absorption:

1. $F_2 / He \xrightarrow{\text{dc discharge}} 2F$
2. $F + DCl \longrightarrow DF + Cl$
3. $Cl + HI \longrightarrow HCl + I$

Curve 2: Gain

4. $Cl + HN_3 \longrightarrow HCl + N_3$
5. $Cl + N_3 \longrightarrow NCl(a) + N_2$
6. $NCl(a) + I \longrightarrow I^* + NCl(X)$

SSG Gain Profile

$NCl(a) + I \longrightarrow I^* + NCl(X)$

F_2 = 0.75 mmole/s (85% dissociated), DCl = 2.0 mmole/s, HI = 0.039 mmole/s
HN_3 = 4.0 mmole/s, P = 16 torr

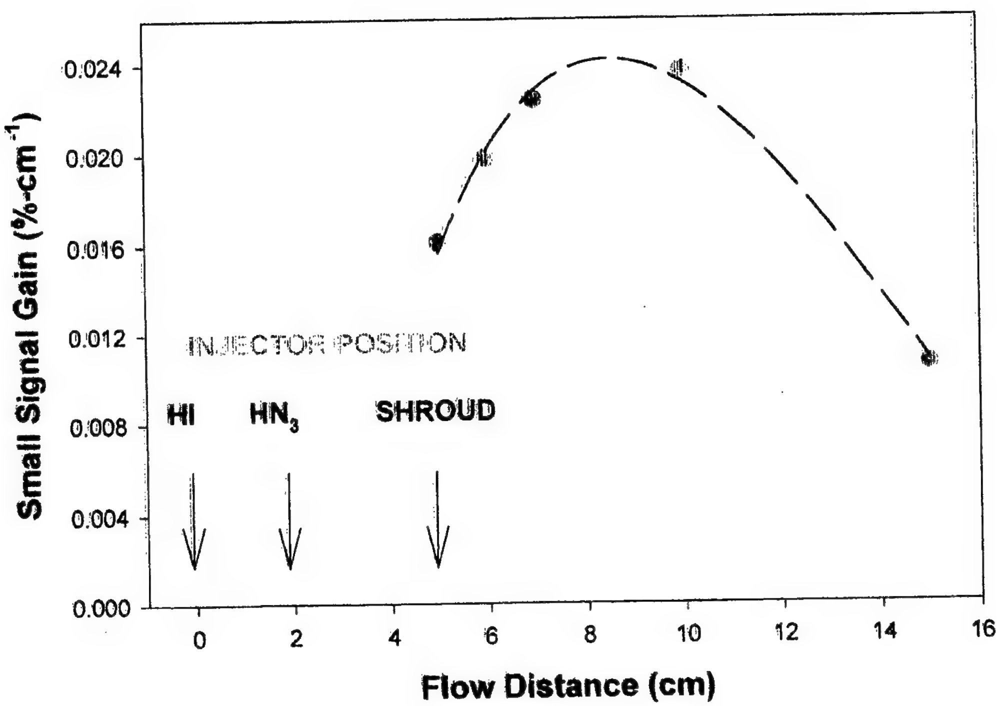

Kinetic 1 D Modeling

Key Rates of $NCl(a^1\Delta)+I$ Model

$F+DCl \rightarrow DF+Cl$	$1.6\cdot10^{-11}$	Based on F+HCl; Nip and Clyne (1977)
$Cl+HN_3 \rightarrow HCl+N_3$	$8.9\pm1.2\cdot10^{-13}$	Yamasaki et al, Chem. Phys. Lett., **94**, 425, (1983) Manke and Setser, J. Phys. Chem, **102**, 153, (1998)
	$2.0\cdot10^{-10}\exp(-1452/T)$	Manke et al. Chem. Phys. Lett. 310, 111 (1999).
$Cl+N_3 \rightarrow NCl(a)+N_2$	$2.25\cdot10^{-11}$	Henshaw et al, J. Phys. Chem., **102**, pp 6239, (1998)
$Cl+N_3 \rightarrow NCl(x)+N_2$	$0.75\cdot10^{-11}$	Manke and Setser, (1998)
$Cl+N_3 \rightarrow NCl(b)+N_2$	$1\cdot10^{-14}$	
$2N_3 \rightarrow 3N_2$	$3.0\cdot10^{-12}$	David and Coombe. J. Phys. Chem., **90**, 3260 (1986)
$2NCl(x) \rightarrow N_2+2Cl$	$8.1\pm1.8\cdot10^{-12}$	Clyne and MacRobert, J. Chem. Soc. Faraday Trans. 2, **79**, pp283-293, (1983)
$NCl(a)+I \rightarrow NCl(x)+I^*$	$1.8\cdot10^{-11}$	Ray and Coombe, J. Phys. Chem., **97**, 3476, 1993
	$1.1\cdot10^{-10}\exp(-519K/T)$	Henshaw et al, J. Phys. Chem., **102**, pp 6239, (1998)
$2NCl(a) \rightarrow NCl(b)+NCl(x)$	$1.5\cdot10^{-13}$	Manke and Setser, (1998)
$2NCl(a) \rightarrow$ products	$7.2\pm0.9\cdot10^{-12}$	Henshaw et al, J. Phys. Chem., **101**, pp 4048, (1997)
$2NCl(a) \rightarrow N_2+2Cl$	$6.8\cdot10^{-12}$	

Previous Gain Demonstration

- Yang, Gylys, Bower, Rubin (1992): Gain in Flow Reactor

$F + DCl \longrightarrow DF + Cl$

$Cl + ICl \longrightarrow Cl_2 + I$

$Cl + HN_3 \longrightarrow HCl + N_3$

$Cl + N_3 \longrightarrow NCl\,(a) + N_2$

$NCl\,(a) + I \longrightarrow I^* + NCl(X)$

- $I^*(^2P_{1/2})$ gain measured *indirectly* via double resonance technique

- Ray and Coombe (1995): Pulsed photolytic laser demonstration

$ClN_3 + h\nu \longrightarrow NCl\,(a) + N_2$

$CH_2I_2 + h\nu \longrightarrow CH_2I + I$

$NCl\,(a) + I \longrightarrow I^* + NCl(X)$

$I + ClN_3 \longrightarrow I + NCl(a) + N_2$

$NCl(a) + ClN_3 \longrightarrow NCl(a,X) + N_2(X,v)$

$N_2(X, v>0) + ClN_3 \longrightarrow NCl(a) + 2N_2(X, v=0)$

$I^* + nh\nu \longrightarrow I + 1.315\,\mu m$ (laser)

- **complex chemistry, $I^*(^2P_{1/2})$ inversion generated via *chain decomposition* of ClN_3, sensitive to $N_2(v)$**

- **Both measurements near threshold conditions**

  ⇨ **quantitative measurements difficult**

Model Calculation of Subsonic SSG Scaling

Gain v. Streamwise Distance from Discharge Tube - Laser Demo Hardware
[F] = 8 mmole/s, [DCl] = 20 mmole/s, [HN_3] = 5 mmole/s, [HI] = 1.2 mmole/s,

P = 28 torr, T = 950 K

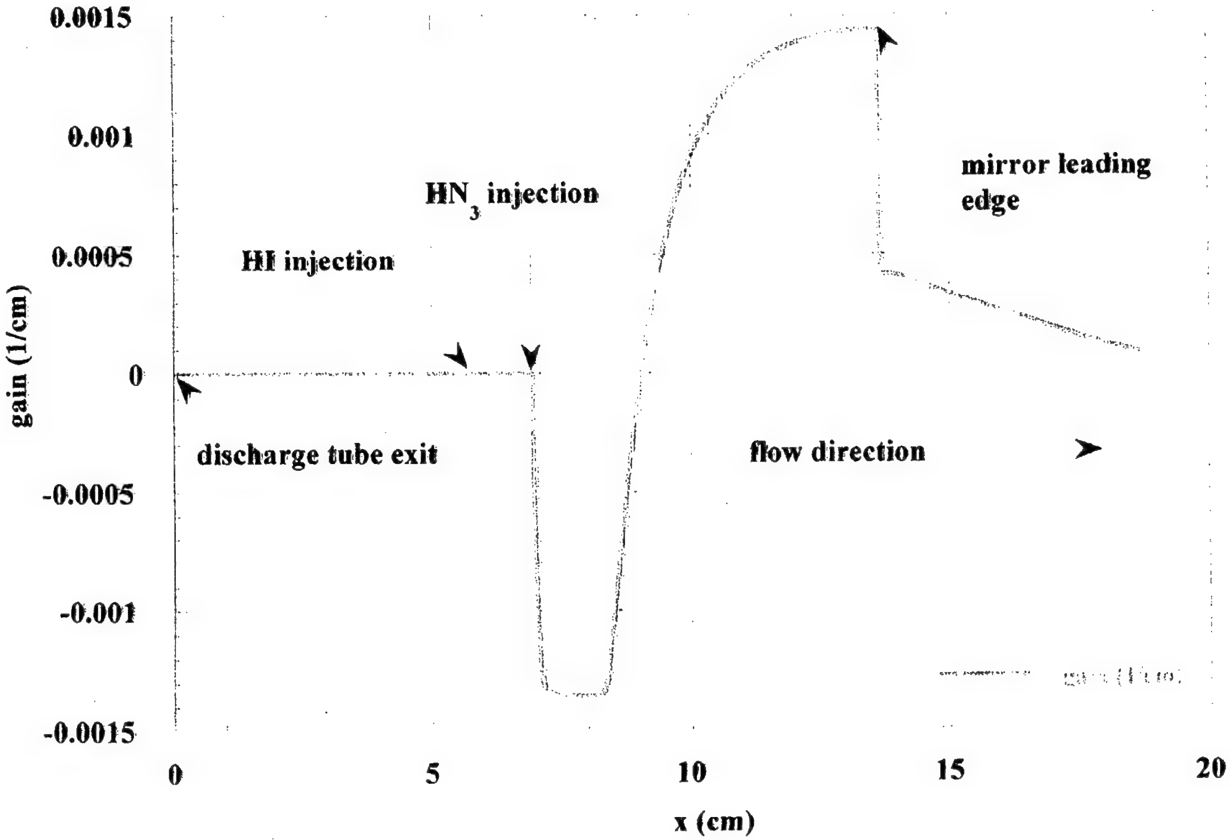

Model Calculation of Subsonic Laser Power Scaling

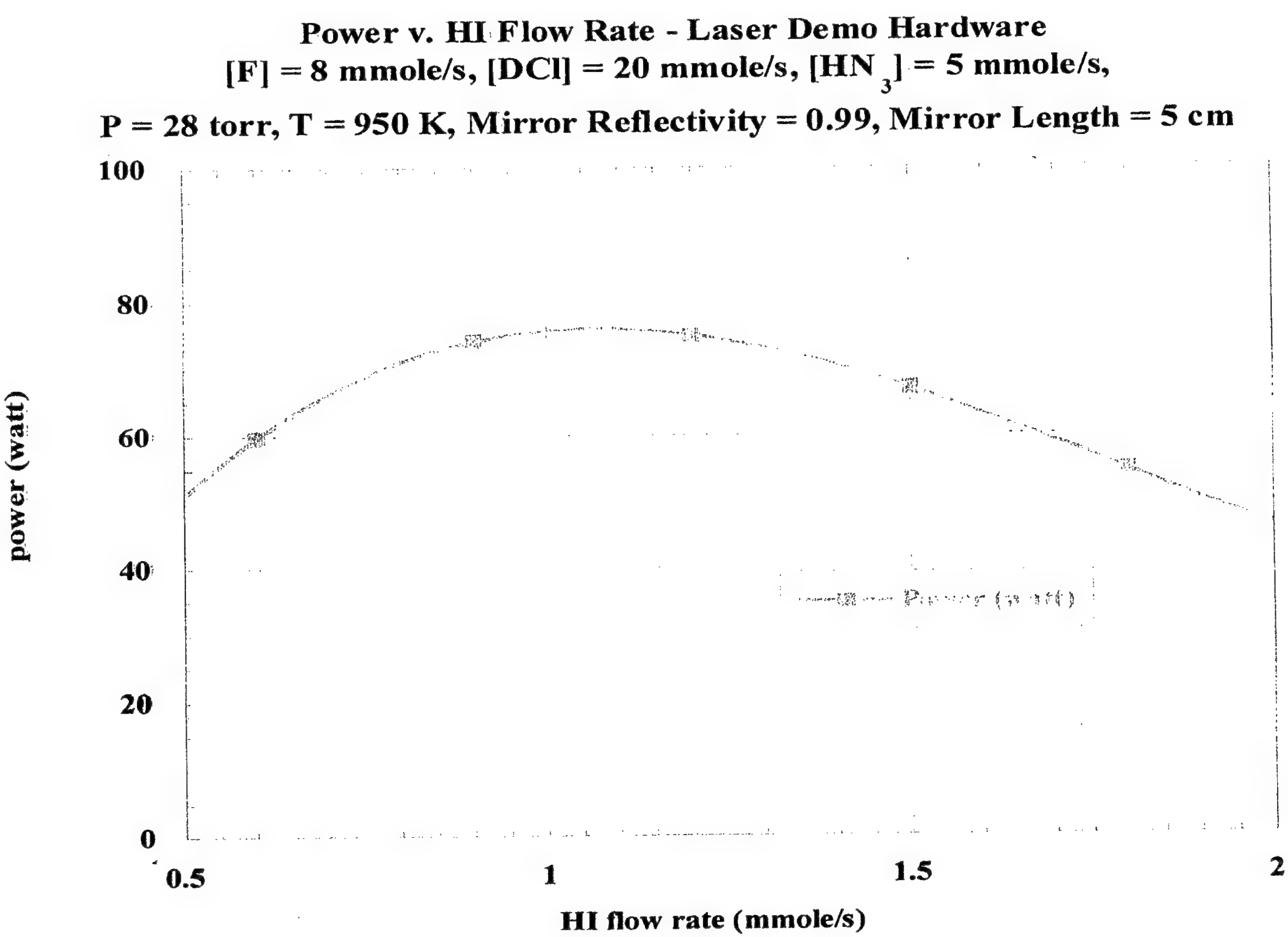

The COIL Laser

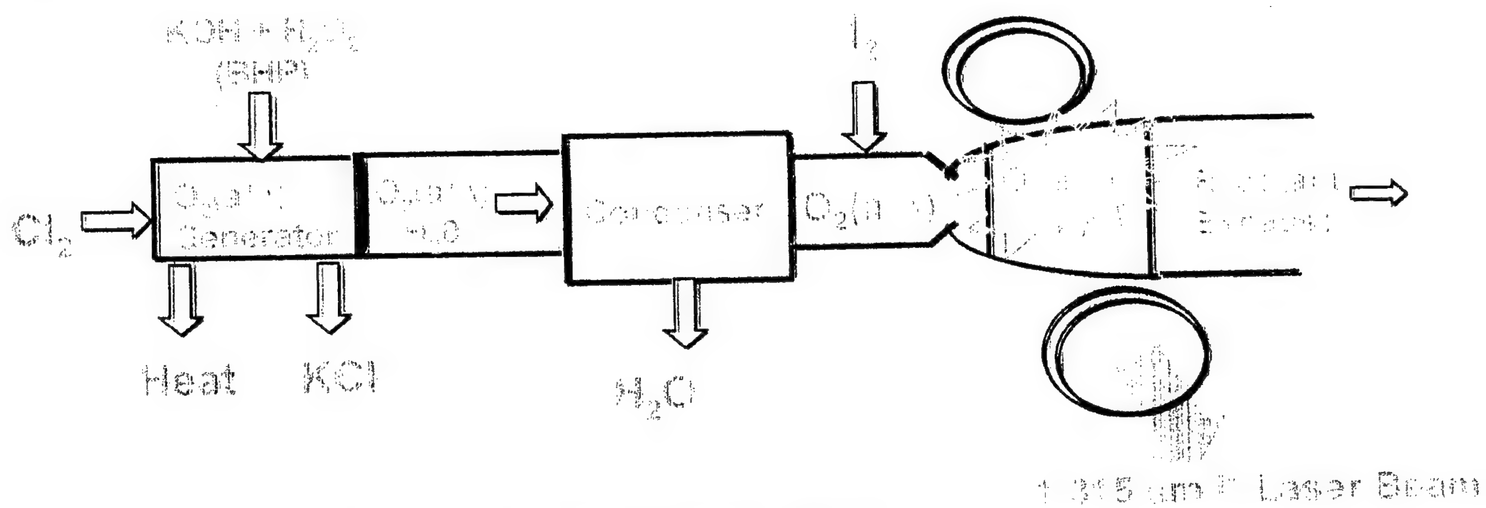

- The CHEMICAL OXYGEN IODINE LASER, COIL
  - Based on chemical production of $O_2(a^1\Delta)$ metastables
  - $O_2(a^1\Delta)$ produced from heterogeneous $KOH/H_2O_2/Cl_2$ mixtures:

$$Cl_2 + H_2O_2 + OH^- \longrightarrow O_2(a^1\Delta) + H_2O + Cl^-$$

- Energy Transfer and Laser:

$$O_2(a^1\Delta) + I(^2P_{3/2}) \longrightarrow I^*(^2P_{1/2}) + O_2(X^3\Sigma), \ \Delta E = 279 cm^{-1}$$

$$I^*(^2P_{1/2}) + nh\nu \longrightarrow I(^2P_{3/2}) + h\nu \text{ (laser 1.315 } \mu m)$$

2D SPATIAL CAVITY SCAN OF I ATOM FLOW

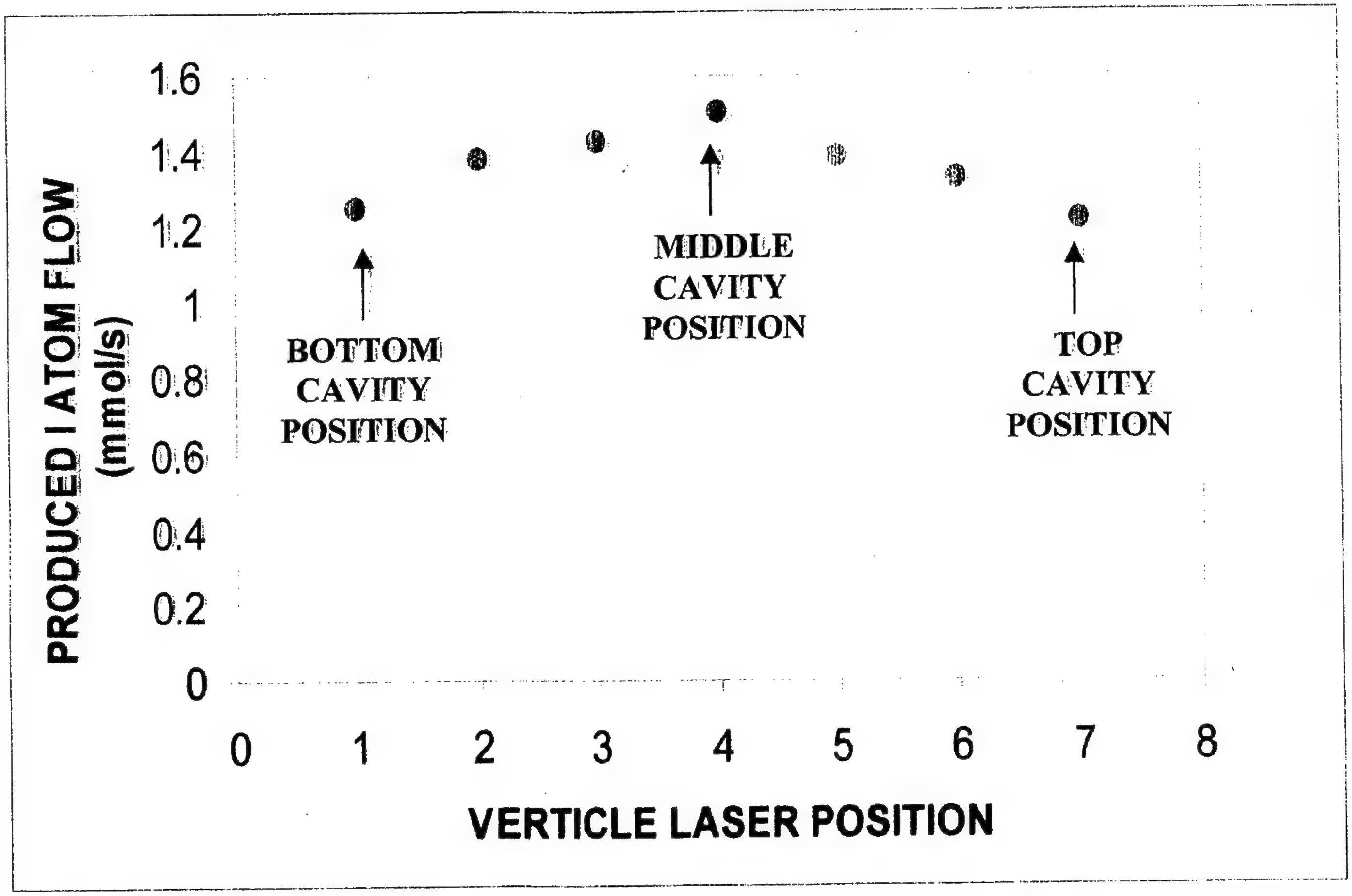

SCALING OF CONVERSION EFFICIENCY, α, WITH PRESSURE, $z = 6$ cm, $i = 2.75$ A

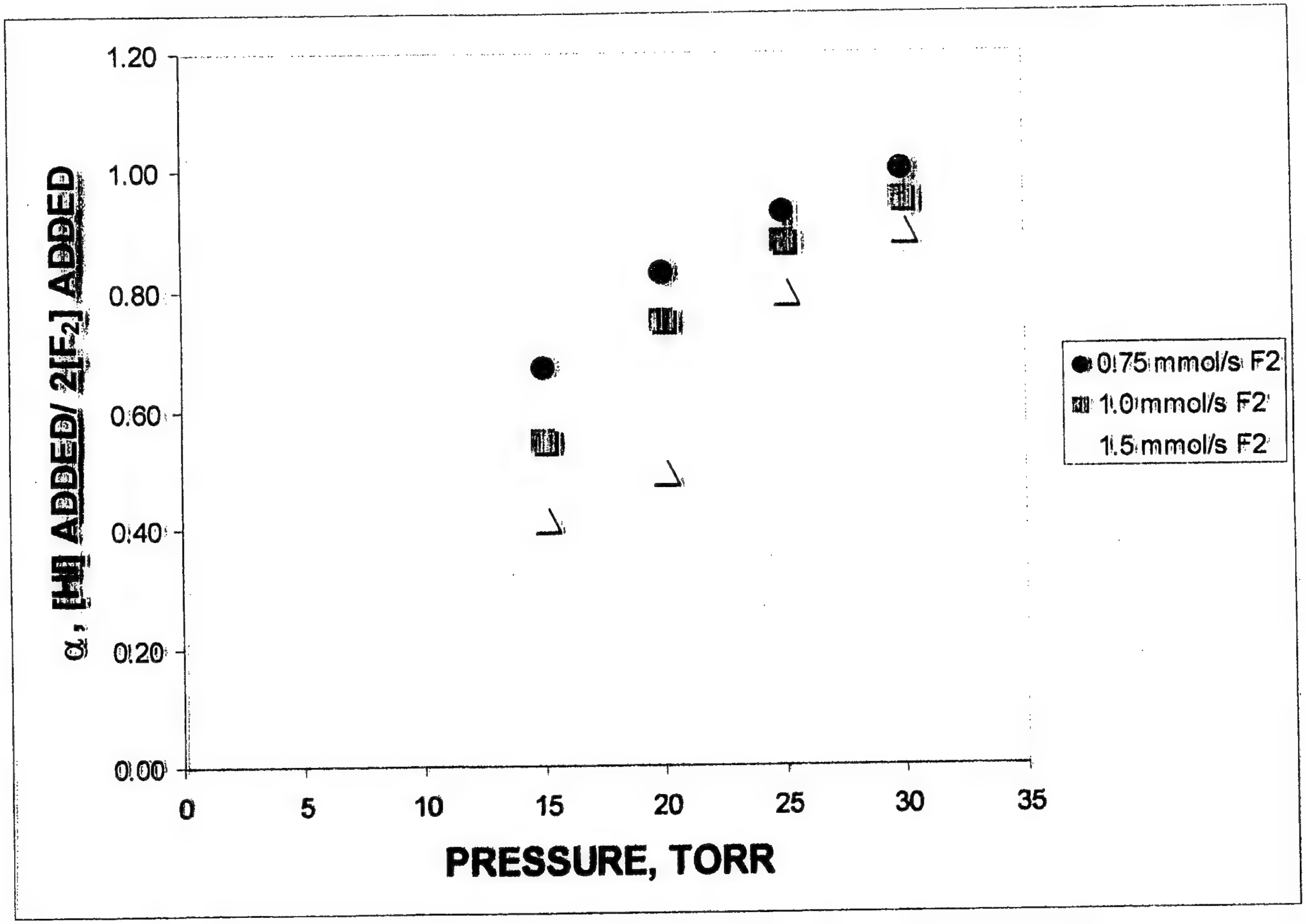

2D TEMPERATURE SCAN OF CAVITY FLOW FIELD

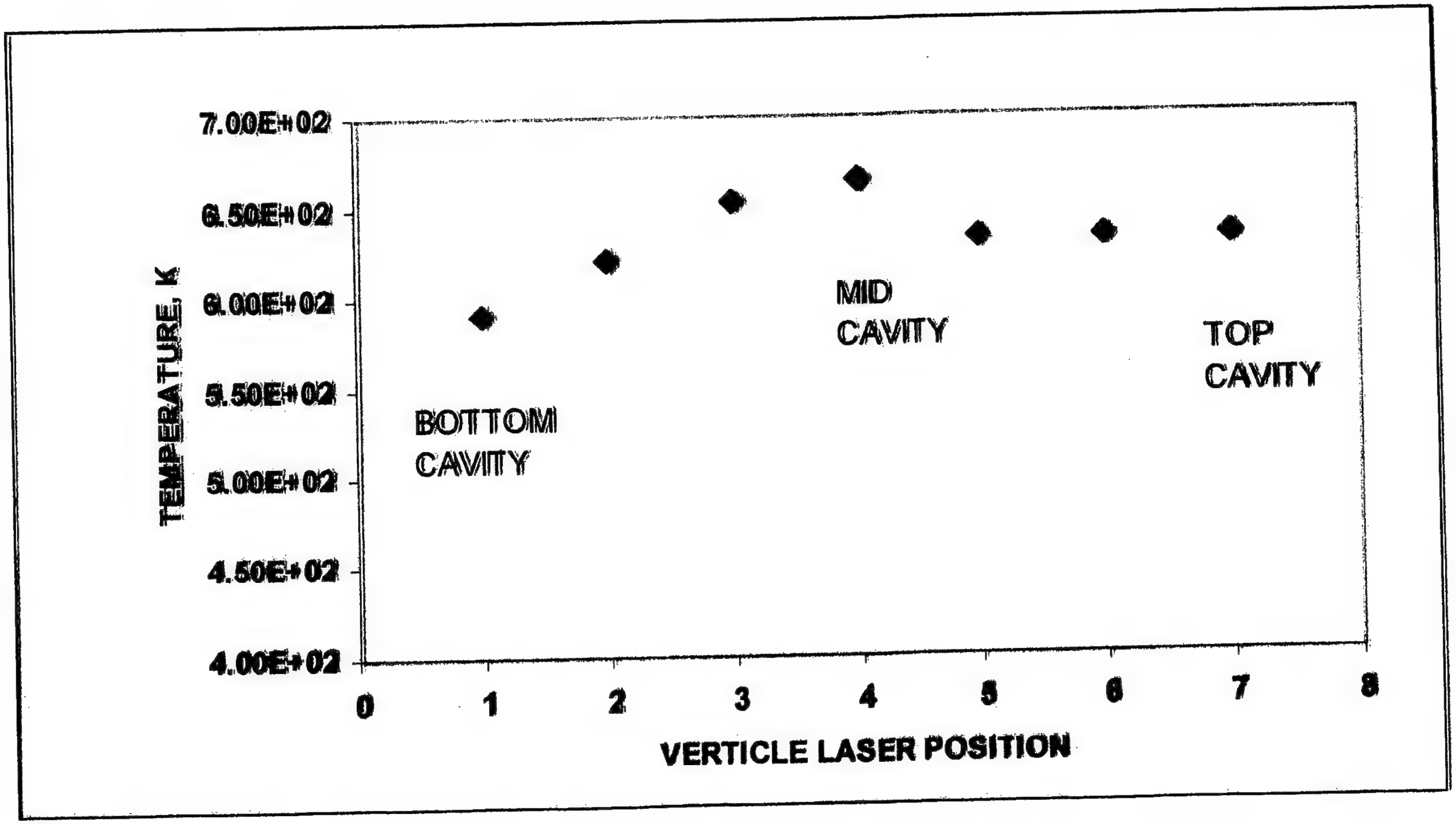

Comparison of Model and Experiment

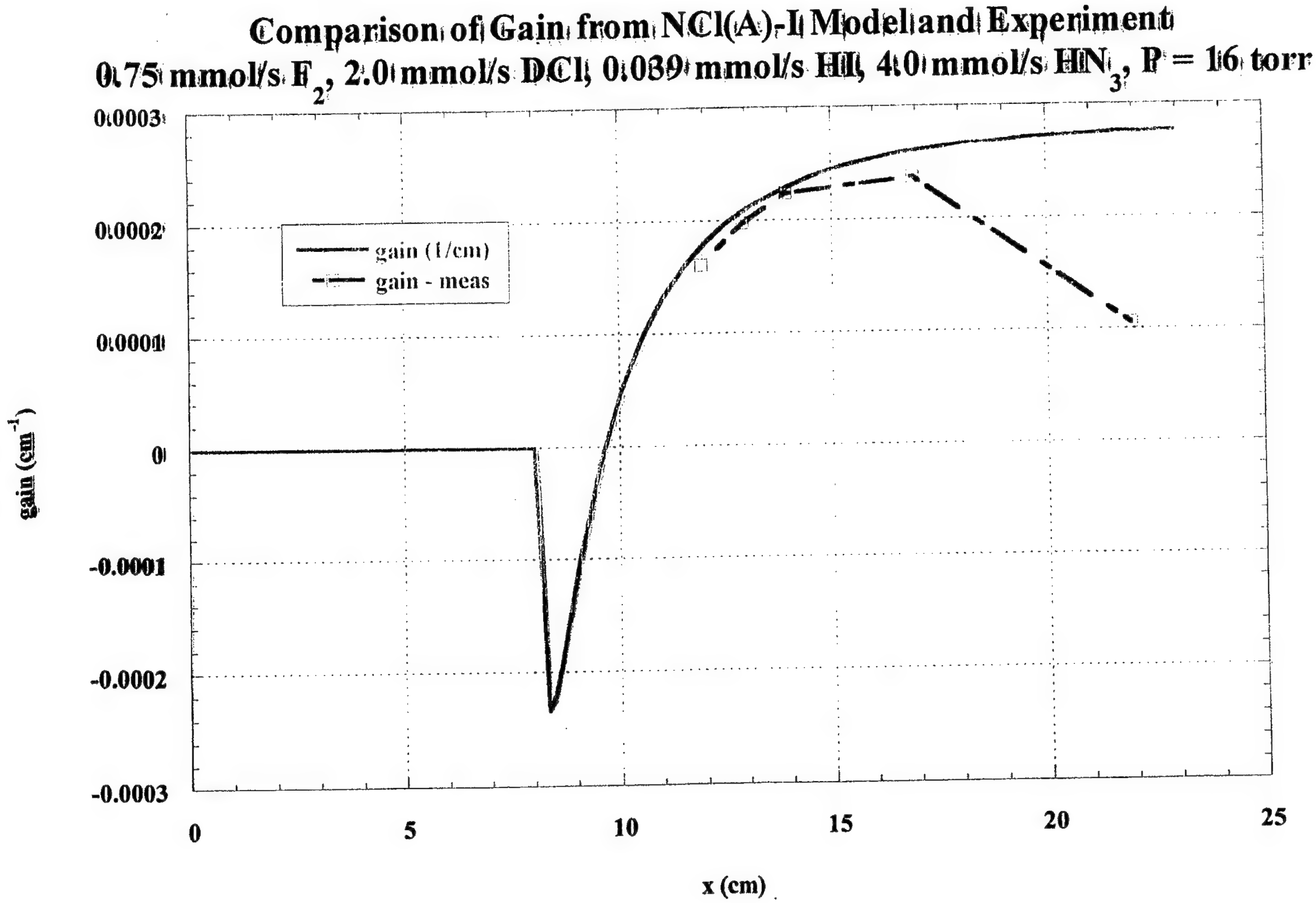

SSG Scaling with Reagent Flow

P = 16 Torr

$F_2 = 0.5$, DCl = 2.0, HI 0.03 mmole/s

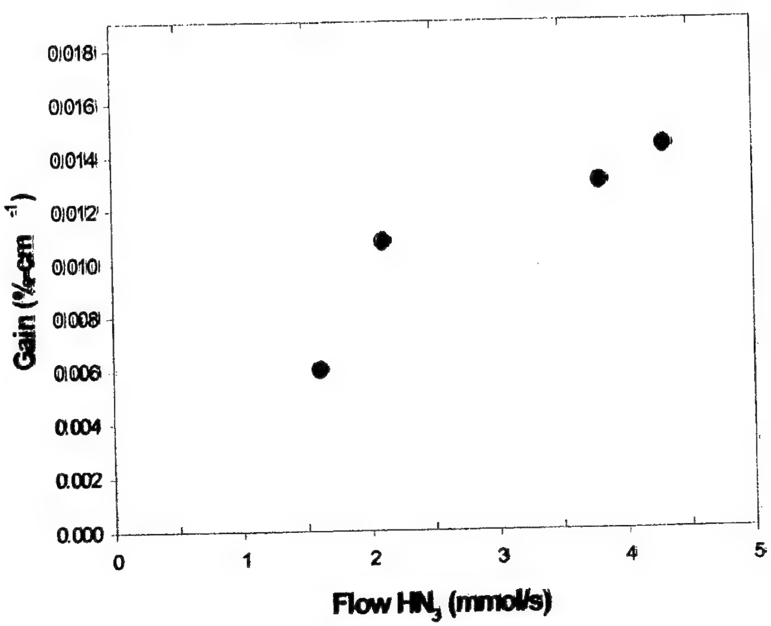

DCl = 2.0, HI 0.03 , HN_3 = 4.5 mmole

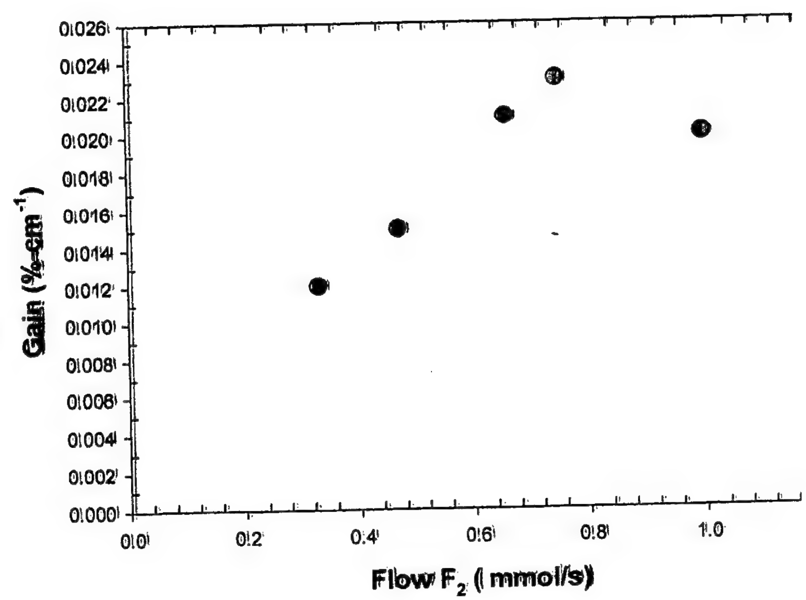

F ATOM DENSITY SCALING WITH PRESSURE

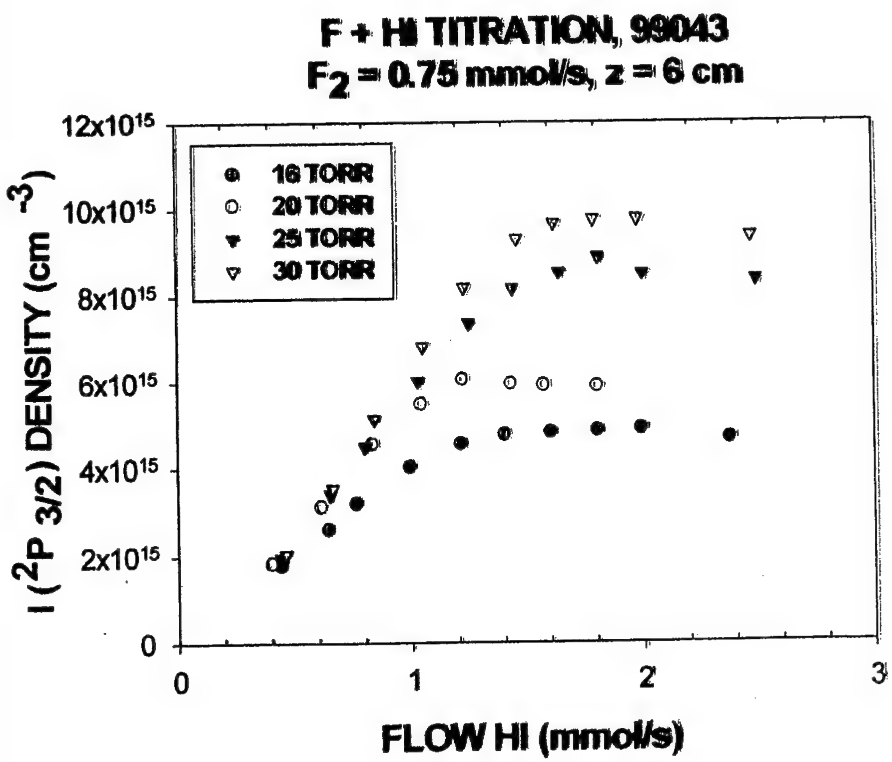

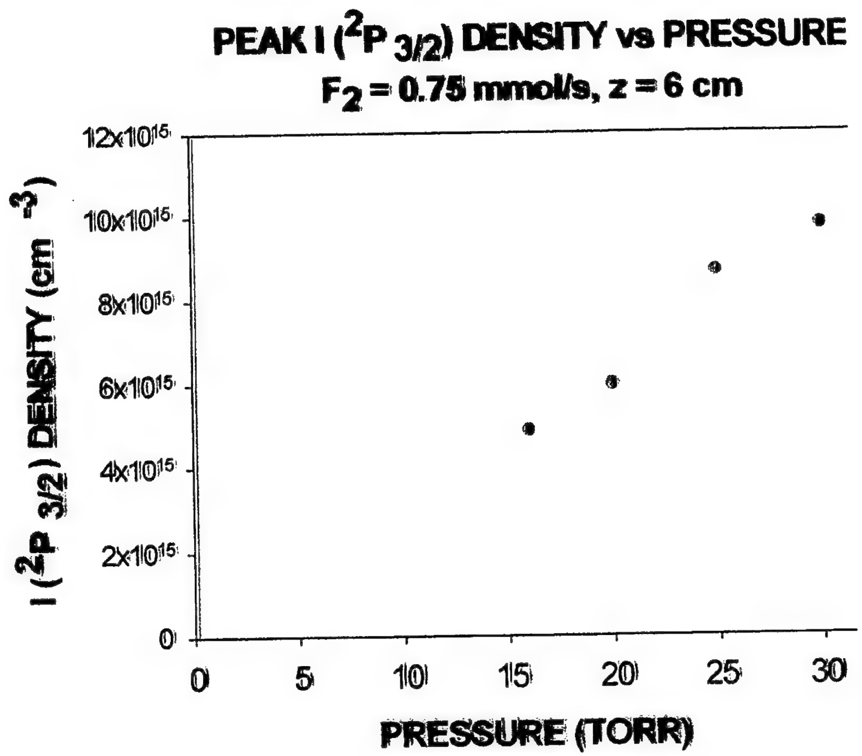

Recent Small Signal Gain (SSG) Scaling: Approx. 2-Fold Improvement in Gain

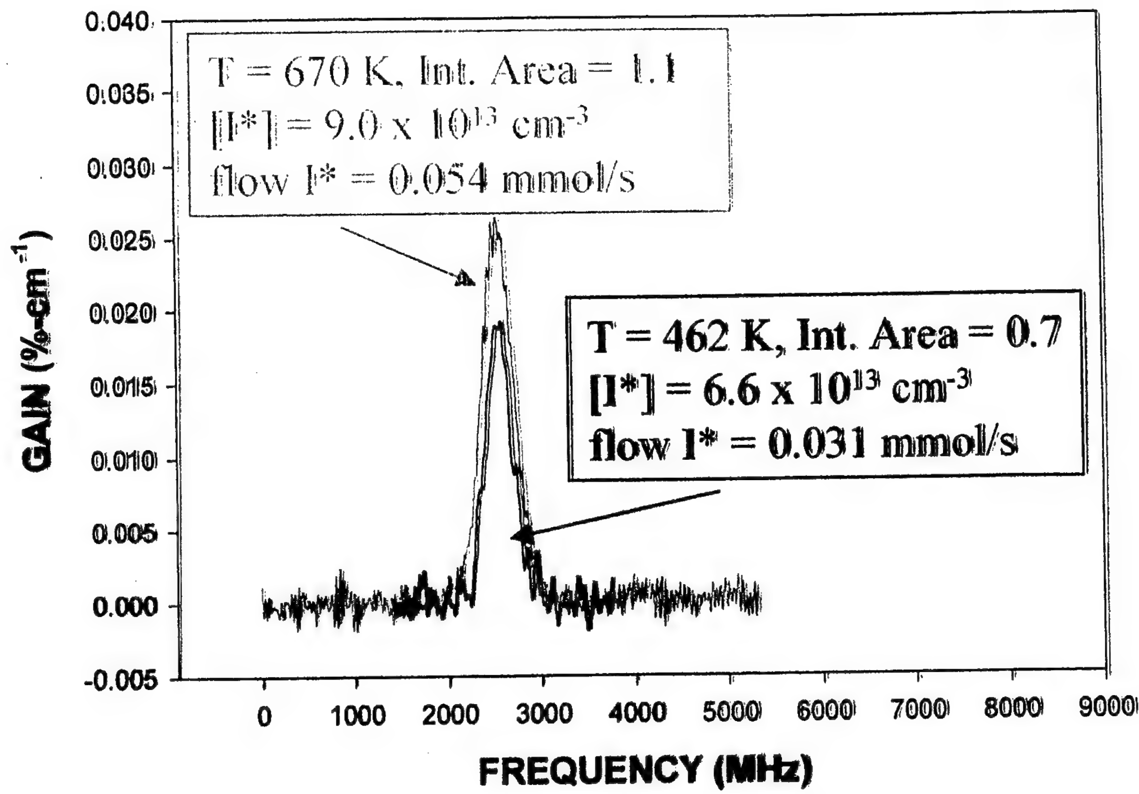

9070N: F_2 = 0.75 mmol/s, DCl = 2.0 mmol/s, HI = 0.04 mmol/s, HN_3 = 3.0 mmol/s
P = 19 TORR, z = 7 cm, NORTHSTAR PS

8176Q: F_2 = 0.66 mmol/s, DCl = 2.0 mmol/s, HI = 0.04 mmol/s, HN_3 = 3.0 mmol/s
P = 15 TORR, z = 7 cm , HELIOS PS

Summary

- Achieved significant milestone in advanced COIL concept
- Demonstrated unambiguous gain in the NCl(a)-I* system
- Current system characterized by low density, limited [F]
- Future experiments:

  scale system to high density, perform laser demonstration

Kinetic and thermodynamic aspects of chemical generation of atomic iodine for a COIL and their consequences for experiments

Vít Jirásek, Otomar Špalek and Jarmila Kodymová
Institute of Physics, Prague

OVERVIEW

1.Introduction into subject

2.Chemical generation of atomic iodine

- chemical generation of $I(^2P_{3/2})$ via atomic fluorine

- chemical generation of $I(^2P_{3/2})$ via atomic chlorine

3.Modelling of the reaction system

- system with atomic fluorine

- system with atomic chlorine

4.Summary

1. Introduction into subject

COIL operation - strongly influenced by a ratio $[I_2]/[O_2(^1\Delta_g)]$

Disadvantage of use of molecular iodine :

- difficult supply, both from solid and liquid phase
- meaningful part of stored energy in $O_2(^1\Delta_g)$ is consumed for I_2 dissociation

$\rightarrow$ use of atomic iodine : an estimated **increase up to 25% in laser power**

Possible techniques for an **atomic iodine production :**

- discharge techniques (dc discharge of alkyliodides[1], microwave discharge technique[2])
- chemical reaction (used for $NCl(a^1\Delta) + I$ laser[3])

---

[1] N.P. Vagin, N.N. Yuryshev, *Proc. SPIE* Vol. **3574**, 321 (1998)
[2] M. Endo, M. Kawakami, S. Takeda, F. Wani, T. Fujioka, *Proc. SPIE* Vol. **3612**, 56 (1999)
[3] T.L. Hanshaw, T.J. Madden, J.M. Herbelin, G. C. Manke, B.T. Anderson, R.T. Tate, G.D. Hager, *Proc. SPIE* Vol. **3612**, 147 (1999)

2. Chemical generation of atomic iodine

Aims:

- purely chemical generation
- method suitable for a cw COIL operation
- use of commercially available gases

Suggested process :

1. production of F or Cl atoms
2. reaction of these atoms with HI :

$$X + HI\ (DI) \rightarrow HX\ (DX) + I(^2P_{3/2}), \quad X = F \text{ or } Cl$$

Chemical generation of $I(^2P_{3/2})$ via atomic fluorine

First step : generation of fluorine atoms

⇒ **proposed reaction :** [4]

$NO + F_2 \rightarrow NOF + \mathbf{F}$ $\quad k_1 = 7 \times 10^{-13}\, e^{-1150/T}\ cm^3s^{-1}$ $\quad$ I-1)

⇒ fast

⇒ exothermic $(-\Delta H^0_{298}=77\ kJ/mole)$[5]

loss processes [6,7]**:**

$F + NO + NO \rightarrow NOF + NO$	$k_2 = 1.7 \times 10^{-31}\ cm^6s^{-1}$	(I-2)
$F + NO + He \rightarrow NOF + He$	$k_3 = 1.1 \times 10^{-31}\ cm^6s^{-1}$	(I-3)
$F + wall \rightarrow products$	$k_w = 12 \pm 19\ s^{-1}$	(I-4)
$F + F + M \rightarrow F_2 + M$	$k_5 = 5.3 \times 10^{-34}\ cm^6s^{-1}$	(I-5)

[4] C.E. Kolb, *J. Chem.Phys.* **64**, 3087 (1976)
[5] S. Johnston, H. J. Bertin, *J. Amer.Chem.Soc.* **81**, 6402 (1959)
[6] F.G. Skolnik, S.W. Veysey, M.G. Ahmed, W.E. Jones, *Can. J. Chem.* **53**, 3188 (1975)
[7] C.A. Helms, L. Hanko, K. Healey, G. Hager, G.P. Perram, *J. Appl.Phys.* **66**, 6093 (1989)

by-product: NOF formed partly as $NOF^* \rightarrow$ decays[6] :

$NOF^* \rightarrow NO + F$ $\qquad k_6 = 3.3 \times 10^{-14}\ cm^3s^{-1}$ (I-6)

$NOF^* \rightarrow NOF + h\nu$ $\qquad k_7 \sim 10^{-5}\ s^{-1}$ (I-7)

$NOF^* + M \rightarrow NOF + M$ $\qquad k_8 = 3.3 \times 10^{-10}\ cm^3s^{-1}$ (I-8)

F production efficiency :

- critically depended on the dilution[7] and $[F_2]$:[NO] ratio
- 18 % predicted[8]
- 20-30 % measured[7]

<u>Second step : reaction of fluorine atoms with HI</u>

$F + HI \rightarrow HF\ (HF^*) + \mathbf{I(^2P_{3/2})}$ $\qquad k_9 = 7.3 \times 10^{-11}\ cm^3s^{-1}$ (I-9)

$\Rightarrow$ **very exothermic** (ΔH^o_{298} = - 216.7 kJ/mole), 75% transformed to vibrational energy of HF^* ($v \leq 6$)[9]

---

[7] C.A. Helms, L. Hanko, K. Healey, G. Hager, G.P. Perram, *J. Appl.Phys.* **66**, 6093 (1989)
[8] J.M. Hoell, F. Allario, O. Jarrett, R.K. Seals, *J. Chem.Phys.* **38**, 2896 (1973)

also electronically excited iodine atoms $I^*(^2P_{1/2})$ may be formed [10]:

$F + HI \rightarrow HF + \mathbf{I^*(^2P_{1/2})}$ (I-9a)

$\Rightarrow$ insufficient for a laser action due to the actual branching ratio of $\mathbf{I^*(^2P_{1/2})}$

HI molecule - **inefficient quencher of $O_2(^1\Delta_g)$[11]:**

$O_2(^1\Delta_g) + HI \rightarrow O_2(^3\Sigma_g) + HI \quad k_{10} \leq 2 \times 10^{-17}\ cm^3s^{-1}$ ((I-10)

quenching of I^* :

$HI + I^* \rightarrow HI + I \quad k_{11} = 5.7 \times 10^{-14}\ cm^3s^{-1}$ (I-11)

$\Rightarrow$ important for COIL operation

---

[9] N. Jonathan, C.M. Melliar-Smith, S. Okuda, D.H. Slater, D. Timlin, *Molecular Physics* **22**, 561 (1971)
[10] U. Dinur, R. Kosloff, R.D. Levine, *Chem.Phys.Lett.* **34**, 199 (1975)
[11] J.B. Koffend, C.E. Gardner, R.F. Heidner, *J. Chem.Phys.* **80**, 1861 (1984)

Chemical generation of $I(^2P_{3/2})$ via atomic chlorine

First step : generation of chlorine atoms

overall process[12] :

$ClO_2 + 2\,NO \rightarrow 2\,NO_2 + Cl$ (II-1)

chain-branching reaction scheme[12,13]:

$ClO_2 + NO \rightarrow NO_2 + ClO$ $k_2 = 3.4 \times 10^{-13}\ cm^3s^{-1}$ (II-2)

$ClO + NO \rightarrow NO_2 + Cl$ $k_3 = 1.7 \times 10^{-11}\ cm^3s^{-1}$ (II-3)

$Cl + ClO_2 \rightarrow 2\,ClO$ $k_4 = 5.9 \times 10^{-11}\ cm^3s^{-1}$ (II-4)

---

[12] S.J. Arnold. K.D. Foster. D.R. Snelling, R.D. Suart, *Appl.Phys.Lett.* 30, **637** **(1977)**

[13] S.J. Arnold, K.D. Foster, D.R. Snelling, R D. Suart, *IEEE J. Quant.Electr.* **QE-14**, 293 (1978)

loss processes :

$$Cl + NO_2 + He \rightarrow NO_2Cl + He \qquad k_5 = 7.2 \times 10^{-31}\ cm^6s^{-1} \quad (II\text{-}5)$$

$$Cl + ClNO_2 \rightarrow Cl_2 + NO_2 \qquad k_6 = 3.0 \times 10^{-11}\ cm^6s^{-1} \quad (II\text{-}6)$$

$$ClO + NO_2 + He \rightarrow NO_3Cl + He \qquad k_7 = 1.0 \times 10^{-31}\ cm^6s^{-1} \quad (II\text{-}7)$$

$$Cl + Cl + M \rightarrow Cl_2 + M \qquad k_8 = 6.4 \times 10^{-33}\ cm^6\,s^{-1} \quad (II\text{-}8)$$

Second step : reaction of chlorine atoms with HI

$$Cl + HI \rightarrow HCl^* + \mathbf{I(^2P_{3/2})}\ ^{17,18} \qquad k_9 = 1.64 \times 10^{-11}\ cm^3s^{-1} \quad (II\text{-}9)$$

⇒132.5 kJ/mole exothermic[9], 70% transformed to vibrational energy in HCl^*[14]

---

[14] J.C. Polanyi, K.B. Woodall, *J.Chem.Phys.* 56, 1563 (1972)

side reactions [13,15,16] :

$I + Cl + M \rightarrow ICl + M$	$k_{10} = 1.0 \times 10^{-32}\ cm^6s^{-1}$	(II-10)
$I + I + M \rightarrow I_2 + M$	$k_{11} = 4.2 \times 10^{-33}\ cm^6s^{-1}$	(II-11)
$HI + O_2(^1\Delta_g) \rightarrow HI + O_2(^3\Sigma_g)$	$k_{12} \leq 2 \times 10^{-17}\ cm^3s^{-1}$	(II-12)
$HCl + O_2(^1\Delta_g) \rightarrow HCl + O_2(^3\Sigma_g)$	$k_{13} = 4 \times 10^{-18}\ cm^3s^{-1}$	(II-13)
$HCl + I^* \rightarrow HCl + I$	$k_{14} = (0.32\text{-}1.5) \times 10^{-14} cm^3s^{-1}$	(II-14)

method successfully applied in operating purely chemical HCl and HCl/CO_2 transfer lasers[12.13]

[15] Kulagin. Yarygina et al[94]
[16] J.P. Singh, J. Bachar, D.W. Setser, S. Rosenwaks, *J. Phys.Chem.* 89, 5347 (1985)

3. Modelling of the reaction systems

specifications :

- one dimensional model
- reactants introduced directly into the primary flow of COIL
- instantaneous mixing
- heat transfer to the walls neglected
- fluid dynamic neglected
- enthalpy balance with $c_p \neq c_p(T)$ included

flow and pressure conditions → typical for the subsonic channel of our SCOIL :

Cl_2 flowrate	40 mol/s
pr. He flowrate	80 mmol/s
sec. He flowrate	40 mmol/s
total pressure	4 kPa
$O_2(^1\Delta_g)$ pressure	580 Pa
flow speed	100 m/s

Reaction system with atomic fluorine as intermediate reactant

First step : production of atomic fluorine

- reactions (I-1) - (I-3) and (I-5) included
- wall recombination neglected
- reactions with primary flow components neglected
- ΔH_r of reactions (I-1) and (I-3) included

Results :

- 30 % maximum efficiency of F atoms at ratio $[F_2]:[NO]:[He]=1:2:30$
- high temperature (550 K)
- 10 cm reaction path for maximum [F]
- high residual concentrations of NO, F_2 and NOF

Second step : HI added into the system

1. HI injected together with F_2+NO+He mixture
2. HI injected downstream to the primary flow at the place of maximum [F] concentration

- reaction (I-9) and recombination of I atoms (II-11) added
- quenching processes by HI neglected

Results :

- 100 % conversion of HI to I
- HI injected together with F_2+NO+He mixture :

- long reaction path
  - 90 % conversion at 50 cm
  - temperature 525 K

- HI injected 9.6 cm downstream of F_2+NO+He mixture :

- 55 % conversion at 23 cm
  - temperature 800 K

Reaction system with atomic chlorine as intermediate reactant

First step : production of atomic chlorine :

- reactions (II-2) - (II-7) included
- ΔH_r of reactions (II-2), (II-3) included
- recombination of Cl atoms neglected
- reactions with primary flow components neglected

Results :

- ClO is the main product at ratio $[ClO_2]:[NO]:[He]=1:1:75$
- 56 % maximum efficiency of Cl atoms at ratio $[ClO_2]:[NO]:[He]=1:2:75$
- temperature 450 K
- short reaction path for maximum [Cl] (0.46 cm)
- high concentration of NO_2

Second step : HI added into the system

1. HI injected together with ClO_2+NO+He mixture
2. HI injected downstream to the primary flow at the place of maximum

- reaction (II-9) and recombination of I atoms (II-11) added
- quenching processes by HI neglected

Results :

- best results if HI is injected together with ClO_2+NO+He mixture
- 80 % I yield at 5 cm, **maximum 90 % yield** at 20 cm
- temperature 480 K

4. Summary

- **<u>the most efficient production of atomic iodine :</u>**

  - ClO_2, NO and HI injected as reactants into the subsonic channel

  - 90 % conversion of HI to I when HI injected simultaneously

  - 3 cm reaction path when HI injected 0.46 cm downstream

- reaction scheme with **fluorine atoms :**

  - reaction path substantially longer (50cm)

  - lower yields of atomic iodine (~60 %)

  - separate reactor at higher pressure needed

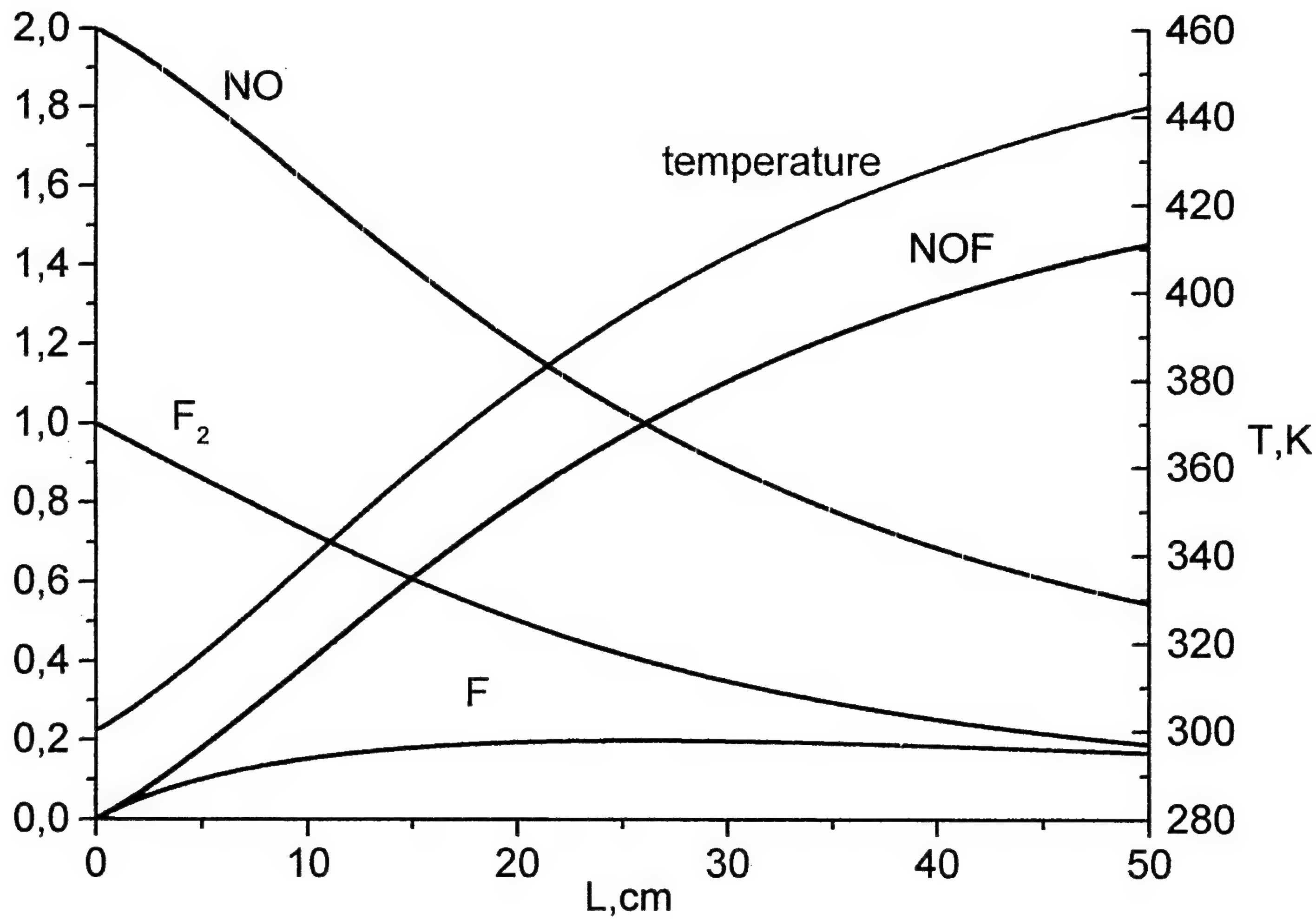

Fig.1a. PRODUCTION OF F ATOMS

Relative concentrations and temperature in reaction system

$[F_2] : [NO] : [He] = 1 : 2 : 75$

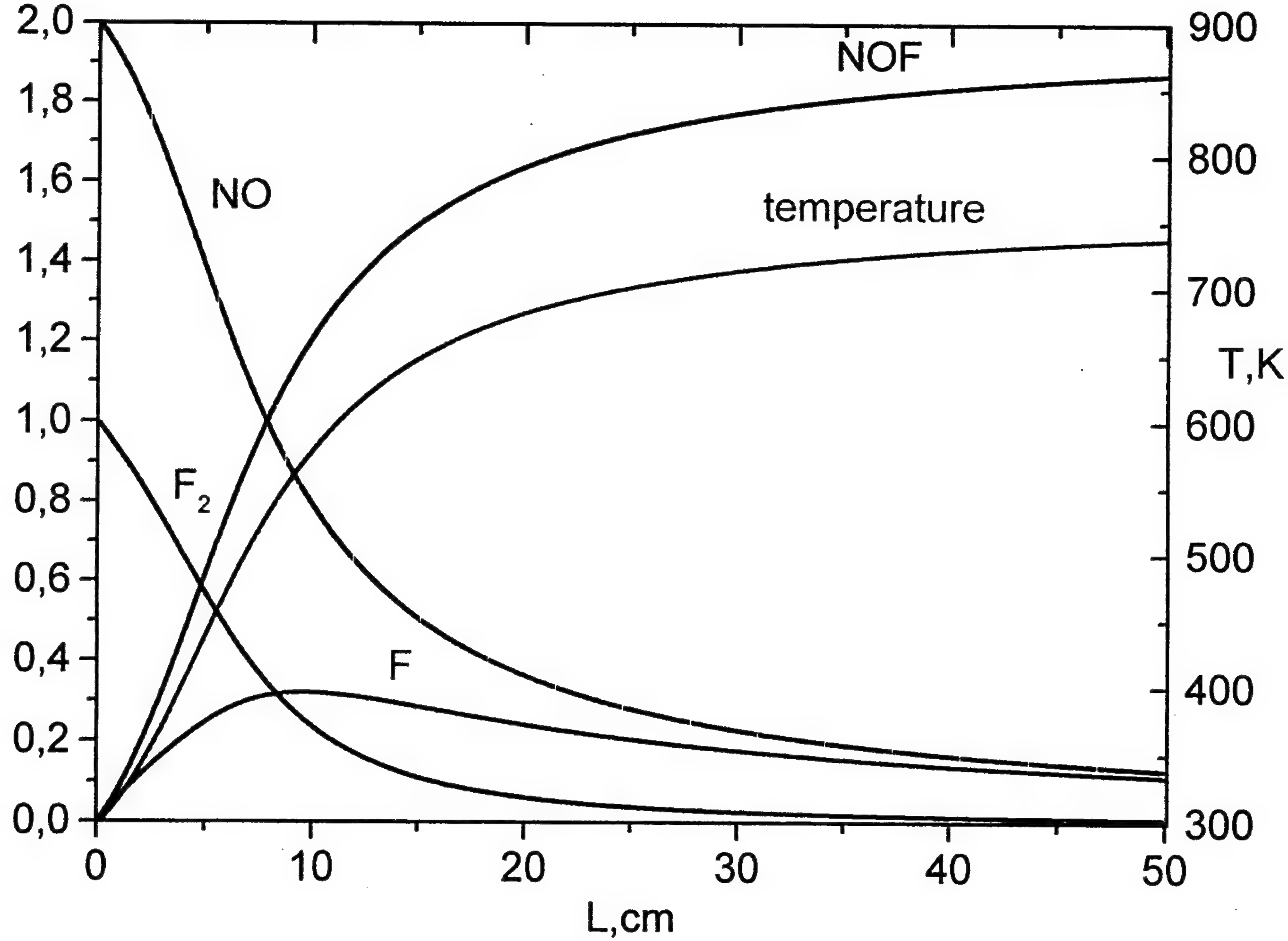

Fig.1b. PRODUCTION OF F ATOMS

Relative concentrations and temperature in reaction system

$[F_2] : [NO] : [He] = 1 : 2 : 30$

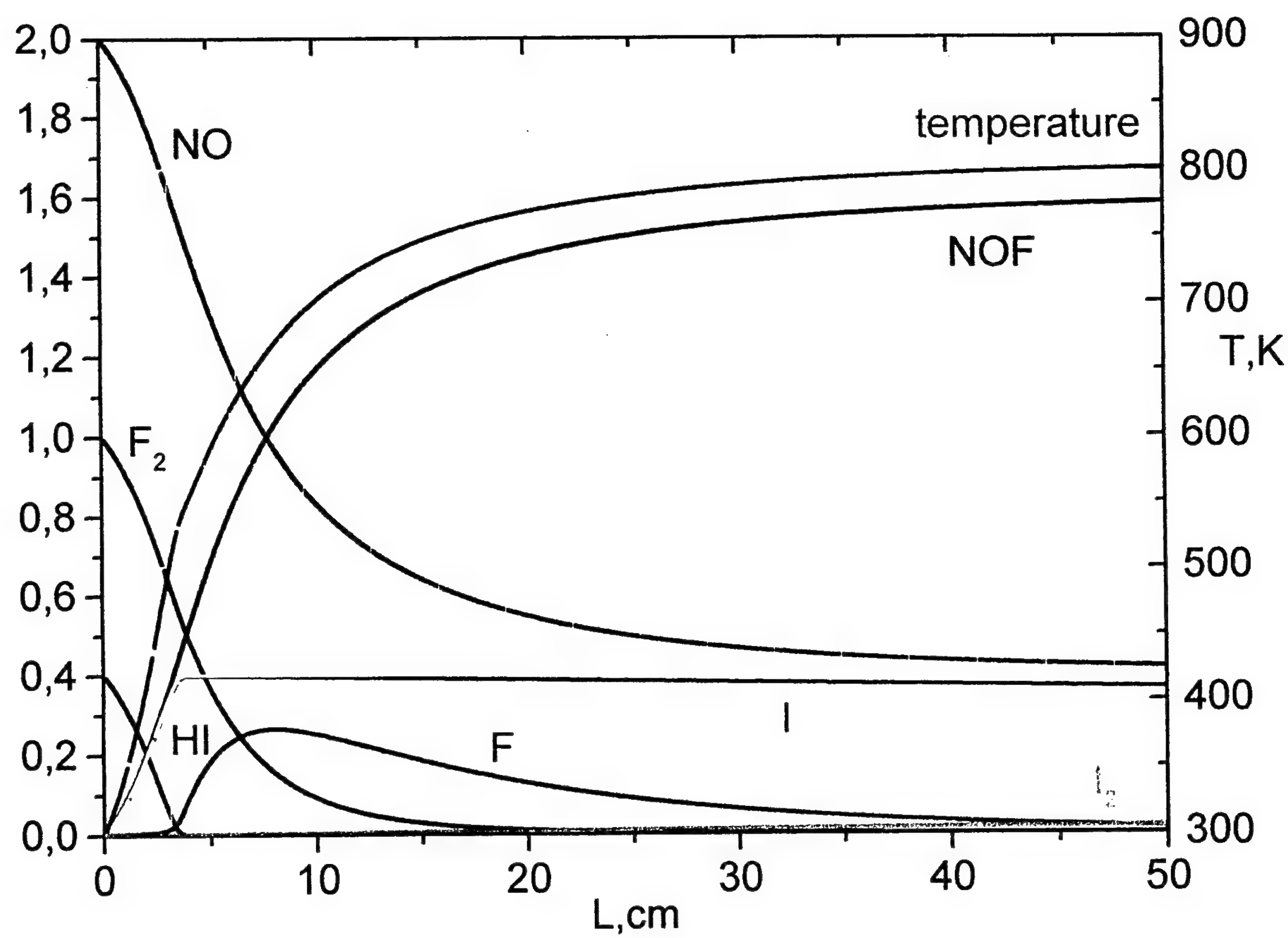

Fig.2. PRODUCTION OF I ATOMS

Relative concentrations and temperature in reaction system

$[F_2] : [NO] : [HI] : [He] = 1 : 2 : 0.4 : 30$

HI injected together with F_2 + NO + He mixture

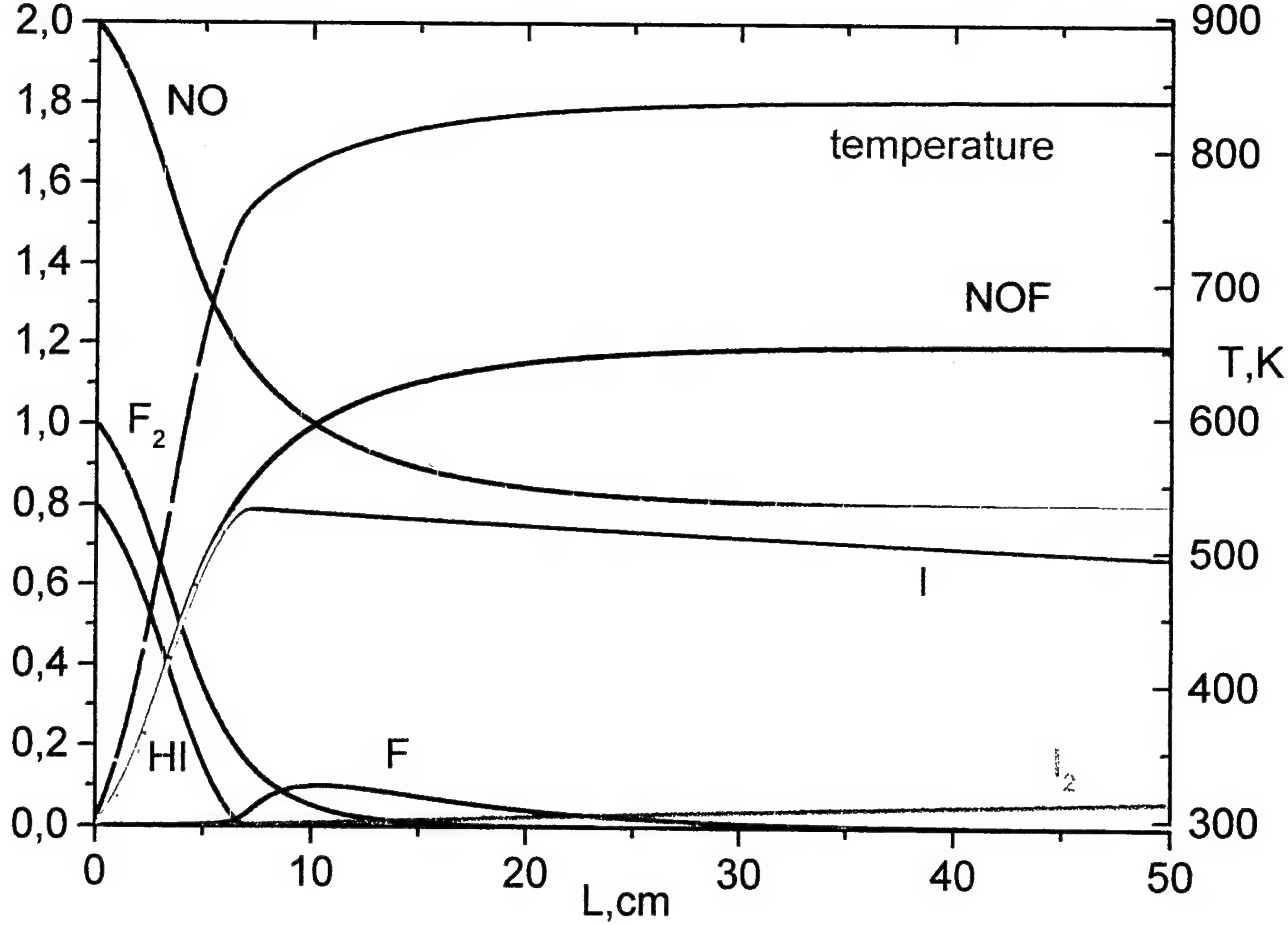

Fig.3. PRODUCTION OF I ATOMS

Relative concentrations and temperature in reaction system

$[F_2] : [NO] : [HI] : [He] = 1 : 2 : 0.8 : 30$

HI injected together with F_2 + NO + He mixture

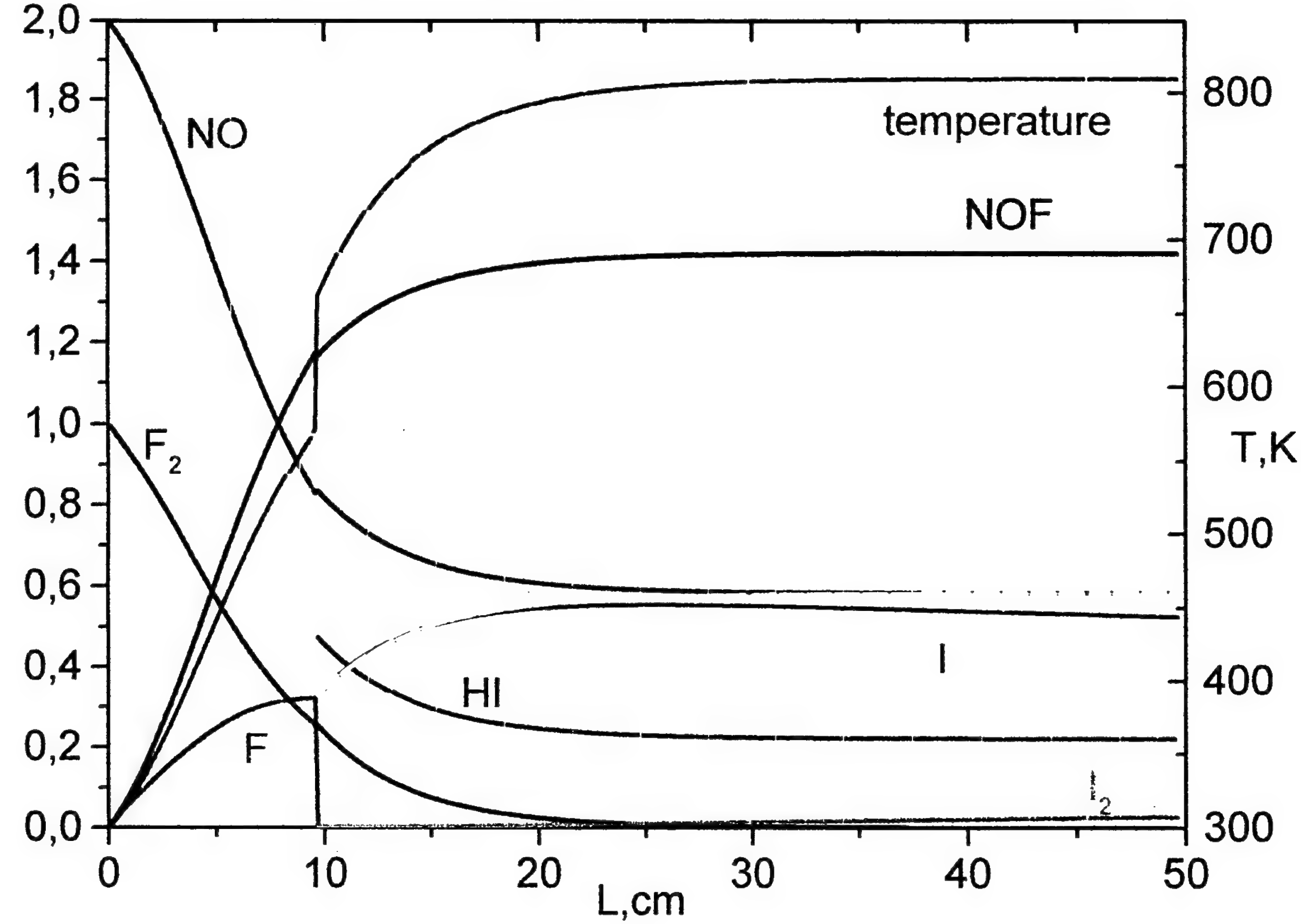

Fig.4. PRODUCTION OF I ATOMS

Relative concentrations and temperature in reaction system

$[F_2] : [NO] : [HI] : [He] = 1 : 2 : 0.8 : 30$

HI injected 9.6 cm downstream of F_2 + NO + He mixture

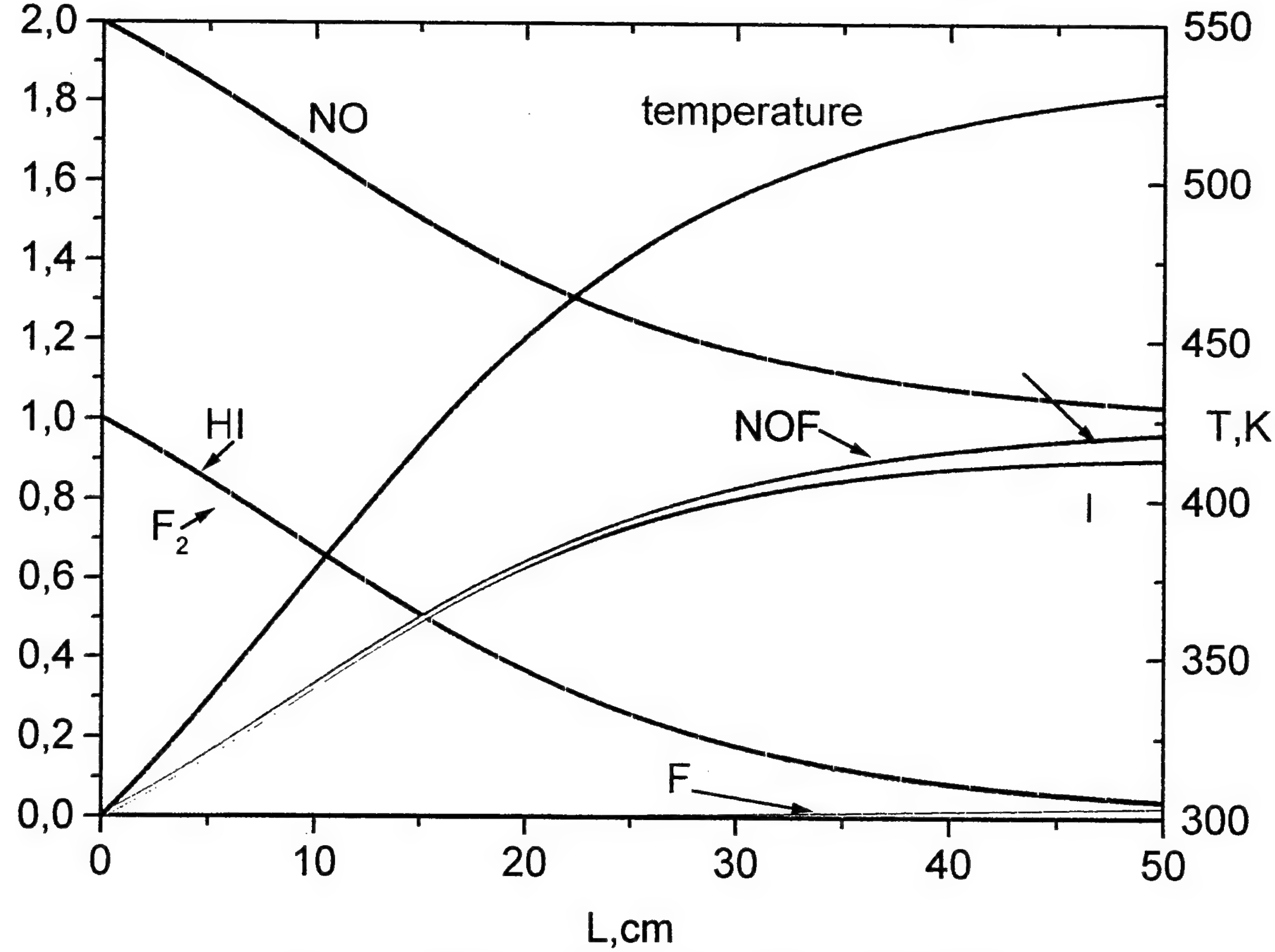

Fig.5. PRODUCTION OF I ATOMS

Relative concentrations and temperature in reaction system

$[F_2] : [NO] : [HI] : [He] = 1 : 2 : 1 : 75$

HI injected together with F_2+ NO + He mixture

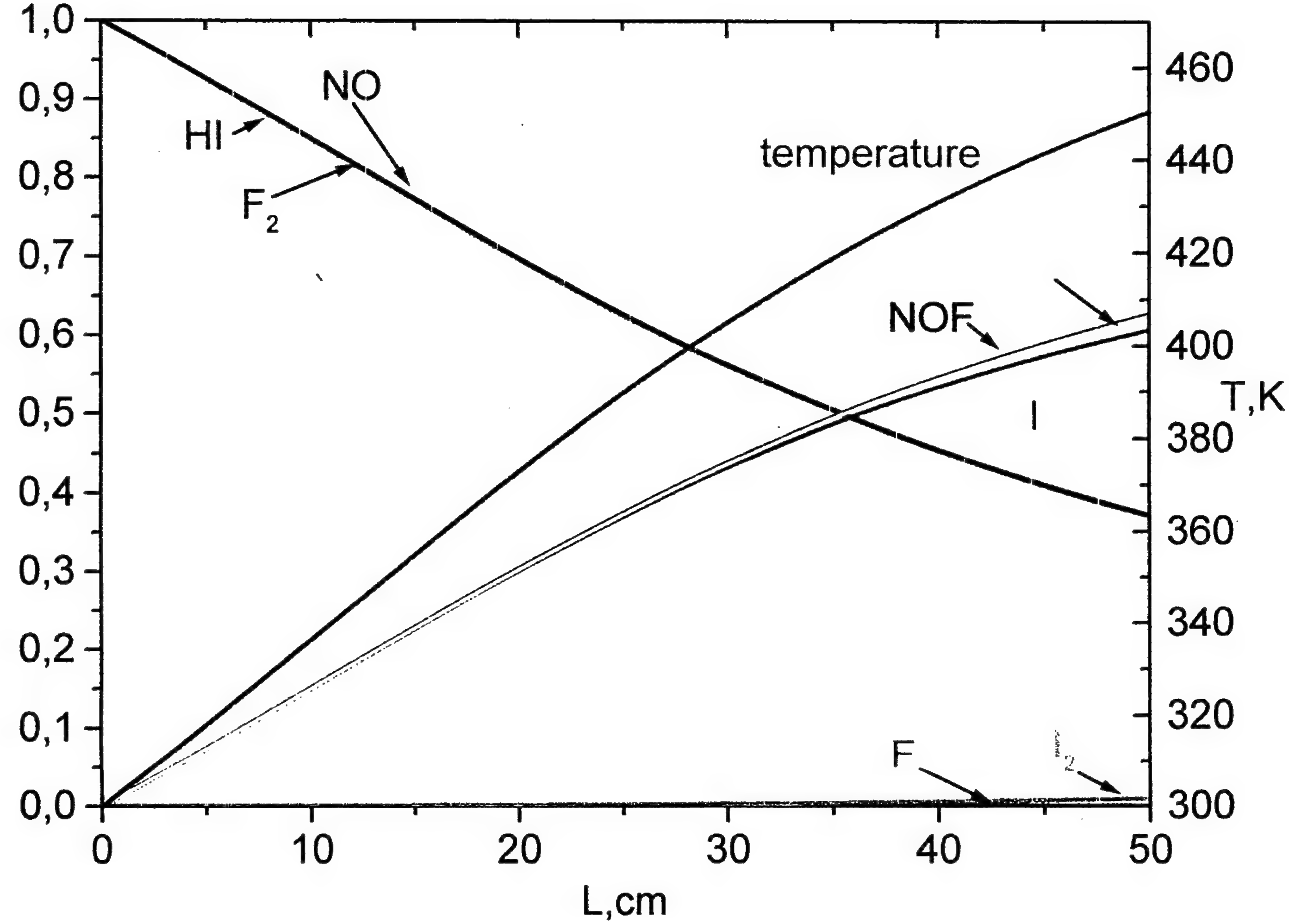

Fig.6. PRODUCTION OF I ATOMS

Relative concentrations and temperature in reaction system

$[F_2] : [NO] : [HI] : [He] = 1 : 1 : 1 : 75$

HI injected together with F_2 + NO + He mixture

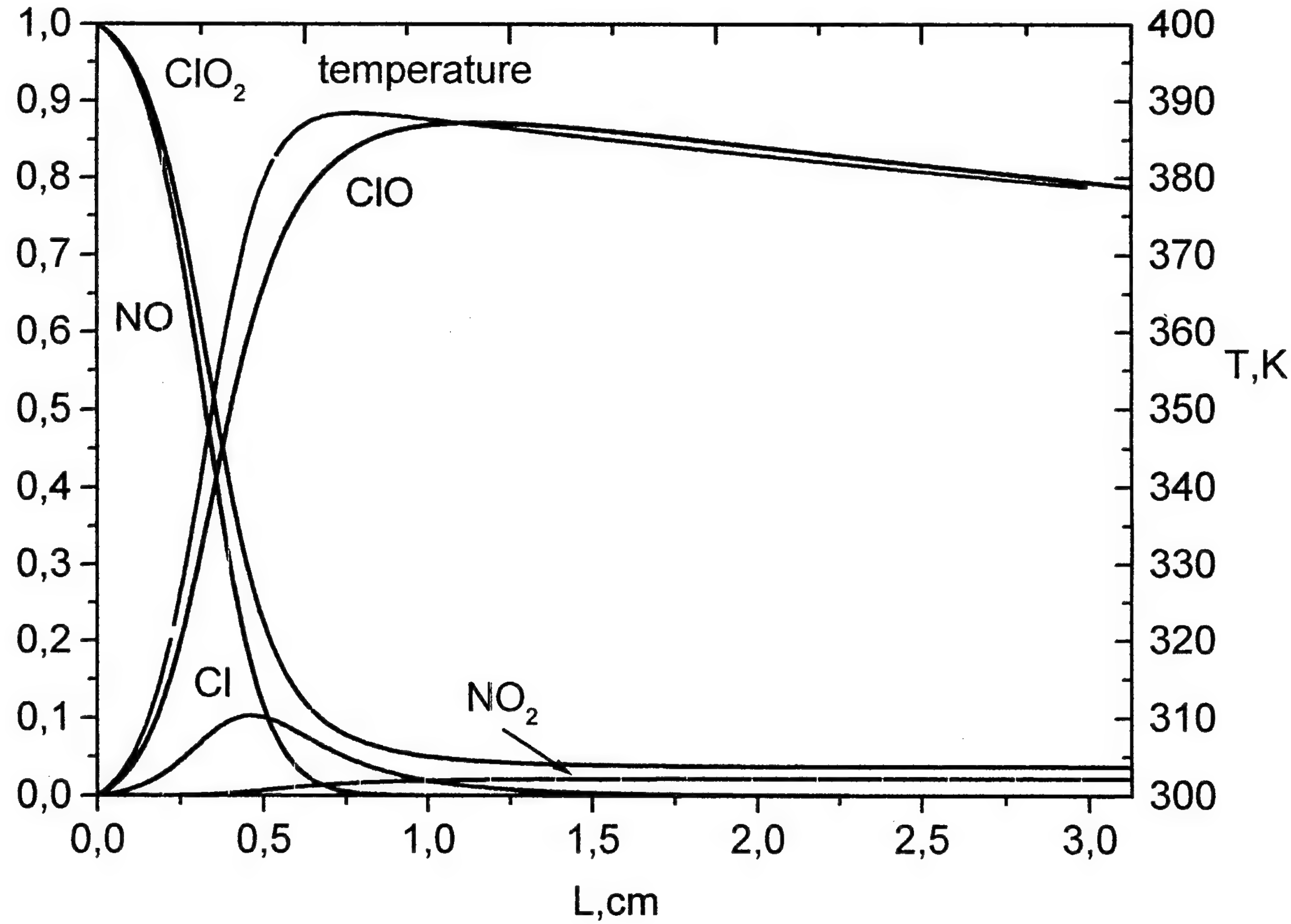

Fig.7 PRODUCTION OF Cl ATOMS

Relative concentrations and temperature in reaction system
$[ClO_2] : [NO] : [He] = 1 : 1 : 75$

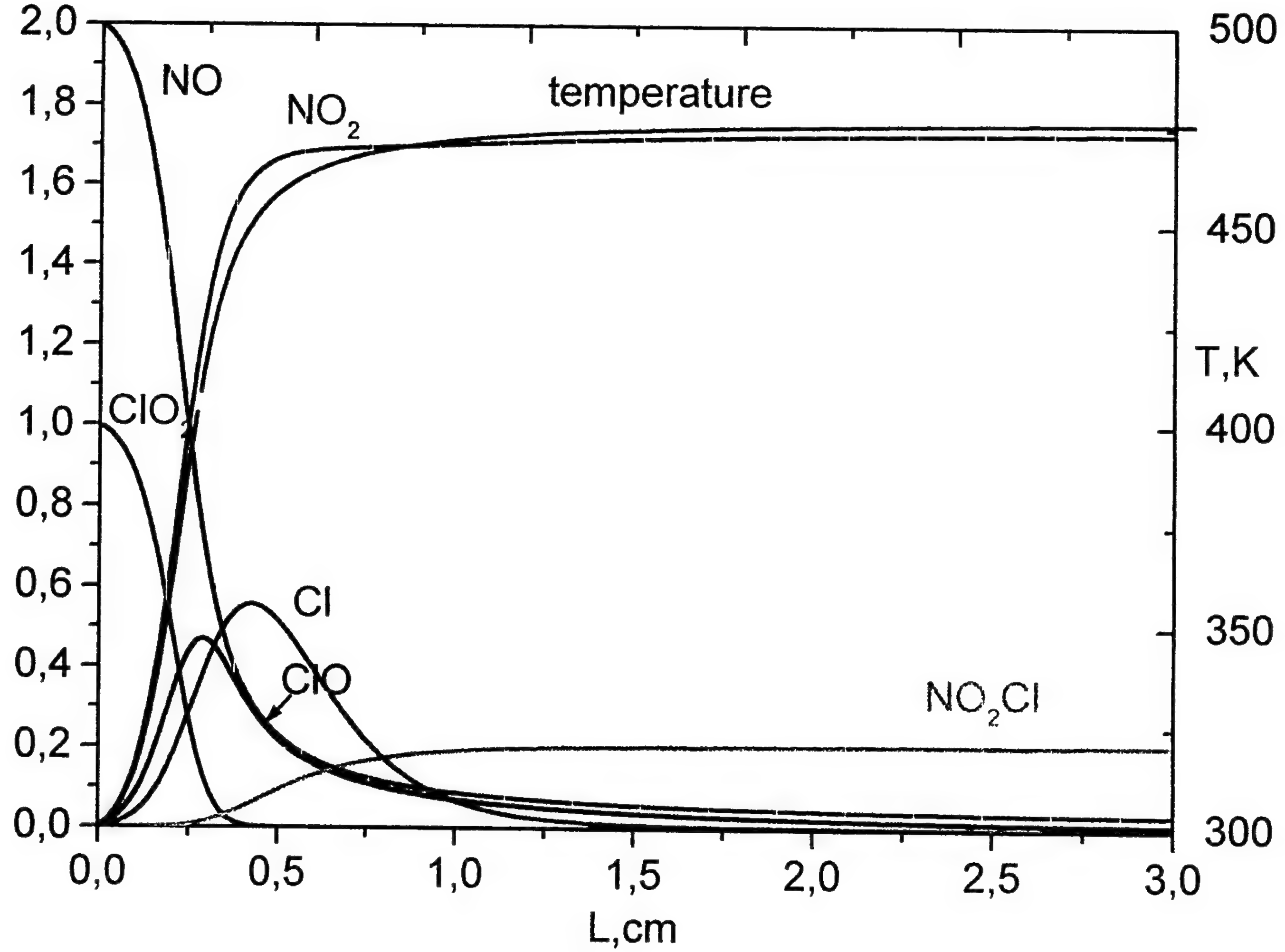

Fig.8 PRODUCTION OF Cl ATOMS

Relative concentrations and temperature in reaction system

$[ClO_2] : [NO] : [He] = 1 : 2 : 75$

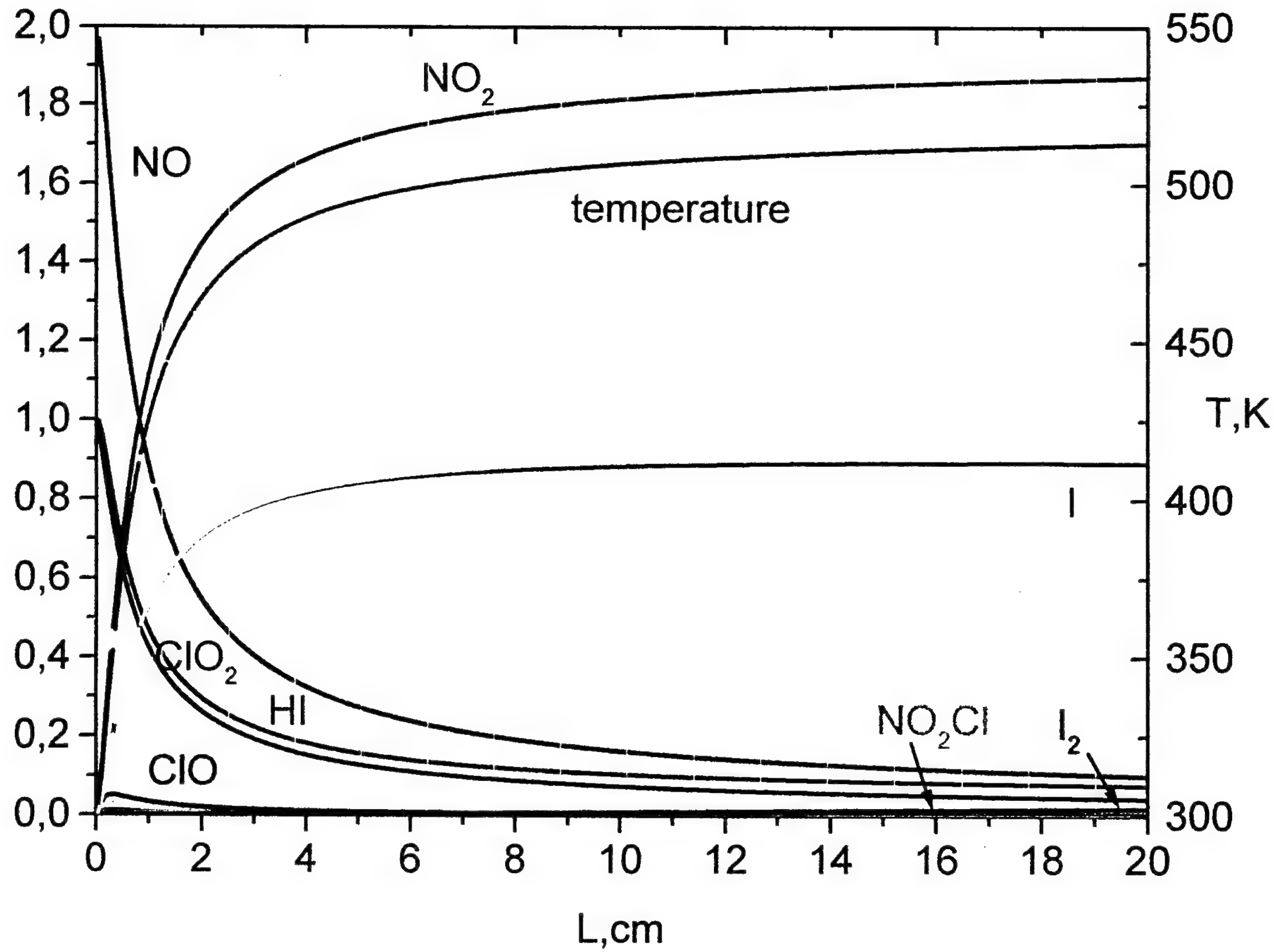

Fig.9 PRODUCTION OF I ATOMS

Relative concentrations and temperature in reaction system

$[ClO_2] : [NO] : [HI] : [He] = 1 : 2 : 1 : 75$

HI injected together with ClO_2 + NO + He mixture

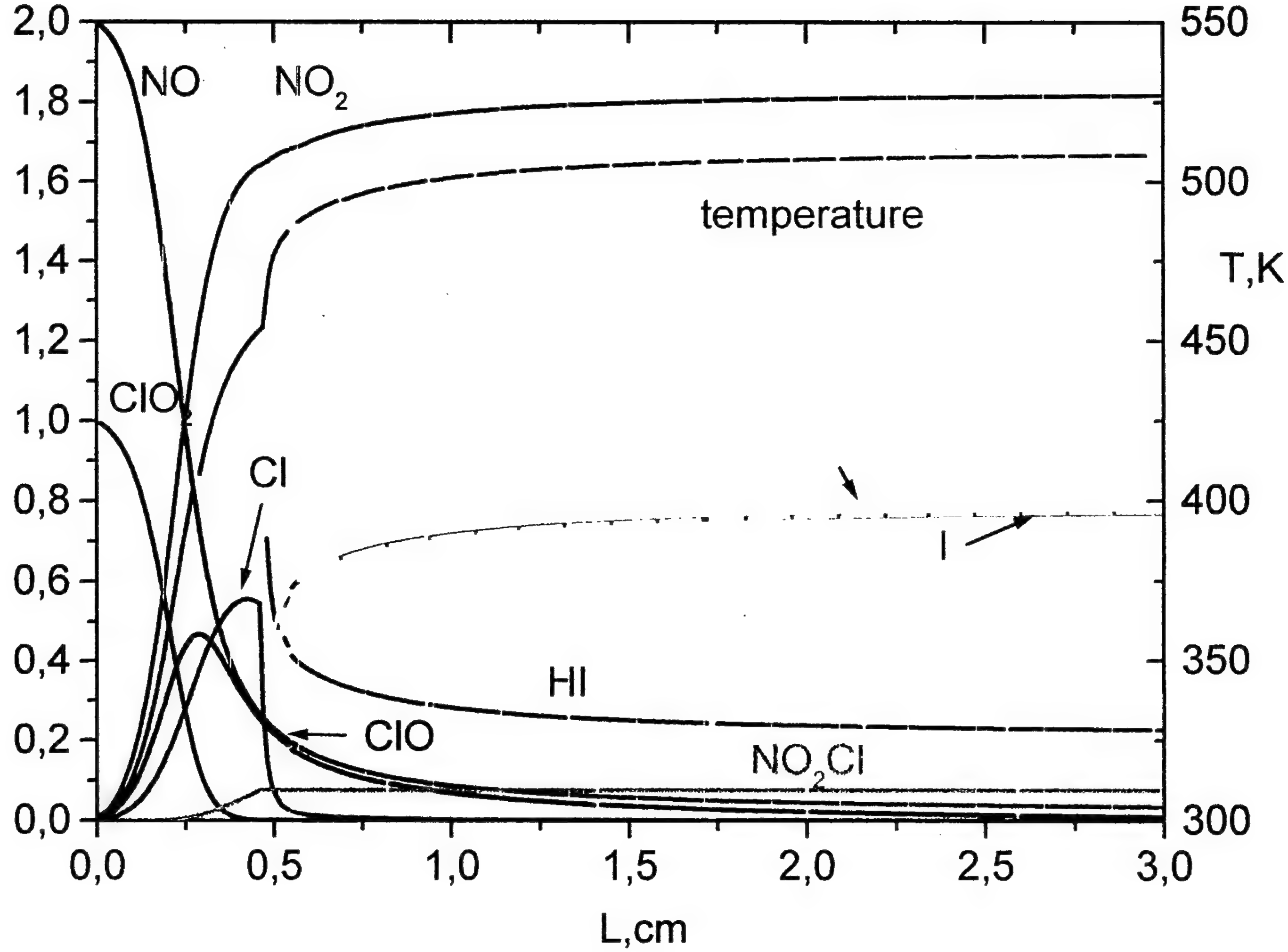

Fig.10 PRODUCTION OF I ATOMS

Relative concentrations and temperature in reaction system

$[ClO_2] : [NO] : [HI] : [He] = 1 : 2 : 1 : 75$

HI injected 0.46 cm downstream of with ClO_2 + NO + He mixture

PULSED CHEMICAL OXYGEN-IODINE LASER WITH VOLUME GENERATION OF IODINE ATOMS.

Yuryshev N. N.

P.N. Lebedev Physics Institute
117924 Moscow, Leninski prospekt 53, Russia

Contents

1. Introduction.
2. Different ways of pulsed mode realization in COIL.
3. Water vapor influence.
4. Pulsed COIL with photolysis.
5. Pressure dependence of output energy. Ozone photolysis as singlet oxygen source.
6. Iodide influence.
7. Pulsed COIL with electric discharge.
8. Pulsed COIL with AOM.
9. COIL pumped solid-state laser.
10. Pulsed COIL as a simulator for the high-power CW laser.
11. Investigation of plasma in oxygen with high singlet oxygen content.

CW COIL with Q-switching

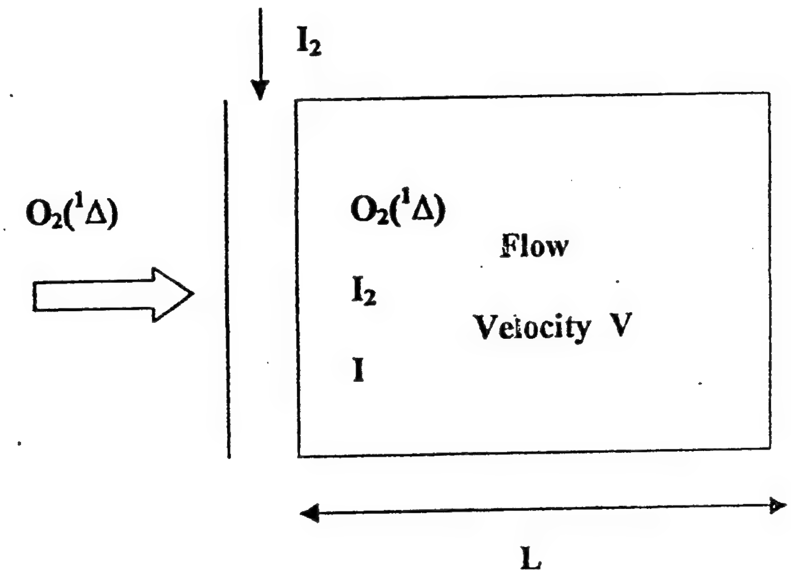

Relaxation process $O_2(^1\Delta) + I(^2P_{1/2}) \rightarrow O_2(^1\Sigma) + I(^2P_{3/2})$ $\qquad K_3 = 1\cdot10^{-13}\ cm^3/s$

$$\tau_{rel\,1} = 1 / K_3 [I(^2P_{1/2})] \approx 1 / K_3 [I]$$

$$L_{max} = V\cdot\tau_{rel\,1}$$

$$E_{stored} = h\nu\, [O_2(^1\Delta)]\, S\, V / K_3 [I]$$

$$\tau_{pulse} = 1 / K_{transfer} [I]$$

$P_{pulse} = h\nu [O_2(^1\Delta)] S V K_{transfer} / K_3$ $\qquad P_{pulse} / P_{CW} = K_{transfer} / K_3 = 7.7\cdot10^2$

For limited aperture

$$P_{pulse} / P_{CW} = L\, K_{transfer} [I] / V$$

Experiment

$$P_{pulse} / P_{CW} = 16$$

Pulsed COIL with Volume Generation of Iodine Atoms

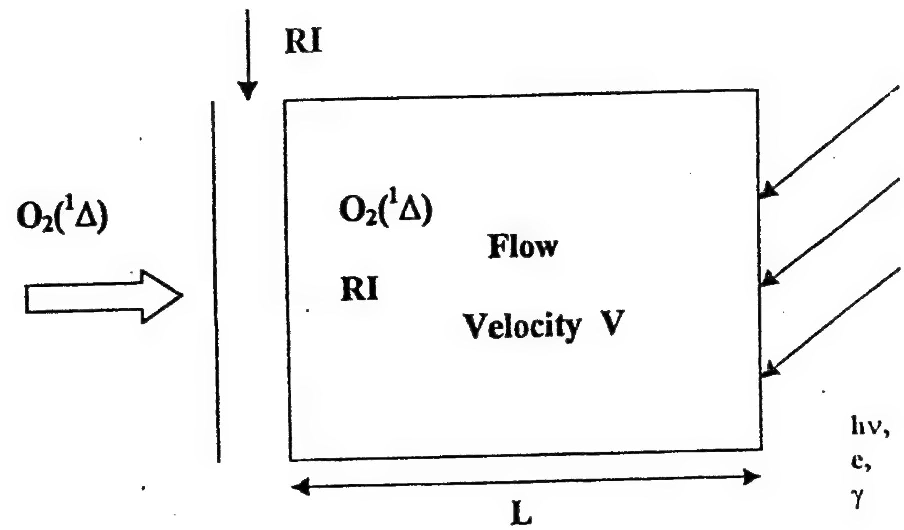

Relaxation process $O_2(^1\Delta) + O_2(^1\Delta) \rightarrow O_2(^1\Sigma) + O_2(^3\Sigma)$ $\quad K_4 = 2\cdot10^{-17}\ cm^3/s$

$$\tau_{rel\,2} = 1.7 / K_4 [O_2(^1\Delta)]_0$$

$$L_{max} = V\cdot\tau_{rel\,2}$$

$$\tau_{rel\,2} / \tau_{rel\,1} = 1.7K_3[I] / K_4 [O_2(^1\Delta)]_0 = 8.5\cdot10^3\cdot\{ [I] / [O_2(^1\Delta)] \}$$

E_{stored} is a function of active medium volume and singlet oxygen pressure.

Pulse duration and small signal gain are the functions of iodine atom concentration.

Influence of Water Vapor Content on Output Energy

$[I(^2P_{1/2})] + [H_2O] \rightarrow [I(^2P_{3/2})] + [H_2O]$, $\quad K_q = 2\cdot10^{-12}\ cm^3/s$

$$K_{transfer}\,[O_2(^1\Delta)]\,[I(^2P_{3/2})] \gg K_q\cdot[I(^2P_{1/2})]\cdot[H_2O]$$

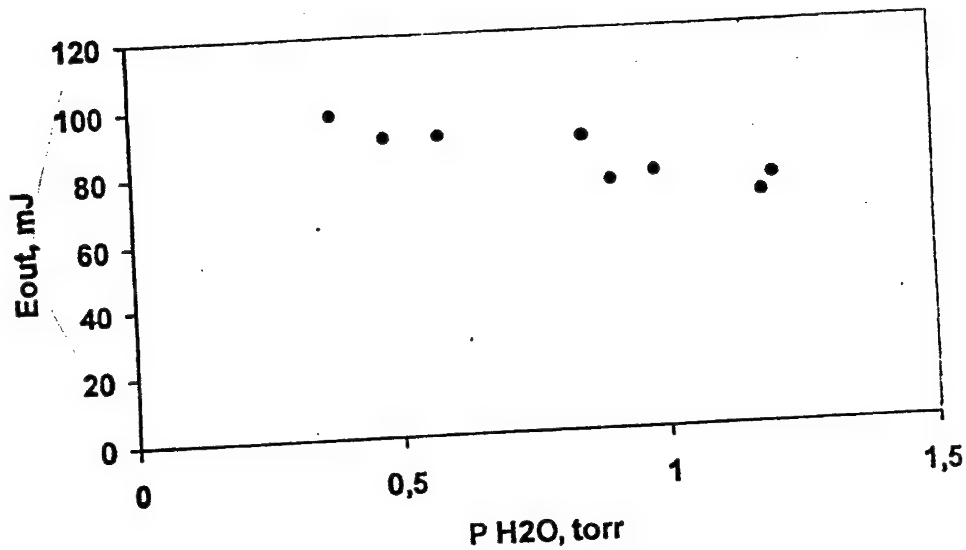

Dependence of output energy on the partial pressure of the water vapor, $P_{O2} = 0.35$ torr, $P_{RI} = 0.12$ torr

Pulsed COIL with photolysis

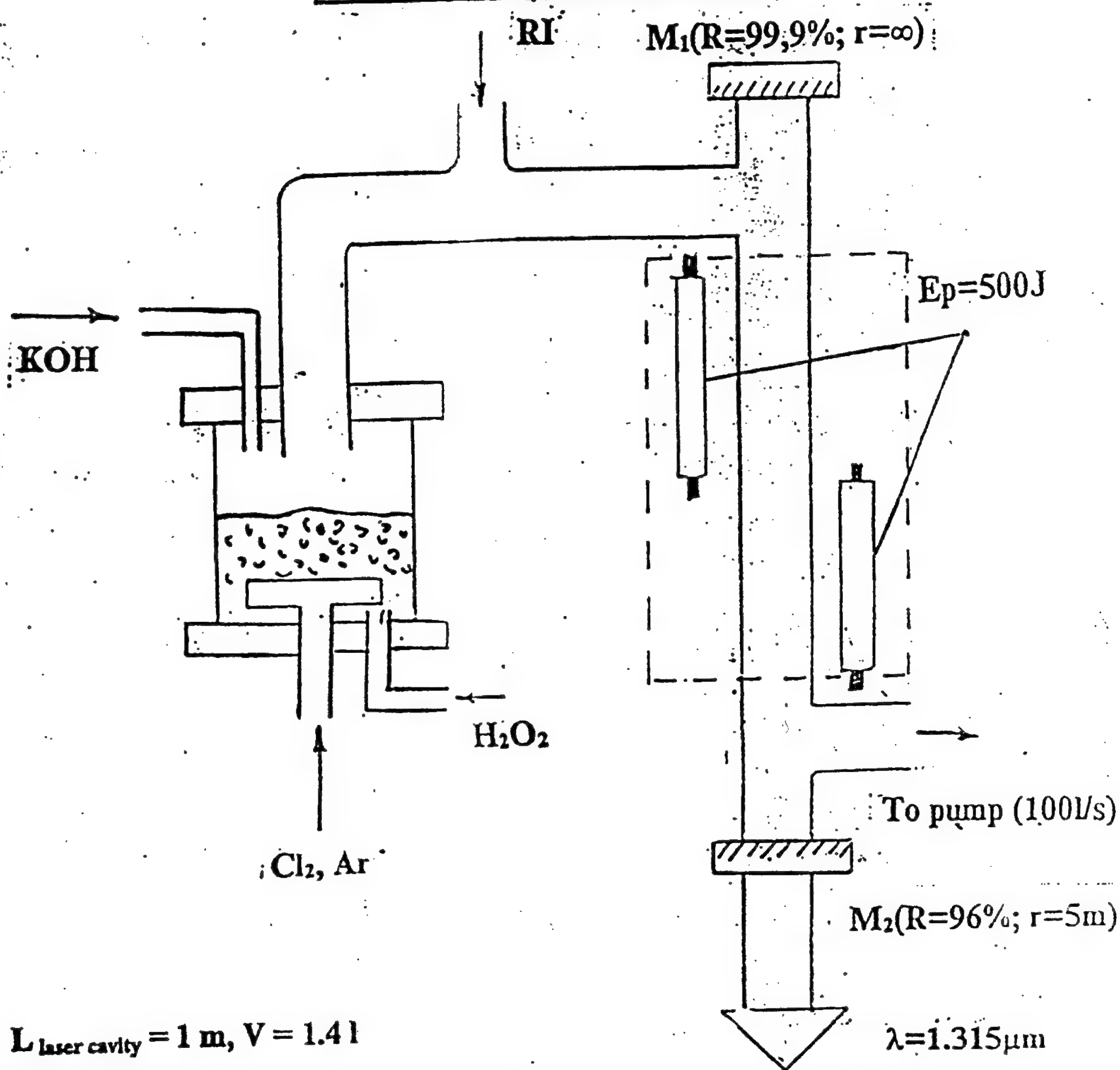

$L_{laser\ cavity} = 1$ m, $V = 1.4$ l

Iodides investigated: CH_3I, CF_3I, C_3F_7I, C_3H_7I

$P_{O2} = 3$ Torr, Cl_2 flowrate = 20 mmole

$E_{out} = 4.4$ J, $\varepsilon_{max} = 3.1$ J / l, $\tau = 15 - 500$ μs

$P_{pulse} = 300$ kW

Intrinsic efficiency = 700 % (depends on iodine concentration produced)

Flash lamp efficiency – 10…20% ⇒Total efficiency – 70…140%

IODIDE INFLUENCE

CH_3I, CF_3I, C_3F_7I

1. High Cl_2 utilization

$$\mathbf{M + R + O_2 \rightarrow RO_2} \qquad k = \begin{array}{l} 1.9 \cdot 10^{-29}\ CF_3I \\ 4.5 \cdot 10^{-31}\ CH_3I \end{array}$$

$$\begin{array}{l} \mathbf{O_2(^1\Delta)} \\ \mathbf{I(^2P_{1/2})} \end{array} + CF_3O_2 \rightarrow \begin{array}{l} O_2(^3\Sigma) \\ I(^2P_{3/2}) \end{array} \qquad \begin{array}{l} k \sim 4.5 \cdot 10^{-11} \\ k \sim 2.5 \cdot 10^{-11} \end{array}$$

CH_3I is preferable

2. Deficient Cl_2 utilization

$$\mathbf{O_2(^1\Delta)} + Cl_2 + CH_3I \rightarrow I + \text{ products}$$

$$k = 4 \cdot 10^{-32} \quad cm^6 \cdot s^{-1}$$

$C_nF_{2n+1}I$ – no reaction

$[Cl_2]$ control method

Pulsed COIL with Electric Discharge

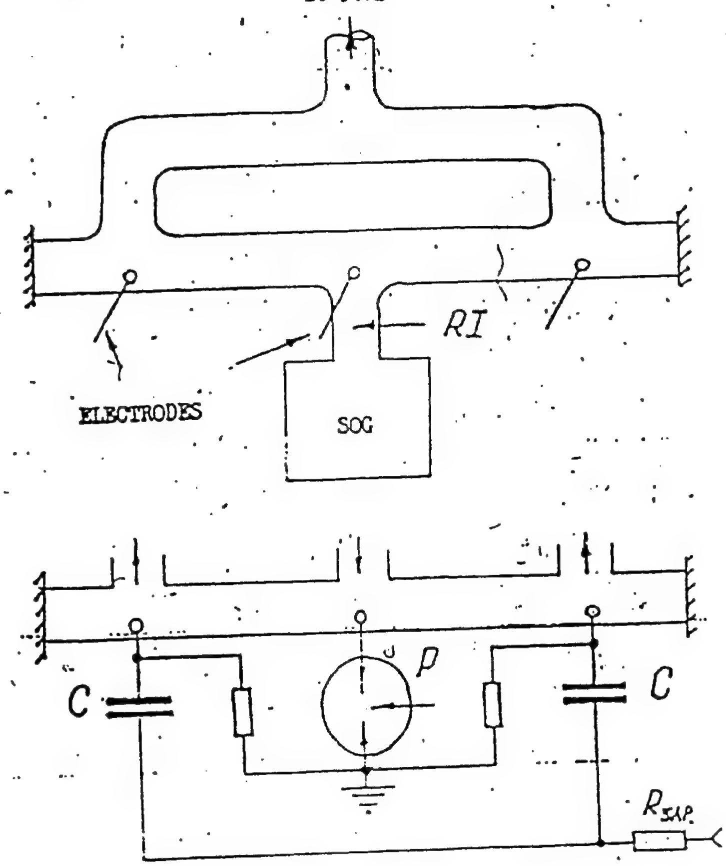

Sparger Type Singlet Oxygen Generator

NO WATER VAPOR TRAP

Typical mixture composition: O_2 – to 2 Torr, CF_3I – to 1 Torr, He(Ar) – to 3 Torr

Chlorine flowrate – 11 mmole / s, Flow velocity – 34 m / s

Discharge parameters: U = 14 – 28 kV / 60 cm, τ = 3 μs
Capacitor – 5 – 10 nF

Energy stored – 1 – 8 J

Pulsed COIL with Electric Discharge
Experimental results

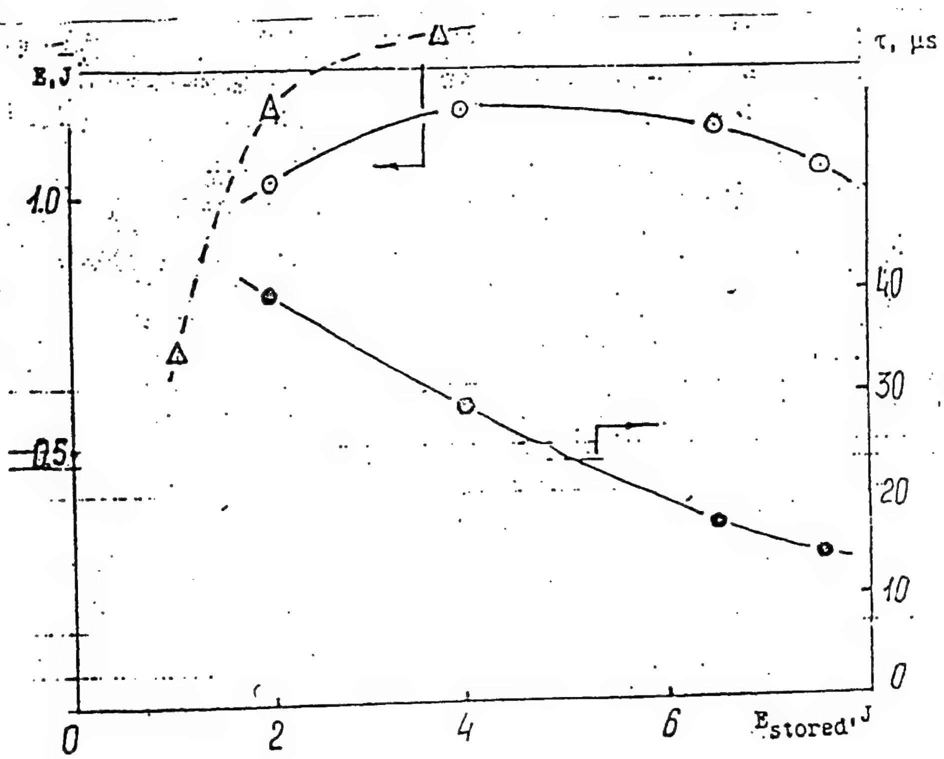

$21\ eV \leq \varepsilon_{\text{Iodine atom}} \leq 29\ eV$, **Photolysis:** $\varepsilon_{\text{Iodine atom}} = 5\ eV$

Buffer gases: He, Ar, N_2, $E_{He} : E_{Ar} : E_{N2} = 2 : 1,4 : 1$

R = CH_3I, E_{out} = 1.8 J, Efficiency = 91%, $\eta_{chem} = 10\%$

P_{pulse} = 100 kW at Chlorine flowrate of 14 mmole / s

Repetition operation to 20 Hz

TE facility is under manufacturing

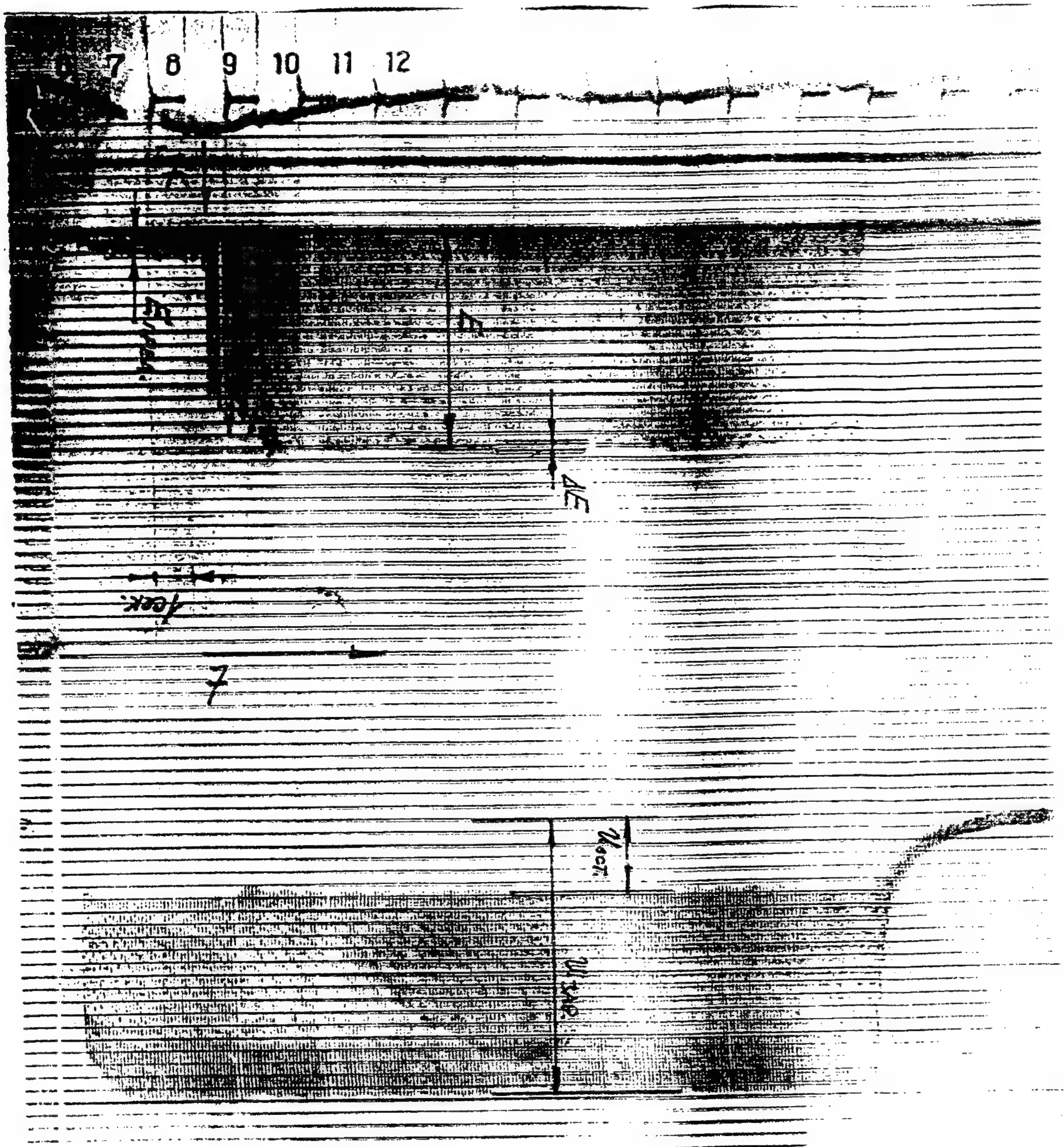
7 8 9 10 11 12

Transfer Flow Transfer Excitation COIL

Motivation: ---degradation of output energy of a longitudinal COIL at increased repetition rate

relaxation of energy stored in active medium due to reaction
$Cl_2 + O_2(^1\Delta) + RI$

Background: --Apollonov and coworkers --simple electrode configuration to drive
HF nonchain laser. P_{SF6} — 70 Torr, electrode gap --- 15 cm

The problem of matching for transverse excitation.

The experimental units designed:

1. 50-cm length laser cell with simple electrode configuration and electrodes treated with sand paper— unseccessful result $4 \times 4 \times 50\ cm^3$
→transfer to preionization with surface discharge

2. 5-cm length laser cell with barrier discharge preionization — in progress $2 \times 2 \times 5$

3. 20-cm length laser cell with resistively loaded pin electrodes — laser generation is obtained. E_{out} = 10 mJ, $\tau_{1/2}$ = 30 μs. Optimization

O_2 - 1 Torr, He - 3 Torr, CH_3I - 0,5 Torr

$V = 1{,}5 \times 2 \times 20 = 60\ cm^3$

$\varepsilon = 160\ mJ/\ell \qquad \eta_{chem} = 3{,}3\%$

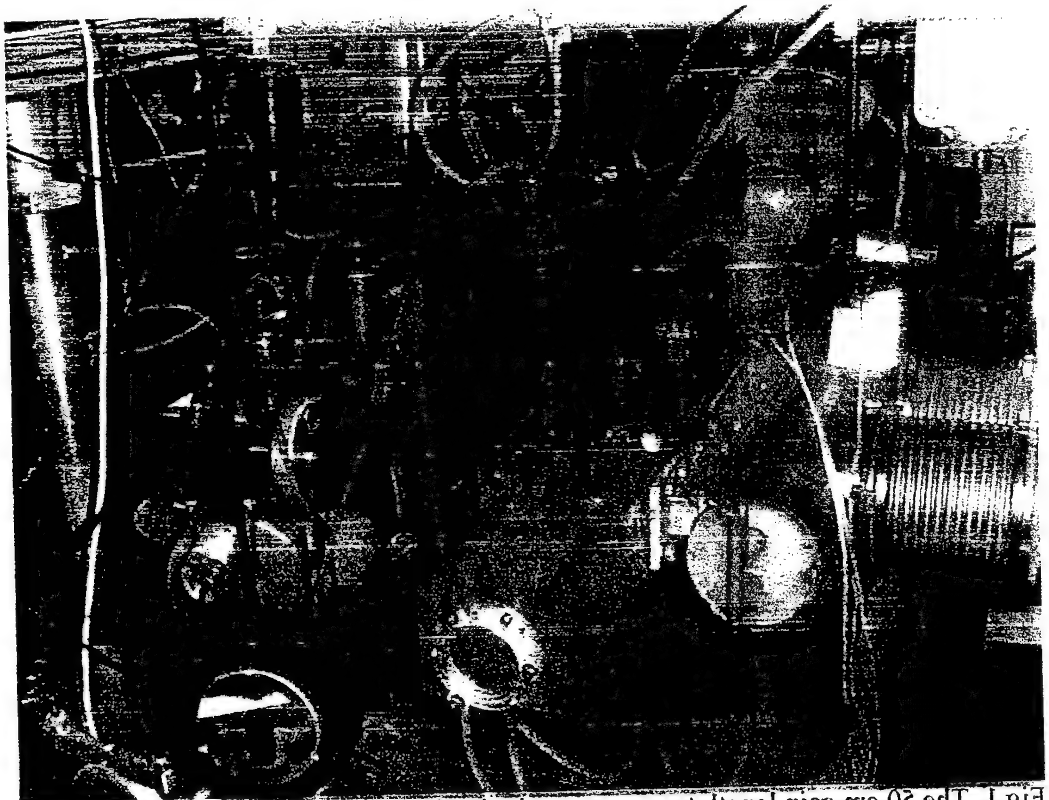

Fig.1. The 50 cm gain length transverse excitation laser chamber

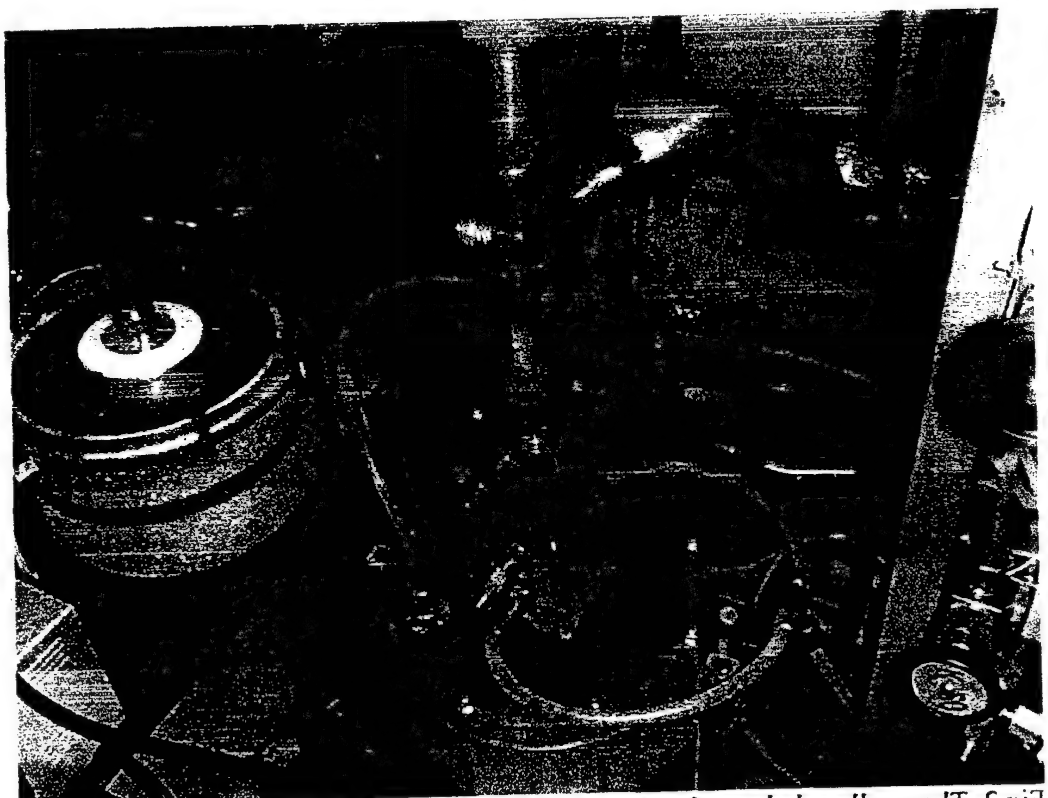

Fig.2. The small-scale laser chamber with jet SOG

The break-down parameters of gas oxygen with high SO content

Motivation: –electrical discharge as a source of singlet oxygen
–discharge generation of atomic iodine for COIL

Expected goal: -kinetic information necessary to describe the singlet oxygen behavior in plasma

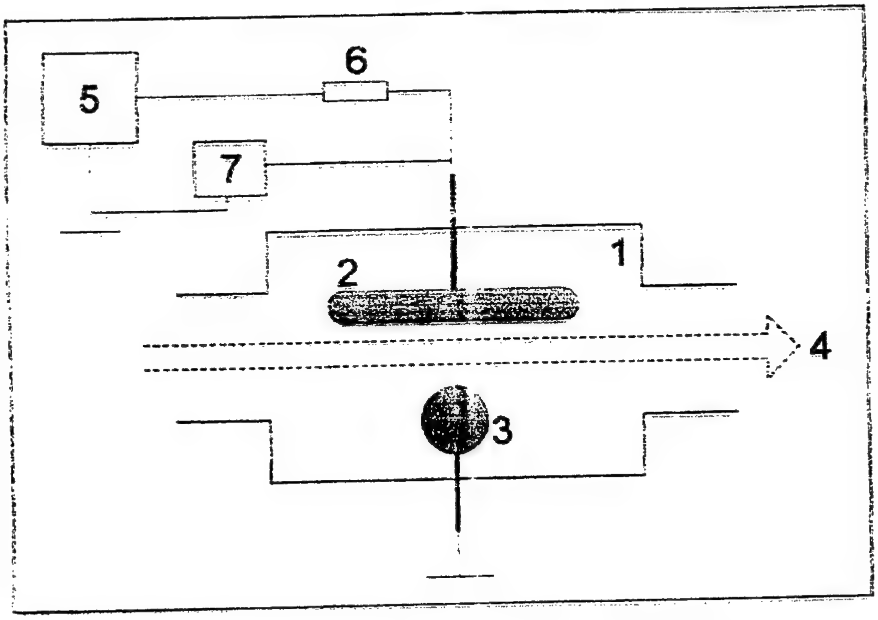

Schematic diagram of experiment: 1-discharge chamber, 2-disk electrode 54.8 mm o.d., 3 negative spherical electrode 20.2 mm o.d., 4-flow direction, 5-regulated high voltage supply, 6-resistor,
7-voltmeter. Electrode gap 6.6 mm

Таблица 1.

№ п/п	O_2 + $O_2(^1\Delta)$ (Торр)	$O_2(^1\Delta)$	H_2O (Торр)	U В	Nd (10^{18} см$^{-2}$)	E/N (10^{-16}Всm^2)	αd
1	1.4	-	0.1	543	0.0327	166.2	11.31
2	1.4	+	0.1	520	0.0327	159.2	11.32
3	2.1	-	0.15	604	0.0490	123.3	13.86
4	2.0	+	0.15	565	0.0468	120.7	13.52
5	2.1	-	0.09	606	0.0477	127.1	13.82
6	2.0	+	0.09	552	0.0455	121.3	13.22
7	1.4	-	0.2	541	0.0348	155.2	11.56
8	1.4	+	0.2	533	0.0348	152.9	11.83
9	2.1	-	0.03	600	0.0464	129.3	13.62
10	2.1	-	0.27	611	0.0516	118.4	14.12
11	2.0	+	0.7	603	0.0588	102.5	14.66
12	0.88	-	0.01	495.6	0.0194	255.7	8.23
13	0.9	+	0.01	478	0.0198	241.2	8.37
14	0.9	+	0.03	479	0.0203	236.5	8.46
15	0.9	+	0.06	482	0.0209	230.5	8.59
16	0.9	+	0.07	490	0.0211	231.9	8.68
17	0.97	-	-	535.8	0.0211	253.6	12.27
18	1.66	-	-	579.6	0.0362	160.3	8.96

IONIZATION CROSS SECTION

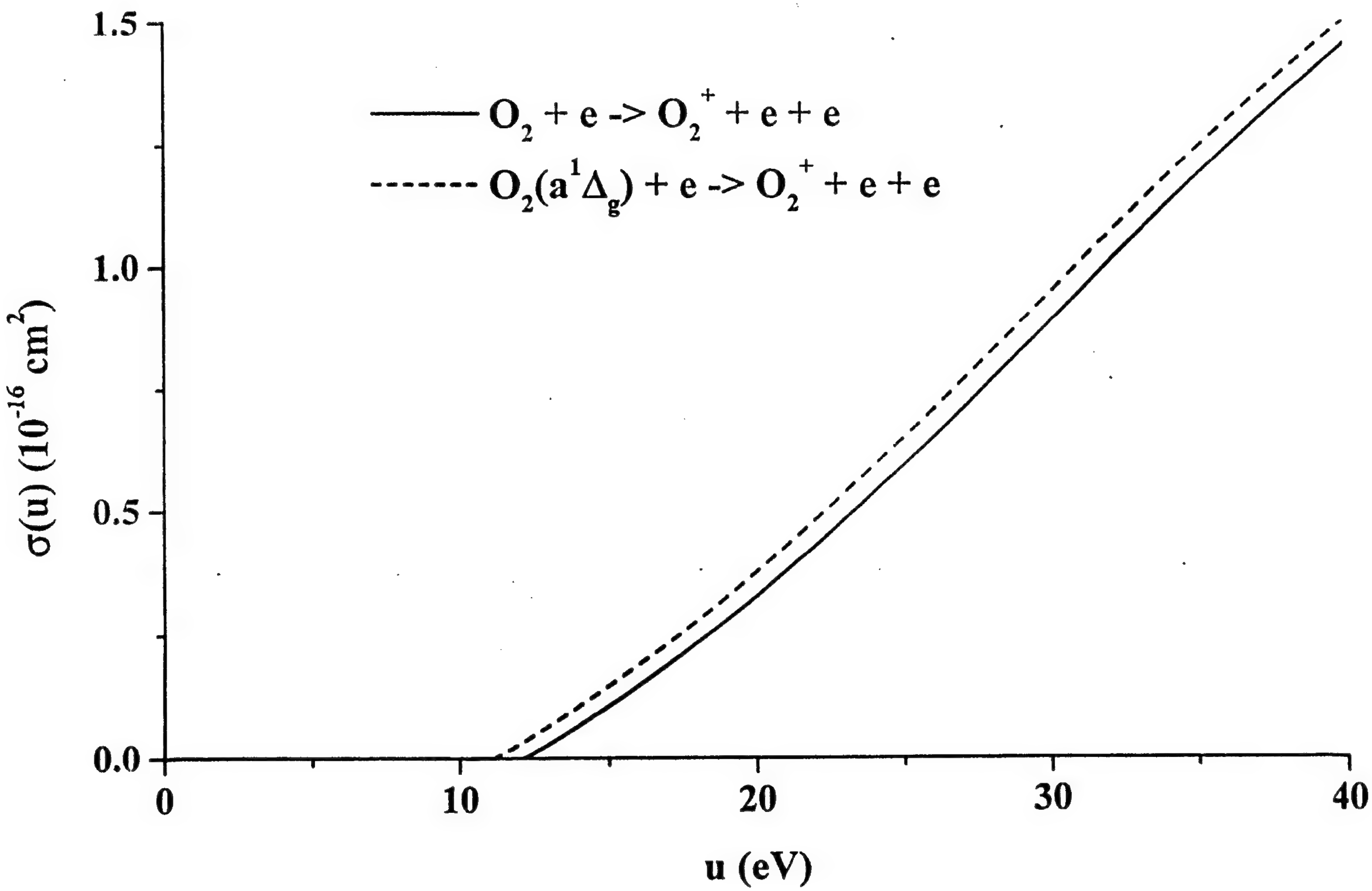

IONIZATION COEFFICIENT CALCULATED FOR EXPERIMENTALI MEASURED ELECTRIC FIELD STRENGTHS

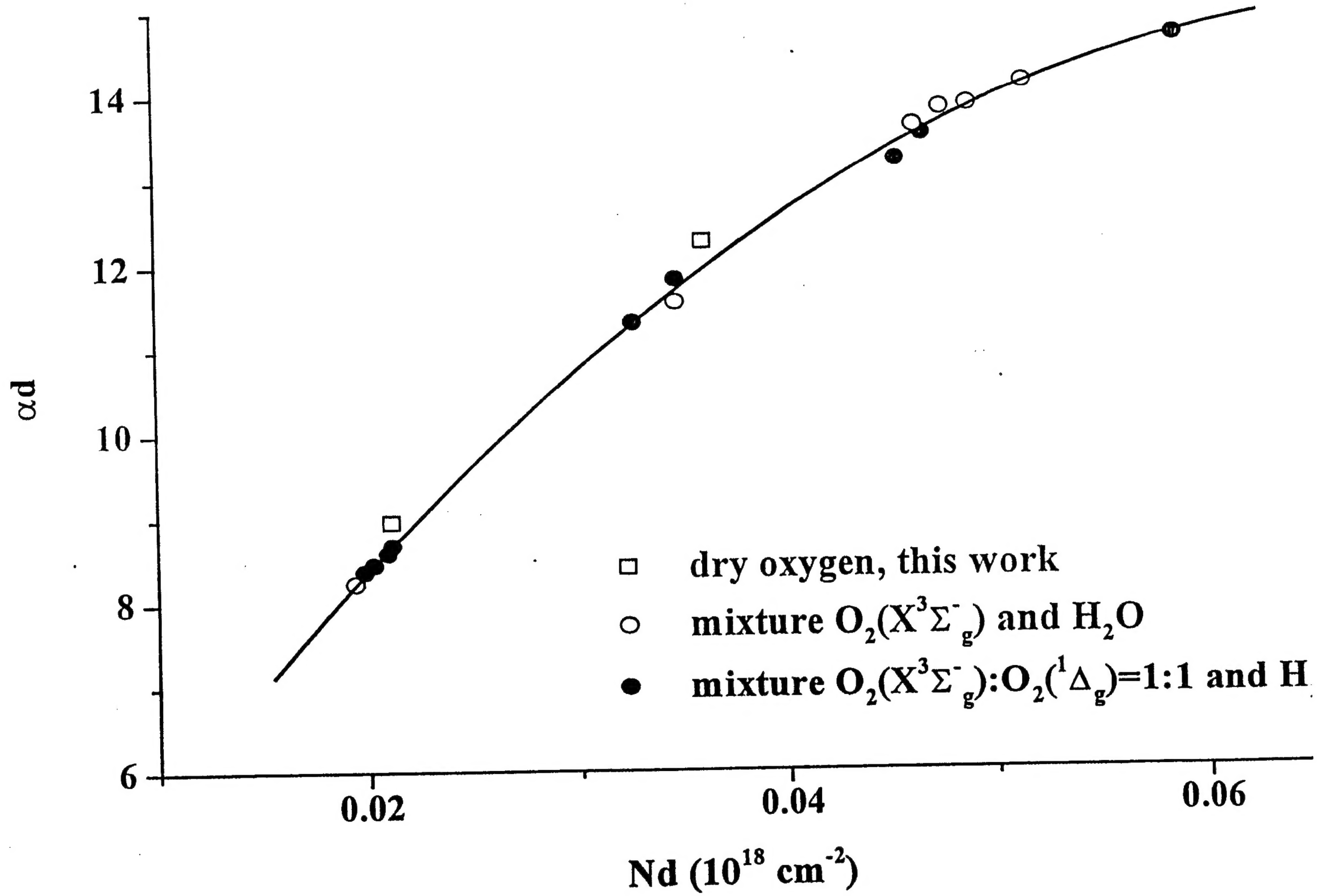

PROCEDURE FOR CALCULATION OF THE BREAKDOWN VOLTAG]
FOR $O_2(^1\Delta_g)$ CONTAINING MIXTURE

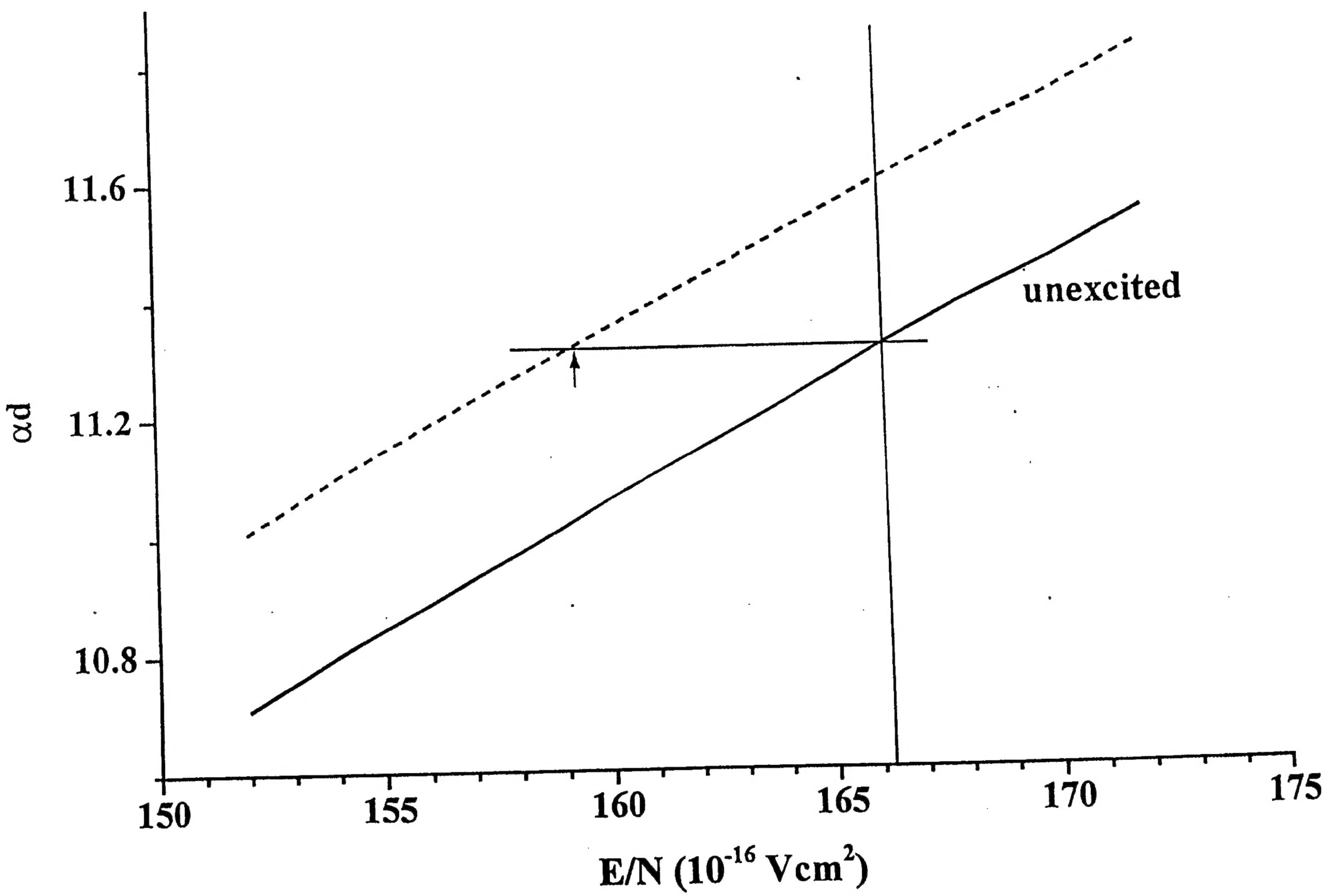

The study of VCC

Experimental set-up

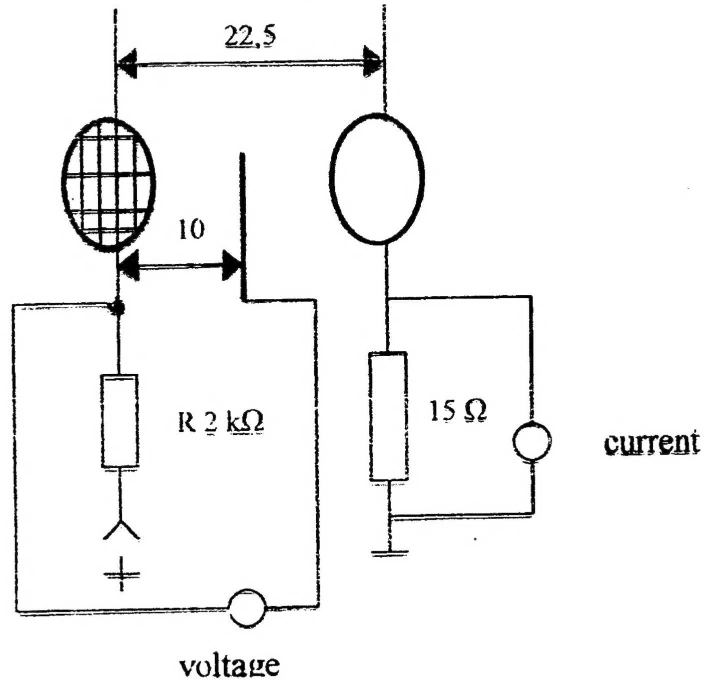

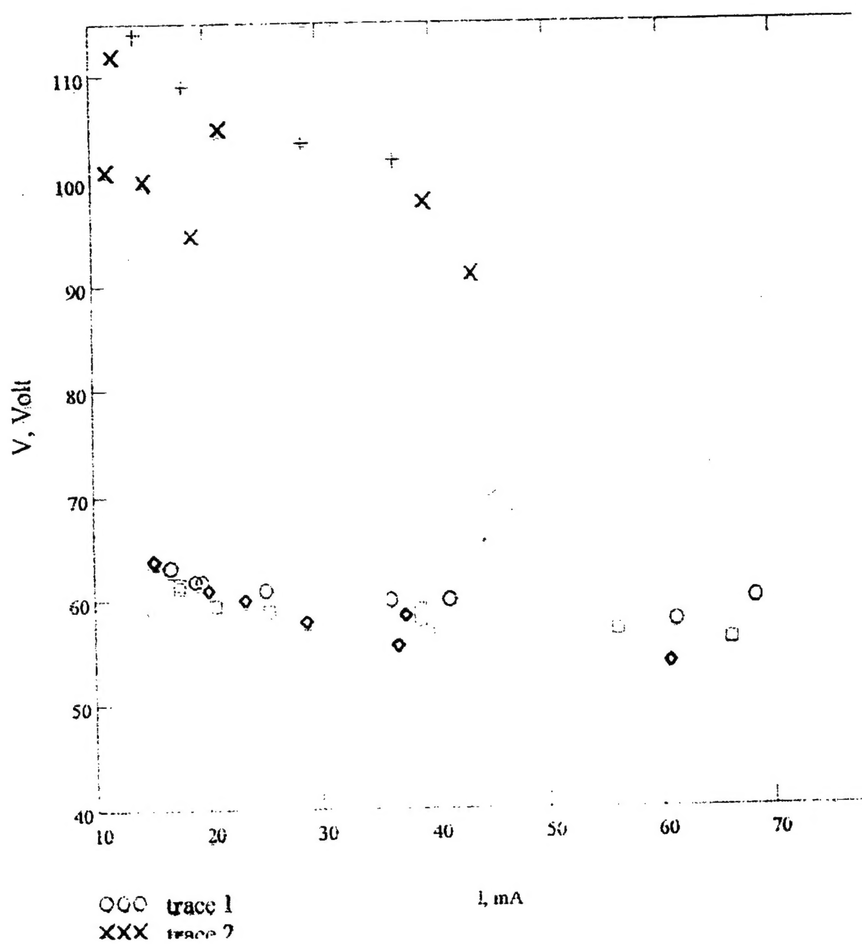

The study of VCC

Experimental set-up